Terms and Conditions of Use of Digitised Theses from Trinity College Library Dublin

Copyright statement

All material supplied by Trinity College Library is protected by copyright (under the Copyright and Related Rights Act, 2000 as amended) and other relevant Intellectual Property Rights. By accessing and using a Digitised Thesis from Trinity College Library you acknowledge that all Intellectual Property Rights in any Works supplied are the sole and exclusive property of the copyright and/or other IPR holder. Specific copyright holders may not be explicitly identified. Use of materials from other sources within a thesis should not be construed as a claim over them.

A non-exclusive, non-transferable licence is hereby granted to those using or reproducing, in whole or in part, the material for valid purposes, providing the copyright owners are acknowledged using the normal conventions. Where specific permission to use material is required, this is identified and such permission must be sought from the copyright holder or agency cited.

Liability statement

By using a Digitised Thesis, I accept that Trinity College Dublin bears no legal responsibility for the accuracy, legality or comprehensiveness of materials contained within the thesis, and that Trinity College Dublin accepts no liability for indirect, consequential, or incidental, damages or losses arising from use of the thesis for whatever reason. Information located in a thesis may be subject to specific use constraints, details of which may not be explicitly described. It is the responsibility of potential and actual users to be aware of such constraints and to abide by them. By making use of material from a digitised thesis, you accept these copyright and disclaimer provisions. Where it is brought to the attention of Trinity College Library that there may be a breach of copyright or other restraint, it is the policy to withdraw or take down access to a thesis while the issue is being resolved.

Access Agreement

By using a Digitised Thesis from Trinity College Library you are bound by the following Terms & Conditions. Please read them carefully.

I have read and I understand the following statement: All material supplied via a Digitised Thesis from Trinity College Library is protected by copyright and other intellectual property rights, and duplication or sale of all or part of any of a thesis is not permitted, except that material may be duplicated by you for your research use or for educational purposes in electronic or print form providing the copyright owners are acknowledged using the normal conventions. You must obtain permission for any other use. Electronic or print copies may not be offered, whether for sale or otherwise to anyone. This copy has been supplied on the understanding that it is copyright material and that no quotation from the thesis may be published without proper acknowledgement.

A role for amyloid-β in Alzheimer's pathology: evidence from cellular, animal and pre-clinical studies

Raasay Jones

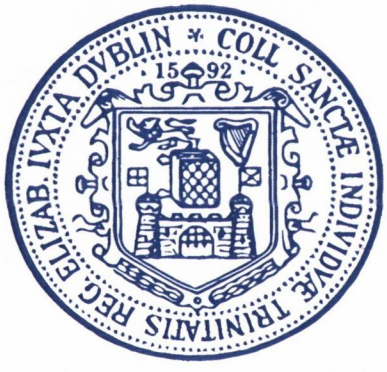

A thesis submitted to Trinity College Dublin for the degree of Doctor of Philosophy

Department of Physiology
Trinity College Institute of Neuroscience
2012

I: Declaration of authorship

I declare that this thesis has not been submitted as an exercise for a degree at this or any other university and it is entirely my own work, with the exception of certain results kindly donated by Dr. Eric Downer. I agree to deposit this thesis in the University's open access institutional repository or allow the library to do so on my behalf, subject to Irish Copyright Legislation and Trinity College Library conditions of use and acknowledgement.

Raasay Jones

II: Acknowledgements

Firstly, I would like to thank my supervisors, Professor Marina Lynch and Professor Thomas Connor, for their constant guidance and unwavering support throughout the course of my PhD. The enthusiasm you have for your work was always such an encouragement, and the time you have given to me over the years is much appreciated.

On both a personal and a professional level I would like to thank Dr. Aedín Minogue and Dr. Eric Downer for being an endless source of knowledge and advice (and on the rare occasion company in the Gingerman), especially over the past year throughout the course of our big studies.

I'd like to thank all the past and present members of TC, AH and MAL labs, it's been a pleasure working with you over the past few years and we've had some great times together (especially Milan!). A special thanks goes to Sinead and Eimear, both for the science, but also for being such good friends along the way. Thanks also to Brendan and Rob, both of whom have been there for my entire journey through TCIN. I'd like to wish you all the best of luck in your future endeavours.

I would like to acknowledge all the staff in TCIN and the Department of Physiology, places I have really enjoyed working over the past four years. My appreciation also goes to the Health Research Board for continuing to provide financial support for this study.

I'd like to thank John for his never-ending patience, reassurance and positive attitude on the many days when things weren't going quite to plan. Last but by no means least, I'd like to say a heartfelt thank you to Mum, Dad, Eppie and Matthew, for your love, support and frequent words of encouragement. I'm so lucky to have you all.

III: Abstract

One of the well-documented histopathological features of Alzheimer's disease (AD) is the progressive accumulation of amyloid-β (Aβ) within the brain, thought to result from inefficient clearance of Aβ by phagocytes and/or increased processing of amyloid precursor protein (APP). While neuroinflammatory changes, largely mediated by glial cells, are believed to be intricately involved in the pathogenesis of this chronic neurodegenerative disorder, the effect of inflammation on Aβ clearance remains to be firmly established. One of the primary objectives of this study was to assess the impact of exogenous and endogenous Aβ on microglia and astrocytes both *in vitro* and *in vivo,* with a specific interest in analysing its effect on astrocytes.

One of the most significant and novel findings is that astrocytes are efficient phagocytes. The data demonstrate that astrocytes, in addition to microglia, exhibit an enhanced capacity for phagocytosis following stimulation with Aβ *in vitro*. This was accompanied by increased mRNA expression of markers of glial activation, pro-inflammatory cytokines and putative Aβ receptors. While such markers of inflammation were also increased *in vivo* following intracerebroventricular infusion of Aβ for 28 days, only astrocytes were found to exhibit enhanced phagocytic potential following the treatment period, suggesting they have a more important role to play in clearing Aβ *in vivo* under these experimental conditions. Results further demonstrate that three receptors, toll-like receptor 2 (TLR2), the scavenger receptors CD36 and CD47, play a part in the complex response of astrocytes to Aβ, as Aβ induced their expression in isolated astrocytes, and specific neutralising antibodies modulated the Aβ-induced release of pro-inflammatory cytokines and phagocytosis.

In addition to the stimulatory effect of exogenously-delivered Aβ, the data demonstrate that an age-related increase in soluble and insoluble Aβ in the brains of transgenic mice genetically engineered to overexpress mutant forms of human APP and presenilin 1 (PS1) was accompanied by enhanced glial activation. Thus

expression of activation markers of microglia and astrocytes, including CD11b, CD68 and glial fibrillary acidic protein (GFAP) were increased with age in transgenic mice. Furthermore, an enhanced inflammatory profile of markers of classical activation was evident in the brains of APP/PS1 mice, and this was paralleled by BBB breakdown and infiltration of T-cells, monocytes/macrophages and neutrophils into the brain parenchyma. Further characterisation of these infiltrating immune cells identified them as likely to reinforce the pro-inflammatory status in the brain, thus exacerbating the pathogenic capacity of glia.

In an effort to translate the findings, which indicate inflammation is a key component in age-related changes in a mouse model of AD, monocyte-derived macrophages (MDMs) were isolated from the blood of healthy elderly adults classified as IQ memory-discrepant (low-performing, LP) compared with those that were IQ memory-consistent (high-performing, HP). In line with a role for inflammatory changes in the very early stages of cognitive deterioration, MDMs from the LP group displayed hypersensitivity to lipopolysaccharde (LPS) evidenced by the enhanced release of pro-inflammatory cytokines, associated with increased expression of TLR2 and TLR4. These observations identify a potential blood-based biomarker that may correlate with progression of cognitive dysfunction and is appropriate for routine and repeated assessment.

IV: Table of contents

v: List of figures

VI: List of tables

VII: Abbreviations

Abs	Absorbance
Ach	Acetylcholine
AChE	Acetylcholinesterase
aCSF	Artificial cerebrospinal fluid
AD	Alzheimer's disease
AGER	Advanced glycosylation end product receptor
ANOVA	Analysis of variance
APC	Antigen-presenting cell
APC	Allophycocyanin
APC-Cy	Allophycocyanin-cyanine
apoE	Apolipoprotein E
APP	Amyloid precursor protein
ATP	Adenosine triphosphate
Aβ	Amyloid-β
BBB	Blood brain barrier
BCA	Bicinchoninic acid
BDNF	Brain-derived neurotrophic factor
bp	Base pairs
BSA	Bovine serum albumin
Ca	Calcium
CC	C-C motif
CCL	Chemokine (C-C motif) ligand
CD	Cluster of differentiation
cDMEM	Complete Dulbecco's modified Eagle medium
cDNA	Complementary DNA
CL	Chemiluminescence
CNS	Central nervous system
CRP	C-reactive protein

CSF	Cerebrospinal fluid
CVO	Circumventricular organ
CXC	C-X-C motif
CXCL	Chemokine (C-X-C motif) ligand
DAPI	4'-6-Diamidino-2-phenylindole
DC	Dendritic cell
dH2O	Distilled water
DMEM	Dulbecco's modified Eagle medium
DMSO	Dimethyl sulfoxide
DNA	Deoxyribonucleic acid
DSM-IV	Diagnostic and Statistical Manual of Mental Disorders
EAAT	Excitatory amino acid transporter
ECM	Extracellular matrix
EDTA	Ethylenediaminetetraacetic acid
ELISA	Enzyme-linked immunosorbent assay
ELR	Glutamic acid-leucine-arginine motif
Em	Emission
EtOH	Ethanol
FACS	Fluorescence-activated cell sorting
FAM	6-carboxyfluorescein
FDA	Food and Drug Administration
FDG	fluorodeoxyglucose
FITC	Fluorescein isothiocyanate
FIZZ	Found in inflammatory zone
FMO	Fluorescence minus one
FW	Formula weight
GDP	Gross domestic product
GFAP	Glial fibrillary acidic protein
GLAST	Glutamate aspartate transporter

GLT-1	Glutamate transporter 1
GM-CSF	Granulocyte-macrophage colony-stimulating factor
GTP	Guanosine-5'-triphosphate
H_2O_2	Hydrogen peroxide
H_2SO_4	Sulfuric acid
HBSS	Hank's balanced salt solution
HMGB1	High-mobility group box
HP	High performer
HPLC	High-performance liquid chromatography
ICAM	Intercellular Adhesion Molecule 1
IFN	Interferon
IgG	Immunoglobulin G
IL	Interleukin
iNOS	Inducible nitric oxide synthase
INT	Tetrazolium salts
IP-10	Interferon γ-induced protein 10
IQ	Intelligence quotient
JAK	Janus kinase
JNK	c-Jun N-terminal kinase
K	Potassium
KC	Keratinocyte chemoattractant
kDa	Kilodalton
LAMP	Lysosom-associated membrane protein
LDH	Lactate dehydrogenase
LP	Low performer
LPS	Lipopolysaccharide
LTP	Long-term potentiation
MACS	Magnetic-activated cell sorting
MAPK	Mitogen-activated protein kinase

MCI	Mild cognitive impairment
MCP-1	Monocyte chemotactic protein-1
M-CSF	Macrophage colony-stimulating factor
MDM	Monocyte derived macrophage
MFI	Median fluorescent intensity
MGB	Minor groove binder
MHC	Major histocompatibility complex
MIP-1α	Macrophage inflammatory protein-1α
MMP	Matrix metalloproteinase
MMSE	Mini–mental state examination
MR	Mannose receptor
MRI	Magnetic resonance imaging
mRNA	Messenger RNA
MS	Multiple sclerosis
NADPH	Nicotinamide adenine dinucleotide phosphate oxidase
NaOH	Sodium hydroxide
NART	National Adult Reading Test
NFT	Neurofibrillary tangles
NFκB	Nuclear factor κB
NGF	Nerve growth factor
NH_4OH	Ammonium hydroxide
NK	Natural killer
NO	Nitric oxide
NSAID	Nonsteroidal anti-inflammatory drug
PAMP	Pathogen-associated molecular pattern
PBMC	Peripheral blood mononuclear cell
PBS	Phosphate buffered saline
PBS-T	Phosphate buffered saline with Tween
PD	Parkinson's disease

PE	Phycoerythrin
PE-Cy	Phycoerythrin-cyanine
PerCP	Peridinin chlorophyll protein
PET	Positron emission tomography
PLA_2	Phospholipase A_2
PRR	Pattern recognition receptor
PS1	Presenelin 1
PSD-95	Postsynaptic density protein 95
RAGE	Receptor for advanced glycation end products
RANTES	Regulated and normal T cell expressed and secreted
RNA	Ribonucleic acid
ROS	Reactive oxygen species
rpm	Revolutions per minute
RPMI	Roswell Park Memorial Institute
RT-PCR	Real time polymerase chain reaction
SD	Standard deviation
SDS	Sodium dodecyl sulfate
SEM	Standard error of the mean
SIP	Stock isotonic Percoll
SIRP	Signal-regulatory protein
SNARE	N-ethylmaleimide-sensitive factor attachment protein receptors
SR	Scavenger receptor
SR-A	Scavenger receptor class A
SR-B	Scavenger receptor class B
STAT	Signal transducer and activator of transcription
TBS-T	Tris buffered saline with tween
TGFβ	Transforming growth factor β
Th	T helper
THP-1	Human acute monocytic leukemia cell line

ThT	Thioflavin T
TLR	Toll-like receptor
TMB	3,3',5,5'-Tetramethylbenzidine
TNF	Tumour necrosis factor
Treg	T regulatory
UV	Ultraviolet
V	Volt
WASP	Wiskott–Aldrich syndrome protein
WMS	Wechsler Memory Scale
WT	Wild type

1: Introduction

1.1 Glial cells

The human brain, described as a 'marvellous, interconnected jungle of neurons and glia', is reported to contain approximately 86.1 billion neurons roughly equalled by glial cells (Azevedo, 2009). Comprised of three principal subtypes, glia have vital roles in neural development, function and health. Microglia act as resident immune cells of the central nervous system (CNS), astrocytes are classically assigned with providing metabolic, trophic and structural support to neurons, and oligodendrocytes function to surround the axons of neurons, generating myelin sheaths and thus allowing the rapid conduction of action potentials. A further glial subtype, ependymal cells, line the ventricles and play an important role in maintaining the volume of cerebrospinal fluid (CSF).

Microglia, comprising 10 – 20% of the total glial population, were initially described by del Rio-Hortega in 1919 following his studies on the brains of young animals using a silver carbonate method of staining. These cells derive from primitive myeloid progenitors that infiltrate the CNS during early embryonic development and differentiate into brain resident microglia (Ginhoux *et al.*, 2010), consequently displaying many surface antigens also present on macrophages. As the primary immune cells of the brain, microglia respond to insult and injury, playing a fundamental role in tissue repair (Harry and Kraft, 2012). Beyond their role inflammation and pathology, microglia have emerged as essential contributors to normal brain physiology. In the healthy brain, microglia structurally and functionally interact with neuronal and non-neuronal elements, carrying out important processes such as synaptic pruning during development and active remodelling of the perisynaptic environment (Tremblay *et al.*, 2011).

The density of microglia varies greatly between brain regions, for example the substantia nigra and corpus callosum are reported to comprise roughly 12% and 5% microglial cells respectively (Tremblay *et al.*, 2011). Morphological differences are also

apparent, with white matter microglia displaying elongated somata and processes, while those in the circumventricular organs (CVOs) exhibit compact morphology with few short processes (Lawson *et al.*, 1990). Microglia possess numerous filopodia and pseupodia, in addition to well-developed cytoplasmic vacuoles, morphological features indicative of their phagocytic ability. These cells are considered to be the most perceptive sensors of brain pathology, with their many ramifications perpetually extending and retracting in order to survey the CNS parenchyma for evidence of insult or injury (Davoust *et al.*, 2008). Upon detection of danger, microglia undergo a complex, multistage activation process resulting in their migration, proliferation, enhanced phagocytosis and the release of immunomodulatory mediators.

Astrocytes, the most abundant type of glia, are large, star-shaped cells originally regarded as merely providing 'brain glue' to support neuronal function. Three subtypes of mature astrocytes have been identified: spherically bushy protoplasmic astrocytes of the grey matter, less bushy process-bearing fibrous astrocytes of the white matter and elongated, non-excitable Bergmann glia of the cerebellum and Müller cells of the retina (Kimelberg and Nedergaard, 2010). This diverse group of cells represent a population with essential functions in homeostasis, neurotransmission, blood flow regulation, energy metabolism and immune defence within the CNS. Astrocytes express a large repertoire of receptors, including G-protein coupled and ionotropic receptors in addition to those for growth factors, chemokines, steroids and innate immune responses (Wang and Bordey, 2008).

In the healthy brain, astrocytes are responsible for processes such as K^+ buffering, control of extracellular pH, water transport, blood brain barrier (BBB) modulation, and the conversion of glucose to lactate that acts as a major fuel source for neurons (Kimelberg and Nedergaard, 2010). Following reports that astrocytes possess the machinery to release glutamate and other neurotransmitters in a Ca^{2+}-dependent manner (Parpura *et al.*, 1994), their role in intracellular communication has been identified. These cells also play an important role in recycling and metabolising

glutamate, helping to protect neurons against excitotoxicity. In addition, astrocytes carry out important antioxidant functions as they contain key proteins involved in the neutralisation of damaging free radicals (Jou, 2008).

1.2 The innate immune system

The immune system consists of a highly developed network of specialised cells and organs operating throughout the body in order to clear antigens that are foreign or perceived as being foreign, thus promoting host survival. The innate immune response relies on non-specific cellular and biochemical defence mechanisms designed to ensure a rapid response to pathogens, while the adaptive immune response provides long-lasting, highly specific reactions to particular inducing pathogens. The innate and adaptive immune responses function together, through the co-operation of numerous cells and molecules, in order to maintain homeostasis and successfully protect the host from antigenic challenge.

Elements of innate immunity are the major focus of this thesis, but it is appropriate to briefly refer to adaptive immunity, a far more elaborate and sophisticated coordination of defence. Cells of this system include B cells, which play a role in humoral immunity and the secretion of antibodies, and T cells, intricately involved in cell-mediated responses. Without the restraint of reliance on germline-encoded receptors to recognise invading pathogens, adaptive immunity benefits from the ability to generate a diverse repertoire of antigen receptors on B and T cells. The subsequent activation and clonal expansion of cells carrying the appropriate antigen-specific receptor for a particular inducing pathogen allows for a highly specific and adaptive immune response (Schenten and Medzhitov, 2011). The additional benefit of cellular memory permits a stronger and faster response to subsequent infections, resulting in the

infection being halted with less reliance on stimulation by the innate immune system (see table 1.1 for a brief comparison).

Property	Innate immune system	Adaptive immune system
Receptors	Fixed in genome Rearrangement is not necessary	Encoded in gene segments Rearrangement necessary
Distribution	Non-clonal All cells of a class identical	Clonal All cells of a class distinct
Recognition	Conserved molecular patterns (LPS, mannans, glycans)	Details of molecular structure (proteins, peptides, carbohydrates)
Self-nonself discrimination	Perfect - selected over evolutionary time	Imperfect – selected in individual somatic cells
Action time	Immediate activation of effectors	Delayed activation of effectors
Response	Co-stimulatory molecules Cytokines Chemokines	Clonal expansion Cytokines Chemokines

Table 1.1 A comparison of innate and adaptive immunity (adapted from Medzhitov and Janeway, 1997).

In contrast, the innate immune system is described as a universal and ancient form of host defence, with similar effector molecules found in plants and animals (Janeway and Medzhitov, 2002). Cells of innate immunity include monocytes, macrophages, dendritic cells (DCs), mast cells, granulocytes and natural killer (NK) cells, while non-cellular components include barriers between the organism and its environment, such as the skin and epithelia, and complex pathways such as the complement cascade.

The innate immune system has evolved to recognise conserved pathogen-associated molecular patterns (PAMPs), ranging from lipopolysaccharides (LPS) to mannans and bacterial DNA using a variety of germline-encoded pattern recognition receptors (PRRs). These receptors recognise conserved products of microbial metabolism, allowing the innate immune system to distinguish between infectious non-self and non-infectious self (Janeway and Medzhitov, 2002). Such receptors are expressed on the surface of numerous immune cells, as well as in intracellular compartments and secreted into the bloodstream and tissue fluids. Stimulation of these receptors leads to opsonisation, activation of complement and pro-inflammatory signalling cascades, phagocytosis and the induction of apoptosis (Medzhitov and Janeway, 1997).

Toll-like receptors (TLRs), fist identified in *Drosophila* in 1985, are particularly important in pathogen recognition and the initiation of an innate immune response. A total of 13 have so far been described in human and mouse, differing from each other in their ligand specificities, expression patterns and target genes (Hanamsagar *et al.*, 2012). For example, TLR1, TLR2 and TLR6 recognise bacterial lipoproteins; TLR3, TLR7, TLR8 and TLR9 are specific for nucleic acids; TLR5 binds to flagellin and TLR4 has a wide spectrum of ligands, including LPS and fungal zymosan (Farina *et al.*, 2007). Binding of TLRs to their microbial ligands stimulates nuclear factor κB (NFκB) signalling pathways and leads to phagocytosis, the release of pro-inflammatory cytokines and anti-microbial peptides, and the direct killing of pathogens (Takeda *et al.*, 2003). Activation of TLRs triggers maturation of phagocytic cells such as DCs, resulting in the expression of co-stimulatory molecules and increased antigen-presenting capacity, thus helping to direct adaptive immune responses (Janeway and Medzhitov, 2002).

1.3 Cells of the peripheral innate immune response

The lifespan of many of cells involved in the innate immune response is thought to be in the order of hours to days, a relatively short time period compared to those involved in the adaptive immune response, which persist for months to years (Sun *et al.*, 2011). Monocytes, comprising 5-10% of white blood cells, originate in the bone marrow from a common myeloid progenitor shared with neutrophils. These cells are released into the bloodstream where they circulate for several days before entering tissues to replenish tissue macrophage and DC populations (Gordon and Taylor, 2005). Monocytes show distinct morphological heterogeneity, including variability of size, granularity and nuclear morphology, thought to reflect the specialisation of function adopted by macrophages in different anatomical locations (Kurihara *et al.*, 1997). Monocytes, and their macrophage and DC progeny, serve three main functions in the immune system, namely phagocytosis, antigen presentation and cytokine production. DCs are believed to play an important role in linking innate and adaptive immunity via the induction of T cell responses. While immature DCs have high endocytic activity, they do not express T cell co-stimulatory signals and therefore have a low activation potential of these cells. Following exposure to pathogens, maturation of DCs and the subsequent upregulation of co-stimulatory molecules such as CD40, CD80 and CD86, results in potent activation of T cell responses (Janeway and Medzhitov, 2002).

Granulocytes, comprising neutrophils, eosinophils and basophils, are so named due to the presence of numerous granules within their cytoplasm. These granules contain a variety of molecules that act to destroy invading pathogens, including antimicrobial peptides and proteases such as cathepsin G, neutrophil elastase and proteinase 3 (Pham, 2006). Neutrophils, which constitute 50-70% of circulating white blood cells, originate from bone marrow myeloid precursor cells. They circulate in the blood and migrate rapidly to sites of infection via chemotaxis, resulting in the phagocytosis and destruction of invading pathogens, generation of reactive oxygen species (ROS) and

the release of microbicidal substances from their cytoplasmic granules. Eosinophils and basophils, whilst far less numerous, are involved in modulating immune responses in a similar manner, and reportedly play an important role acting as effector cells in allergic inflammation (Hogan *et al.*, 2008, Schroeder, 2009).

NK cells are a type of cytotoxic lymphocyte whose primary functions are described in the killing of virally- and cancer-infected cells through initiation of the granule exocytosis pathway. Following cell-cell interactions, NK cells form a cytotoxic synapse with their target, resulting in the release of granzymes that enter the infected cell with the aid of perforin, which forms pores in the cell membrane, leading to the initiation of apoptosis or osmotic cell lysis (Leong and Fehniger, 2011).

1.4 Mediators of the innate immune response

Activation of the innate immune system is associated with release of a plethora of inflammatory mediators, such as cytokines, chemokines and ROS. These inflammatory mediators appropriately direct cells of the adaptive immune response to change their phenotype in order to eliminate a particular inducing pathogen.

$CD4^+$ T helper (Th) cells play an important role in adaptive immune responses by recruiting and activating B cells, $CD8^+$ T cells, macrophages and neutrophils (Zhu and Paul, 2010). Based on their functions and cytokine secretion, Th cells can be are classified into four major lineages, Th1, Th2, Th17 and T regulatory (Treg) cells. These phenotypes are characterised by the cytokines they produce, with Th1 and Th2 responses effective against intracellular and extracellular pathogens respectively (Zygmunt and Veldhoen, 2011). Th1 cells produce interferon γ (IFNγ) and tumour necrosis factor α (TNFα), which activate macrophages and are responsible for cell-mediated immunity, while Th2 cells produce interleukin-4 (IL-4), interleukin-10 (IL-10) and interleukin-13 (IL-13), responsible for antibody production and the inhibition of

several macrophage functions (Zhu and Paul, 2010). It is important to note that these cytokines rarely act in isolation, with many having somewhat overlapping physiological effects. The pattern of cytokine release from Th cells further affects antigen-presenting cells (APCs) which adopt diverse phenotypes depending on the environment they are exposed to (Classen *et al.*, 2009).

Interleukin-12 (IL-12) was originally identified as a product of Epstein–Barr virus transformed human B cell lines that could activate NK cells and induce IFNγ production and T cell proliferation (Stern *et al.*, 1990). A heterodimer, composed of a p35 light chain and p40 heavy chain, IL-12 signals through its cognate IL-12 receptor (IL-12R), expressed mainly on activated T cells and NK cells (Presky *et al.*, 1996). Microbial products such as bacteria, intracellular parasites, fungi, double-stranded RNA and bacterial DNA induce the production of IL-12 by phagocytes such as macrophages, neutrophils and DCs (Ma and Trinchieri, 2001). IL-12 strongly evokes expression of IFNγ, thus favouring a Th1 immune response and providing a bridge between innate and adaptive immunity (Trinchieri, 2003). Some of its other functions include enhancing the cytotoxic activity of NK and $CD8^+$ T cells, in part by inducing the transcription of genes encoding cytotoxic granule-associated molecules such as granzymes and perforin, and by upregulating expression of various adhesion molecules (Trinchieri, 1998).

IFNs, first discovered in 1957, were originally described as agents that interfere with viral replication (Isaacs and Lindenmann, 1957). IFNγ is the sole type II IFN, signalling through the IFNγ receptor (IFNγR), comprised of IFNγRI and IFNγRII subunits. IFNγ is a hallmark cytokine of the Th1 immune response, acting to induce antimicrobial and antitumor mechanisms in addition to upregulating antigen processing and presentation pathways (George *et al.*, 2012). IFNγ directs the migration, maturation and differentiation of numerous leukocyte subsets, in addition to activating NK cells and regulating B cell functions such as antibody production (Schroder *et al.*, 2004).

Interleukin-1β (IL-1β) is often referred to as the 'prototypic' inflammatory cytokine (Rothwell and Luheshi, 2000). The most studied members of the IL-1 family, IL-1α and IL-1β are less than 30% homologous, yet they bind to the same cell surface receptors and mediate similar biological effects. IL-1 receptor I (IL-1RI) is expressed on almost all cell types, acting as the key receptor in IL-1β-mediated responses, while IL-1 receptor II (IL-1RII) acts as a decoy by competitively inhibiting IL-1β from binding to IL-1RI. IL-1β increases the expression of vascular adhesion molecules and further induces a number of pro-inflammatory cytokines, chemokines, and inflammatory molecules that form an amplifying immune cascade. The net effect of this is to recruit and activate macrophages, lymphocytes and neutrophils to fight infection and stimulate wound healing in response to tissue damage (Dinarello, 1996). IL-1β release is often accompanied by that of TNFα and IL-6, with these cytokines having many redundant physiological effects (Rachal Pugh *et al.*, 2001).

TNFα, a further multifunctional pro-inflammatory cytokine, is originally synthesised as a membrane bound 26kDa polypeptide precursor, proteolytically cleaved by a membrane-associated metalloproteinase to release a 17kDa polypeptide. Three of these polypeptide chains then polymerise to form the circulating 51kDa protein (Munoz-Fernandez and Fresno, 1998). TNFα exerts its effects through activation of two distinct TNF receptors, but it is TNF receptor I (TNF-RI) thought to be responsible for mediating most of the biological actions of TNFα, including its antiviral activity and ability to induce apoptosis and cytokine production (Chen and Goeddel, 2002). TNFα, chiefly produced by activated macrophages, is described as a 'master regulator' of pro-inflammatory cytokine production, and plays a key role in stimulation of the acute-phase response (Parameswaran and Patial, 2010).

Interleukin-6 (IL-6) is described as a pleiotropic cytokine that influences antigen-specific immune responses and inflammatory reactions. The receptor system for IL-6, expressed on the surface of many immune cells, comprises IL-6 receptor (IL-6R) and gp130, a signal transducing component of cytokines related to IL-6 (Taga *et al.*, 1989).

IL-6 is released in response to infection and plays a key role in acute-phase protein induction as well as being particularly involved in the stimulation of T and B lymphocytes to effector cells (Barton, 1997). IL-6 can itself have a direct effect on cells, or be co-agonistic or antagonistic in combination with other cytokines (Tamm, 1989).

In contrast, IL-10 is an anti-inflammatory cytokine that plays an important role in the prevention of pro-inflammatory and autoimmune pathologies. Acting to keep inflammatory events under control, IL-10 serves to protect against excessive immune responses and tissue damage (Glocker *et al.*, 2011). IL-10 is expressed by many cells of the innate immune system, including DCs, macrophages, NK cells, eosinophils and neutrophils (Saraiva and O'Garra, 2010). In order to exert its effects, IL-10 dimerises and binds to a surface-bound cytokine receptor made up of two molecules of the IL-10 receptor α-chain (IL-10RI) and two molecules of the accessory IL-10 receptor β-chain (IL- 10RII) (Moore *et al.*, 2001). The many roles of IL-10 include downregulating the expression major histocompatibility (MHC) antigens, co-stimulatory molecules and release of pro-inflammatory Th1 cytokines such as TNFα, IL-1β, IL-6 and IL-12, (Zhang *et al.*, 2010).

Nitric oxide (NO) is a radical effector of the innate immune response that can act to directly block pathogen replication by inhibiting the synthesis of, and causing double-stranded breaks in, bacterial DNA (Fang, 1997). Inducible NO synthase (iNOS) is expressed following activation of various immune cells and results in the production of NO for periods of time lasting from hours to days (Kroncke *et al.*, 1997). iNOS utilises oxygen and electrons from nicotinamide adenine dinucleotide phosphate (NADPH) to oxidise L-arginine into the intermediate OH-L-arginine, which is then converted to NO and L-citrulline (Lowenstein and Padalko, 2004).

Chemokines, derived from a shortened version of 'chemotactic cytokines', comprise a family of small soluble proteins whose main function is to act as chemoattractants for cell migration, adhesion and chemotaxis (Bajetto *et al.*, 2002). Divided into four

families, depending on the location of their first two cysteine residues, the 50 members of the chemokine family often show similar, somewhat overlapping, specificities. The CC chemokine family encompasses monocyte chemotactic protein-1 (MCP-1; CCL2), macrophage inflammatory protein-1 (MIP-1α; CCL3) and 'regulated and normal T-cell expressed and secreted' protein (RANTES; CCL5). Together they function to attract monocytes, basophils, eosinophils, NK cells and T lymphocytes to sites of infection, but have little or no action on neutrophils (Bajetto *et al.*, 2002). Keratinocyte chemoattractant protein (KC; CXCL1) and IFNγ-inducible protein-10 (IP-10; CXCL10) are members of a second CXC subfamily of chemokines, which can be subdivided into two groups depending on the presence or absence of a glutamic acid-leucine-argninine (ELR) motif near the N-terminus. CXC chemokines containing this ELR motif, such as CXCL1, provide specificity for neutrophils, whereas those without it, such as IP-10, act primarily on lymphocytes and monocytes (Savarin-Vuaillat and Ransohoff, 2007).

1.5 Phagocytosis

The ability of a cell to internalise material from its surroundings is important for many biological processes including the uptake of essential nutrients, the removal of dead or damaged cells from the body and defence against invading pathogens. Endocytosis, the process by which a cell absorbs fluids and macromolecules from its surroundings, is therefore vital for its survival. Three forms of endocytosis can be distinguished according to the size of vesicle formed, its contents and the uptake machineries involved. Phagocytosis typically involves the internalisation of solid particles from the external milieu via large endocytic vesicles called phagosomes, while pinocytosis is associated with uptake of fluids and solutes via smaller pinocytic vesicles. Receptor-mediated endocytosis is a mechanistically distinct process stimulated by ligand binding

to specific cell-surface receptors resulting in the internalisation of receptor and ligand via clathrin-coated or uncoated vesicles.

Phagocytosis, first described by Eli Mechnikov in 1882, is generally defined as the internalisation of particles with a diameter greater than 0.5μm, such as bacteria, viruses, parasites, large immune complexes, apoptotic cells and cell debris (Ernst, 2006). While in unicellular eukaryotes such as protozoa, phagocytosis is an important feeding mechanism, in humans and animals it has developed as a vital element of the innate immune response, critical for the ingestion, destruction and processing of infectious or foreign material in response to infection (Aderem, 2003). Phagocytosis is not only effective in the clearance of pathogenic microorganisms, it also acts to process internalised targets, thus enabling antigen presentation to T cells, and resulting in the production of pro-inflammatory cytokines and chemokines that orchestrate the development of adaptive immune responses (Underhill and Goodridge, 2012).

In mammals, macrophages, DCs and neutrophils act as the professional phagocytic cells of the innate immune response. One litre of human blood contains an average of six billion polymorphonuclear and mononuclear phagocytes, with each group differing in structure and function depending on its origin (Hoffbrand, 2005). Macrophages, originating from monocytes, migrate into tissues to become multifunctional tissue-specific phagocytes following differentiation. The transformation from a monocyte to a macrophage involves the cell enlarging up to ten-fold, increasing the number and complexity of its intracellular organelles and producing higher levels of hydrolytic enzymes in order to increase its phagocytic capability. Macrophages usually enter tissue within hours to a few days following the initiation of inflammation, where their main biological function is to ingest and destroy foreign material and subsequently process and present it to lymphocytes. Activated macrophages also produce cytokines that serve an important role in innate and adaptive immune responses. Neutrophils migrate faster and react more aggressively to infection than do macrophages,

generally being the first cell to arrive at a site of inflammation, where they kill invading pathogens using lytic enzymes and bactericidal substances present in their cytoplasmic granules.

The process of phagocytosis can be divided into a number of distinct stages as shown in figure 1.1. The phagocyte binds to the target particle via any of a number of cell-surface phagocytic receptors, stimulation of which results in activation of multiple intracellular signalling pathways leading to membrane motility and the initiation of downstream effector functions. The plasma membrane extends to surround the pathogen and pinches off around it, resulting in internalisation of the target particle by the ingesting cell. Following engulfment, the ingested material is localised in an acidified cytoplasmic vacuole called a phagosome. These phagosomes acquire proteolytic activity through sequential fusion with lysosomes, eventually resulting in the ingested material being destroyed.

Phagocytosis is an adhesion-dependent process that involves numerous receptors, cytoskeletal elements and signalling cascades (see figure 1.2). Professional phagocytes such as macrophages display several classes of phagocytic receptors, including TLRs and scavenger receptors (SRs), which bind pathogens and mediate their internalisation. Within 30-60 minutes of TLR stimulation *in vitro*, phagocytic cells redeploy their actin cytoskeletons to enhance antigen capture (West *et al.*, 2004). In order to aid phagocytosis, pathogens may be coated with naturally occurring soluble factors such as immunoglobulin G (IgG) antibodies, complement molecules and lectins, that act to enhance phagocyte binding. These molecules, known as opsonins, may be constitutively present in serum or released following stimulation (Hart *et al.*, 2004). Once pathogens are opsonised, phagocytosis can occur more efficiently via activation of Fc and complement receptors.

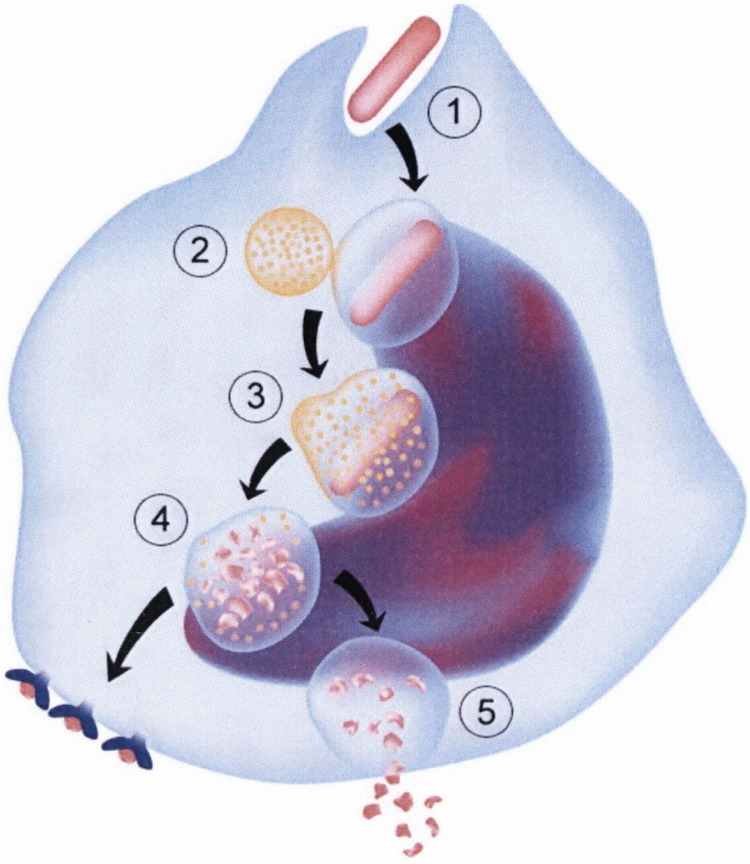

Figure 1.1 Stages of phagocytosis.

(1) Phagocyte binds to the target particle via any of a number of cell-surface phagocytic receptors resulting in the extension of pseudopods and internalisation of the pathogen by the ingesting cell (2) Following engulfment, the ingested material is localised within an acidified cytoplasmic vacuole (3) Phagosomes acquire proteolytic activity through the sequential fusion with lysosomes, eventually resulting in the ingested material being destroyed (4) Digested pathogens are processed for display on the cell surface by MHC peptide complexes where they are presented to cells of the adaptive immune response (5) Leftover fragments are released by exocytosis. (adapted from http://www.fotolia.com/id/32157847).

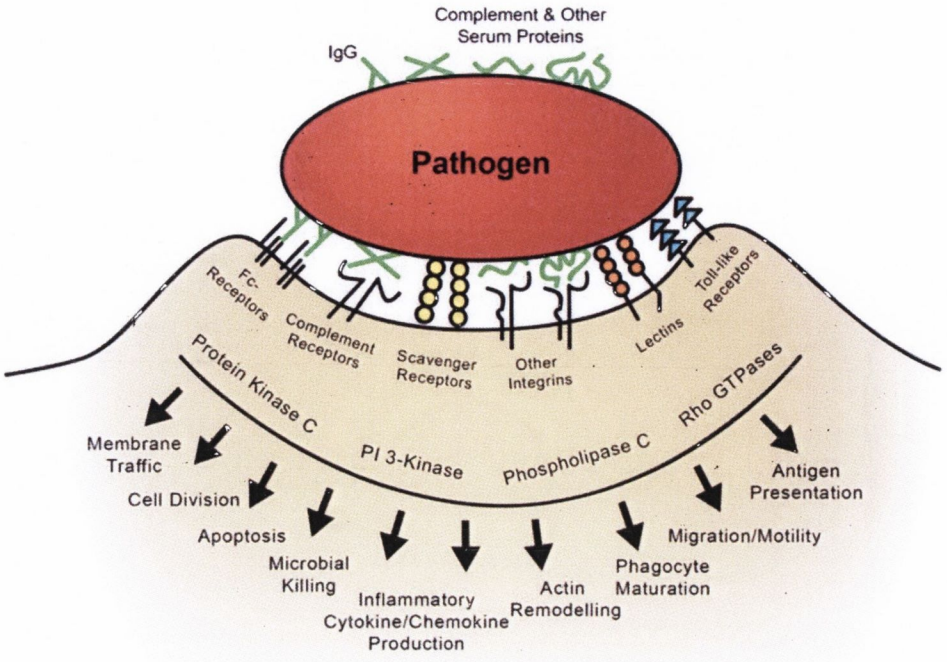

Figure 1.2 Cellular receptors involved in phagocytosis.

Multiple receptors simultaneously recognise pathogens via direct and indirect receptor binding, engagement of which induces numerous intracellular signals that can act in an overlapping manner. Stimulation of these pathways serves to activate or inhibit further phagocytosis and/or pathogen-induced responses (adapted from Underhill and Ozinsky, 2002).

Stimulation of phagocytic receptors results in the activation of a series of intracellular signalling pathways leading to dynamic and rapid reorganisation of the actin cytoskeleton (Kong and Ge, 2008). One of the initial events in cytoskeletal reorganisation is actin polymerisation, controlled by proteins belonging to the family of Rho GTPases, such as Rac and Cdc42 (Groves *et al.*, 2008). The effects of these small GTPases are mediated by GTP-dependent interactions with downstream effectors such as Wiskott-Aldrich syndrome protein (WASP). WASP family proteins

activate actin nucleation, allowing rapid filament growth and the extension of pseudopods around target particles (Insall and Machesky, 2009). In addition to reorganisation of the actin cytoskeleton, stimulation of phagocytic receptors leads to enhanced expression of MHC peptide complexes and co-stimulatory molecules, which play an important role in recruiting cells to the site of inflammation and initiating an adaptive immune response.

Following engulfment, scission from the plasma membrane and entry into the cell, the ingested material is trapped in a localised acidic phagosome. This initially innocuous vacuole undergoes a dramatic transformation in order to acquire the microbicidal and degradative features associated with innate immunity. Following sequential fusion with early endosomes, late endosomes and lysosomes, the resultant phagolysosome has a highly acidic, oxidative and degradative internal milieu (Flannagan *et al.*, 2009). Phagosomal pH generally drops from pH5.5 to pH 4.5 between early and late phagosomes, with acidification achieved through insertion of additional proton-pumping V-ATPases and tightening of the H^+ 'leak'. Collectively, this creates a hostile environment which favours the activity of many hydrolytic enzymes with acidic pH optima. Phagosomes are also equipped with an assortment of defensins, cathelicidins, lysozymes, lipases, proteases, hydrolases and endopeptidases that assist in degrading various pathogenic components (Kagan *et al.*, 1994).

The process of phagosomal maturation is achieved through a series of fusion and fission events with involvement of proteins such as members of the Rab family of small GTPases and lysosomal-associated membrane proteins (LAMPs). In particular, Rab5 appears to be involved in the fusion of phagosomes with early endosomes, and Rab7 mediates fusion with late endosomes (Ernst, 2006). N-ethylmaleimide-sensitive factor attachment protein receptors (SNAREs) are also important in phagosomal maturation, playing a vital role in membrane fusion and recycling.

Cells such as macrophages and DCs act as APCs by displaying antigen from digested pathogens associated with MHC peptide complexes on their cell surfaces. Following formation of a phagolysosome, contents of the phagosome interact with MHC molecules where they are transported to the cell surface and present pathogens to T cells to initiate an adaptive immune response. The goal of MHC class I molecules is to report on intracellular events, such as vial infection, to $CD8^+$ T cells, while that of MHC class II molecules is to sample the extracellular milieu and present antigens to $CD4^+$ T cells (Vyas *et al.*, 2008).

Finally, phagocytosis stimulates a process known as 'respiratory burst', where increased cellular oxygen consumption results in the production of a series of highly toxic oxygen derived compounds such as superoxide, hypochlorous acid, hydrogen peroxide and NO (Knight, 2000). The production of these highly reactive microbicidal agents is achieved by a multi-component NADPH oxidase complex that assembles on the phagosomal membrane (Minakami and Sumimotoa, 2006). These ROS are produced for the purpose of killing invading microorganisms and initiating an inflammatory response, however they can also inflict damage on neighbouring tissues and are thought to be of pathogenic significance in a number of diseases (Babior, 2000).

1.6 Innate immunity in the CNS

In comparison to the periphery, the CNS is relatively immune-privileged as it lacks a lymphatic drainage system and is shielded from the circulatory system by the BBB. As the brain has limited regenerative potential, it is important to maintain its integrity in order to reduce the loss of postmitotic neurons following immune-mediated toxicity (Colton, 2009). In the normal brain, low expression of cytokines are observed, however upregulation of molecules involved in the innate immune response is induced by the

presence of pathogens, in response to brain injury and also in a variety neurodegenerative disorders (Vitkovic *et al.*, 2000).

An innate immune response in the brain can be achieved through stimulation of a number of PRRs, including TLRs. Increasing evidence indicates that TLRs play a role in several inflammatory conditions within the CNS and, for example, genetic polymorphisms in human TLR4 have been linked to increased susceptibility in developing meningitis (Emonts *et al.*, 2003). Furthermore, the extent of TLR expression appears to correlate with neurodegenerative changes in diseases such as Alzheimer's disease (AD), Parkinson's disease (PD) and multiple sclerosis (MS) (Carty and Bowie, 2011). TLR expression and signalling has been demonstrated in many resident CNS cells, with evidence of increased expression following bacterial and viral infection (Carpentier *et al.*, 2008). Stimulation of TLRs on microglia and astrocytes is likely a contributing factor to the induction of neuroinflammation, resulting in the activation of neighbouring cells which both amplifies the initial response, modifies BBB permeability, and leads to recruitment of cells from the periphery that support initiation of an adaptive immune response (Hanisch *et al.*, 2008).

Microglia are the resident immunocompetent, phagocytic and APCs within the CNS, playing a similar role to macrophages in the periphery. These cells remain quiescent in the brain until injury or infection activates them to perform inflammatory and APC functions. So called 'resting' microglia in the healthy adult brain are characterised by a small cell body with fine, ramified processes and low expression of surface antigens (Garden and Moller, 2006). Once activated, microglia actively participate in the neurological immune response by secreting inflammatory cytokines, NO, increasing expression of MHC and co-stimulatory molecules, and acquiring an array of cell surface receptors that trigger or amplify innate immune responses (Hanisch, 2002).

Evidence is emerging to suggest that astrocytes are also intricately involved in innate immunity within the brain. These cells display a wide array of molecules involved in an innate immune response, including TLRs, mannose receptor, SRs, double-stranded RNA-dependent protein kinase and components of the complement system (Farina *et al.*, 2007). Following stimulation via TLRs, astrocytes actively participate in innate immune reactions, acting as a key CNS source of inflammatory mediators such as complement, IL-1β, IL-6, and chemokines MCP-1, CXCL1 and IP-10 (Ransohoff and Brown, 2012).

Although microglia are described as the resident phagocytic and APCs within the CNS, reports indicate that astrocytes also have phagocytic potential. For example, astrocytes have been shown to play a phagocytic role in axon elimination during embryonic and early post-natal development (Berbel and Innocenti, 1988). In addition, astroglial filaments have been found adjacent to demyelinating myelin sheaths in experimental gliomas, which they were shown to phagocytose and process (Lantos, 1974). More recently, a population of constitutively-phagocytic astrocytes, capable of engulfing large axonal evulsions were identified in the postlaminar optic nerve head myelination transition zone, and these cells were found to express Mac-2, a protein typically present in phagocytic cells (Nguyen *et al.*, 2011).

Astrocytes have also been shown to become phagocytic subsequent to brain trauma, evidenced by their ability to engulf colloidal carbon particles following their injection into the brain (al-Ali and al-Hussain, 1996) and phagocytic astrocytes appear in the middle molecular layer of the dentate gyrus six days after lesioning the entorhinal cortex (Bechmann and Nitsch, 1997). Interestingly, astrocytes *in vitro* have been shown to present antigen to T cells in a manner restricted by MHC, and thus a role for these cells in immune and phagocytic responses within the CNS is of great interest (Fontana *et al.*, 1984).

1.7 Alzheimer's disease

AD was initially described as an 'intriguing pathologic condition' by the German psychiatrist and neuropathologist, Alois Alzheimer, in 1906. The first documented case, detailed during a lecture at the 37th Conference of South-West German Psychiatrists in Tübingen, was identified by Alzheimer as 'an unusual disease of the cerebral cortex' which had affected a woman by the name of Auguste D. Prior to her untimely death at the age of 55, Auguste suffered from progressive cognitive impairment, disorientation, hallucinations and psychosocial incompetence. Following her death in 1906, post-mortem analysis of her brain showed various abnormalities including 'atrophy', the appearance of 'neurofibrils' and 'miliary focuses [senile plaques] resulting from the deposition of a peculiar substance in the cerebral cortex'.

Over 100 years later, AD is described as an age-related, progressive neurodegenerative disorder that affects over 35.6 million people worldwide (Ittner and Gotz, 2011). Clinically, patients present with short-term memory loss followed by a progressive decline in cognitive and executive functioning (Bekris *et al.*, 2010). In addition to extensive neuronal and synapse loss, the post-mortem AD brain is characterised by the build-up of two hallmark proteins, amyloid-β (Aβ), which accumulates in extracellular senile plaques, and microtubule-associated tau, which localises to intracellular neurofibrillary tangles (NFTs). These abnormal protein accumulations are believed to act in concert to cause the progressive neuronal degradation that leads to subsequent symptoms of the disease.

Little is known about the normal function of tau, although it appears to act as a microtubule-binding protein that regulates their stability and transport (Dixit *et al.*, 2008). Interestingly, the accumulation of hyperphosphorylated and aggregated tau within neurons in the AD brain has been shown to proceed the formation of senile plaques and their appearance to better correlate with neurodegeneration and cognitive impairment (Braak and Braak, 1991). Transgenic overexpression of a human tau

variant in mice resulted in animals developing progressive, age-related NFTs, neuronal loss and behavioural impairments (Santacruz *et al.*, 2005). While tau can clearly be described as a major player in AD, it is Aβ, the second hallmark protein associated with disease pathology that is the focus of this thesis.

AD is associated with significant neuroinflammation, which likely plays a fundamental role in disease pathogenesis. Evidence from epidemiological studies has revealed that treatment with non-steroidal anti-inflammatory drugs (NSAIDs) reduces the risk and delays the onset of developing AD (Pasinetti, 2002). Numerous mediators of inflammation are increased in the AD brain, including chemokines, cytokines, ROS and complement. This inflammation is suggested to occur in response to plaques and tangles associated with dystrophic neurons as well as reactive microglia and astrocytes (Rubio-Perez and Morillas-Ruiz, 2012). Such chronic, self-propagating, cytokine-mediated inflammation helps to explain the progressive neurodegeneration and dementia that occurs in AD. Therapeutic strategies aiming to control this inflammation may therefore be extremely valuable in halting progression of the disease.

1.8 Amyloid-β

Aβ is a proteolytic product derived from amyloid precursor protein (APP), an integral type I transmembrane protein expressed in many tissues throughout the body but principally concentrated in the synapses of neurons (Priller *et al.*, 2006). The primary function of APP is largely unknown, however it has been implicated as a regulator of synapse formation and plasticity, with its expression found to be upregulated during neuronal differentiation and following neuronal injury (Turner *et al.*, 2003).

APP contains three main proteolytic cleavage sites, two close to the membrane (α and β) and one within the transmembrane domain (γ). The cleavage of each of these

domains is catalysed by α-, β- and γ-secretases respectively (see figure 1.3), and can occur via one of two pathways:

1. In the amyloidogenic pathway, APP is initially cleaved by β-secretase, resulting in the production of a soluble NH_2 terminal fragment, sAPPβ, and a membrane bound COOH terminal fragment, C99, which is further cleaved by γ-secretase to yield Aβ.

2. In the non-amyloidogenic pathway, APP is initially cleaved by α-secretase, resulting in the production of a soluble NH_2 terminal fragment, sAPPα, and a membrane bound COOH terminal fragment, C83, which is further cleaved by γ-secretase to yield P3.

As α-secretase cleaves within the Aβ peptide domain, it precludes generation of the Aβ peptide, and therefore methods to increase its biological activity are being investigated in the treatment of AD. The large extracellular domains liberated by α- or β-secretase cleavage appear to participate widely in neurotrophic activity, intercellular communication and membrane-to-nucleus signalling (Turner *et al.*, 2003). However, while these fragments differ in size by only 17 amino acids at the carboxyl terminus, the effects induced by sAPPα are reported to be roughly 100 times more potent than those induced by sAPPβ (Mattson *et al.*, 1993).

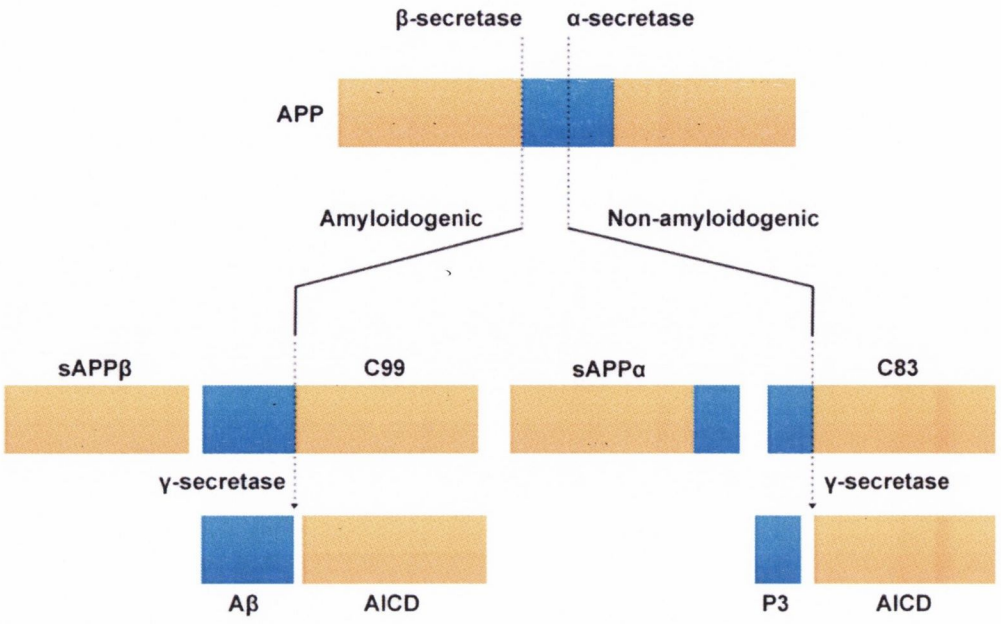

Figure 1.3 Schematic view of the cleavage sites of APP.

Cleavage of APP by β-secretase results in the formation of sAPPβ and C99, which is further cleaved by γ-secretase to yield Aβ and the APP intracellular domain (AICD). Alternatively, cleavage of APP by α-secretase results in the formation of sAPPα and C83, which is further cleaved by γ-secretase to yield P3.

The membrane-bound fragments, C83 or C99, are subsequently cleaved by γ-secretase. Cleavage of C99 results in formation of the Aβ peptide, whilst C83 cleavage generates a shortened Aβ-like fragment termed P3 (Turner *et al.*, 2003). Interestingly, cleavage of C99 by γ-secretase can occur at a number of sites, thus generating multiple Aβ species of varying lengths. $A\beta_{1-40}$ is the species most predominantly produced, compared to trace amounts of the more insoluble $A\beta_{1-42}$.

Aβ is initially produced as a single monomer, with its transition to dimers, trimers and higher oligomers resulting in its aggregation and pathogenic transformation (Nag *et al.*, 2011). Further aggregation yields protofibrils and fully-fledged fibrils that constitute the bulk of senile plaques found in the AD brain (Walsh *et al.*, 1999). Interestingly, lower

order oligomers appear to be the most potent neurotoxins, and, as $A\beta_{1-42}$ spontaneously aggregates to form these oligomers, it is thus considered the most toxic species. Recent studies have suggested there is a relatively weak correlation between the severity of dementia and the density of fibrillar amyloid plaques in the AD brain; a more robust association has been observed between levels of oligomeric Aβ, synaptic loss and cognitive impairment (Walsh and Selkoe, 2007).

1.9 Phagocytosis of Aβ

Microglia act as tissue macrophages within the CNS and have been shown to play an important role in the internalisation and degradation of Aβ (Lee and Landreth, 2010). The presence of large numbers of activated microglia in the AD brain, specifically surrounding Aβ plaques, suggests they play a significant role in disease progression. Evidence that Aβ is phagocytosed by microglial cells comes from several sources. *In vitro*, microglia have been shown to actively phagocytose monomeric, oligomeric and fibrillar Aβ (Lee and Landreth, 2010). *In vivo*, numerous ultrastructural studies have reported that microglia in the AD cortex contain intra-cytoplasmic fragments of Aβ (Lewandowska *et al.*, 2004).

Microglia, endowed with numerous cell-surface molecules capable of detecting physiological disturbances, are thought to interact with Aβ through receptors such as the SRs, TLR2, TLR4 and the receptor for advanced glycation endproducts (RAGE) (see figure 1.4). Engagement of these molecules results in the activation of multiple parallel signalling cascades responsible for the complex cellular responses to Aβ (Lucin and Wyss-Coray, 2009). SRs, a family of cell-surface molecules that bind to a variety of unrelated ligands, were the first receptors reported to be involved in Aβ uptake (Paresce *et al.*, 1996). Mononuclear phagocytes, such as microglia, are known to express multiple SRs, including SR-A, SR-BI and CD36. A role for TLRs as Aβ

receptors was identified subsequent to the observation that blocking TLR signalling via interference with receptor–ligand interactions decreased Aβ-induced signalling and phagocytosis (Bamberger *et al.*, 2003). Aβ binding to RAGE is a powerful activator of microglial inflammation and analysis of RAGE expression in non-demented and AD brains indicates that an increase in RAGE protein and RAGE-expressing microglia parallels disease severity (Lue *et al.*, 2001).

Although microglia have the ability to internalise Aβ via receptor-mediated uptake, it has been suggested they may be unable to degrade it efficiently. Studies have shown that inactivated microglia have weakly acidic lysosomes and need to be stimulated by inflammatory agents in order to allow them to degrade and remove Aβ efficiently (Majumdar *et al.*, 2007). It has been postulated that as AD progresses, the inability of microglia to clear the mounting Aβ leads to 'frustrated phagocytosis', contributing to the persistent release of pro-inflammatory mediators and widespread neuronal degeneration observed in later stages of the disease (El Khoury and Luster, 2008).

In comparison to microglia, the role of astrocytes in clearance of Aβ from the AD brain is less well characterised. Adult mouse astrocytes placed *in situ* on Aβ-laden brain sections from transgenic AD mice were shown to associate with Aβ deposits and reduce the presence of Aβ in these sections (Wyss-Coray *et al.*, 2003). Furthermore, when adult mouse astrocytes were transplanted into the hippocampi of transgenic mice, a 57% reduction in Aβ burden was observed compared with WT animals (Pihlaja *et al.*, 2008). This study was followed up with the demonstration that astrocytes respond to human Aβ by upregulating expression of neprilysin, a zinc-dependent metalloprotease enzyme that degrades Aβ (Pihlaja *et al.*, 2011). When astrocytes were incubated with an inhibitor of neprilysin, the removal of Aβ was significantly reduced.

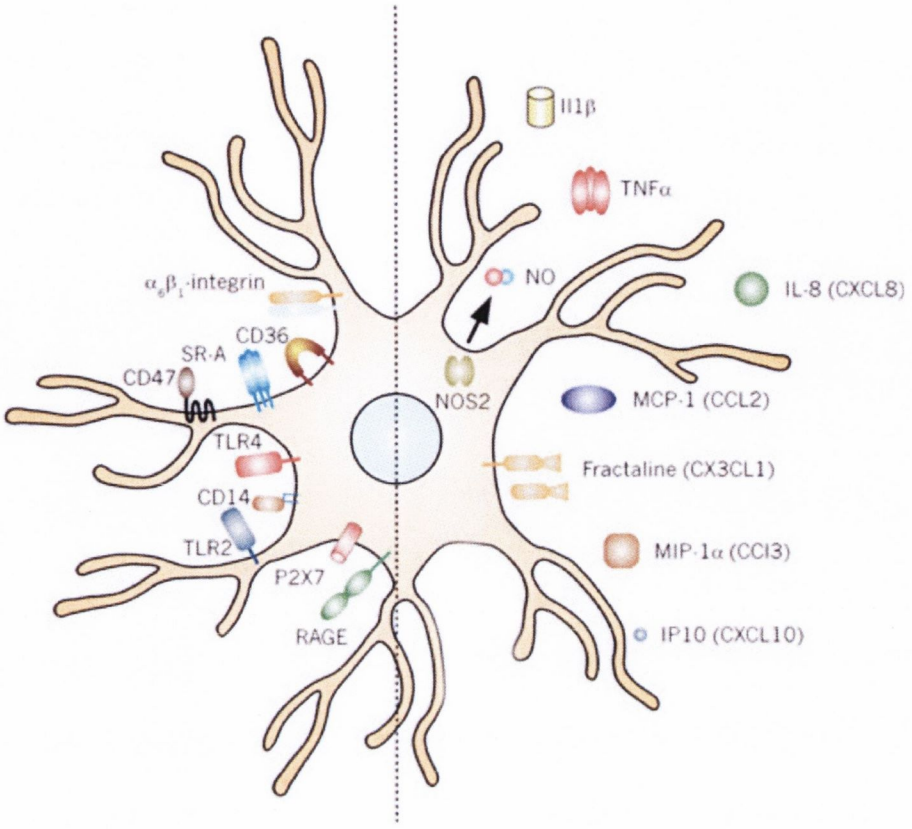

Figure 1.4 Pathways of microglial activation by Aβ

Microglia are endowed with numerous receptors capable of detecting physiological disturbances. Aβ has the ability to stimulate microglia through a variety of cell surface molecules (left), including CD36, SR-A, TLR2, TLR4 and RAGE. Stimulation of these receptors results in the release of cytokines, neurotoxic substrates (right), and activation of cellular pathways such as phagocytosis (adapted from Heneka *et al.*, 2010).

In post-mortem human AD brains, Aβ immunopositive material has been demonstrated within astrocytes throughout the entorhinal cortex (Nagele *et al.*, 2003). Additionally, primary human astrocytes derived from AD and non-AD brains have been shown to bind to and internalise aggregates of $A\beta_{1\text{-}42}$ (Nielsen *et al.*, 2009). Interestingly, this study demonstrated that foetal astrocytes were more efficient at internalising $A\beta_{1\text{-}42}$ than adult astrocytes, and that both foetal and adult astrocytes were better at internalising fluorescent $A\beta_{1\text{-}42}$ than primary adult microglia (Familian *et al.*, 2007,

Nielsen *et al.*, 2010). Interestingly, astrocytes were also reported to be more efficient in phagocytosing oligomeric compared with fibrillar species of $A\beta_{1-42}$ (Nielsen *et al.*, 2010). The mechanisms by which astrocytes internalise and degrade Aβ are largely unknown. SRs such as SR-B1 and the macrophage receptor with collagenous structure (MARCO) have been implicated (Alarcon *et al.*, 2005), however the role of receptors involved in microglial phagocytosis of Aβ, such as RAGE, TLR2, TLR4, CD36 and CD47, remains to be seen.

1.10 Genetics of AD

Age is the single biggest risk factor for AD, with incidence of the disease doubling every 5 years after the age of 65. This leads to a prevalence greater than 25% in people over the age of 90 (Qiu *et al.*, 2009). The cause of late-onset sporadic AD is, as of yet, unknown, however it is likely to be the result of a complex interaction between ageing and numerous environmental and genetic risk factors.

Molecular analyses of families with early-onset AD, accounting for roughly 5% of total cases, have identified mutations in three main genes to be responsible for the disease (Hoenicka, 2006). To date, over 230 mutations in PS1 and PS2, the catalytic subunits of γ-secretase, and APP have been associated with early-onset AD, most of which affect the synthesis and proteolysis of APP (Wu *et al.*, 2012). A double mutation in APP reported in a Swedish family (APPswe) that leads to increased cleavage of APP by β-secretase, has been shown to result in up to an 8-fold increase in Aβ production *in vitro* (Citron *et al.*, 1992). Mutations in PS1 and PS2 are reported to be associated with favouring the production of $A\beta_{1-42}$ over $A\beta_{1-40}$ (Albani *et al.*, 2007). Taken together, this is further supportive evidence of a causal role for Aβ in AD pathogenesis.

Interestingly, a recently reported coding mutation within the β-secretase cleavage site of APP (A673T) has been demonstrated to protect against AD and cognitive decline in

humans. When this mutation was cloned into 293T human embryonic kidney cells *in vitro*, it resulted in an approximate 40% reduction in the formation of Aβ (Jonsson *et al.*, 2012). Roughly 0.5% of Icelanders are reported to be carriers of this mutation, as are 0.2–0.5% of Finns, Swedes and Norwegians. It has been stated that harbouring the A673T mutation makes carriers five times more likely to reach 85 without developing AD (Callaway, 2012).

The most significant genetic risk factor of AD described to date is harbouring the ε4 variant of the lipid transport protein apolipoprotein E (apoE) (Huang, 2010). ApoE, a protein involved in cholesterol transport, exists in three major isoforms: ε2, ε3 and ε4 (Zhong and Weisgraber, 2009). In both sporadic and familial forms of AD, the prevalence of the apoE ε4 allele increases from 14% in the control population to roughly 40% in those suffering from AD (Poirier *et al.*, 1993). While the reasons for this are still largely unknown, it has been suggested that it could be due to interactions of apoE with Aβ, or as a result of its involvement in the mediation of CNS cholesterol and lipid homeostasis (Laws *et al.*, 2003).

1.11 Transgenic models of AD

The use of transgenic mouse models of AD provides an invaluable tool to investigate disease progression, in addition to assessing therapeutic interventions and biomarkers that could potentially prove effective in humans. Although transgenic mice undoubtedly mimic a number of the pathological hallmarks of AD, such as plaque deposition, neuroinflammation and cognitive deficits, they by no means recapitulate all aspects of the disease, in particular showing only moderate neuronal loss (Johnston *et al.*, 2011).

The first transgenic model of AD was generated using a platelet-derived growth factor (PDGF)-promoter driving a human APP770 minigene with a V717F mutation (PDAPP), (Games *et al.*, 1995). These mice expressed high levels of mutant human APP and

progressively developed many pathological hallmarks of AD, including Aβ deposits, neuritic plaques, synapse loss and gliosis. PDAPP mice showed significant memory impairments in the Morris water maze, radial arm maze, operant bar pressing and visual object recognition tasks compared with age matched controls (Chen *et al.*, 2000, Dodart *et al.*, 1999, Mullan *et al.*, 1993). Numerous other models incorporating mutations in APP have since been generated, including Tg2576 mice that overexpress human APP695 with a K670N M671L double mutation (Hsiao et al., 1996).

Perhaps the most commonly used transgenic model of AD today incorporates mutations in both APP and PS1. The APPswe/PS1dE9 model used in the current study contains one transgene encoding a chimeric APP with a double K595N M596L mutation, and a second encoding PS1 with a deltaE9 mutation, linked to increased Aβ plaque formation and early-onset AD respectively. These animals develop large numbers of Aβ plaques in the cerebral cortex and hippocampus far earlier than singly transgenic Tg2576 littermates (Borchelt *et al.*, 1997).

A 5XFAD transgenic model has recently been generated carrying 5 familial AD mutations, including a human APP transgene with Swedish, Florida, and London mutations, and a PS1 transgene carrying a double M146L L286V mutation *(Oakley et al.*, 2006). Compared with other models of AD, these animals develop synaptic loss, neurodegeneration, neuroinflammation and memory deficits unusually early by 4 months of age (Oakley *et al.*, 2006). More recently again, an APPSwDI/NOS2(-/-) mouse model has been developed, reported to closely model AD by exhibiting extensive Aβ pathology, hyperphosphorylated and aggregated normal mouse tau, significant neuronal loss, and cognitive deficits (Wilcock *et al.*, 2008). While one has to exercise caution in interpreting findings from transgenic models of AD, they present key features of the human disease and are thus a valuable tool in attempting to elucidate the molecular basis of cognitive impairment that occurs during the course of this debilitating disease.

1.12 Treatment of AD

There are currently only five drugs approved by the US Food and Drug Administration (FDA) for the symptomatic treatment of AD. Although these drugs are partially effective in improving symptoms, they do not halt progression of the disease or address the fundamental processes underlying AD. Four of these drugs target cholinergic function, which is compromised in AD following early loss of basal forebrain cholinergic neurons (Van der Zee *et al.*, 2011). Current treatments focus on inhibiting acetylcholinesterase (AChE), an enzyme involved in breakdown of the neurotransmitter acetylcholine (ACh). The first of these drugs, approved in 1993, was tacrine hydrochloride, an AChE inhibitor purported to slow the loss of cholinergic-mediated neural pathways important in memory function and cognition (Osborn and Saunders, 2010). AChE inhibitors approved since include donepezil, rivastigmine and galantamine. Meta-analyses based on randomised controlled trials have demonstrated that AChE inhibitors confer moderate and short-term improvements in cognition and global outcome, in addition to limited evidence of modest enhancements in mood and social interaction (Corbett and Ballard, 2012).

The most recent drug approved by the FDA, memantine hydrochloride, acts as an antagonist of the N-methyl-D-aspartate (NMDA) receptor, and is licensed for the treatment of moderate to severe AD, either on its own or in combination with AChE inhibitors. Neuronal excitotoxicty, following excessive exposure to the neurotransmitter glutamate, has long been associated with AD and thus targeting NMDA receptors was a novel approach in treatment of the disease following the limited efficacy of drugs targeting the cholinergic system.

A further innovative approach in the treatment of AD was stimulation of Aβ clearance by immunisation with Aβ antigens (active vaccination) or anti-Aβ antibodies (passive vaccination). The first vaccine of a pre-aggregated preparation of synthetic human Aβ, AN1792, was abandoned in 2002 due to the occurrence of meningoencephalitis in

approximately 6% of treated patients (Birmingham and Frantz, 2002). Follow up studies of Phase IIa participants have shown that AN1792 immunisation induced a modest but significant positive effect on some cognitive and functional outcome measures, including a significant reduction in Aβ load (Serrano-Pozo *et al.*, 2010). Several second-generation Aβ vaccinations have since been developed, including solanezumab and bapineuzumab. Solanezumab is a humanised monoclonal antibody developed with affinity for the central region of Aβ that selectively binds to soluble Aβ with little or no binding capacity for fibrillar forms (Delrieu *et al.*, 2012), whereas bapineuzumab binds Aβ plaques more strongly than it does soluble Aβ (Kerchner and Boxer, 2010). Unfortunately, phase III clinical trials of both drugs very recently failed to meet specified end-points in slowing cognitive and functional decline in AD, and their development is to be halted.

Emerging antibody therapies include crenezumab, due to be studied in asymptomatic subjects with a PS1 E280A mutation that predisposes carriers to early onset of AD (Miller, 2012). Further therapeutic approaches include modulation of the secretase enzymes, for example CTS-21166 which acts as an inhibitor of β-secretase. Several compounds that inhibit γ-secretase have also been identified, the most advanced of which is LY-450139, now in Phase III clinical development. Compounds that stimulate α-secretase activity are also being studied, including EHT-0202, which has recently commenced evaluation in a Phase II study. However while these drugs look promising, if the risk factors and pathogenic mechanisms involved in AD were more clearly understood, novel treatments, and perhaps even a cure for this devastating disease may be uncovered. Similarly, if an early diagnostic marker were to be identified, the efficacy of both current and future treatments would surely be enhanced.

1.13 Aims of study

The initial objective of this study was to examine the impact of exogenous Aβ on microglia and astrocytes *in vitro*, with specific regard to its effect on phagocytosis, markers of cellular activation, cytokine release and expression of putative Aβ receptors by both cell types. A significant issue was to investigate how astrocytes respond to Aβ by using a range of neutralising antibodies to establish the involvement of specific receptors and signalling pathways in these cells, both in terms of phagocytosis and cytokine release. The second objective was to examine the effect of exogenously-administered Aβ and the accumulation of endogenous Aβ (in APP/PS1 mice) on similar markers of glial activation. In APP/PS1 mice, the age-related expression profile of markers of alternative activation, acquired deactivation and classical activation was also examined. Finally, a cohort of human subjects with IQ-discrepant memory was recruited with the objective of assessing whether plasma concentrations of Aβ might correlate with phenotypic or functional changes in peripheral monocytes/macrophages.

2: Materials & Methods

2.1 Cell culture

2.1.1 Aseptic technique

All cell culture work was carried out in a laminar flow hood and aseptic technique was employed throughout. Use of the laminar flow hood ensured a constant supply of filtered air to the work area thus preventing the entry of normal air-borne pathogens from the surrounding atmosphere. To ensure the laminar flow hood remained sterile, the interior was sprayed with 70% ethanol (EtOH) in autoclaved distilled water (dH_2O) prior to use. Following use, the hood was exposed to ultraviolet (UV) light for 30 minutes. UV light causes adjacent thymine molecules in DNA to dimerise thus inhibiting replication of pathogens. Any materials passed into the flow hood were sprayed with 70% EtOH. Pipette tips and dH_2O were sterilised prior to use by autoclaving at 121°C for 1 hour and sterile disposable plasticware was employed where possible to further ensure asepsis. Disposable latex gloves were worn at all times and hands were sprayed with 70% EtOH before being placed in the hood. Dissection equipment was sterilised by thorough cleaning with Virkon followed by overnight baking at 200°C. Cells were maintained in an incubator at 37°C in a 5% carbon dioxide (CO_2) humidified atmosphere. Both the incubator and the laminar flow hood were cleaned regularly with Biocidal ZF™, Mycoplasma-OFF, Virkon and 70% EtOH to maintain a continually-sterile environment.

2.1.2 Preparation of culture media and test compounds

Primary glial culture media: Heat-inactivated foetal bovine serum (FBS; 50ml; 10%), penicillin-streptomycin (5ml; 1%) and fungizone (500µl; 0.25µg/ml) were filter-sterilised into a bottle of Dulbecco's modified Eagle's medium (DMEM; 500ml) using a syringe filter (0.2µm) to give complete DMEM (cDMEM) which was used in the preparation of all primary glial cell cultures. cDMEM was stored at 4°C for up to 2 weeks.

Cytochalasin-D: A stock solution (3mM) was prepared by dissolving cytochalasin-D (1mg; FW 507.6g/mol) in dimethyl sulfoxide (DMSO) and frozen at -20°C. Stock solution was diluted to working concentrations in pre-warmed cDMEM prior to use. Vehicle control was prepared containing DMSO as appropriate.

Macrophage colony-stimulating factor (M-CSF): A stock solution (100µg/ml) was prepared by reconstituting M-CSF (50µg) in bovine serum albumin (BSA; 0.1%) in sterile 1X phosphate-buffered saline (PBS). Stock solution was frozen at -20°C and diluted to a working concentration of 20ng/ml in pre-warmed cDMEM prior to use.

Granulocyte macrophage colony-stimulating factor (GM-CSF): A stock solution (50µg/ml) was prepared by reconstituting GM-CSF (50µg) in BSA (0.1%) in sterile 1X PBS. Stock solution was frozen at -20°C and diluted to a working concentration of 10ng/ml in pre-warmed cDMEM prior to use.

$A\beta_{1-40}$, $A\beta_{1-42}$ and $A\beta_{40-1}$: Lyophilised peptide (1mg) was dissolved in high performance liquid chromatography (HPLC) grade water at 6mg/ml and diluted to 1mg/ml with 1X PBS taking account of the peptide content for each batch used. In order to prepare a more aggregated species, stock solutions were incubated for 24 hours at 37°C with continuous rotation at 220 revolutions per minute (rpm). Aβ aggregation states were assessed using a thioflavin T (ThT) assay (see figure 2.1) and sodium dodecyl sulphate (SDS) gel electrophoresis followed by silver nitrate staining. ThT is a benzothiazole dye that fluoresces strongly upon binding to the cross β-sheet quaternary structure of amyloid fibrils (Abs/Em=440/490nm). Stock solutions were frozen at -20°C and diluted to a working concentration in pre-warmed cDMEM prior to use.

HiLyte Fluor™ 488-labeled $A\beta_{1-42}$: Lyophilised peptide (0.1mg) was dissolved in ammonium hydroxide (NH_4OH; 1%) and diluted to a 0.25µg/ml stock solution using 1X PBS. In order to prepare a more aggregated species, stock solutions were incubated for 24 hours at 37°C with continuous rotation at 220rpm. Stock solutions

were frozen at -20°C and diluted to a working concentration in pre-warmed cDMEM prior to use.

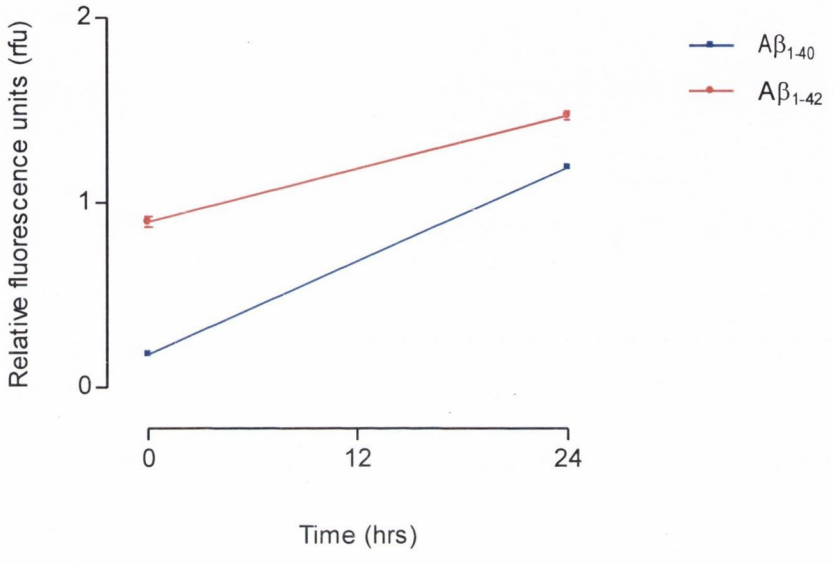

Figure 2.1 Representative ThT graph.

An increase in ThT fluorescence occurs following incubation of $A\beta_{1-40}$ and $A\beta_{1-42}$ at 37°C with continuous rotation for 24 hours.

Wedelolactone: A stock solution (100mM) was prepared by reconstituting Wedelolactone (1mg; FW 314.3g/mol) in DMSO. Stock solution was frozen at -20°C and diluted to a working concentration (25μM) in pre-warmed cDMEM prior to use. Vehicle control was prepared containing DMSO as appropriate.

Neutralising antibodies (see table 2.1) and IgG controls: All antibodies were diluted to a working concentration (2.5μg/ml) in pre-warmed cDMEM prior to use and added to cells in the presence of aggregated Aβ for 24 hours.

Antibody	Company
CD36 Antibody Rabbit Polyclonal IgG	Santa Cruz Cat # sc9154
CD47 Antibody Mouse Monoclonal IgG	Santa Cruz Cat # sc70716
TLR2 Antibody Mouse Monoclonal IgG	Hycult Biotech Cat # HM1054
RAGE Antibody Goat Polyclonal IgG	R&D Systems Cat # AF1616

Table 2.1 Neutralising antibodies.

2.1.3 Preparation of primary mixed glial cultures.

Primary mixed glial cell cultures were prepared from the brains of 1-3 day old male neonatal Wistar rats. An incision was made along the midline of the scalp with a small sterile scissors and the skin was peeled back to reveal the skull. A cut was made along each side of the skull cap at the level of the ears and it was removed using a curved forceps. A straight forceps was used to discard the meninges along with any adherent blood vessels and cortical tissue was pinched out from both hemispheres of 3 rat pups and pooled in a few drops of pre-warmed cDMEM. Tissue was finely cross-chopped using a sterile scalpel, transferred to a sterile falcon tube containing warmed cDMEM (6ml) and placed in an incubator for 20 minutes. Subsequently, tissue was gently triturated using a sterile Pasteur pipette until all visible clumps were removed. The cell suspension was passed through a nylon cell strainer (40µm) into a sterile falcon tube and centrifuged at 850 x *g* for 3 minutes at 20°C. Supernatant was discarded and the cell pellet re-suspended in cDMEM (1ml) using a Pasteur pipette. At this stage, cells were counted using the trypan blue exclusion method (as described in section 2.1.7). Cells were split over 6-well plates at a density of $5x10^5$ cells/ml. Plates were placed in an incubator and the cells were left to adhere for a minimum of 2 hours, at which point each well was flooded with cDMEM (1.5ml). Cells were maintained at 37°C in a 5% CO_2 humidified atmosphere

and culture media was replaced every 3-4 days. Cells were treated when confluent and periodically stained for CD11b and GFAP in order to assess purity (as described in section 2.4.1).

2.1.4 Preparation of enriched microglial cultures

Enriched primary microglial cultures (see figure 2.2A) were prepared as described in 2.1.3 above with the following adaptations. Cells were initially seeded onto T25cm^2 tissue culture flasks and 24 hours later media was replaced with cDMEM containing M-CSF (20ng/ml) and GM-CSF (10ng/ml). On day 7, the necks of the flasks were wrapped in parafilm, placed on an orbital shaker and agitated at ~130rpm until microglia were dissociated into solution. Flasks were tapped to detach any remaining adherent microglia and the supernatant centrifuged at 850 x *g* for 5 minutes. The pellet was resuspended in cDMEM, a cell count was carried out and microglia were plated onto 6-well plates at a density of 5x10^5 cells/ml. Plates were placed in an incubator and the cells were left to adhere for a minimum of 2 hours, at which point each well was flooded with cDMEM (1.5ml). Microglia were maintained at 37°C in a 5% CO_2 humidified atmosphere for 2 days prior to treatment.

2.1.5 Preparation of enriched astrocytic cultures

Enriched cultures of primary astrocytes (see figure 2.2B) were prepared as described in section 2.1.3 above with the following adaptations. On day 10-12, the necks of the flasks were wrapped in parafilm and placed on an orbital shaker at ~200rpm until microglia were dissociated into solution. Flasks were tapped vigorously to detach any remaining adherent microglia. The supernatant was removed, discarded and replaced with trypsin-ethylenediaminetetraacetic acid solution (EDTA; 2ml). Flasks were placed in the incubator for 5 minutes or until cells were sufficiently loosened at which point cDMEM was added to terminate the action of trypsin-EDTA. Cells were centrifuged at 850 x *g* for 3 minutes, counted and plated onto 6-well plates at a

density of $5x10^5$ cells/ml. Plates were placed in an incubator and the cells were left to adhere for a minimum of 2 hours, at which point each well was flooded with a further 1.5ml cDMEM. Astrocytes were maintained at 37°C in a 5% CO_2 humidified atmosphere for 2 days prior to treatment.

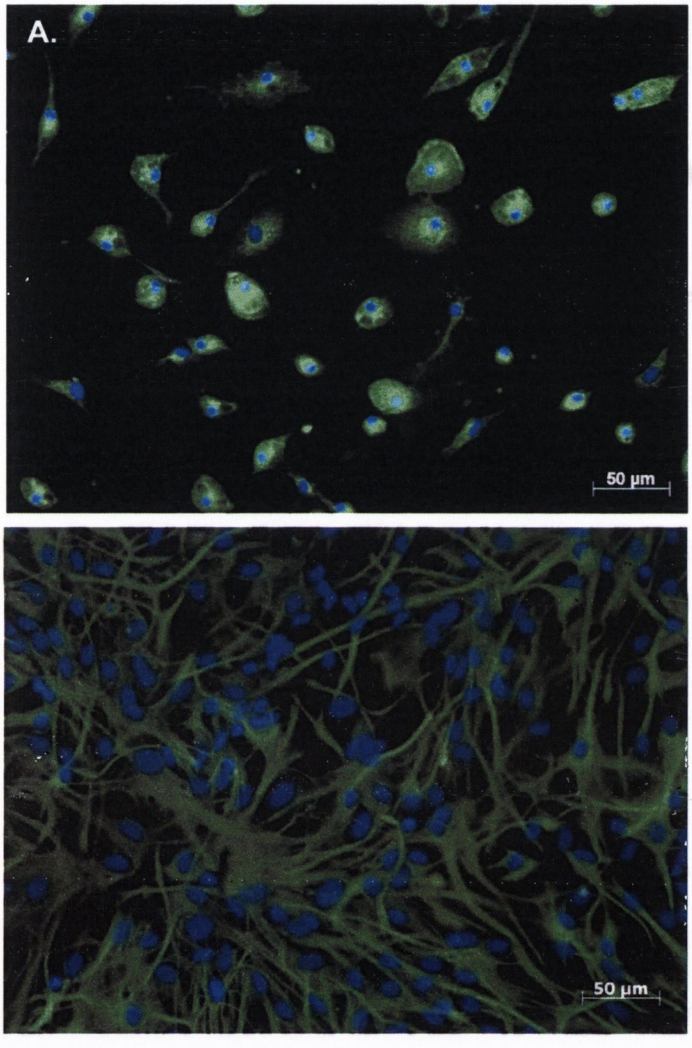

Figure 2.2 Confocal images demonstrating the purity of microglial and astrocytic cultures.

CD11b (A; green) and glial fibrillary acidic protein (B; green) immunocytochemistry was used to demonstrate the purity of enriched microglial and astrocytic cultures. Nuclei were counterstained using 4'-6-diamidino-2-phenylindole (DAPI).

2.1.6 Preparation of coverslips for immunocytochemistry

Glass coverslips for cell culture were first sterilised with 70% EtOH for 30 minutes and left under the UV light for an additional 30 minutes. Poly-$_D$-lysine (25mg) was reconstituted in autoclaved dH_2O and thoroughly vortexed to yield a stock solution of 1mg/ml which was sterilised using a syringe filter (0.2µm), aliquoted and frozen at -20°C. Prior to use, poly-$_D$-lysine was diluted to a final concentration of 40µg/ml using autoclaved dH_2O. Coverslips were immersed in poly-$_D$-lysine at 37°C for 30 minutes, washed twice with autoclaved dH_2O and left to fully dry prior to use. When dry, 1 coverslip was added to each well of a 24-well plate for immunocytochemistry.

2.1.7 Cell counting

Cells were resuspended in a known volume of media and viable cells counted using the trypan blue exclusion method. Live cells possessing intact cellular membranes have the ability to exclude trypan blue dye whereas dead cells do not. Cell suspension was diluted in trypan blue (1:10) and a plastic haemocytometer used to count the cells under a light microscope. The number of cells/ml was determined using the formula: cell count x dilution factor x 10^4.

2.2 Cell viability assays

2.2.1 Lactate dehydrogenase CytoTox 96® assay

Lactate dehydrogenase (LDH), which catalyses the interconversion of pyruvate and lactate, is a stable cytosolic enzyme that is released upon cell lysis. Release of LDH into supernatants is assessed by evaluating the conversion of a tetrazolium salt (INT) to a red formazan product; the colour produced is proportional to the number of lysed cells.

The LDH CytoTox 96® assay was carried out as per manufacturer's instructions. Prior to collecting cell supernatants, appropriate wells were incubated with lysis buffer in cDMEM (1:10) for 1 hour. Assay buffer (12ml) was used to reconstitute a bottle of substrate mix. Aliquots of supernatants (50µl) were transferred in duplicate to a 96-well flat-bottomed plate. The following controls were set up (1) wells containing cDMEM only (2) wells containing supernatant from cells incubated with lysis buffer for 1 hour (3) lysis buffer in cDMEM and (4) a LDH positive control in 1X PBS (1:5000). Reconstituted substrate mix (50µl) was added to each well and the plate was incubated in the dark at room temperature for 30 minutes. Stop solution (50µl) was added to each well and absorbance was read at 490nm using a BioTek EI_x800 Microtitre Plate Reader. Experimental LDH release was calculated using the following equation:

$$\% \text{ Cytotoxicity} = \frac{\text{Experimental LDH release } (OD_{490})}{\text{Maximum LDH release } (OD_{490})} \times 100$$

2.2.2 Alamar blue cell viability assay

A stock solution of alamar blue (440µM) was prepared by dissolving resazurin (25mg; FW 251.17g/mol) in dH_2O and stored in a dark bottle for future use. The alamar blue assay is based upon the ability of viable cells to reduce resazurin to resorufin with the amount of fluorescence produced being proportional to the number of living cells. Damaged and non-viable cells have lower innate metabolic activity and thus generate a proportionally lower signal when compared with healthy cells.

The dye was added to the cells at a 1:10 dilution in cDMEM. In addition, resazurin was added to a set of wells that contained cDMEM only and to cells that had been

treated with lysis buffer for 1 hour (see LDH assay protocol). Plates were incubated at 37°C until a colour change was observed i.e. pink in non-treated cells and dark blue in lysed cells. Once this change was observed, aliquots of supernatant (100µl) from each well were transferred in duplicate to a fresh 96-well flat-bottomed plate. Absorbance was read at 595nm using a BioTek El_x800 Microtitre Plate Reader and percentage cell viability was calculated using the following equation:

$$\% \text{ Cell viability} = ((A_m - A_s)/(A_m - A_c)) \times 100$$

where A_m = Average absorbance of wells containing cDMEM only

A_m = Average absorbance of wells containing cells without treatments

A_s = Absorbance of a particular sample

2.3 Opsonised zymosan assay

This assay was used to compare the oxidative burst that occurs following phagocytosis in primary rat microglia and astrocytes, using rat peripheral blood mononuclear cells (PBMCs) as a positive control (see section 2.12.2 for isolation procedure). Zymosan, a protein present in the unicellular yeast *Sachromyces cervisae*, is opsonised by complement and immunoglobulins (IgG) in plasma in order to facilitate its phagocytosis. The assay is based on luminol-dependent chemiluminescence that results from reactive oxygen species (ROS) released during the oxidative burst that follows phagocytosis.

In order to opsonise zymosan, serum was obtained from whole rat blood by centrifugation at 3400 x *g* at 4°C for 15 minutes. Zymosan was diluted in 1X Hank's balanced salt solution (HBSS; 1mg/ml) and incubated with serum at a ratio of 3 parts zymosan: 1 part serum for 30 minutes at 37°C. Samples were centrifuged at 500 x *g*

for 10 minutes and the opsonised zymosan pellet was washed, centrifuged again and resuspended in 1X HBSS (1ml).

Luminol (1mM) was prepared by dissolving 5-amino-2,3-dihydro-1,4-phthalazinedione in sodium hydroxide (NaOH; 0.1M). Opsonised zymosan (50µl) was added to each well of a black 96-well microplate containing microglia, astrocyte or PBMC suspension (50µl) in 1X HBSS ($3x10^6$ cells/ml) and luminol solution (1mM; 50µl). Chemiluminescence measurements were taken with appropriate controls using a BioTek Synergy HT Multi-Mode Microplate Reader. Readings were carried out at 2 minute intervals with a total run time of 44 minutes.

2.4 Immunocytochemistry

2.4.1 CD11b and GFAP immunocytochemistry

Fluorescent immunocytochemistry was routinely carried out on mixed glial cells and isolated microglia/astrocytes grown on glass coverslips in order to assess purity (see figure 2.2) and to visualise the uptake of fluorescent latex beads (1µm diameter) and HiLyte Fluor™ 488-labeled $A\beta_{1-42}$. Cells were fixed using ice-cold methanol for 5 minutes at -20°C and washed 3 times (1X PBS containing 0.02% Triton X-100). Cells were blocked at room temperature for 2 hours (10% normal goat serum in wash buffer) and incubated with primary antibody (see table 2.2; in 5% goat serum in wash buffer) overnight at 4°C. Negative controls were performed by replacing the primary antibody with wash buffer.

Following overnight incubation, coverslips were washed 3 times with wash buffer and incubated in the dark for 2 hours with secondary antibody (in 5% goat serum in wash buffer). Cells were washed 3 times, mounted onto glass slides using Vectashield

mounting medium with DAPI, sealed with nail polish and stored at 4°C for fluorescent microscopy.

	Antibody	Company	Dilution
Primary	Mouse anti-rat CD11b	Serotec Cat # MCA2759	1:200
	Rabbit anti-GFAP	Dako Cat # Z0334	1:2000
Secondary	Alexa Fluor 633 goat anti-mouse	Invitrogen Cat# A21050	1:4000
	Alexa Fluor 633 goat anti-rabbit	Invitrogen Cat # A21070	1:4000

Table 2.2 Antibodies used for immunocytochemistry.

2.4.2 Confocal microscopy

Images were acquired using a LSM 510 Confocal Laser Scanning Microscope and visualised using LSM Image Browser Rel. 4.2. All images were obtained using a 40x objective lens with immersion oil and default configurations: 512 x 512, 8-bit data depth, bidirectional scanning and linear mode. Z-stacking was used to obtain images of planes at various depths in order to confirm that fluorescently-labelled latex beads or $A\beta_{1-42}$ had been phagocytosed by the cells of interest.

2.5 *In vivo* studies

2.5.1 Groups and maintenance of animals

Animals were maintained under constant veterinary supervision in a specific pathogen-free environment at the Bioresources Unit of Trinity College Dublin, housed in groups of 2 or 3 per cage, at 22-23°C with a 12-hour light-dark cycle. All animals used in these studies had free access to food and water and were fed a standard laboratory diet. Experiments were carried out under licence obtained from the Department of Health and Children (Ireland) under the Cruelty to Animals Act 1876, the European Community Directive, 86/609/EEC, and in agreement with experimental procedures laid down by the local ethics committee. Every effort was made to minimise stress to the animals at all stages of studies undertaken.

2.5.2 Chronic Aβ infusion study

Male Wistar rats aged 3–4 months were used in these studies. Sterile technique was employed during filling and handling of pumps as well as throughout the surgical implantation procedure. Rats were randomly divided into 2 groups (n=8), half of which received intracerebroventricular infusion of a cocktail of aggregated $A\beta_{1-40}$ (26.9μM) and $A\beta_{1-42}$ (36.9μM; Miller *et al.*, 2008), while the other half received artificial cerebrospinal fluid (aCSF; see Appendix).

ALZET mini-osmotic pumps (model 2004) were primed at 37°C in saline (0.9%) prior to use and loaded with Aβ cocktail or aCSF (250μl) for a calculated delivery rate of 0.25μl/h (±0.05 μl) for 28 days.

Prior to pump implantation, animals were placed in an induction chamber and anaesthesia was induced with 5% isofluorane in 100% oxygen at a delivery rate of 1 litre/minute. Respiration rates were closely monitored until deep anaesthesia was

confirmed by loss of the pedal reflex. Once anesthetised, the rat was moved to a stereotaxic frame and the rate of flow of isofluorane was maintained at ~2% in 100% oxygen.

The surgical area was shaved and 2 aseptic washes were carried out using povidone-iodine scrub and solution. Starting slightly behind the eyes, a midline sagittal incision (roughly 2.5cm long) was made with a sterile scalpel to expose the skull. The skin and subcutaneous tissue were clamped with forceps to open the surgical field and, using a bone scraper, the exposed skull was scraped to remove the periosteal connective tissue until bregma and lambda were clearly visible. Remaining tissue was removed from the periosteum using a few drops of hydrogen peroxide (H_2O_2) to improve the visual field.

The location for intracerebroventricular cannula placement was determined and marked using the stereotactic coordinates 0.9 mm posterior to bregma, 1.3 mm lateral to the midline and 4 mm ventral to the dura. A hole was drilled through the skull at the marked location and the cannula attached to the ALZET pump was inserted. The cannula was affixed to the skull using cryanoacetate gel and secured in place using a smooth covering of dental cement. A subcutaneous pocket, in which the mini-osmotic pump was placed, was prepared in the midscapular area behind the neck by opening and closing a hemostat. The pump was inserted into the subcutaneous pocket leaving a generous amount of slack to permit free motion of the animals head and neck.

Following pump implantation, the scalp wound was closed using interrupted sutures. Post-operative care consisted of topical application of lidocaine hydrochloride (4%) and a subcutaneous injection of the analgesic, rimadyl (5 mg/kg). Rats were closely monitored and kept under a heat lamp to prevent hypothermia until fully recovered.

After 28 days, rats were perfused and sacrificed by decapitation. Animals were anaesthetised by injection of urethane (~1g/kg) and a scalpel used to make a median

incision from underneath the chin to below the sternum. The connective tissue beneath was cut away and an incision made in the diaphragm to gain entry to the thoracic cavity. The ribs were removed to expose the heart, and a cannula connected to a perfusion pump was inserted into the left ventricle. The right atrium was pierced using a forceps and ice-cold sterile 1X PBS was peristaltically pumped through the heart into the vascular system. Following perfusion, areas of the cortex and hippocampus were dissected out on a Petri dish containing dry ice for microglial and astrocytic isolation (see section 2.6) or snap frozen in nuclease-free tubes in liquid nitrogen and stored at -80°C for RNA extraction (see section 2.8).

2.5.3 APP/PS1 studies

APP/PS1 mice contain 2 transgenes inserted at a single locus; a chimeric APP and a deltaE9 mutation of human PS1. Genotyping was carried out as described in section 2.5.4.

In the first study, groups of middle-aged (13-14 months; *n*=7-8) and aged (23-24 months; *n*=4-8) WT and APP/PS1 mice were used. The second study consisted of a cohort of slightly older middle-aged animals (17-19 months, *n*=8). For the first study, mice were sacrificed by decapitation whilst under anaesthesia induced by inhalation of isofluorane. For the second study, animals were perfused with ice-cold 1X PBS prior to sacrifice in order to remove any contaminating cells from peripheral blood. Brains were placed on a Petri dish containing dry ice, the cerebellum was removed and cortex and hippocampus were dissected out. Portions of cortex and hippocampus were snap-frozen in liquid nitrogen and stored at -80°C in nuclease-free tubes for mRNA and protein analysis. In the first study, the remaining brain tissue was used for isolation of microglia and astrocytes as described in section 2.6.2, while in the second study all mononuclear cells were isolated as described in section 2.6.3.

2.5.4 Genotyping

Tail snips (0.5 cm) were collected from all animals following sacrifice and stored at -80°C for DNA isolation using a Qiagen DNeasy kit as per manufacturer's instructions.

Tail snips were placed into nuclease-free tubes and ATL buffer (180µl; supplied in Qiagen DNeasy kit) was added followed by proteinase K (20µl). Tubes were vortexed well and incubated at 56°C overnight until tissue was completely lysed. AL buffer (200µl) was then added followed by ethanol (200µl; 96 – 100%), samples were transferred to DNeasy Mini spin columns in collection tubes and centrifuged at 6,000 x *g* for 1 minute. Columns were placed in new collection tubes, AW1 (500µl) buffer was added and the centrifugation step was repeated. Columns were removed and placed in new collection tubes, AW2 (500µl) buffer was added and centrifuged at 20,000 x *g* for 3 minutes. DNeasy Mini columns were placed in nuclease-free tubes and AE buffer (100µl) was pipetted onto the membrane and incubated for 1 minute at room temperature. This was followed by centrifugation for 1 minute at 6,000 x *g* to elute DNA which was assessed for yield using a NanoDrop® ND1000 spectrophotometer (as described in section 2.8.4).

The presence of APPswe and PS1dE9 transgene products in wild-type and APP/PS1 mice was assessed using polymerase chain reaction (PCR) and visualised by running products on agarose gels. Primers (as described in table 2.2) were reconstituted using nuclease-free H_2O to yield stock solutions of 125pmol/µl.

APPswe and PS1dE9 PCR reactions (in 25µl volumes) were set up separately using DNA (10.5µl; ~5ng), forward and reverse primer for the transgene of interest (1µl each; 0.5µM) and GoTaq® Green Master Mix (12.5µl) in order to enable efficient amplification of DNA templates. Positive control reactions (prion) were prepared to indicate whether DNA was suitable for use. PCR cycling parameters consisted of 5 stages (as described in table 2.4).

Primer	Sequence	Product
Prion forward	5'-CTAGGCCACAGAATTGAAAGATCT-3'	
Prion reverse	5'-GTAGGTGGAAATTCTAGCATCATCC-3'	324bp product
APPswe forward	5'-AGGACTGACCACTCGACCAG-3'	
APPswe reverse	5'-CGGGGGTCTAGTTCTGCAT-3'	377bp product
PS1dE9 forward	5'-AATAGAGAACGGCAGGAGCA-3'	
PS1dE9 reverse	5'-GCCATGAGGGCACTAATCAT-3'	608bp product

Table 2.3 Primers used for DNA amplification.

Step	Temperature	Duration	Note
Step 1	94°C	3 minutes	
Step 2	94°C	30 seconds	
Step 3	54°C	1 minute	
Step 4	72°C	1 minute	*Steps 2-4 were repeated for 35 cycles*
Step 5	72°C	2 minutes	

Table 2.4 PCR cycling parameters for DNA amplification.

Equal volumes of PCR product from each sample (10µl) and a 100 pair base ladder (6µl) were loaded onto agarose gels (1.5% w/v) made up in Tris/Borate/EDTA buffer containing GelRed™ (1:10,000 dilution) in order to visualise products. Gels were run at 100V for 45 minutes and visualised under UV light (see figure 2.3).

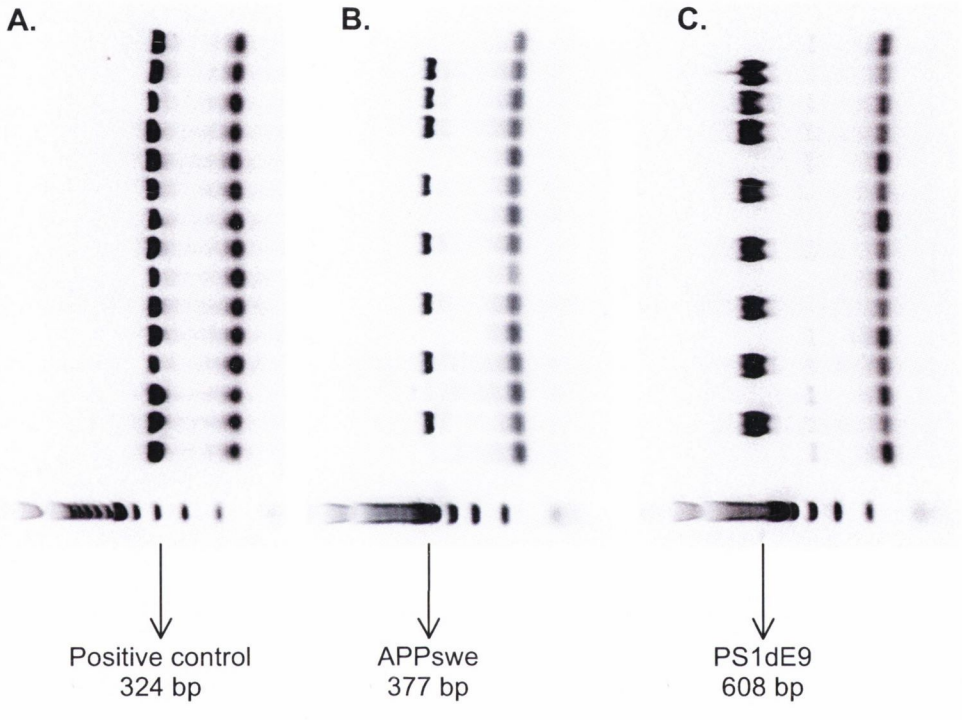

Figure 2.3 Representative gels from APP/PS1 genotyping.

Prion products were present at 324 bp in all samples (A), indicating DNA was suitable for PCR. APPswe (B) and PS1dE9 (C) products were present at 377 bp and 608 bp respectively in APPswe/PS1dE9 mice whilst being absent in WT mice.

2.6 *Ex vivo* cell isolation

2.6.1 Microglia

Prior to the separation procedure, a stock isotonic Percoll (SIP) solution was prepared by mixing 9 volumes of Percoll with 1 volume of 10X PBS. Two ice-cold Percoll gradients of 75% and 25% were prepared from SIP using 1X PBS.

Following sacrifice, brains were immediately placed in medium A (see Appendix). Tissue was cross-chopped using a sterile scalpel and placed in a hand-held homogeniser where it was mechanically dissociated. The suspension was triturated using fire-polished Pasteur pipettes with 3 decreasing diameters and flushed onto a filter (70μM) where the flow-through was collected and brought to 25ml with medium A. Cells were pelleted by centrifugation at 200 x *g* for 10 minutes at 4°C with the brakes turned off. The resultant pellet was re-suspended in 75% Percoll (10ml) and overlaid with 25% Percoll (10ml) and 1X PBS (6ml). The gradient was centrifuged at 800 x *g* for 30 minutes at 4°C with the brakes turned off. Following centrifugation, a thick myelin-containing layer collected at the 0-25% Percoll interface and an enriched microglial population at the 25-75% interface (see figure 2.4). Cells were gently removed using a Pasteur pipette and washed in 3 volumes of Roswell Park Memorial Institute media-1640 (RPMI) for the phagocytic assay (section 2.7.1) or FACS buffer (see Appendix) for cell surface immunofluorescence analysis by flow cytometry. The purity of isolated $CD11b^+$ microglia was assessed using flow cytometry as described in section 2.7.2.

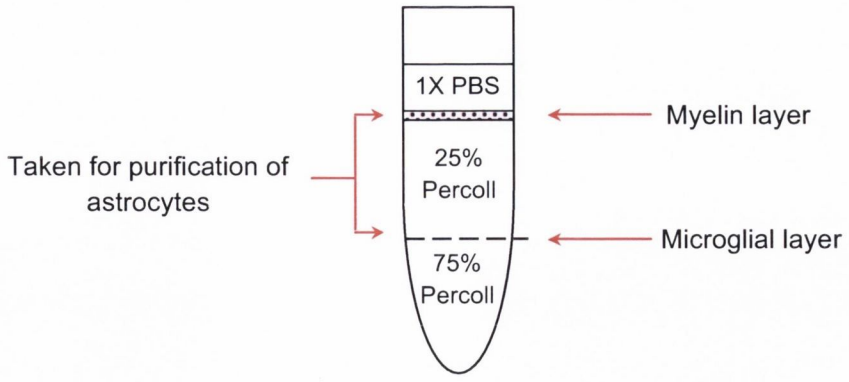

Figure 2.4 Percoll gradient, following centrifugation, for the isolation of glial cells from brain tissue

A 3-layer Percoll gradient was set up as illustrated above and centrifuged at 800 x *g* for 30 minutes. An enriched microglial population was present at the at the 25-75% interface while the layers above were taken for further processing to result in a population of enriched astrocytes.

2.6.2 Astrocytes

To obtain an enriched *ex vivo* astrocyte population, the myelin layer down to the 25-75% interface (as shown in figure 2.4) was removed using a Pasteur pipette and washed with medium A. The resultant pellet was re-suspended in OptiPrep™ so that the final iodixanol concentration was 9%. This was centrifuged at 800 x *g* for 30 minutes, the myelin discarded and the cell containing fraction washed in 3 volumes of RPMI for the phagocytic assay or FACS buffer for cell surface immunofluorescence analysis. The purity of isolated $GLAST^+$ astrocytes was assessed using flow cytometry as described in section 2.7.2.

2.6.3 Mononuclear cell isolation

A slightly modified version of the protocol described in section 2.6.1 was used to isolate all mononuclear cells from the brain. Briefly, the brain was isolated to a 6-well plate containing ~2ml RPMI, homogenised using a hand-held homogeniser, dissociated through a cell strainer (70μM) into a falcon tube and centrifuged for 7 minutes at 300 x *g*. The pellet was re-suspend in 1X PBS (10ml) and centrifuged again for 7 minutes at 300 x *g*. The pellet was re-suspend in 70% Percoll (9ml), underlaid with SIP (5ml), and overlaid with 57% Percoll (9ml), 21.5% Percoll (9ml) and 1X PBS (9ml). The gradient was centrifuged at 1250 x *g* for 45 minutes with the brakes off. Cells were removed from the third and fourth interfaces, taking roughly 9ml, washed with 1X PBS and stained as described in section 2.7.

2.7 Flow cytometry

2.7.1 Phagocytic assay

Primary mixed glial cells and *ex vivo* microglia and astrocytes were set up at a density of ~$5x10^5$ cells/ml in DMEM or RPMI in FACS tubes. Cells were incubated with HiLyte Fluor™ 488-labeled Aβ (Abs/Em=503/528nm; 0.15-10μM) or fluorescently-labelled yellow/green latex beads (Abs/Em=470/505nm; 1:200 dilution) for 2 hours as appropriate. Media was replaced with trypan blue (0.2mg/ml) and samples were incubated for 2 minutes to quench extracellular fluorescence. Cells were washed 3 times with FACS buffer, centrifuged at 350 x *g* for 5 minutes and resuspended in the appropriate blocking solution (see table 2.5). Following this, cells were centrifuged at 350 x *g* for 5 minutes and resuspended in FACS buffer with the appropriate antibodies for 30 minutes (see table 2.6 for mouse and rat antibodies and table 2.10 for human antibodies). Cells were washed and re-suspended in FACS buffer 3 times. After the final wash, cells were re-suspended in FACS buffer (300μl)

and immunofluorescence was immediately read on a DAKO CyAn-ADP 7 colour flow cytometer with Summit software v4.3 for acquisition. Further flow cytometric analysis was carried out in FlowJo v7.6.5.

	Block	Duration
Mouse	Rat Anti-Mouse CD16/CD32 (Mouse BD Fc Block™ Cat# 553141)	5 minutes
Rat	50% FBS in FACS buffer	30 minutes
Human	1mg/ml human IgG from serum	20 minutes

Table 2.5 Blocking solutions used for mouse, rat and human cells.

Unstained cells and fluorescence minus one (FMO) tubes were used to gate the percentage of positive cells in any channel. Compensation beads were used to optimise fluorescence settings for multicolour flow cytometric analyses. These beads consist of two polystyrene microparticle populations, one which binds any κ light chain-bearing IgG and one lacking any binding capacity. When mixed together with a fluorochrome-conjugated antibody, the compensation beads provide distinct positive and negative populations used to manually set compensation levels.

In the case of microglial and astrocytic analysis, phagocytic cells were represented as the percentage of $CD11b^+$, $CD11b^-$ or $GLAST^+$ cells positive in the fluorescein isothiocyanate (FITC) channel. In the case of human PBMC analysis, phagocytic monocytes/macrophages were represented as the percentage of $CD11b^+CD45^+$ cells positive in the FITC channel.

2.7.2 Cell surface staining

For analysis of cell surface immunofluorescence by flow cytometry, cells were washed 3 times with FACS buffer, centrifuged at 350 x *g* for 5 minutes and resuspended in the appropriate blocking solution (see table 2.5). Cells were centrifuged at 1200rpm for 5 minutes and resuspended in FACS buffer with appropriate antibodies at room temperature for 30 minutes (see table 2.7 for mouse and rat antibodies and table 2.11 for human antibodies). Following this, cells were washed and re-suspended in FACS buffer 3 times. Cells were finally re-suspended in FACS buffer (300µl) and immunofluorescence was read on a DAKO CyAn-ADP 7 colour flow cytometer with Summit software v4.3 for acquisition. Further flow cytometric analysis was carried out in FlowJo v7.6.5. Unstained cells, FMOs and compensation tubes were set up as appropriate to gate the percentage of positive cells in any channel.

2.7.3 Intracellular staining

In order to identify T cell subsets, a stimulation protocol was used to permit the enhanced detection of intracellular cytokines by flow cytometry. Stimulation of cells with phorbol myristate acetate (PMA) and ionomycin activates them to produce cytokines. When such activation is performed in the presence of brefeldin-A (BFA), intracellular transport of proteins is inhibited, and thus antigens and cytokines produced during activation are retained within the cell. Mononuclear cells isolated as described in section 2.6.3 were incubated with PMA (10ng/ml), ionomycin (1µg/ml) and BFA (5µg/ml) at 37°C for 5 hours. Following this, cells were washed 3 times with 1X PBS, centrifuged at 350 x *g* for 5 minutes, resuspended in Viability Dye eFluor 780 (1:1000; eBioscience Cat # 65-0865), and incubated in the dark at room temperature for 15 minutes. This Viability Dye irreversibly labels dead cells prior to fixation and permeabilsation procedures.

After 15 minutes, cells were washed 3 times with FACS buffer, extracellular antibodies were added at the appropriate dilution (see table 2.7), and incubated at room temperature for 30 minutes. Prior to incubation with intracellular antibodies, cells were fixed and permeabilised by re-suspending them in paraformaldehyde (2% in FACS buffer) for 15 minutes, washing 3 times and re-suspending in saponin (0.5% in FACS buffer). Cells were then washed once more and resuspended in saponin (0.5%; 100µl) with intracellular antibodies at the appropriate dilution. Following this, cells were washed and re-suspended in FACS buffer 3 times. Cells were finally re-suspended in FACS buffer (300µl) and immunofluorescence was read on a DAKO CyAn-ADP 7 colour flow cytometer with Summit software v4.3 for acquisition. Further flow cytometric analysis was carried out in FlowJo v7.6.5.

Antibody	Company	Dilution
Anti-mouse CD11b Alexa Fluor 647	BD Bioscience Cat # 557686	1:100
Anti-mouse CD11b PerCP/Cy5.5	BioLegend Cat # 10227	1:100
Anti-GLAST (ACSA-1) APC	Miltenyi Biotec Cat # 130 095 814	1:200
Anti-mouse IL-4Rα PE	R&D Systems Cat # FAB530F	1:100
Anti-mouse IL-10Rβ PerCP	R&D Systems Cat # FAB53681C	1:100
Anti-mouse IFNγR PE	eBioscience Cat # 12-1191-80	1:100
Anti-mouse CD3 PE-Cy7	BioLegend Cat # 100219	1:100
Anti-mouse CD4 PE-Alexa Fluor 610	Invitrogen Cat # MCD0422	1:100
Anti-mouse CD45 PE-Cy7	BD Bioscience Cat # 552848	1:100
Anti-mouse Ly6G FITC	BioLegend Cat # 127605	1:100
Anti-mouse IFNγ FITC	BD Bioscience Cat # 555441	1:100
Anti-mouse IL-4 PerCP-Cy5.5	BD Bioscience Cat # 560700	1:100
Anti-mouse IL-17A PE	BD Bioscience Cat # 559502	1:100
Anti-Rat CD11b Alexa Fluor 647	Serotec Cat # MCA275A647	1:100
Anti-Rat CD45 PE-Cy7	BD Bioscience Cat # 561588	1:100
Anti-GLAST (ACSA-1) APC	Miltenyi Biotec Cat # 130 095 814	1:200

Table 2.6 Mouse and rat antibodies used for flow cytometry.

2.8 Analysis of mRNA by RT-PCR

2.8.1 Harvesting glial cells for mRNA isolation

Following treatment, supernatants were aspirated and RA1 lysis buffer (350µl containing 1% β-mercaptoethanol; supplied in Total RNA isolation kit) was added directly to each well. Cells were scraped using a cell scraper to remove adherent cells and lysates were transferred to nuclease-free tubes. If RNA isolation did not take place immediately following harvesting, samples were frozen at -80°C for further processing.

2.8.2 Preparation of brain tissue for mRNA isolation

RNA was isolated from snap-frozen cortical and hippocampal tissue. In all cases, samples were thawed on ice and RA1 lysis buffer (350µl containing 1% β-mercaptoethanol) was added to the nuclease-free tubes. A hand-held mechanical homogeniser was rinsed with RNase away before use and samples were homogenised for approximately 30 seconds. Homogeniser tips were rinsed with RNAse free dH_2O between samples to prevent cross-contamination.

2.8.3 RNA isolation

Total RNA was isolated using a Total RNA isolation kit as per manufacturer's instructions. Following preparation (as described in sections 2.8.1 and 2.8.2), lysates were added to NucleoSpin® Filter units and filtered by centrifugation at 11,000 x *g* for 1 minute. EtOH (70%; 350µl) was added to each sample lysate and mixed by pipetting up and down. The lysate was placed in NucleoSpin® RNA II columns and centrifuged at 11,000 x *g* for 30 seconds in order to bind RNA to the silica column.

Following this, the columns were placed in new collecting tubes, membrane desalting buffer (350µl) was added and the tubes were centrifuged at 11,000 x *g* for 1 minute.

Any contaminating DNA was digested with a 1:10 dilution of rDNase in DNase reaction buffer which was pipetted directly onto the centre of the silica column and left to stand at room temperature for 15 minutes. This was followed by washing with RA2 and RA3 buffers to remove any contaminating salts, metabolites or macromolecular cellular components. RA2 buffer (200µl) was added to each column and centrifuged at 11,000 x *g* for 30 seconds. Columns were placed in new collecting tubes and RA3 (600µl) buffer was added to each column and centrifuged at 11,000 x *g* for 30 seconds. The flow-through was discarded and the collecting tube re-used for a second wash, where RA3 buffer (250µl) was added and centrifuged at 11,000 x *g* for 2 minutes. Columns were placed into fresh 1.5ml RNase-free micro-centrifuge tubes and pure RNA was eluted under low ionic strength conditions by adding RNase free H_2O (60µl) and centrifuging at 11,000 x *g* for 1 minute. Eluted RNA was frozen at -80°C for quantification and reverse transcription.

2.8.4 Spectrophotometric quantification of RNA

Total RNA concentrations were measured using a NanoDrop® ND1000 spectrophotometer. Before making a sample measurement, a blank was first taken and stored. Aliquots of each sample (1µl) were pipetted onto the end of the fibre optic cable for measurement. Sample RNA concentrations were given in ng/µl based on absorbance at 260 nm and the selected analysis constant. The ratio of absorbance at 260 and 280 nm was used to assess the purity of RNA. A ratio of ~2.0 is generally indicative of pure RNA. All RNA samples used had an A260:A280 ratio >1.5. RNA was aliquoted in equal volumes and adjusted to a standard concentration with RNase-free H_2O prior to complementary DNA (cDNA) synthesis.

2.8.5 cDNA synthesis

RNA was reverse transcribed into cDNA using a High Capacity cDNA Archive Kit as per manufacturer's instructions. Briefly, master mix was made up with a 1:5 dilution of 10X Reverse Transcription Buffer, 1:12.5 dilution of 25X dNTPs, 1:5 dilution of Random Primers, 1:10 dilution of MultiScribe Reverse Transcriptase and 1:2.381 dilution of RNase free H_2O. For each sample, equalised RNA (20µl) together with an equal volume of 2X master mix was placed into a PCR mini-tube. Samples were placed in a PTC-200 Peltier Thermal Cycler DNA Engine, incubated at 25°C for 10 minutes, 37°C for 2 hours and 85°C for 5 minutes. The resultant cDNA was stored at -20°C for further RT-PCR analysis.

2.8.6 Multi-target (Multiplex) quantitative RT-PCR

Assessment of target genes was performed using TaqMan® Gene Expression Assays, containing specific target primers and a FAM® dyelabelled minor groove binding (MGB) target probe. Primers used for rat and mouse gene expression studies are listed in tables 2.7 and 2.8 respectively.

Briefly, a 1:4 dilution of cDNA was prepared with RNase-free water. An aliquot of this (10µl) was pipetted into a PCR plate, along with target primer (1.25µl), β-actin primer (1.25µl) and TaqMan® Universal PCR Master Mix (12.5µl). Electronic pipettes were used in order to ensure pipetting accuracy. RT-PCR was carried out using an ABI Prism 7300 Sequence Detection System. Samples were assayed in 1 run composed of 3 stages: 50°C for 2 minutes, 95°C for 10 minutes and 40 cycles of 95°C for 15 seconds and 60°C for 1 minute. Target gene expression was calculated relative to β-actin, the endogenous control.

2.8.7 RT-PCR analysis

The Ct method was used to assess gene expression for all real-time PCR analysis. This method assesses the relative gene expression of treated sample groups compared to its endogenous control. In this manner the fold-difference (increase or decrease) can be assessed between groups.

Gene name	TaqMan Gene Expression Assay
Aldehyde dehydrogenase 1	Rn01426187_m1
CD11b (Integrin alpha M)	Rn00709342_m1
CD36	Rn01442639_m1
CD40	Rn01423583_m1
CD47	Rn00569914_m1
CD68	Rn01495634_m1
GFAP	Rn00566603_m1
GLAST (EAAT1, GluT-1)	Rn00570130_m1
GLT-1 (EAAT2, GLT-1)	Rn00568080_m1
Glutamine synthetase	Rn01483107_m1
IFN-γ	Rn01483107_m1
IL-1β	Rn00580432_m1
IL-6	Rn00561420_m1
iNOS (NOS2)	Rn00561646_m1
MHC class II (RT1 class II)	Rn01768597_m1
RAGE (AGER)	Rn00584249_m1
S100β	Rn00566139_m1
SR-B1	Rn00580588_m1
TLR2	Rn02133647_m1
TLR4	Rn00569848_m1
TNFα	Rn99999017_m1

Table 2.7 Rat TaqMan Gene Expression Assay numbers.

Gene name	TaqMan Gene Expression Assay
Arginase-1	Mm00475988_m1
BDNF	Mm04230607_s1
CD11b (Integrin alpha M)	Mm00434455_m1
CD68	Mm03047340_m1
FIZZ-1	Mm00445109_m1
GFAP	Mm01253033_m1
GLAST (EAAT1, GluT-1)	Mm00600697_m1
Glutamine synthetase	Mm00725701_s1
IFNγR-1	Mm00599890_m1
IL-4Rα	Mm01275139_m1
iNOS (NOS2)	Mm00440502_m1
IP-10 (CXCL10)	Mm00445235_m1
Mannose receptor-1	Mm00485148_m1
MCP-1 (CCL2)	Mm00441242_m1
MIP-1α (CCL3)	Mm00441258_m1
NGF	Mm00443039_m1
RANTES (CCL5)	Mm01302428_m1
TLR2	Mm00442346_m1
TLR4	Mm00445273_m1
TNFα	Mm00443258_m1

Table 2.8 Mouse TaqMan Gene Expression Assay numbers.

2.9 Mesoscale multiplex assays

2.9.1 Tissue preparation for Mesoscale

For the Aβ Triplex Assay, hippocampal tissue (~20mg) was homogenised in lysis buffer (100µl; see Appendix) using a hand-held homogeniser. Samples were centrifuged at 21,500 x *g* for 20 minutes at 4°C and supernatants removed in order to assess concentrations of soluble Aβ. A bicinchonic acid (BCA) protein assay (as described in section 2.9.2) was first carried out on the supernatants and they were equalised to 5mg/ml in lysis buffer prior to carrying out further analysis.

To analyse insoluble Aβ, the remaining pellet was digested in guanidine buffer (200µl; see Appendix) for 4 hours at room temperature with gentle agitation. Samples were centrifuged at 16,000 x *g* for 20 minutes at 4°C. A BCA protein assay was carried out on the supernatants. Samples were equalised to 0.5mg/ml in guanidine buffer and a further 1:400 dilution with 1X Tris-wash buffer (supplied with Mesoscale kit) was carried out prior to Mesoscale analysis of concentrations of insoluble Aβ.

For the Pro-Inflammatory 7-Plex Assay, a separate piece of hippocampal tissue (~20mg) was homogenised in 1% Triton-X in 1X PBS (100µl) using a hand-held homogeniser. Samples were centrifuged at 21,500 x *g* for 20 minutes at 4°C. A BCA protein assay was carried out on the supernatant and samples were equalised to 2mg/ml in 1% Triton-X in 1X PBS prior to further analysis.

2.9.2 BCA protein assay

Protein concentrations were determined using a BCA protein assay kit as per manufacturer's instructions. Samples were diluted in dH_2O (1:20) prior to assessing protein concentrations. A working solution of BSA (2mg/ml) was prepared in the

appropriate buffer and a series of dilutions were carried out to give standards with final BSA concentrations ranging from 0 – 2mg/ml. Samples and standards (25µl) were added in duplicate to wells of a 96-well plate. BCA working reagent (200µl; 50:1 Reagent A:B, supplied with kit) was added to each well, plates were covered, incubated for 30 minutes at 37°C and absorbance read at 595nm using a BioTek El_x800 Microtitre Plate Reader. Protein concentrations were corrected for the dilution factor calculated relative to the standard curve.

2.9.3 Human/Rodent (4G8) Aβ Triplex Assay

Both soluble and insoluble hippocampal concentrations of $A\beta_{1-38}$, $A\beta_{1-40}$ and $A\beta_{1-42}$ were measured using a MULTI-SPOT® Human/Rodent (4G8) Abeta Triplex Ultra-Sensitive Assay as per manufacturer's instructions. Briefly, blocker A solution (1%; 150µl; supplied with assay) was added to each well of the 96-well plate and incubated at room temperature for 1 hour. The plate was washed 3 times with 1X Tris-wash buffer. Standards for $A\beta_{1-38}$ (0 – 3000pg/ml), $A\beta_{1-40}$ (0 – 10,000pg/ml) and $A\beta_{1-42}$ (0 – 3000pg/ml) were prepared by dissolving the 100X peptides in blocker A (1%) and carrying out 3-fold serial dilutions to generate 7 standards. Detection antibody was prepared by diluting 50X sulfo-tag 4G8 detection antibody (60µl) in 100X blocker G (30µl) and 1% blocker A (2910µl). Detection antibody (25µl) was added to each well and sample or standard (25µl) was dispensed on top of this into relevant wells. The plate was covered and incubated at room temperature for 2 hours with vigorous shaking (300–1000 rpm). Following this, the plate was washed 3 times with 1X Tris-wash buffer and 2X MSD read buffer T (150µl) was added to each well. The plate was read using a Mesoscale Sector Imager and Aβ concentrations were calculated relative to the standard curve (expressed as pg/mg of protein).

2.9.4 Mouse Pro-Inflammatory 7-Plex Kit

Briefly, blocker A solution (1%; 150µl) was added to each well of the 96-well plate and incubated at room temperature for 1 hour. The plate was washed 3 times with 1X Tris-wash buffer. Standards were prepared as per manufacturer's instructions and sample or standard (25µl) was dispensed into separate wells of the MSD plate and incubated overnight at 4°C with vigorous shaking. Following overnight incubation, the plate was washed 3 times with 1X Tris-wash buffer and detection antibody solution (25µl) was added to each well. The plate was sealed and incubated with vigorous shaking for 2 hours at room temperature. The plate was again washed 3 times with 1X Tris-wash buffer and 2X MSD read buffer T (150µl) was added to each well. The plate was read using a Mesoscale Sector Imager and cytokine concentrations were calculated relative to the standard curve (expressed as pg/mg of protein).

2.10 Western Immunoblotting

Following treatment, cells were gently rinsed with 1X PBS, followed by incubation with lysis buffer for 10 minutes. A scraper was used to remove cells from the base of the 6-well plate and samples were centrifuged at 21,500 x *g* for 20 minutes at 4°C. A BCA protein assay was carried out on the supernatants and samples were equalised to 2mg/ml with lysis buffer prior to further analysis. Samples were then diluted with 2X Laemmli sample buffer (see Appendix), heated to 80°C for 2 minutes and separated on polyacrylamide gels (1mm thick) with a monomer concentration of 7.5% or 10% (see Appendix). Sample (20µg total protein) and protein ladder were loaded onto gels and run at 100V for approximately 1.5 hours.

Proteins were transferred to nitrocellulose membrane (0.45µM) and blocked in 5% non-fat dried milk in 1X Tris buffered-saline containing 0.05% Tween (TBS-T; see

Appendix) at room temperature for 2 hours. Primary and peroxidase-conjugated secondary antibodies were made up in 5% non-fat dried milk in TBS-T.

Membranes were incubated overnight at 4°C with primary antibody (see table 2.9), washed for 1 hour with TBS-T, and incubated with the appropriate secondary antibody (see table 2.9) for 2 hours at room temperature. Immunoreactive bands were detected by enhanced chemiluminescence using a Fujifilm LAS-4000 system. Blots were stripped using Re-Blot Plus, re-probed for β-actin and imaged as described above.

	Antibody	Company	Dilution
Primary	Polyclonal anti-GFAP	Abcam Cat # ab7620	1:5000
	Anti-EAAT1 antibody	Abcam Cat # ab416	1:500
	Monoclonal anti-S100β	Sigma Cat # S2532	1:1000
	Monoclonal anti-β-actin	Sigma Cat # A5441	1:5000
Secondary	Goat anti-rabbit IgG	Invitrogen Cat # ALI4401	1:5000
	Goat anti-mouse IgM	Sigma Cat # A8786	1:5000

Table 2.9 Primary and secondary antibodies used for Western immunoblotting.

2.11 Enzyme-linked immunosorbent assay

Concentrations of IL-1β (Rat IL-1β DuoSet, R&D Systems, Cat # DY501), IL-6 (Rat IL-6 ELISA Set, BD Bioscience, Cat # 550319) and TNFα (Rat TNF ELISA Set, BD Bioscience, Cat # 558535) were measured in the supernatant as per manufacturer's instructions. Briefly, a 96-well Nunc F96 MaxiSorp Immuno Plate was coated with an appropriate dilution of capture antibody (100µl) and incubated overnight at 4°C. The capture antibody was aspirated and wells were washed 4 times with wash buffer (0.05% Tween-20 in 1X PBS; 200µl). Any excess wash buffer remaining in the wells was removed by blotting the plate dry on a paper towel. The plate was blocked by adding assay diluent (1% BSA in 1X PBS; 200µl) for 1 hour at room temperature. Wells were washed as before and blotted dry.

A top standard of 2000pg/ml or 4000pg/ml as appropriate was prepared from a stock standard (supplied in kit) and a series of 2-fold serial dilutions were carried out to obtain an 8-point standard curve. Sample or standard (100µl) were added in duplicate to each well and incubated for 2 hours at room temperature. Following this, samples and standards were aspirated and the plate washed as before. Detection antibody (100µl) was added to each well and incubated for 1 hour at room temperature. The plate was washed as before and streptavidin-horseradish peroxidise (100µl) was added to each well and incubated for 30 minutes at room temperature. Following this, the plate was washed a final time and 3,3',5,5'-tetramethylbenzidine substrate solution (TMB; 100µl) was added to each well and incubated for 30 minutes in the dark until colorimetric saturation was reached, at which point the reaction was stopped by adding sulfuric acid (H_2SO_4; 1M; 50µl) to each well and absorbance was read at 450nm using a BioTek EL_x800 Microtitre Plate Reader. A standard curve was constructed by plotting known standards against absorbance values and determining unknown cytokine concentrations against the standard curve (expressed as pg/ml).

2.12 Human study

2.12.1 Background

Adults (35 female, 12 male) with a mean age of 71.5 years (ranging from 65 to 82) were recruited from the older adult participant panel of the Trinity College Institute of Neuroscience. A battery of tests were administered in one session, focusing on memory and executive function. The Mini Mental State Exam (MMSE) was used as a screening measure, the National Adult Reading Test (NART) as a proxy measure of general intellectual status and memory was assessed using three subtests of Wechsler Memory Scale (WMS): Logical Memory I and II, Verbal Paired Associates I and II, Visual Reproduction I and II.

Participants were assigned to low and high performing sub-groups based on their memory performance relative to an estimate of their intelligence. Z-scores were used to relate their performance on the WMS test to their scores on the NART. Participants were defined as low performers (LP) if they scored more than 0.75 standard deviations below their NART-estimated IQ on the WMS. All other participants were classified as high performers (HP). This approach yielded 35 HP subjects (26 female, 9 male) with a mean age of 71.9 (SD = 4.7) and 12 LP subjects (9 female, 3 male) with a mean age of 71.1 (SD = 4.8). No significant difference was observed in MMSE scores between the two groups.

Participants received reimbursement of travel expenses to the maximum value of €20. This study was approved by the Ethics Committee of the School of Psychology at Trinity College Dublin, and all participants provided informed consent. Participants completed a detailed questionnaire about their health and current medications, as well as any relevant health issues in their family prior to assessment. Those with a history of head injury, stroke, epilepsy, neurological conditions, major psychiatric disorder, heart attack or diabetes were excluded from the study. All

neuropsychological assessments were carried out by Ms. Eleonora Greco and Dr. Sabina Brennan under the supervision of Professor Ian Robertson.

2.12.2 PBMC isolation from whole blood

Human PBMCs were isolated from heparinised venous whole blood samples (50ml per donor) immediately after collection by density separation over Lymphoprep™. Blood samples were diluted 1:1 with sterile 1X PBS and 2 volumes of diluted blood were gently layered over 1 volume sterile Lymphoprep™. Gradients were centrifuged at 480 x *g* for 30 minutes with the brakes off. Following centrifugation, mononuclear cells formed a distinct band at the sample/medium interface. Plasma was removed to the level of the interface, aliquoted and stored at -80°C for further analysis. The layer of PBMCs was gently removed using a Pasteur pipette, transferred to a fresh falcon tube and centrifuged at 350 x *g* for 10 minutes. Supernatant was discarded, the pellet re-suspended in 1X PBS and centrifuged for 10 minutes at 350 x *g*. Cells were resuspended in RPMI following isolation and roughly $2x10^6$ cells were taken for analysis of phagocytic activity as described in section 2.7.1 and cell surface immunofluorescence analysis by flow cytometry as described in section 2.7.2. Remaining PBMCs were used for isolation of monocytes to be differentiated into monocyte-derived macrophages (MDMs) as described in section 2.12.4.

2.12.3 Human (4G8) Aβ Triplex Assay

Plamsa concentrations of $A\beta_{1-38}$, $A\beta_{1-40}$ and $A\beta_{1-42}$ were measured as described in section 2.9.3 with the exception that no Blocker G was added to the detection antibody mix.

2.12.4 Preparation and analysis of MDMs

$CD14^+$ monocytes were isolated from PBMCs by Dr. Eric Downer using magnetically-activated cell sorting (MACS) MicroBeads and a MACS separator. The principle of MACS is based on cells being magnetically-labelled with CD14 MACS MicroBeads and separated on a column placed in the magnetic field of a MACS separator. When passed through the column, magnetically labelled $CD14^+$ cells are retained while unlabeled $CD14^-$ cells flowed through. Once the column is removed from the magnetic field, the magnetically retained $CD14^+$ cells are free to be eluted.

PBMCs were re-suspended in MACS buffer (see Appendix) and centrifuged at 350 x *g* for 10 minutes. The pellet was re-suspended in MACS buffer (80μl per $1x10^7$ cells) and CD14 MACS MicroBeads (10μl per $1x10^7$ cells) were added and incubated for 15 minutes at 4°C. Cells were washed in 10 volumes MACS buffer and passed slowly through a MACS LS^+ column. The column was washed 3 times with MACS buffer, removed from the magnet and $CD14^+$ monocytes were eluted in RPMI. This method is reported to result in a population of 85–92% pure $CD14^+$ cells as estimated by flow cytometry (Rowan *et al.*, 2008). Cell counts of $CD14^+$ monocytes isolated from the total PBMC population did not find any significant difference between HP and LP groups, with the percentage of $CD14^+$ monocytes in PBMCs being 20.5 ± 1.0 and 18.48 ± 1.7 respectively (p=0.289, Student's *t*-test for independent means).

Freshly isolated monocytes were allowed to differentiate into MDMs in RPMI supplemented with FBS (10%), penicillin-streptomycin (1%), and GM-CSF (10ng/ml) for 7 days. Equal MDM counts were cultured from both cohorts and CD14 mRNA expression in MDMs was similar in LP and HP subjects following 7 days in culture, indicating no difference in the number of MDMs at the end of the experiment, and that differentiation of monocytes to macrophages was similar in LP and HP groups.

Antibody	Company	Dilution
Anti-human CD11b APC-eFluor 780	eBioscience Cat # 47-0118-42	1:100
Anti-human CD45 PE-Cy7	eBioscience Cat # 25-0459-42	1:100
Anti- human CD119 Alexa Fluor 488	Serotec Cat # MCA1450A488	1:200
Anti-human IL-4Rα PE	R&D Systems Cat # FAB230P	1:400
Anti-human TLR2 Alexa Fluor 488	eBioscience Cat # 53-9024-82	1:100
Anti-human TLR4 PE-Cy7	eBioscience Cat # 25-9917-41	1:100

Table 2.10 Human antibodies used for flow cytometry.

2.12.5 Stimulation of MDMs with lipopolysaccharide (LPS)

In a separate series of experiments, MDMs that had been allowed to differentiate for 7 days were stimulated with LPS (100ng/ml) for 24 hours and harvested for mRNA and cytokine analysis. Supernatants were assesed for the release of IL-1β, IL-12p70, IFN-γ, IL-6, IL-8, IL-10 and TNF-α using a Mesoscale Human Pro-Inflammatory 7-plex Ultrasensitive Kit.

2.12.6 Human Pro-Inflammatory 7-plex Ultrasensitive Kit

This assay was carried out as described in section 2.9.4 with the exception that supernatants and standards (25µl) were incubated for 2 hours at room temperature with vigorous shaking rather than overnight. Cytokine concentrations were calculated from the standard curve and expressed as pg/ml of protein.

2.13 Statistical analysis

All data were analysed using the statistical packages Graph Pad Prism (GraphPad Software, Inc.) or GB-STAT (Dynamic Microsystems, Inc.). Statistical comparisons were performed using a Student's *t*-test for independent means or 1- or 2-way analysis of variance (ANOVA) as indicated in the experimental sections. If significant changes were observed following ANOVA, the data was further analysed using a Newman-Keuls *post hoc* test as appropriate. A p value less than 0.05 was deemed statistically significant. Results are expressed as means + standard error of the mean (SEM).

3: Examining the effect of Aβ on phagocytosis by glial cells *in vitro* & *in vivo*

3.1 Introduction

Phagocytosis, an essential component of the innate immune response, is a complex cellular process involving numerous cytoskeletal elements and signalling cascades acting in concert to process and destroy material that is foreign or perceived as being foreign. Microglia are the resident immunocompetent and phagocytic cells within the CNS, sharing several characteristics with peripheral macrophages, including their ability to phagocytose. These cells continuously extend and retract ramified processes into the surrounding tissue with a radius of about 80μm and thus the entire brain undergoes surveillance by these cells every few hours (Cameron and Landreth, 2010). In comparison to microglia, the role of astrocytes as phagocytic cells within the CNS is less well understood.

Inefficient clearance of Aβ from the brain is thought to contribute to the pathogenesis of AD and thus removing the build-up of this peptide is a major target in ongoing research. Evidence from numerous sources indicates that microglia mediate the clearance of Aβ through receptor-mediated phagocytosis. Uptake of Aβ by microglia and its subsequent targeting to the endosome–lysosomal pathway has been investigated in detail with microglia being shown to actively phagocytose monomeric, oligomeric and fibrillar Aβ (Lee and Landreth, 2010). Various ultra-structural studies have also reported that microglia in the cortex of AD patients contain intra-cytoplasmic fragments of Aβ, thus further strengthening the phagocytic role of microglia in the AD brain (Lewandowska *et al.*, 2004).

Studies indicating the role of astrocytes in clearance of Aβ from the AD brain are far less abundant. Astrocytes plated on brain sections from a mouse model of AD have been shown to associate with Aβ deposits and reduce the presence of Aβ in these sections (Wyss-Coray *et al.*, 2003). In addition, astrocytes from enhanced green fluorescent protein expressing mice transplanted into the hippocampus of APP/PS1 animals were found localised near Aβ deposits, with confocal microscopy further

revealing that they contained internalised Aβ immunoreactive material (Pihlaja *et al.*, 2008).

When a recent study crossed two distinct APP transgenic mouse strains with CD11b-HSVTK mice, where ganciclovir treatment led to the ablation of microglia for up to 4 weeks, it was surprisingly found that neither amyloid plaque maintenance nor formation depended on the presence of microglia (Grathwohl *et al.*, 2009). Interestingly, this lack of effect was accompanied by a temporary concomitant activation of astrocytes suggesting they might have a role to play in the progression of AD.

The aims of these studies were as follows:

1. To validate an assay investigating the phagocytosis of fluorescently-labelled latex beads by microglia and astrocytes *in vitro*.
2. To compare the ability of microglia and astrocytes in phagocytosing fluorescently-labelled latex beads, FITC-labelled Aβ and opsonised zymosan *in vitro*.
3. To assess the effect of Aβ on phagocytosis, markers of activation and expression of putative Aβ receptors in isolated microglia and astrocytes *in vitro*.
4. To evaluate the effect of exogenous Aβ administration on phagocytosis, markers of activation and expression of putative Aβ receptors *in vivo*.

3.2 Methods

Primary cultures of mixed glial cells prepared from neonatal rats were incubated with fluorescently-labelled latex beads or aggregated FITC-labelled $A\beta_{1-42}$ and uptake was assessed using flow cytometry as described in section 2.7.1. CD11b, a well-established integrin marker, was used to identify microglia in these glial cultures. The $CD11b^-$ cell population was found to consist predominantly of astrocytes and thus microglia and astrocytes were identified as $CD11b^+$ and $CD11b^-$ cells respectively. Immunocytochemistry and Z-stack confocal microscopy were carried out using anti-CD11b and anti-GFAP antibodies as described in section 2.4.1.

To investigate the effect of Aβ on microglia and astrocytes *in vitro*, isolated cultures of each cell type were incubated with a cocktail of aggregated $A\beta_{1-40}$ (4.2μM) and $A\beta_{1-42}$ (5.8μM) or reverse peptide $A\beta_{40-1}$ (10μM) for 24 hours (Murphy *et al*, 2011). Phagocytosis was investigated as described above and mRNA and protein analysis assessed using RT-PCR and Western immunoblotting as described in sections 2.8 and 2.10 respectively.

The effect of exogenous Aβ on microglia and astrocytes *in vivo* was investigated by implanting male Wistar rats (3–4 months) with mini-osmotic pumps delivering either a cocktail of aggregated $A\beta_{1-40}$ (26.9μM) and $A\beta_{1-42}$ (36.9μM) or aCSF intracerebroventricularly at a rate of 0.25μl/h (+0.05 μl) for 28 days as described in section 2.5.2 (Miller *et al.*, 2008). Following sacrifice, a portion of the hippocampus was taken for mRNA analysis while the rest of the brain was used to isolate glial cells, as described in section 2.6, in order to examine *ex vivo* phagocytosis by microglia and astrocytes.

3.3 Results

3.3.1 Validation of an assay to assess phagocytosis in mixed glial cells

Following incubation of mixed glial cells with fluorescently-labelled latex beads, they appeared to be present within microglia ($GFAP^-$ cells) and astrocytes ($GFAP^+$ cells) as shown in figure 3.1. To demonstrate that beads were located intracellularly, Z-stack confocal microscopy was carried out to generate a three-dimensional image of both cell types. Isolated cultures of microglia and astrocytes were stained with anti-CD11b and anti-GFAP as shown in figures 3.2 and 3.3. These images confirmed that fluorescently-labelled latex beads were located within microglia and astrocytes respectively.

A 1-way ANOVA followed by *post-hoc* analysis demonstrated that pre-treatment with cytochalasin D, a cell permeable and potent inhibitor of actin polymerisation, decreased uptake of latex beads by $CD11b^+$ and $CD11b^-$ cells ($p<0.01$) as shown in figure 3.4. This reduction in uptake was not due to increased cell death or a reduction in cell viability as shown in figure 3.5. A 1-way ANOVA revealed that staurosporine, used as a positive control, resulted in a significant cell death in both alamar blue and LDH ($p<0.01$) assays.

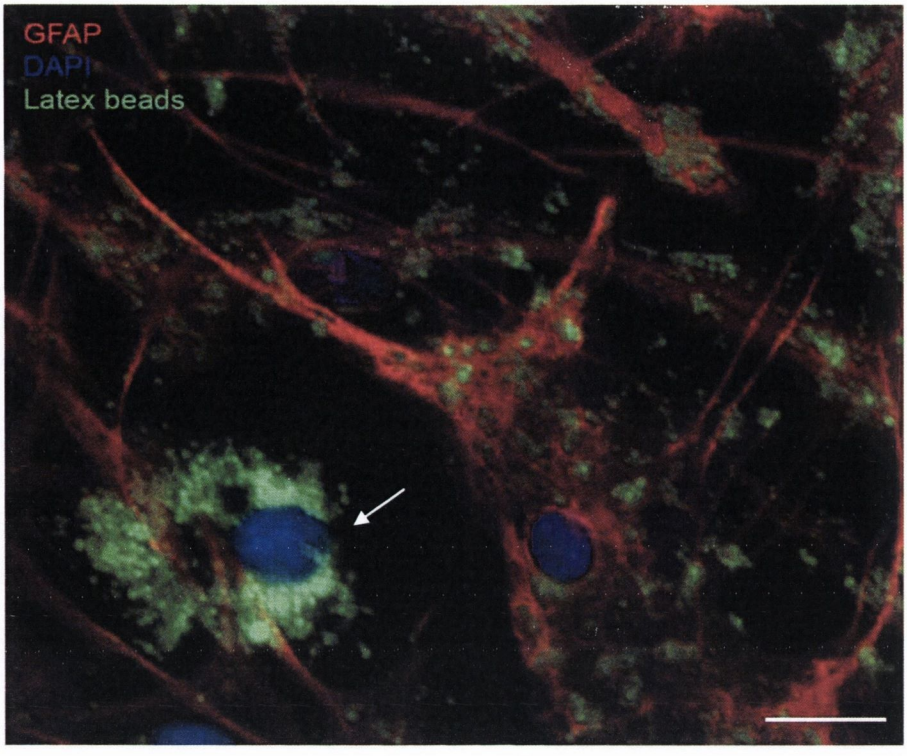

Figure 3.1 Representative micrograph visualising the uptake of fluorescently-labelled latex beads by mixed glial cells *in vitro*.

Primary mixed glial cells were incubated with fluorescently-labelled latex beads (green) for 2 hours and stained with anti-GFAP (red). Nuclei were counterstained using DAPI (blue). The fluorescent micrograph demonstrates cellular localisation of the latex beads. The arrow denotes a probable microglial cell due to its lack of positive GFAP staining. Scale bar at 20μM.

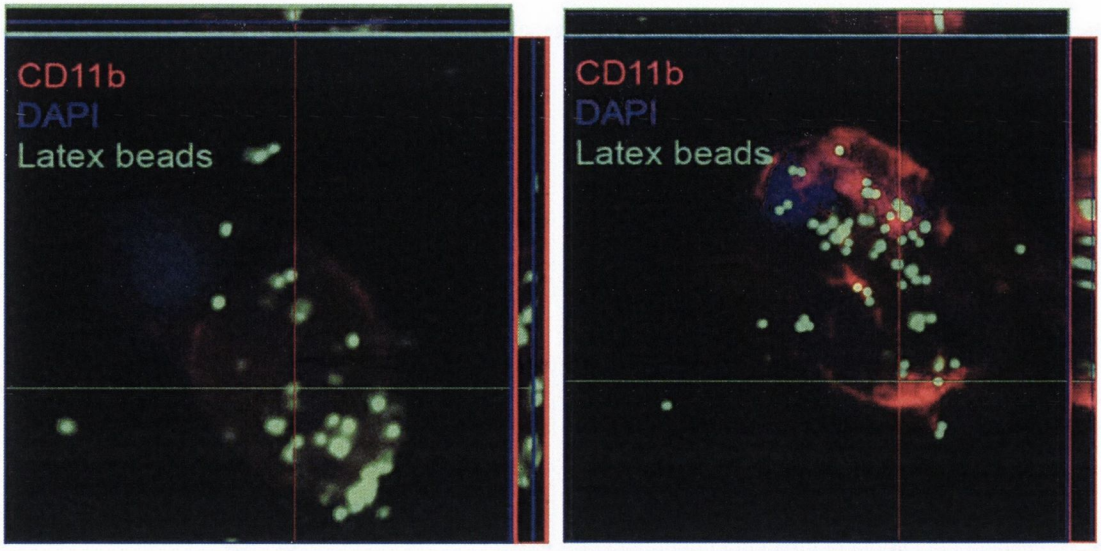

Figure 3.2 Representative micrograph visualising the intracellular localisation of fluorescently-labelled latex beads within CD11b$^+$ microglia.

Representative micrograph of a phagocytosing microglia in orthogonal projections of confocal z-stacks. Isolated microglia were incubated for 2 hours with fluorescently-labelled latex beads (green) and stained with anti-CD11b (red). Nuclei were counterstained using DAPI (blue). The fluorescent micrograph demonstrates intracellular localisation of the latex beads.

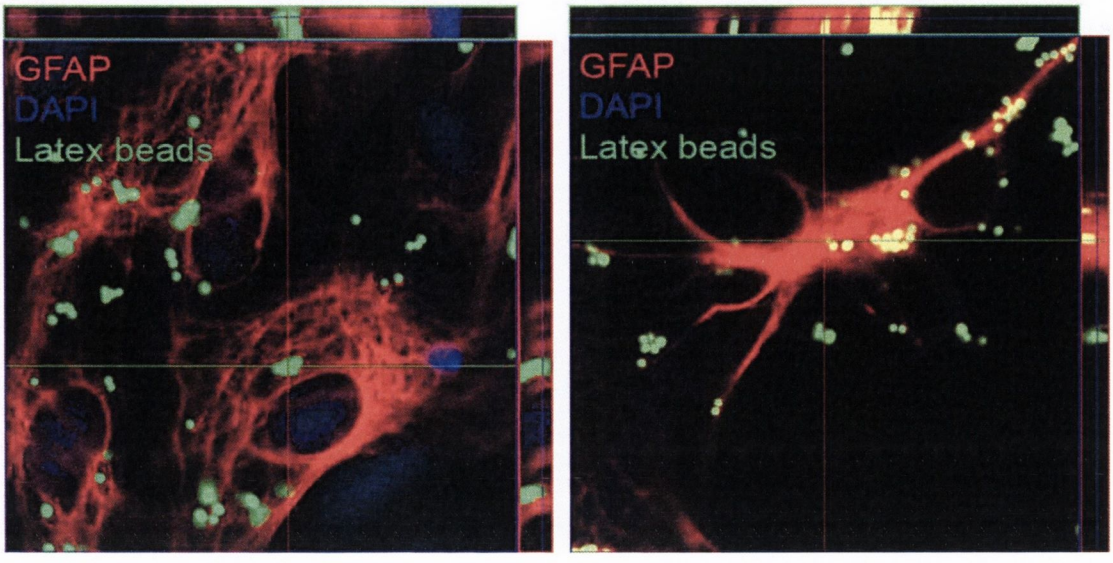

Figure 3.3 Representative micrograph visualising the intracellular localisation of fluorescently-labelled latex beads within GFAP$^+$ astrocytes.

Representative micrograph of a phagocytosing astrocyte in orthogonal projections of confocal z-stacks. Isolated astrocytes were incubated for 2 hours with fluorescently-labelled latex beads (green) and stained with anti-GFAP (red). Nuclei were counterstained using DAPI (blue). The fluorescent micrograph demonstrates intracellular localisation of the latex beads.

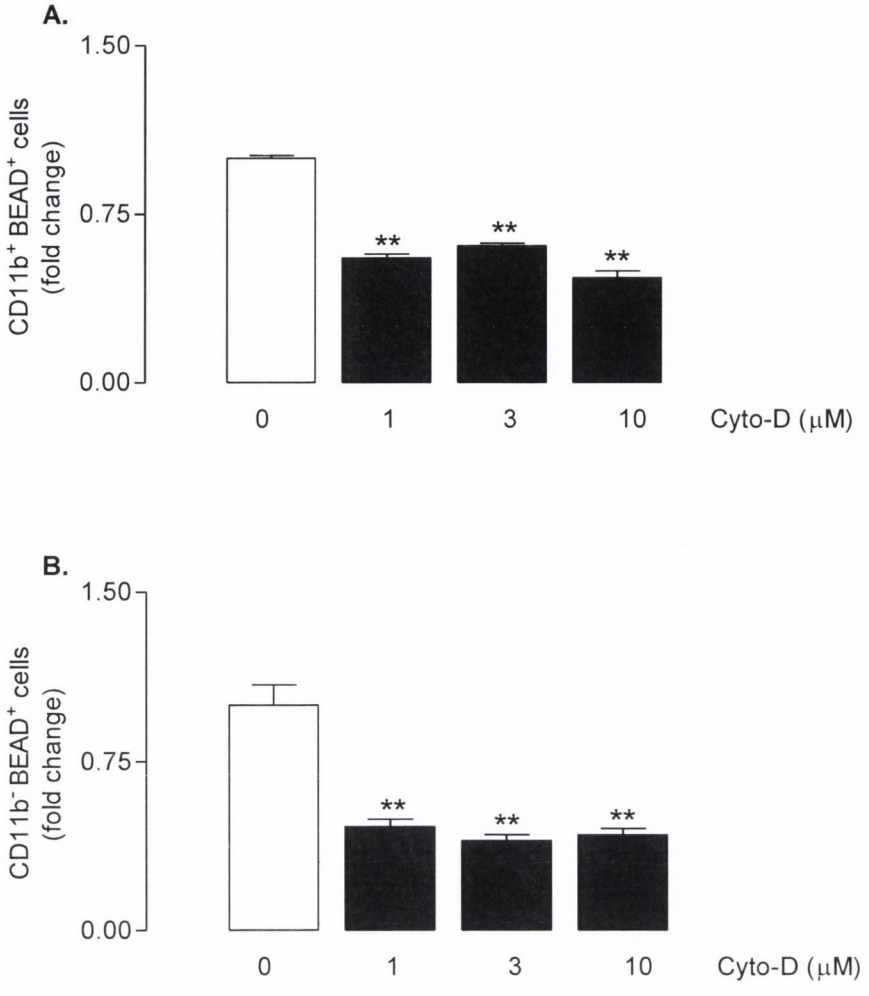

Figure 3.4 Pre-treatment with cytochalasin D inhibited the uptake of fluorescently-labelled latex beads by $CD11b^+$ and $CD11b^-$ cells.

Primary mixed glial cells were pre-treated with cytochalasin D (1, 3 or 10μM) and the phagocytosis of fluorescently-labelled latex beads by $CD11b^+$ (A) and $CD11b^-$ (B) cells was assessed using flow cytometry. The data show that uptake of latex beads by $CD11b^+$ [$F_{(3,12)}$=139.8, p<0.001] and $CD11b^-$ [$F_{(3,12)}$=30.14, p<0.001] cells was significantly decreased following pre-treatment with cytochalasin D. Data are expressed as means + SEM (n=4) from one of three independent experiments with similar results. **p<0.01 versus control (1-way ANOVA followed by Newman-Keuls *post-hoc* analysis).

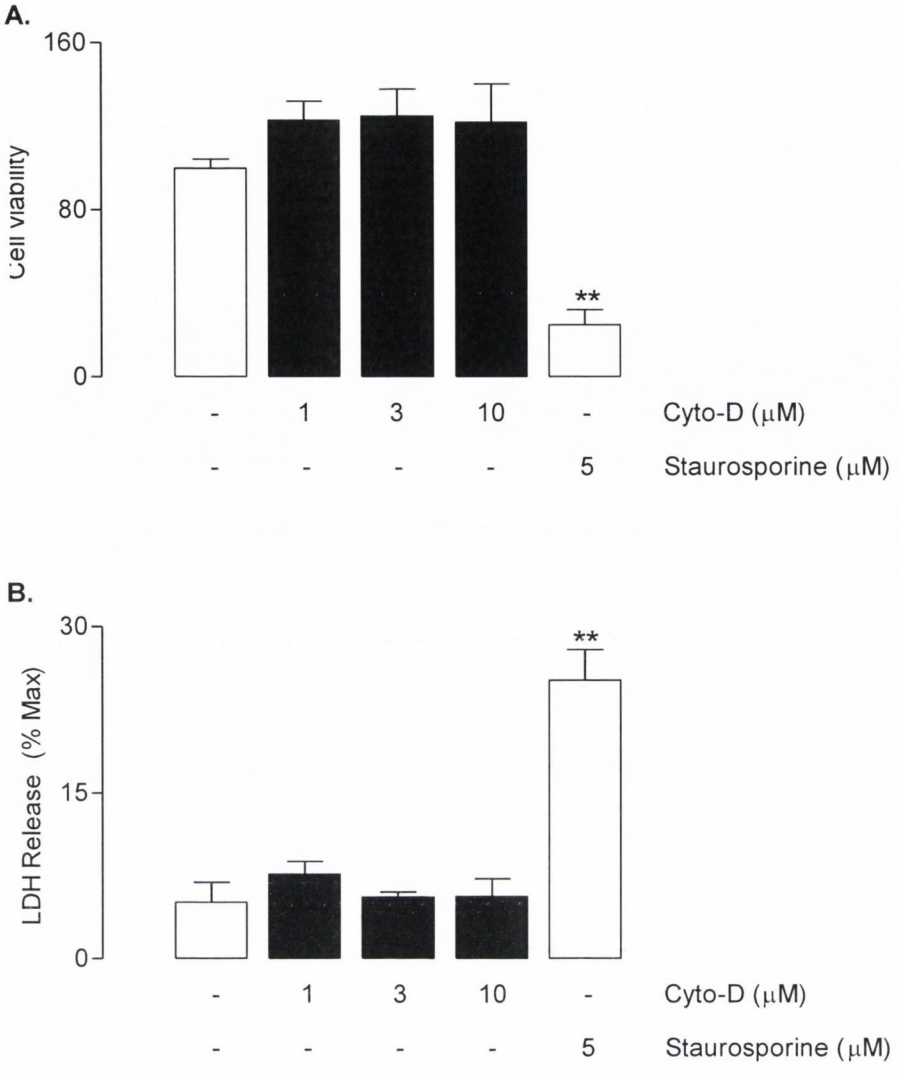

Figure 3.5 Treatment of mixed glial cells with cytochalasin D did not reduce cell viability.

Primary mixed glial cells were treated with cytochalasin D and alamar blue (A) and LDH (B) assays were carried out. The data show that treatment with cytochalasin D had no negative effect on cell viability. Staurosporine (5μM) was used as a positive control and resulted in significant cell death in both alamar blue [$F_{(4,10)}$=13.83, p=0.0004] and LDH [$F_{(4,10)}$=25.82, p<0.001] assays. Data are expressed as means + SEM (n=3). **p<0.01 versus control (1-way ANOVA followed by Newman-Keuls *post-hoc* analysis).

3.3.2 Assessing the phagocytosis of FITC-labelled $A\beta_{1-42}$ by mixed glial cells

A 1-way ANOVA demonstrated that uptake of aggregated FITC-labelled $A\beta_{1-42}$ occurred in a concentration-dependent manner by both $CD11b^+$ and $CD11b^-$ cells ($p<0.01$) as shown in figure 3.6. Representative FACS-plots demonstrating the median fluorescent intensity (MFI) and percentage of FITC-labelled $A\beta_{1-42}$-positive cells for each concentration used (0, 0.15, 0.45, 1.35, 3 or 10μM) are shown in figure 3.7. MFI quantifies the shift in fluorescence intensity of any specific cell population. Based on these studies, a concentration of 3μM aggregated FITC-labelled $A\beta_{1-42}$ was chosen to carry out Z-stack confocal microscopy in order to generate a three-dimensional image of microglia and astrocytes to ensure that FITC-labelled $A\beta_{1-42}$ was located intracellularly. Isolated cultures of microglia and astrocytes were stained with anti-CD11b and anti-GFAP respectively as illustrated in figures 3.8 and 3.9.

A 1-way ANOVA followed by *post-hoc* analysis revealed that pre-treatment with cytochalasin D decreased the uptake of FITC-labelled $A\beta_{1-42}$ by both $CD11b^+$ and $CD11b^-$ cells ($p<0.01$), as shown in figure 3.10. This inhibition was significantly greater when cells were incubated in the presence of 10μM compared with 1 and 3μM concentrations of cytochalasin D ($p<0.05$).

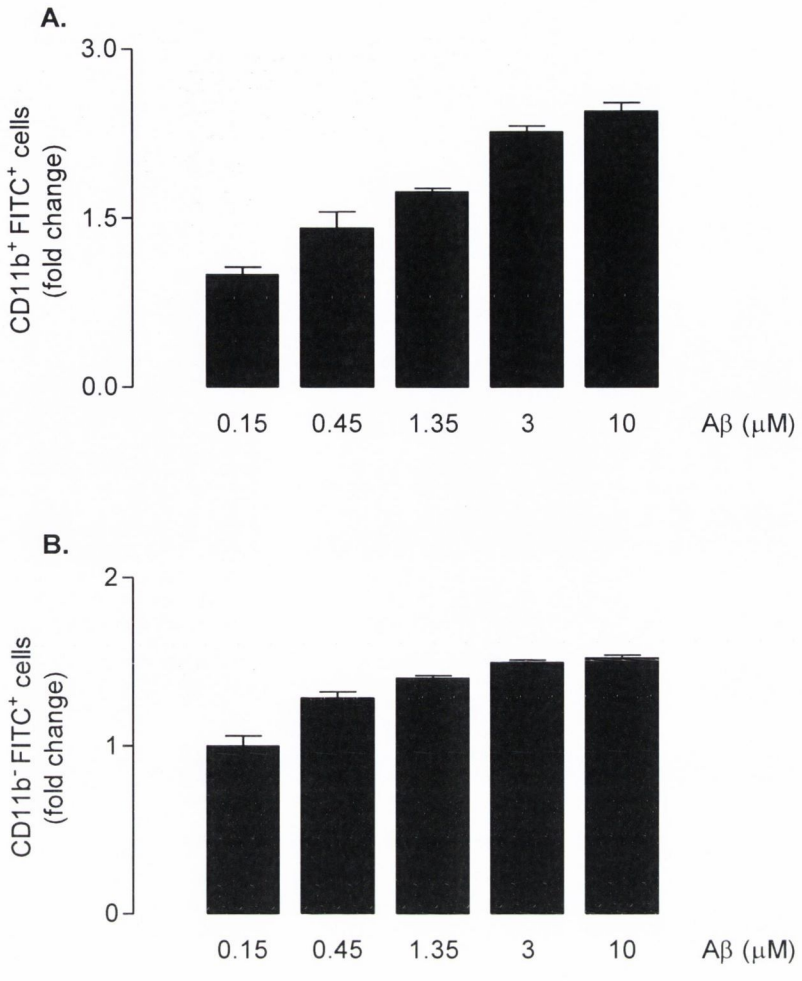

Figure 3.6 Uptake of FITC-labelled $A\beta_{1-42}$ by $CD11b^+$ and $CD11b^-$ cells increased in a concentration-dependent manner.

Primary mixed glial cells were incubated with aggregated FITC-labelled $A\beta_{1-42}$ (0.15, 0.45, 1.35, 3 or 10μM) for 2 hours and its uptake by $CD11b^+$ (A) and $CD11b^-$ (B) cells was assessed using flow cytometry. Data show that uptake of Aβ by $CD11b^+$ [$F_{(4,10)}$=50.69, p<0.001] and $CD11b^-$ [$F_{(4,10)}$=38.2, p<0.001] cells increased in a concentration-dependent manner. Data are expressed as means + SEM (n=4) from one of four independent experiments with similar results.

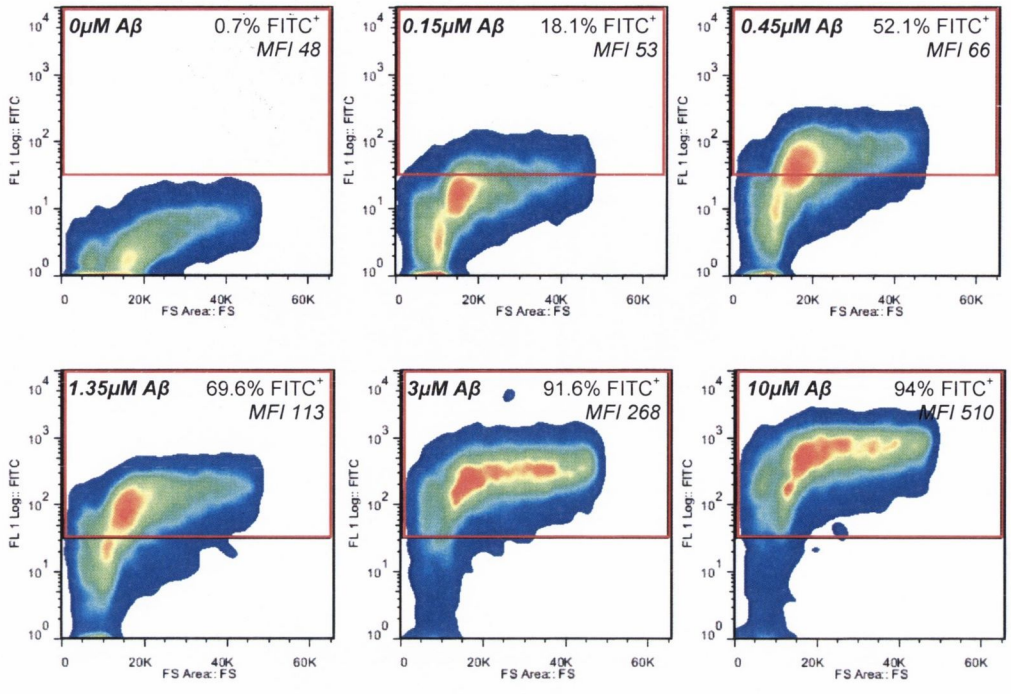

Figure 3.7 Representative FACS-plots demonstrate the uptake of FITC-labelled $A\beta_{1-42}$ by primary mixed glial cells.

Primary mixed glial cells were incubated with aggregated FITC-labelled $A\beta_{1-42}$ (0.15, 0.45, 1.35, 3 or 10μM) for 2 hours and its uptake assessed using flow cytometry. Debris and non-cellular events were initially excluded using forward/side scatter, with the percentage of $FITC^+$ cells then identified using the appropriate FMO. Representative FACS-plots for each $A\beta_{1-42}$ concentration demonstrate that uptake of FITC-labelled $A\beta_{1-42}$ by mixed glial cells was concentration-dependent. The percentage of cells in the top right hand corner were positive for the uptake of FITC-labelled $A\beta_{1-42}$. The shift in fluorescence intensity of these cells is further demonstrated by their MFI.

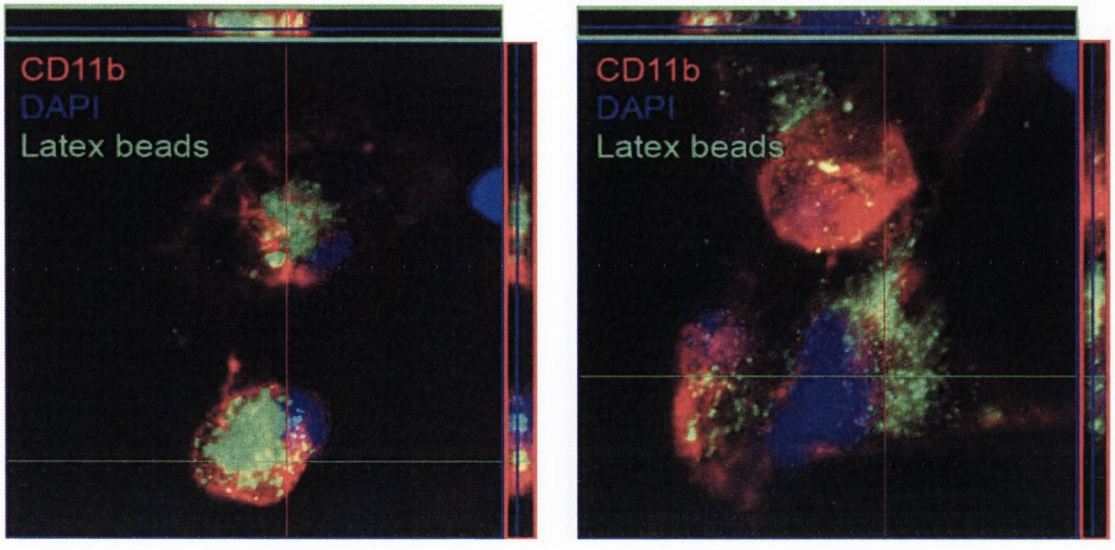

Figure 3.8 Representative micrograph visualising the intracellular localisation of FITC-labelled $A\beta_{1-42}$ following incubation with isolated microglia.

Representative micrograph of a phagocytosing microglia in orthogonal projections of confocal z-stacks. Isolated microglia were incubated for 2 hours with 3μM aggregated FITC-labelled $A\beta_{1-42}$ (green) and stained with anti-CD11b (red). Nuclei were counterstained using DAPI (blue). The fluorescent micrograph demonstrates intracellular localisation of FITC-labelled $A\beta_{1-42}$.

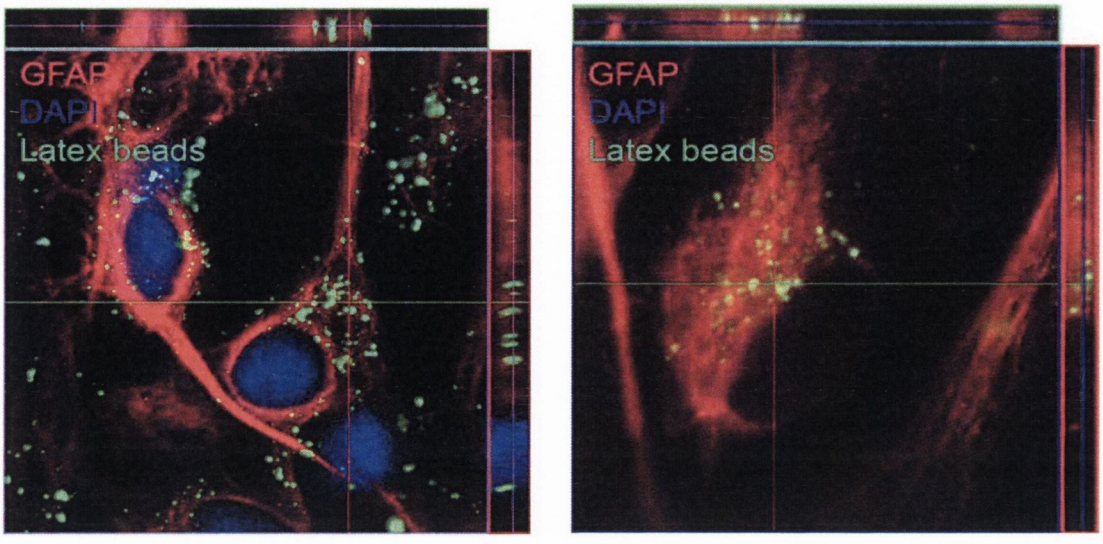

Figure 3.9 Representative micrograph visualising the intracellular localisation of FITC-labelled $A\beta_{1-42}$ following incubation with isolated astrocytes.

Representative micrograph of a phagocytosing astrocyte in orthogonal projections of confocal z-stacks. Isolated astrocytes were incubated for 2 hours with 3μM aggregated FITC-labelled $A\beta_{1-42}$ (green) and stained with anti-GFAP (red). Nuclei were counterstained using DAPI (blue). The fluorescent micrograph demonstrates intracellular localisation of FITC-labelled $A\beta_{1-42}$.

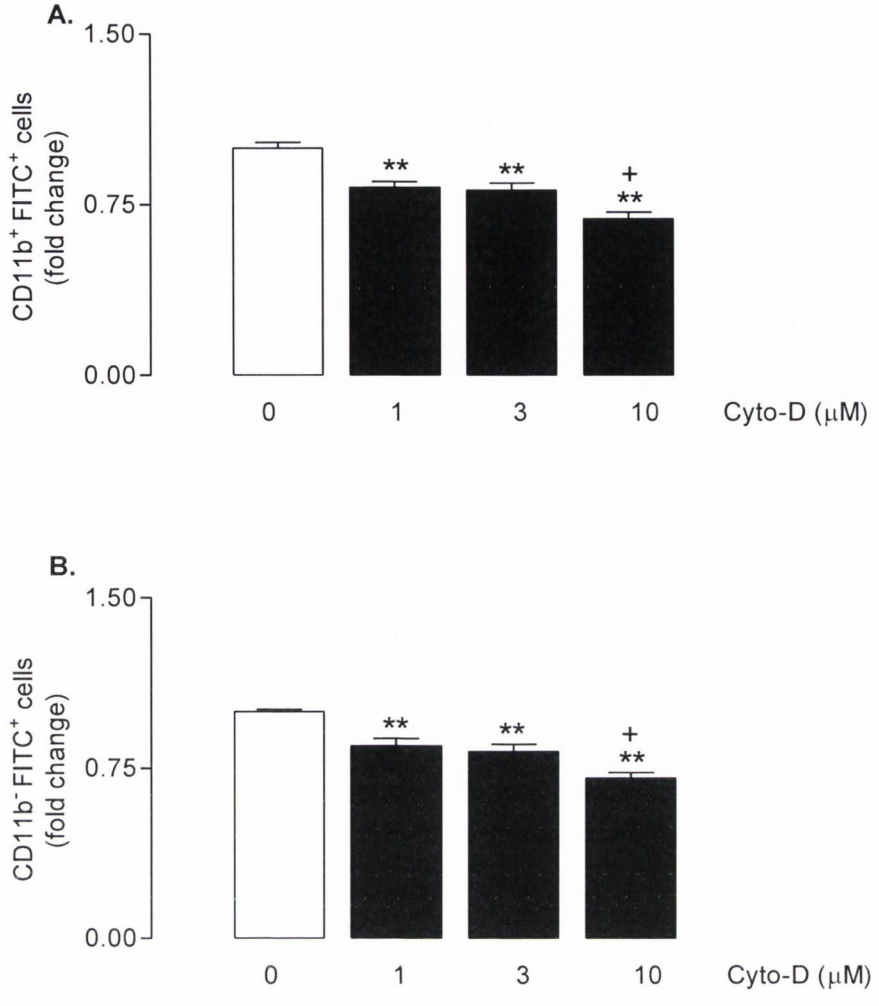

Figure 3.10 Pre-treatment with cytochalasin D inhibited the uptake of FITC-labelled Aβ by $CD11b^+$ and $CD11b^-$ cells.

Primary mixed glial cells were pre-treated with cytochalasin D (1, 3 or 10μM) for 2 hours and the phagocytosis of FITC-labelled Aβ by $CD11b^+$ (A) and $CD11b^-$ (B) cells was assessed using flow cytometry. The data show that uptake of Aβ by $CD11b^+$ [$F_{(3,11)}$=17.42, p=0.0002] and $CD11b^-$ [$F_{(3,12)}$=16.15, p =0.0002] cells was decreased following pre-treatment with cytochalasin D. This inhibition was significantly greater when cells were incubated in the presence of 10μM compared with 1 and 3μM cytochalasin D (p<0.05). Data are expressed as means + SEM (n=4) from one of three independent experiments with similar results. $^{**}p$<0.01, versus control, ^{+}p<0.05 versus 1μM cytochalasin-D (1-way ANOVA followed by Newman-Keuls *post-hoc* analysis).

3.3.3 Analysis of the oxidative burst that occurs following phagocytosis in microglia, astrocytes and PBMCs.

A comparison of the ability of primary rat microglia, astrocytes and PBMCs to mount a phagocytic response to opsonised-zymosan is shown in figure 3.11. This assay is based on the luminol-dependent chemiluminescence that results from ROS released during the oxidative burst that accompanies phagocytosis.

Zymosan was opsonised with serum as described in section 2.3 and luminol (1mM) was prepared by dissolving 5-amino-2,3-dihydro-1,4-phthalazinedione in sodium hydroxide (NaOH; 0.1M). Opsonised zymosan (50µl) was added to each well of a black 96-well microplate containing microglia, astrocyte or PBMC suspension (50µl) in 1X HBSS ($3x10^6$ cells/ml) and luminol solution (1mM; 50µl). Chemiluminescence measurements were taken with readings carried out at 2 minute intervals for a total run time of 44 minutes.

A 1-way ANOVA revealed that all cell types released a significant amount of ROS ($p<0.01$) following incubation with opsonised-zymosan as measured using chemiluminescence. This is indicative of the oxidative burst that accompanies phagocytosis. Further *post-hoc* analysis revealed that PBMCs had a significantly higher response to opsonised-zymosan than microglia or astrocytes ($p<0.01$). In addition, the microglial phagocytic response was more pronounced than that of astrocytes ($p<0.05$).

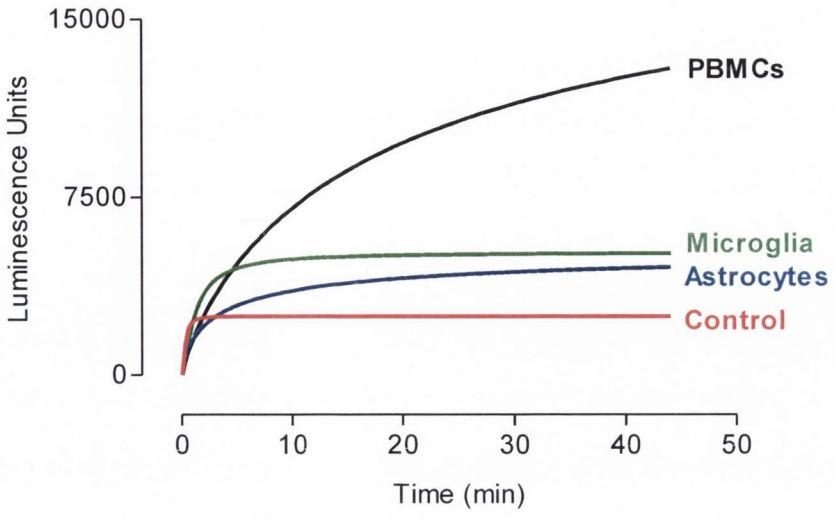

Figure 3.11 Phagocytosis and the associated release of ROS was greater in PBMCs than microglia and astrocytes.

Isolated primary astrocytes, microglia and rat peripheral blood mononuclear cells were incubated with opsonised-zymosan and luminol for 44 minutes. Chemiluminescent readings were taken at 2 minute time points. All cell types were found to mount a significant phagocytic response compared to control [$F_{(3,22)}$=98.18, p<0.0001]. PBMCs had a significantly higher response compared with microglia and astrocytes (p<0.01). The microglial phagocytic response was more pronounced than that of astrocytes (p<0.05). Data are expressed as means + SEM (n=5).

3.3.4 Analysis of the effect of Aβ on isolated microglia *in vitro*

In order to examine the effect of Aβ on microglia *in vitro*, isolated cultures were incubated with a combination of aggregated $A\beta_{1-40}$ (4.2μM) and $A\beta_{1-42}$ (5.8μM), hereafter referred to as Aβ, or reverse peptide $A\beta_{40-1}$ (10μM) for 24 hours (Murphy *et al.*, 2011).

Aβ increased mRNA expression of three markers of microglial activation CD11b, CD68 and CD40 ($p<0.01$), but had no effect on MHC-II mRNA ($p=0.6517$) as shown in figure 3.12. In addition, mRNA expression of IL-1β, IL-6, TNFα and iNOS was increased ($p<0.01$) following incubation with Aβ as shown in figure 3.13

Aβ increased mRNA expression of the putative Aβ receptor TLR2 ($p<0.01$), but had no effect on TLR4 ($p=0.3063$), SR-B1 ($p=0.565$), CD36 ($p=0.3872$), CD47 ($p=0.1765$) or RAGE ($p=0.2667$) mRNA as shown in figure 3.14.

Incubation of isolated microglia with Aβ for 24 hours increased their ability to phagocytose fluorescently-labelled latex beads ($p<0.05$) as shown in figure 3.15.

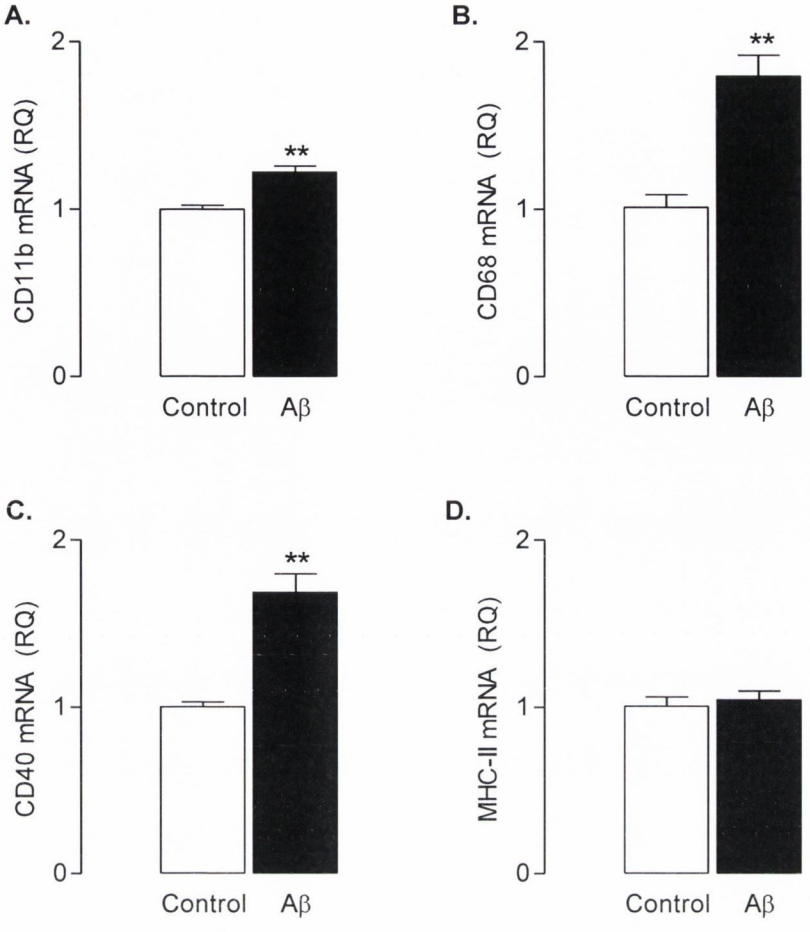

Figure 3.12 Aβ increased mRNA expression of CD11b, CD68 and CD40 in isolated microglia.

Isolated microglia were incubated with Aβ or reverse peptide for 24 hours *in vitro*. Data show that Aβ significantly increased mRNA expression of CD11b, CD68 and CD40 (A-C; $p<0.01$), while MHC-II (D) expression remained unchanged following treatment. Data are expressed as means + SEM ($n=6$) from one of two independent experiments with similar results. $^{**}p<0.01$ versus control (Student's *t*-test for independent means).

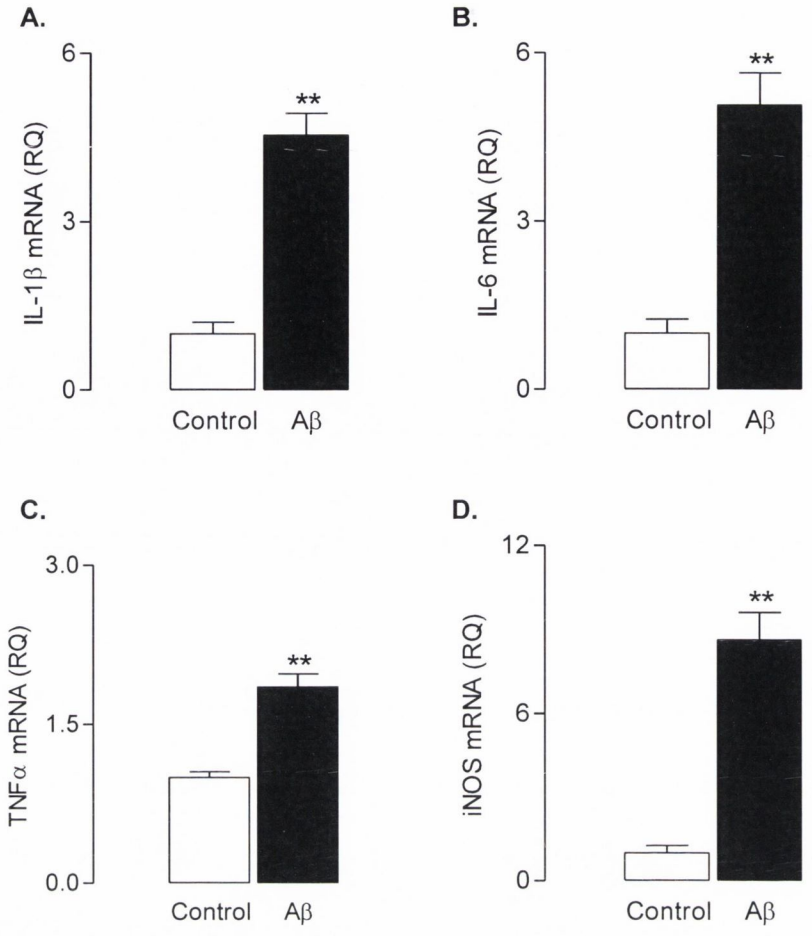

Figure 3.13 Aβ increased mRNA expression of IL-1β, IL-6, TNFα and iNOS in isolated microglia.

Isolated microglia were incubated with Aβ or reverse peptide for 24 hours *in vitro*. Data show that Aβ significantly increased mRNA expression of IL-1β, IL-6, TNFα and iNOS (A-D; $p<0.01$). Data are expressed as means + SEM ($n=6$) from one of two independent experiments with similar results. $^{**}p<0.01$ versus control (Student's *t*-test for independent means).

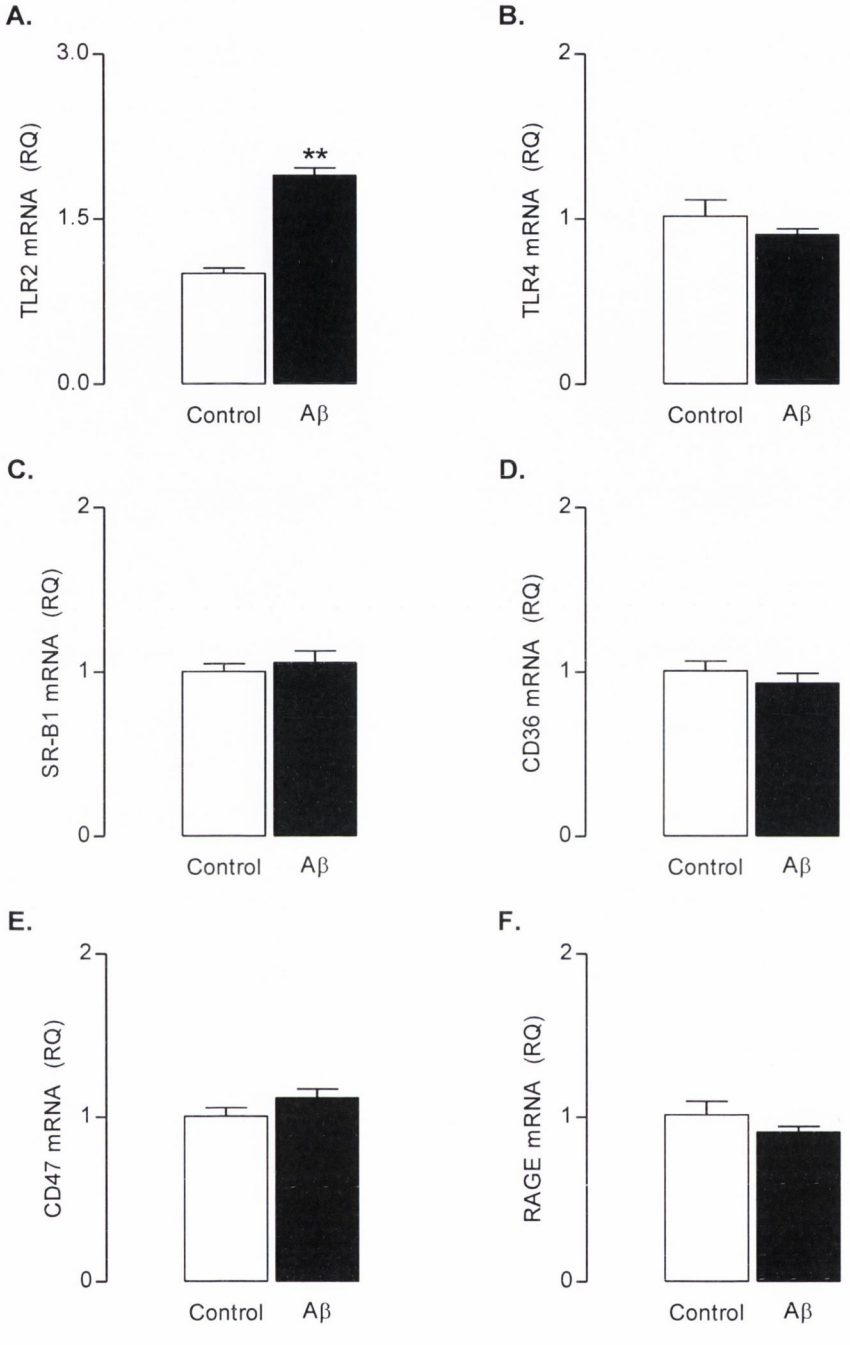

Figure 3.14 Aβ increased mRNA expression of TLR2 in isolated microglia.

Isolated microglia were incubated with Aβ or reverse peptide for 24 hours *in vitro*. Data show that Aβ significantly increased TLR2 mRNA expression (A; $p<0.01$) but TLR4, SR-B1, CD36, CD47 and RAGE mRNA expression (B-F) remained unchanged following treatment. Data are expressed as means + SEM ($n=6$) from one of two independent experiments with similar results. $^{**}p<0.01$ (Student's *t*-test for independent means).

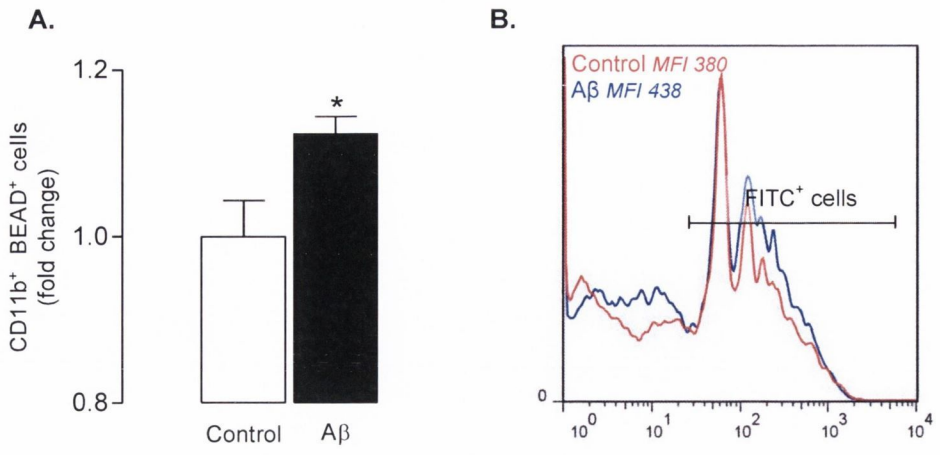

Figure 3.15 Aβ increased the phagocytosis of fluorescently-labelled latex beads by CD11b$^+$ microglia.

Isolated microglia were incubated with Aβ or reverse peptide for 24 hours *in vitro* and the phagocytosis of fluorescently-labelled latex beads was assessed using flow cytometry. Debris and non-cellular events were initially excluded using forward/side scatter, with the percentage of CD11b$^+$FITC$^+$ cells further identified using the appropriate FMOs. The data show that Aβ significantly increased phagocytosis of latex beads by CD11b$^+$ cells (A; $p<0.05$), visualised with a representative FACS-plot and MFI data (B). Data are expressed as means + SEM ($n=6$) from one of three independent experiments with similar results. *$p<0.05$ (Student's *t*-test for independent means).

3.3.5 Analysis of the effect of Aβ on isolated astrocytes *in vitro*

In order to examine the effect of Aβ on astrocytes *in vitro*, isolated cultures were incubated with Aβ or reverse peptide for 24 hours.

Aβ decreased mRNA but not protein expression of the markers of astrocyte activation GFAP ($p<0.05$) and S100β ($p<0.01$) as shown in figure 3.16. Aβ had no effect on GLAST mRNA ($p=0.866$) or protein expression as shown in figure 3.17, however it significantly increased mRNA expression of GLT-1 ($p<0.01$). Aβ had no effect on mRNA expression of glutamine synthetase ($p=0.6513$).

Aβ increased mRNA expression of markers of inflammation IL-1β, IL-6, TNFα and iNOS ($p<0.01$) as shown in figure 3.18, while it also increased expression of the putative Aβ receptors TLR2, TLR4, SR-B1, CD36 and CD47 ($p<0.01$) as shown in figure 3.19. In contrast, RAGE mRNA expression was decreased ($p<0.05$) following incubation of cells in the presence of Aβ.

Incubation of isolated astrocytes with Aβ for 24 hours significantly increased their ability to phagocytose fluorescently-labelled latex beads ($p<0.01$) as shown in figure 3.20.

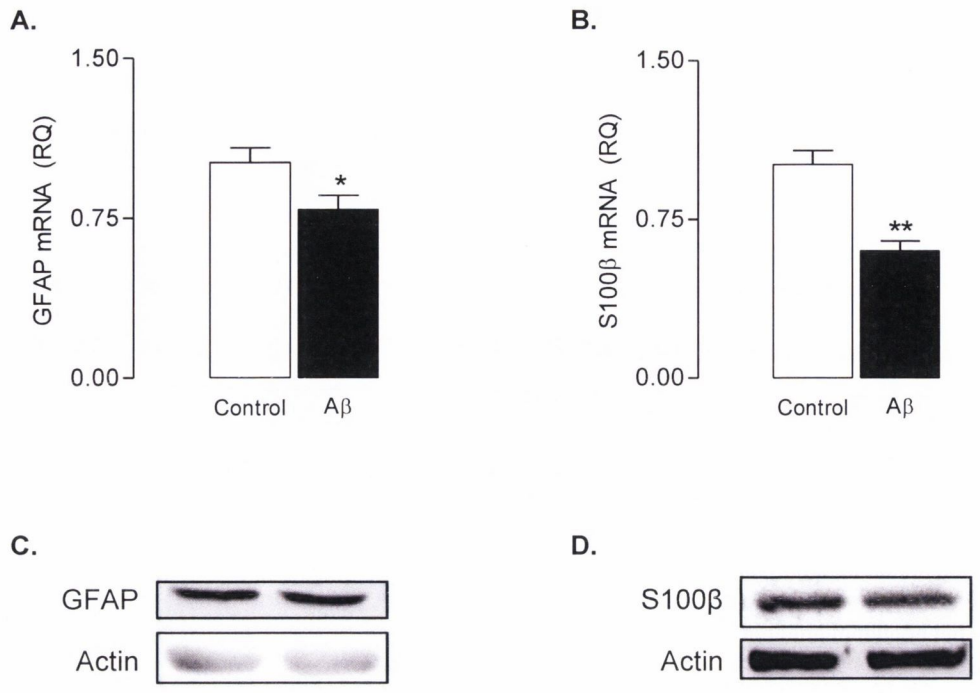

Figure 3.16 Aβ decreased mRNA but not protein expression of GFAP and S100β in isolated astrocytes.

Isolated astrocytes were incubated with Aβ or reverse peptide for 24 hours *in vitro*. The data show that Aβ significantly decreased mRNA expression of GFAP (A; $p<0.05$) and S100β (B; $p<0.01$). Protein expression of GFAP and S100β, as assessed by Western immunoblotting and measured relative to actin, remained unchanged following incubation in the presence of Aβ (C, D). Data are expressed as means + SEM ($n=6$) from one of two independent experiments with similar results. *$p<0.05$, **$p<0.01$ versus control (Student's *t*-test for independent means).

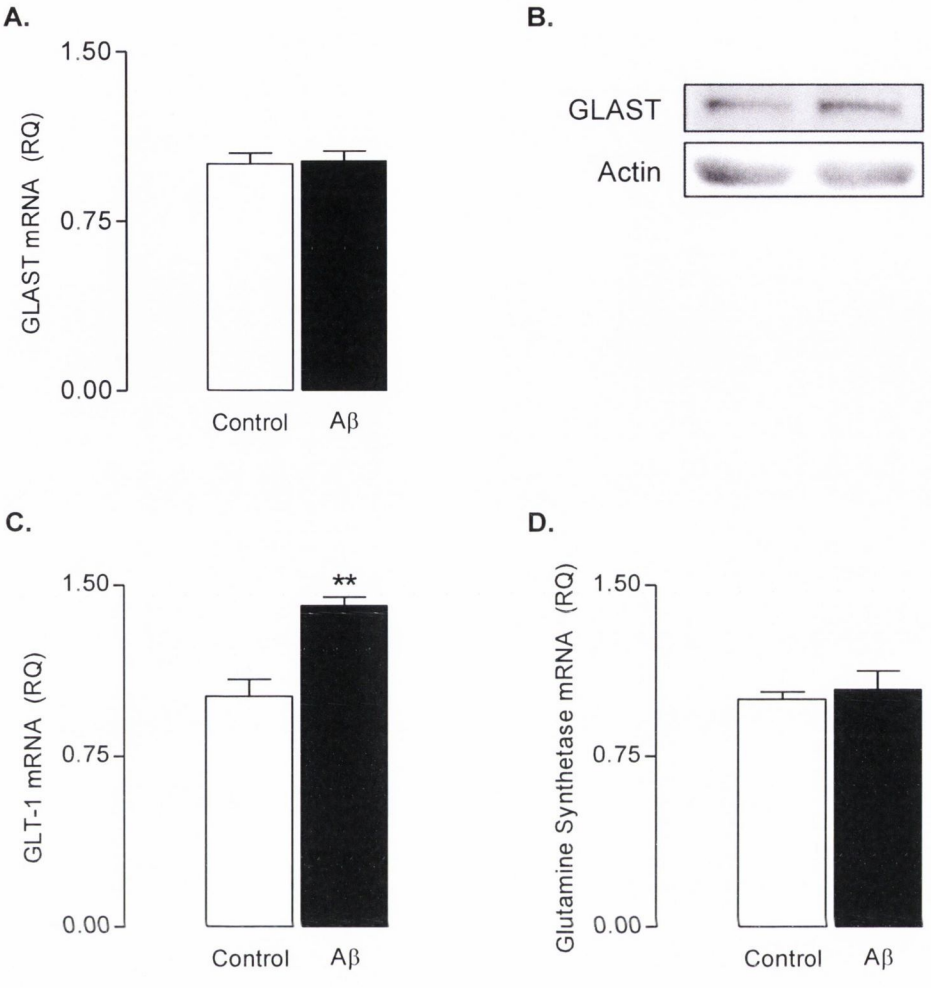

Figure 3.17 Aβ increased mRNA expression of GLT-1 but not GLAST in isolated astrocytes.

Isolated astrocytes were incubated with Aβ or reverse peptide for 24 hours *in vitro*. The data show that GLAST mRNA (A) and protein (B) expression remained unchanged following treatment. Aβ significantly increased mRNA expression of GLT-1 (C; $p<0.01$). Glutamine synthetase mRNA expression remained unchanged following treatment (D). Data are expressed as means + SEM ($n=6$) from one of two independent experiments with similar results. $^{**}p<0.01$ versus control (Student's *t*-test for independent means).

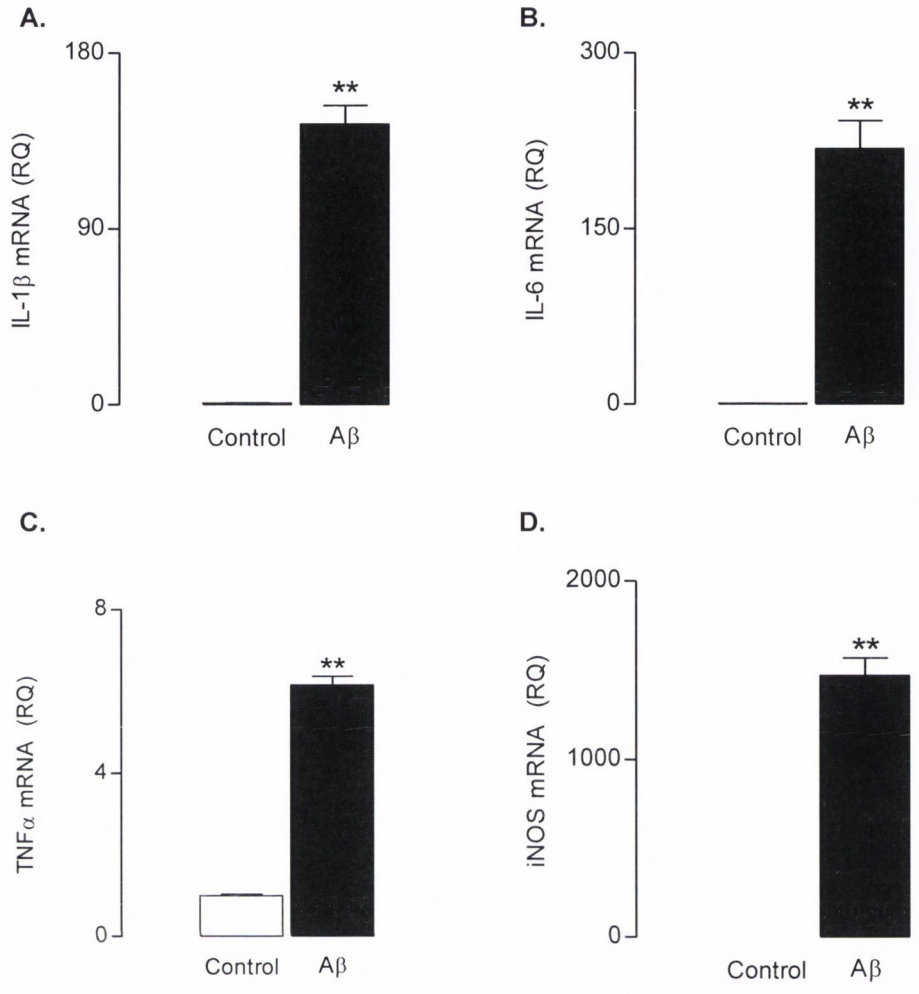

Figure 3.18 Aβ increased mRNA expression of IL-1β, IL-6, TNFα and iNOS in isolated astrocytes.

Isolated astrocytes were incubated with Aβ or reverse peptide for 24 hours *in vitro*. Data show that Aβ significantly increased mRNA expression of IL-1β, IL-6, TNFα and iNOS (A-D; $p<0.01$). Data are expressed as means + SEM ($n=6$) from one of two independent experiments with similar results. **$p<0.01$ versus control (Student's *t*-test for independent means).

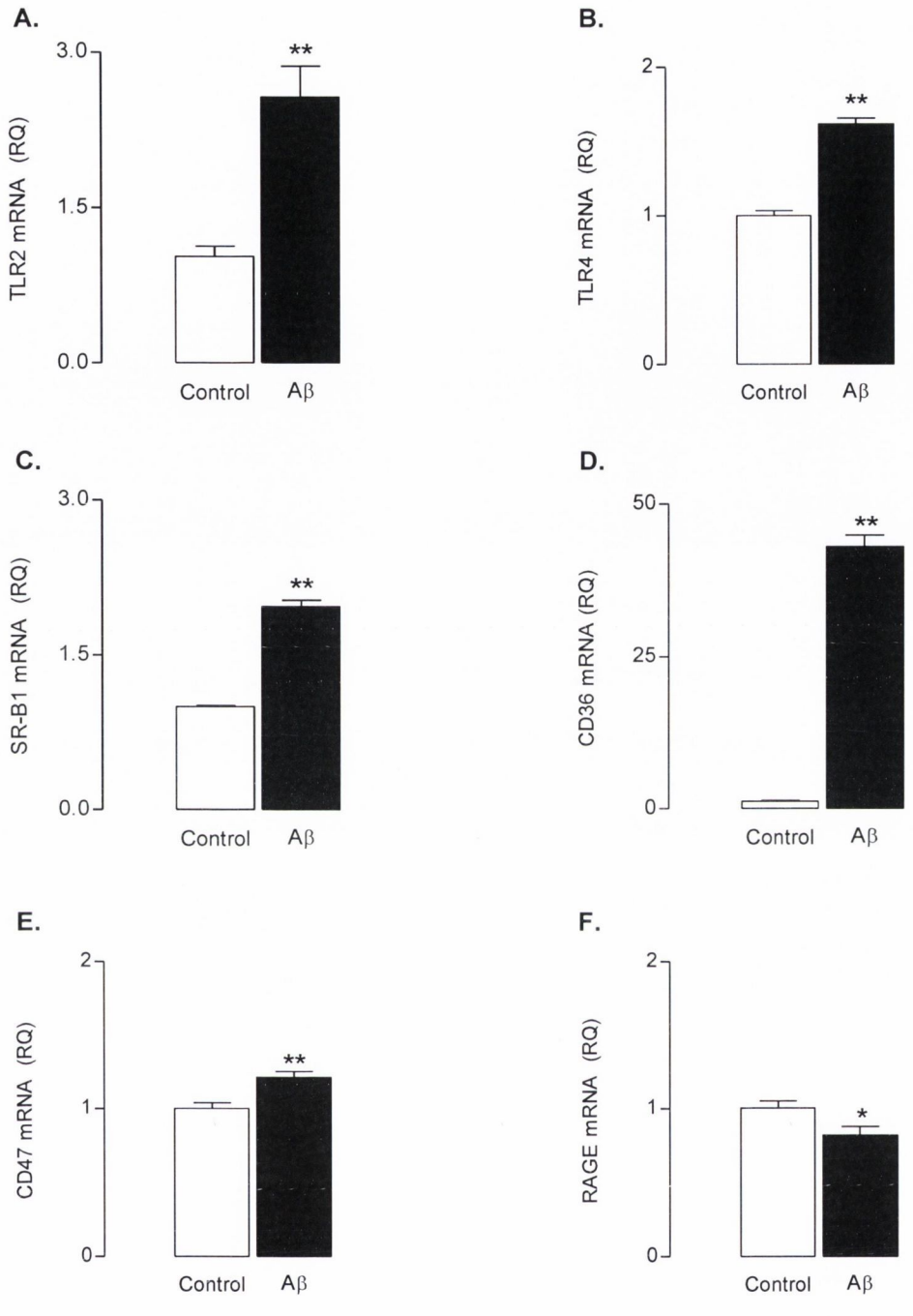

Figure 3.19 Aβ increased mRNA expression of its putative receptors TLR2, TLR4, SR-B1, CD36 and CD47 in isolated astrocytes but decreased the expression of RAGE.

Isolated astrocytes were incubated with Aβ or reverse peptide for 24 hours *in vitro*. The data show that Aβ significantly increased mRNA expression of TLR2, TLR4, SR-B1, CD36 and CD47 (A-E; $p<0.01$). RAGE mRNA expression was significantly decreased following treatment (F; $p<0.05$). Data are expressed as means + SEM ($n=6$) from one of two independent experiments with similar results. *$p<0.05$, **$p<0.01$ versus control (Student's *t*-test for independent means).

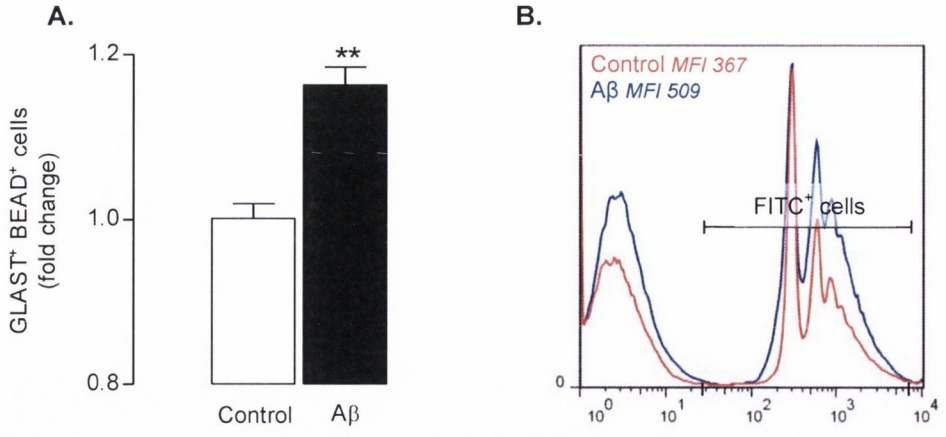

Figure 3.20 Aβ increased the phagocytosis of fluorescently-labelled latex beads by GLAST$^+$ astrocytes.

Isolated astrocytes were incubated with Aβ or reverse peptide for 24 hours *in vitro* and the phagocytosis of fluorescently-labelled latex beads was assessed using flow cytometry. Debris and non-cellular events were initially excluded using forward/side scatter, with the percentage of GLAST$^+$FITC$^+$ cells further identified using the appropriate FMOs. The data show that Aβ significantly increased phagocytosis of latex beads by GLAST$^+$ astrocytes (A; $p<0.01$), visualised with a representative FACS-plot and MFI data (B). Data are expressed as means + SEM ($n=6$) from one of three independent experiments with similar results. $^{**}p<0.01$ versus control (Student's *t*-test for independent means).

3.3.6 Analysis of the effect of exogenous Aβ on its putative receptors and mediators of inflammation *in vivo*

To examine the effects of exogenous Aβ on microglia and astrocytes in vivo, male Wistar rats (3–4 months) were implanted with mini-osmotic pumps delivering a cocktail of aggregated Aβ or aCSF intracerebroventricularly for 28 days.

Intracerebroventricular infusion of Aβ increased hippocampal mRNA expression of IL-1β and TNFα ($p<0.05$) but had no effect on iNOS ($p=0.1131$) or IFNγ ($p=0.6564$) expression as shown in figure 3.21.

Aβ infusion had no effect on hippocampal mRNA expression of the putative Aβ receptors TLR2 ($p=0.5983$), TLR4 ($p=0.7126$), RAGE ($p=0.5277$) or SR-B1 ($p=0.1623$) as shown in figure 3.22.

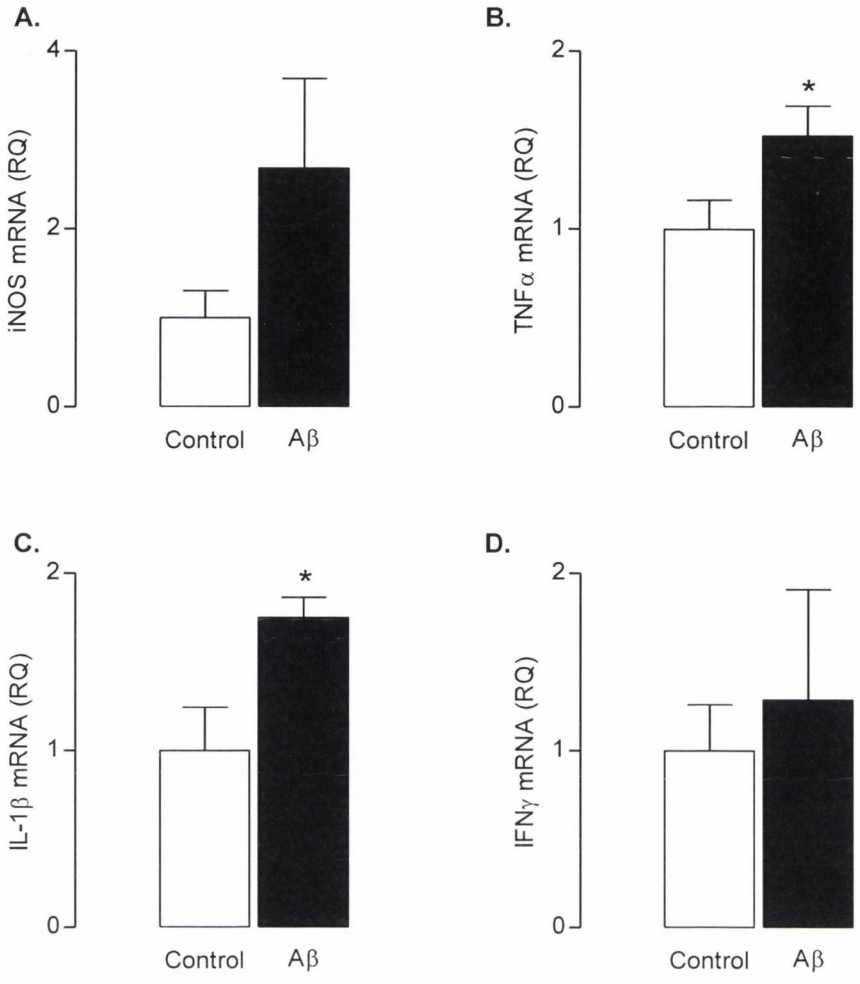

Figure 3.21 Intracerebroventricular infusion of Aβ increased mRNA expression of IL-1β and TNFα in the hippocampus.

Male Wistar rats aged 3–4 months were intracerebroventricularly implanted with mini-osmotic pumps delivering an infusion of aggregated $A\beta_{1-40}$ (26.9μM) and $A\beta_{1-42}$ (36.9μM) or aCSF at a calculated delivery rate of 0.25μl/h (±0.05 μl) for 28 days. Infusion of Aβ increased hippocampal mRNA expression of the pro-inflammatory cytokines, TNFα and IL-1β (B,C; $p<0.05$) but had no effect on iNOS (A) or IFNγ expression (D). Data are expressed as means + SEM ($n=7$). *$p<0.05$ versus control (Student's *t*-test for independent means).

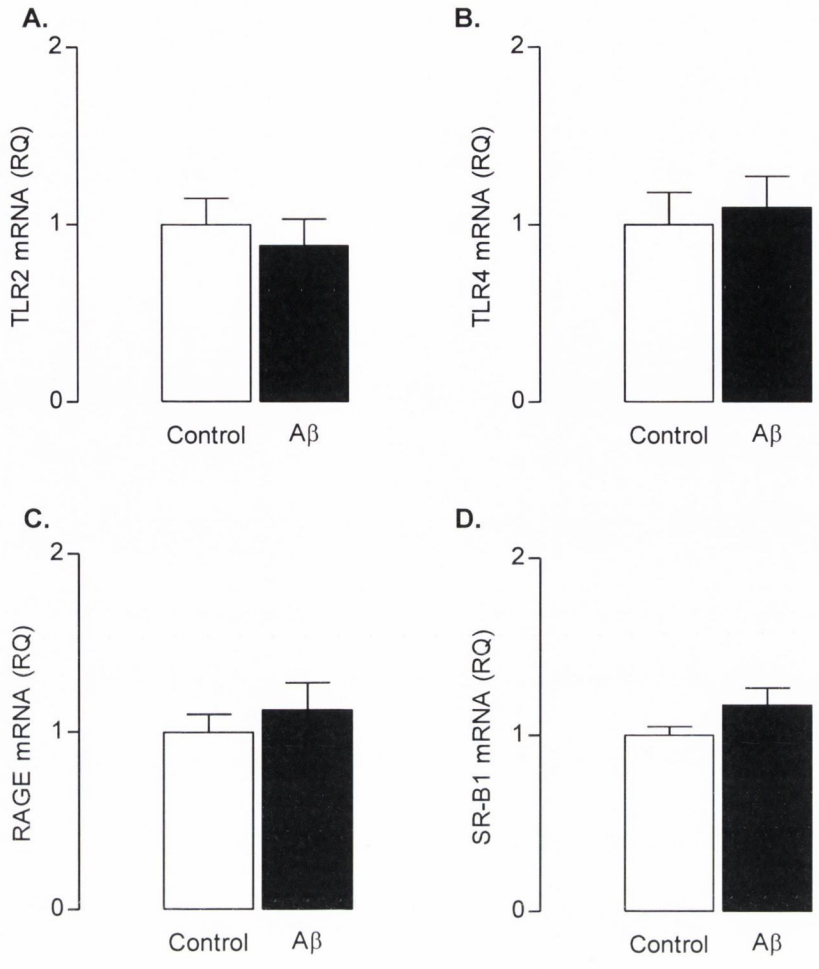

Figure 3.22 Intracerebroventricular infusion of Aβ had no effect on mRNA expression of TLR2, TLR4, RAGE or SR-B1 in the hippocampus.

Male Wistar rats aged 3–4 months were intracerebroventricularly implanted with mini-osmotic pumps delivering an infusion of aggregated $A\beta_{1-40}$ (26.9μM) and $A\beta_{1-42}$ (36.9μM) or aCSF at a calculated delivery rate of 0.25μl/h (±0.05 μl) for 28 days. Infusion of Aβ had no effect on hippocampal mRNA expression of the putative Aβ receptors TLR2, TLR4, RAGE or SR-B1 (A-D). Data are expressed as means + SEM (*n*=7).

3.3.7 Analysis of the effect of exogenous Aβ on microglia *in vivo*

Intracerebroventricular infusion of aggregated Aβ for 28 days had no effect on mRNA expression of two markers of microglial activation, CD68 (p=0.2966) or MHC-II (p=0.9382), in the hippocampus as shown in figure 3.23. While CD11b mRNA expression in the hippocampus was unchanged (p=0.3766) following Aβ infusion, CD11b protein expression was significantly increased (p<0.05) in the cortex following treatment as shown in figure 3.24.

Following isolation of $CD11b^+$ cells from the cortex of vehicle- and Aβ-infused animals, *ex vivo* phagocytosis of fluorescently-labelled latex beads by these cells was unchanged (p=0.6498) between groups as shown in figure 3.25.

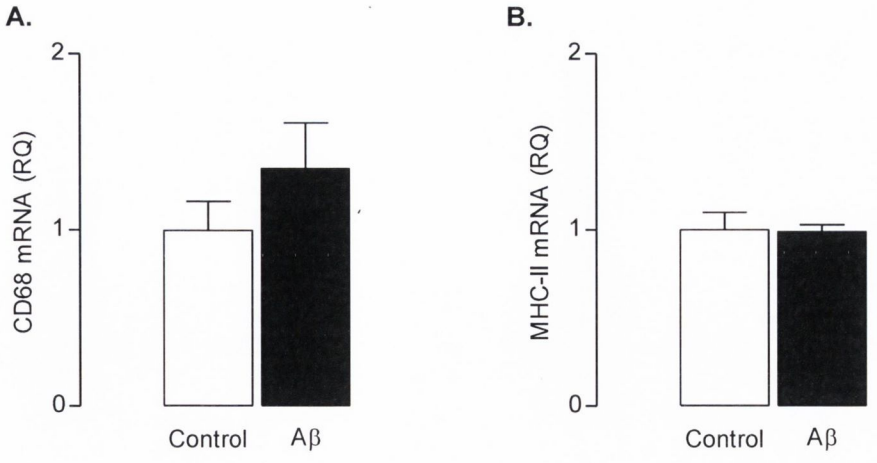

Figure 3.23 Intracerebroventricular infusion of Aβ had no effect on mRNA expression of CD68 or MHC-II.

Male Wistar rats aged 3–4 months were intracerebroventricularly implanted with mini-osmotic pumps delivering an infusion of aggregated $A\beta_{1-40}$ (26.9μM) and $A\beta_{1-42}$ (36.9μM) or aCSF at a calculated delivery rate of 0.25μl/h (±0.05 μl) for 28 days. Intracerebroventricular infusion of Aβ had no effect on mRNA expression of CD68 (A) or MHC-II (B). Data are expressed as means + SEM (*n*=7).

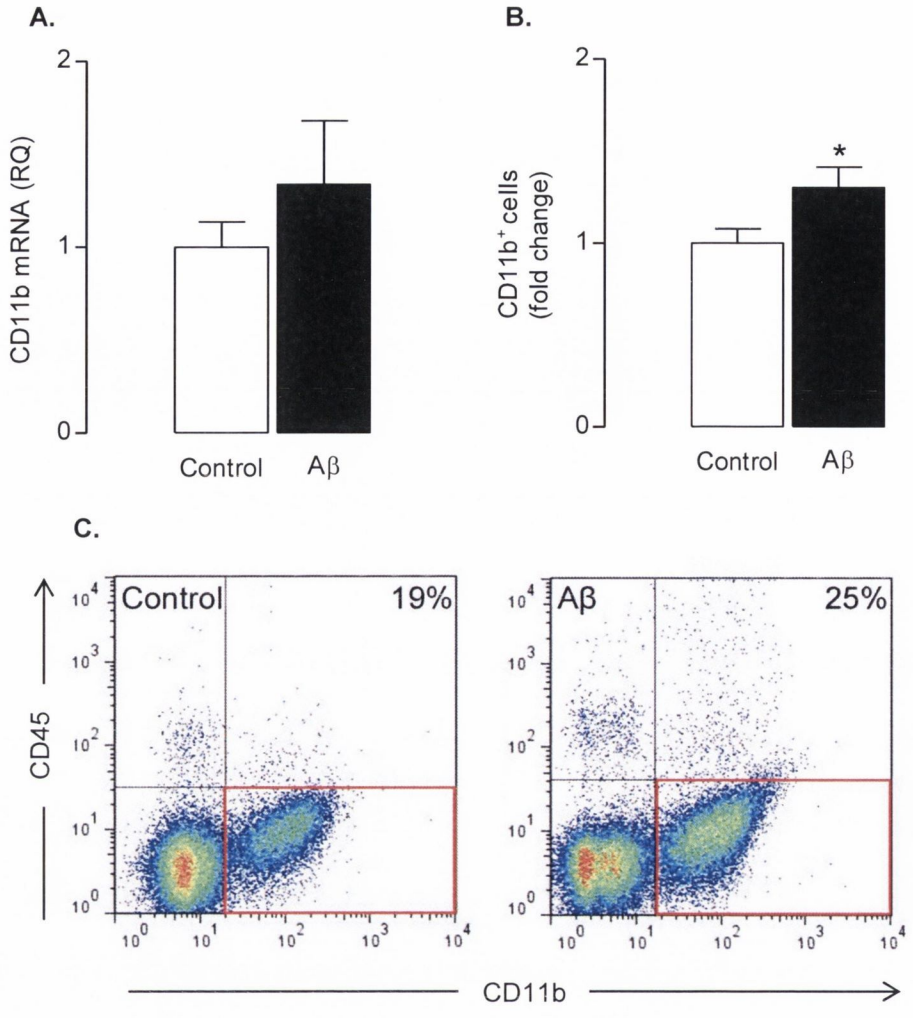

Figure 3.24 Intracerebroventricular infusion of Aβ increased protein but not mRNA expression of CD11b.

Male Wistar rats aged 3–4 months were intracerebroventricularly implanted with mini-osmotic pumps delivering an infusion of aggregated $A\beta_{1-40}$ (26.9μM) and $A\beta_{1-42}$ (36.9μM) or aCSF at a calculated delivery rate of 0.25μl/h (±0.05 μl) for 28 days. Microglial cells were isolated from cortical tissue by density separation over Percoll in order to assess protein expression of CD11b by flow cytometry. Debris and non-cellular events were initially excluded using forward/side scatter, with the percentage of $CD11b^{+}CD45^{low}$ cells further identified using the appropriate FMOs. Infusion of Aβ had no effect on hippocampal mRNA expression of CD11b (A) but significantly increased its protein expression (B; $p<0.05$) in the cortex following 28 days, visualised with representative FACS-plots (C). Data are expressed as means + SEM ($n=7$). *$p<0.05$ versus control (Student's *t*-test for independent means).

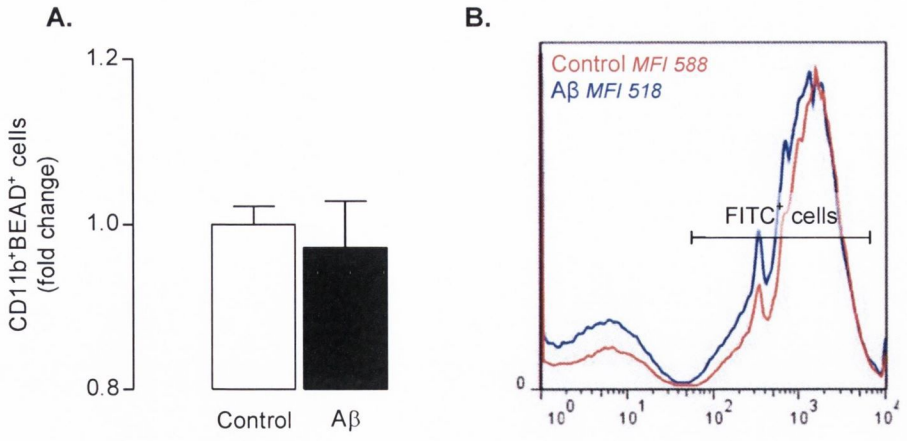

Figure 3.25 *Ex vivo* phagocytosis of fluorescently-labelled latex beads by CD11b$^+$ cells was unchanged following intracerebroventricular infusion of Aβ.

Male Wistar rats aged 3–4 months were intracerebroventricularly implanted with mini-osmotic pumps delivering an infusion of aggregated $A\beta_{1-40}$ (26.9μM) and $A\beta_{1-42}$ (36.9μM) or aCSF at a calculated delivery rate of 0.25μl/h (±0.05 μl) for 28 days. Microglial cells were isolated from cortical tissue by density separation over Percoll in order to assess *ex vivo* phagocytosis. Debris and non-cellular events were initially excluded using forward/side scatter, with the percentage of CD11b$^+$FITC$^+$ cells further identified using the appropriate FMOs. Infusion of Aβ had no effect on the phagocytosis of fluorescently-labelled latex beads by CD11b$^+$ cells (A), visualised with a representative FACS-plot and MFI data (B). Data are expressed as means + SEM (n=7).

3.3.8 Analysis of the effect of exogenous Aβ on astrocytes *in vivo*

Intracerebroventricular infusion of Aβ for 28 days increased mRNA expression of GFAP ($p<0.05$) in the hippocampus but had no effect on other markers of astrocyte activation such as S100β ($p=0.7825$), GLT-1 ($p=0.3379$) or glutamine synthetase ($p=0.6774$) as shown in figure 3.26. GLAST mRNA ($p=0.3147$) and protein expression ($p=0.6212$) were also unaffected following Aβ infusion as shown in figure 3.27.

Following isolation of $GLAST^+$ cells from the cortex of vehicle- and Aβ-infused animals, *ex vivo* phagocytosis of fluorescently-labelled latex beads was increased ($p<0.05$) in cells isolated from Aβ-treated rats as shown in figure 3.28.

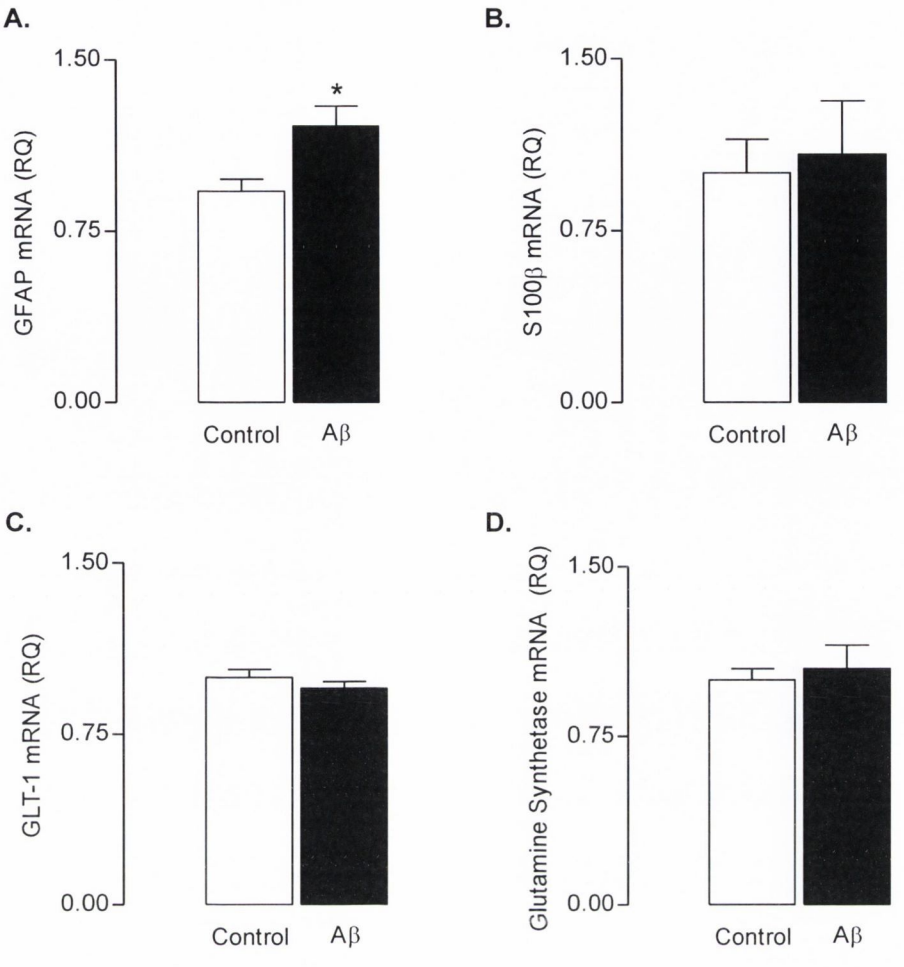

Figure 3.26 Intracerebroventricular infusion of Aβ increased hippocampal mRNA expression of GFAP but not S100β, GLT-1 or glutamine synthetase.

Male Wistar rats aged 3–4 months were intracerebroventricularly implanted with mini-osmotic pumps delivering an infusion of aggregated $A\beta_{1-40}$ (26.9μM) and $A\beta_{1-42}$ (36.9μM) or aCSF at a calculated delivery rate of 0.25μl/h (±0.05 μl) for 28 days. Infusion of Aβ increased hippocampal mRNA expression of GFAP (A; $p<0.05$) but had no effect on the expression of S100β, GLT-1 or glutamine synthetase (B-D). Data are expressed as means + SEM ($n=7$). *$p<0.05$ versus control (Student's *t*-test for independent means).

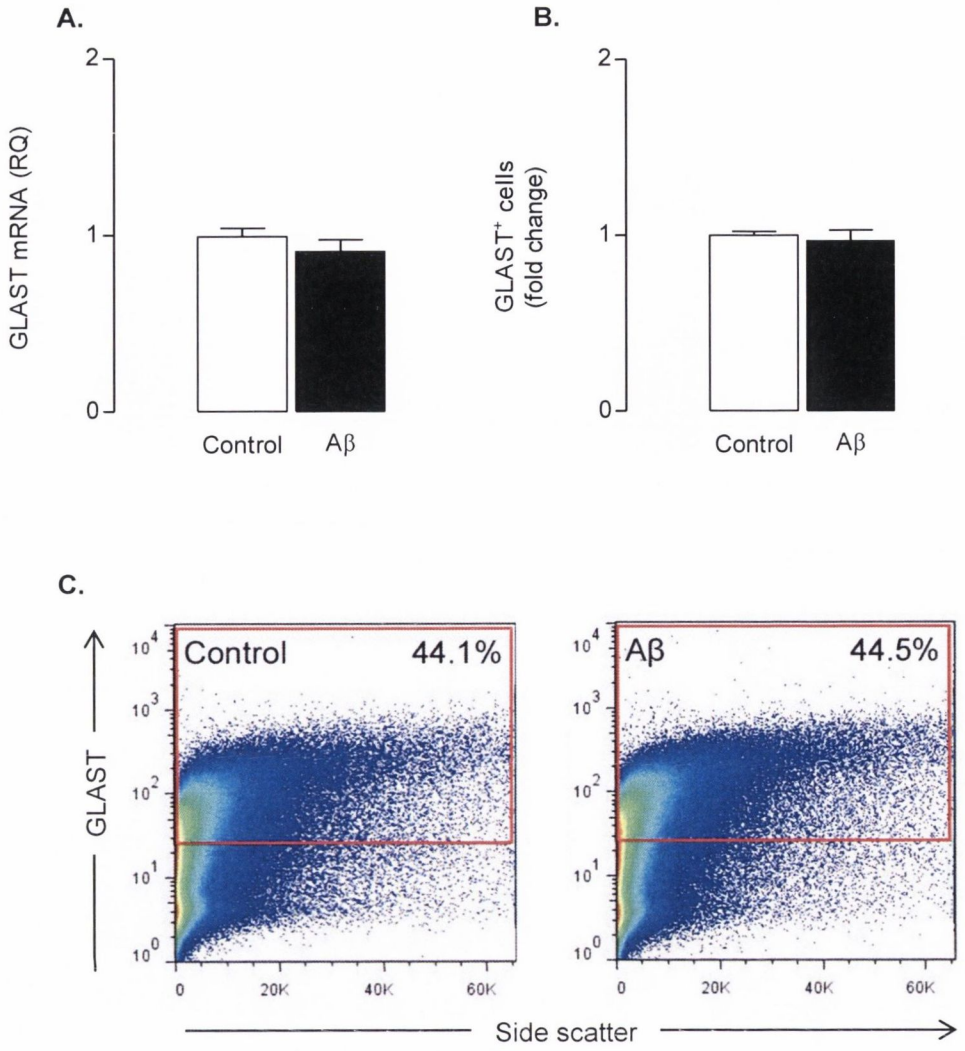

Figure 3.27 Intracerebroventricular infusion of Aβ had no effect on mRNA or protein expression of GLAST.

Male Wistar rats aged 3–4 months were intracerebroventricularly implanted with mini-osmotic pumps delivering an infusion of aggregated $A\beta_{1-40}$ (26.9μM) and $A\beta_{1-42}$ (36.9μM) or aCSF at a calculated delivery rate of 0.25μl/h (±0.05 μl) for 28 days. Astrocytes were isolated from cortical tissue by density separation over Percoll in order to assess protein expression of GLAST by flow cytometry. Debris and non-cellular events were initially excluded using forward/side scatter, with the percentage of $GLAST^+$ cells further identified using the appropriate FMO. Infusion of Aβ days had no effect on hippocampal mRNA (A) or protein (B) expression of GLAST in the cortex of infused animals, visualised with representative FACS-plots (C). Data are expressed as means + SEM (*n*=7).

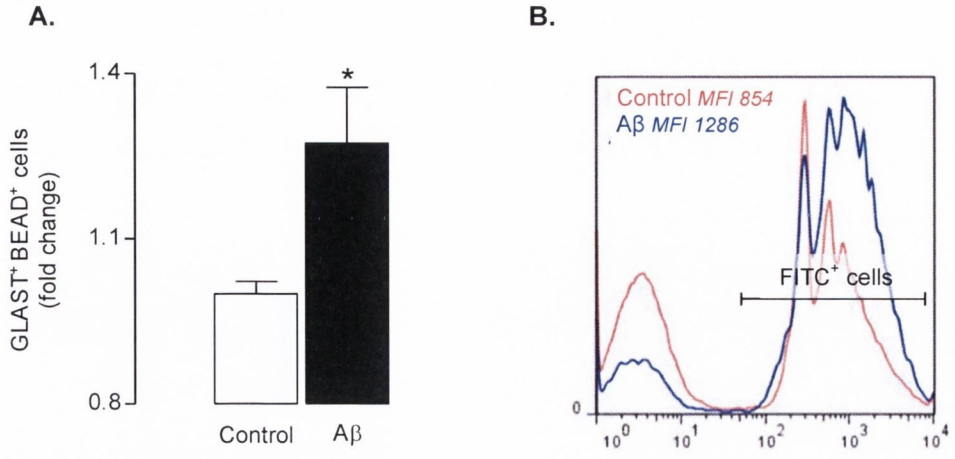

Figure 3.28 *Ex vivo* phagocytosis by GLAST$^+$ cells was increased following intracerebroventricular infusion of Aβ.

Male Wistar rats aged 3–4 months were intracerebroventricularly implanted with mini-osmotic pumps delivering an infusion of aggregated $A\beta_{1-40}$ (26.9μM) and $A\beta_{1-42}$ (36.9μM) or aCSF at a calculated delivery rate of 0.25μl/h (±0.05 μl) for 28 days. Astrocytes were isolated from cortical tissue by density separation over Percoll in order to assess *ex vivo* phagocytosis. Debris and non-cellular events were initially excluded using forward/side scatter, with the percentage of GLAST$^+$FITC$^+$ cells further identified using the appropriate FMOs. Infusion of Aβ significantly increased the *ex vivo* phagocytosis of fluorescently-labelled latex beads by GLAST$^+$ cells. (A; $p<0.05$), visualised with a representative FACS-plot and MFI data (B). Data are expressed as means + SEM ($n=7$). *$p<0.05$ versus control (Student's *t*-test for independent means).

3.4 Discussion

Initial findings in the present studies confirmed that fluorescently-labelled latex beads and FITC-labelled Aβ were taken up in a concentration-dependent manner by both microglia and astrocytes. This was visualised using immunocytochemistry and confocal microscopy where fluorescent micrographs clearly demonstrated intracellular localisation of the beads and Aβ. Microglia have previously been shown to phagocytose FITC-labelled Aβ (Hickman *et al.*, 2008) and internalise it into large, intracellular compartments identified as lysosomes using the lysosomal membrane glycoprotein marker LAMP-1 (Halle *et al.*, 2008).

There are a variety of assays available to study the mechanisms of phagocytosis *in vitro*: the direct visualisation of engulfed particles, spectrophotometric evaluation of phagocytosed paraffin dye-containing droplets and scintillation counting of radiolabeled bacteria (Harvath and Terle, 1999). More recently, flow cytometry has been used to assess the phagocytosis of commercially-available fluorescently-labelled bacteria and latex beads by a variety of cell types. Flow cytometry has the advantage of rapid analysis of thousands of cells combined with the ability to quantify internalised particles for each cell examined. The benefits of speed, accuracy, and the ability to accumulate information on individual cell populations have resulted in flow cytometry being a preferred method for the study of phagocytosis.

The uptake of beads and Aβ was primarily by phagocytosis since it was inhibited by pre-treatment with cytochalasin D, a cell permeable and potent inhibitor of actin polymerisation. Cytochalasin D did not completely abrogate the uptake of beads or Aβ by glial cells; this was unlikely due to the concentration used as, in the case of the beads, a plateau effect was observed at the lowest drug concentration. In contrast, cytochalasin D inhibited the uptake of FITC-labelled Aβ in a concentration-dependent manner, suggesting different uptake methods of latex beads and Aβ.

One possible explanation for the incomplete inhibition of phagocytosis by cytochalasin D may be that beads and/or Aβ are also taken up into the cell by a mechanism independent of actin polymerisation. In this context, it is interesting to note that a recent study also demonstrated uptake of polystyrene particles by phagocytic cells even in the presence of cytochalasin D (Hofer *et al.*, 2009). Another possibility is that the beads and fluorescently-labelled Aβ are incompletely taken up and simply stick to the outside of the cells. However this is unlikely as extracellular fluorescence was routinely quenched using trypan blue to allow discrimination between adherent and ingested fluorescent particles (Van Amersfoort and Van Strijp, 1994). A sensitive procedure based on zymosan-induced luminol-enhanced chemiluminescence (CL) used to assess the phagocytic responses of microglia and astrocytes via indirect measurement of ROS, also confirmed that that both cell types were capable of mounting a significant phagocytic response. In the case of this assay, microglia were found to be slightly more efficient at generating an oxidative burst compared to astrocytes.

While it is well established that microglia act as phagocytes within the CNS, results presented here suggest that astrocytes also have a significant role to play. These findings are consistent with data demonstrating that neurons and astrocytes have the ability to internalise FITC-labelled Aβ *in vitro* (Mandrekar *et al.*, 2009). These authors, however, state that astrocytes were heterogeneous with respect to their ability to take up Aβ; one population of cells internalised Aβ as efficiently as microglia while another population took up no Aβ at all. Results presented here suggest that the uptake of latex beads and FITC-labelled Aβ by astrocytes was homogeneous and that they appeared to be almost as efficient as microglia. As astrocytes express receptors purported to be involved in phagocytosis such as TLR2, TLR4 and RAGE, it could therefore be anticipated that they are efficient phagocytes (Casula *et al.*, 2011).

In order to investigate the effect of Aβ on microglia and astrocytes *in vitro*, isolated cell cultures were incubated with aggregated Aβ which was found to increase mRNA expression of the cytokines IL-1β, IL-6, iNOS and TNFα. This was paralleled by an increase in markers of microglial activation, CD11b and CD40. Interestingly CD68, a protein suggested to be indicative of phagocytic activity (Zotova *et al.*, 2011), was also increased following Aβ treatment. The evidence suggests that Aβ resulted in astrocytic activation as increased mRNA expression of GLT-1 was also observed. In contrast, Aβ decreased GFAP and S100β mRNA, although this did not translate to a change in protein expression. Perhaps most interestingly, results from the current study demonstrate that Aβ significantly increased the phagocytosis of fluorescently-labelled latex beads by both microglia and astrocytes.

Stimulation of microglia and astrocytes with Aβ has previously been shown to dose-dependently increase the release of cytokines such as IL-1β, IL-6, TNFα and the chemokines MIP-1α and MCP-1 (Floden and Combs, 2006, Benveniste *et al.*, 2001, Veerhuis *et al.*, 2005). This is consistent with results observed in the present study. In addition, Aβ stimulation has been shown to result in the production of glutamate (Klegeris and McGeer, 1997), a possible explanation for the observed increase in GLT-1 mRNA. Glutamate transporters on astrocytes are responsible for homeostasis of extracellular glutamate in the CNS, something which is thought to contribute to the prevention of excitotoxic neurodegeneration (Takeuchi *et al.*, 2008).

In the AD brain, accumulation of Aβ is accompanied by various inflammatory changes; several studies have reported increases in IL-1β (Shaftel *et al.*, 2008) and others have suggested that TNFα and IL-6 are also increased (Huell *et al.*, 1995). These changes parallel the well described activation of microglia and astrocytes. While controlled inflammatory changes may stimulate cells to become phagocytic and clear Aβ, it has been proposed that persistent inflammation, which occurs with age and in AD, is associated with microglial senescence. Streit and colleagues

suggest that, in this instance, cells lose their ability to phagocytose and undertake neuroprotective functions, consequently contributing to, or even causing, neurodegenerative changes (Streit *et al.*, 2008).

Multiple Aβ binding proteins have been identified within the CNS, engagement of which result in the activation of numerous parallel signalling cascades leading to the complex cellular responses to Aβ (Lucin and Wyss-Coray, 2009). Some of the putative cellular Aβ receptors include the class A SRs (SR-A), class B SRs (SR-B) including SR-B1, CD36 and CD47, RAGE and TLRs 2, 4, 6 and 9, (Bamberger *et al.*, 2003, Paresce *et al.*, 1996, Reed-Geaghan *et al.*, 2009, Stewart *et al.*, 2010). Microglia have been shown to internalise aggregates of Aβ via SRs, evidenced by the ability of SR ligands to inhibit Aβ uptake (Paresce *et al.*, 1996). Microglia lacking TLR2 and TLR4 are unable to produce ROS or a mount phagocytic response following stimulation with Aβ (Reed-Geaghan *et al.*, 2009), whereas increased expression of TLR2 and TLR4 have been observed in the AD brain and animal models of AD (Reed-Geaghan *et al.*, 2010). Injection of Aβ into the hippocampus induces TLR2 expression (Trudler *et al.*, 2010) whereas functional TLR2 blocking antibodies suppress the Aβ-increased expression of pro-inflammatory cytokines and activation markers in microglia (Jana *et al.*, 2008).

The present findings indicate that Aβ increased mRNA expression of TLR2 in microglia, whereas it increased TLR2, TLR4, SR-B1, CD36 and CD47 expression in astrocytes. In contrast, RAGE mRNA was decreased in astrocytes following stimulation with Aβ. The data indicate that these receptors are involved in the complex cellular responses to Aβ, although their individual roles remain to be further elucidated. It will be of interest to assess the effect of inhibiting the actions of individual receptors on Aβ-induced inflammatory and phagocytic responses.

To assess whether the changes induced by Aβ *in vitro* translated to an *in vivo* setting, animals were infused with Aβ for 28 days and tissue was taken for analysis

of markers of inflammation. The data indicate that Aβ induced increases in IL-1β mRNA expression and also in TNFα and iNOS mRNA, although the latter did not reach statistical significance. Several studies have previously reported that chronic infusion of Aβ for 28 days is associated with persistent inflammatory changes (Craft *et al.*, 2004, Frautschy *et al.*, 2001). Increased hippocampal concentrations of IL-1β and TNFα have been observed 5 weeks subsequent to the infusion period (Craft *et al.*, 2004). These changes are reportedly accompanied by evidence of oxidative changes and loss of synapses (Frautschy *et al.*, 2001).

In addition to the Aβ-induced increase in cytokines, the present data demonstrate there was an increase in expression of some markers of glial activation, for example the number of $CD11b^+$ cells was enhanced in tissue prepared from Aβ- compared with control-treated animals. This is in agreement with a study reporting increased numbers of $F4/80^+$ microglia following Aβ-infusion (Craft *et al.*, 2004). Whereas a single injection of Aβ has been shown to increase other markers of microglial activation such as MHC-II (Lyons *et al.*, 2007, Lynch *et al.*, 2007), chronic Aβ infusion exerted no significant effect on this measure, or on expression of CD68 mRNA. Interestingly, uptake of fluorescently-labelled latex beads by $CD11b^+$ cells was similar in preparations obtained from control- and Aβ-treated rats. This lack of effect of Aβ on microglial phagocytosis contrasts with *in vitro* results; thus highlighting the difficulty in translating findings from one preparation to another and further indicates a limitation of undertaking analysis *in vitro* only.

Several markers of astrocytic activation were examined in tissue prepared from control- and Aβ-treated rats. The data demonstrate there was an increase in GFAP mRNA but not S100β, GLT-1 or glutamine synthetase. While GFAP is the most commonly-used marker of astrocytic activation, it is accepted that it is not expressed on all astrocytes (Walz and Lang, 1998), including astrocytes with end-feet that contact small blood vessels (Simard *et al.*, 2003). Conversely, non-astrocytic ependymal cells have been reported to express GFAP (Chen *et al.*, 2007). The

glutamate transporter, GLT-1, is expressed on astrocytes although its expression is region-specific (Wang and Bordey, 2008) and neuronal expression has also been reported (Yang *et al.*, 2010). Similarly, expression of S100β on different astrocytic populations is not uniform (Steiner *et al.*, 2007) and it has also been identified in other cell types including neurons and microglia (Shapiro *et al.*, 2010). Glutamine synthetase (Gras *et al.*, 2003) and GLAST (van Landeghem *et al.*, 2001) are also reported to be expressed by microglia. Therefore, while there is no ideal marker of activated astrocytes, GFAP is generally accepted as the most appropriate, and the present data indicates that Aβ increased its expression.

As GFAP is expressed intracellularly, it is not appropriate for flow cytometry, and therefore GLAST was selected to identify astrocytes for the purpose of this study. The antibody chosen has been shown to recognise the extracellular epitope of GLAST by immunohistochemistry, immunocytochemistry and flow cytometry (Jungblut *et al.*, 2012). While there was no difference in expression of GLAST mRNA or the number of $GLAST^+$ cells in the preparation obtained from Aβ- compared with control-treated rats, there was a significant increase in the number of $GLAST^+$ cells which phagocytosed fluorescently-labelled latex beads *ex vivo*.

While both astrocytes and microglia exhibit increased Aβ-induced phagocytosis *in vitro*, it appears that astrocytes have a more important role to play in clearing Aβ *in vivo* following a 28-day time point. It would be of interest to infuse Aβ for varying time-periods so as to establish if this occurred as result of a switch from microglial to astrocytic activation over time. The current data is interesting in relation to results observed by Grathwohl and colleagues, who demonstrated that the ablation of microglia in a mouse model of AD for up to 4 weeks resulted in no changes in amyloid plaque maintenance or formation (Grathwohl *et al.*, 2009). This unexpected finding indicates that, at least in some conditions, microglia appear to have minimal impact on Aβ accumulation. The concomitant activation of astrocytes observed in Grathwohl's study perhaps suggests these cells have the ability to perform a role

similar to that of the absent microglia. It might be concluded that, at least as far as phagocytosis is concerned, there is a certain amount of redundancy in the system.

Perhaps the most significant finding described here is that astrocytes appear to be efficient phagocytes. The data also demonstrate that astrocytes, in addition to microglia, exhibit an enhanced capacity for phagocytosis following stimulation with Aβ *in vitro*. This was observed in parallel with increased mRNA expression of markers of activation, pro-inflammatory cytokines and putative Aβ receptors in both cell types. While such markers of inflammation were also increased *in vivo* following infusion of Aβ for 28 days, only $GLAST^+$ astrocytes were found to exhibit enhanced phagocytic properties following the treatment period. A role for astrocytes in the modulation of Aβ phagocytosis is therefore suggested as an area to explore in finding ways to clear Aβ from the AD brain.

4: Investigating the role of some putative Aβ receptors in the Aβ-induced activation of astrocytes *in vitro*

4.1 Introduction

Multiple Aβ binding receptors have been identified within the CNS, engagement of which leads to activation of numerous parallel signalling cascades resulting in the complex cellular responses to Aβ (Lucin and Wyss-Coray, 2009). Recognition of Aβ has been shown to occur through an ensemble of cell-surface receptors including CD36, CD47, TLR2, TLR4 and RAGE (Jana et al., 2008, Reed-Geaghan et al., 2009, Bamberger et al., 2003). While numerous studies detail the role of these receptors in the Aβ-induced stimulation of microglia; reports of their function in the response of astrocytes to Aβ are far less plentiful. The previous chapter demonstrated that Aβ increased mRNA expression of CD36, CD47, TLR2 and TLR4 in primary astrocytes, while it decreased that of RAGE mRNA, thus suggesting these receptors are involved in the Aβ-induced activation of astrocytes. Therefore, it was of interest to confirm this proposal by assessing the effect of blocking these receptors to try and further elucidate their role in Aβ-induced inflammatory and phagocytic responses.

TLRs play a critical role in the innate immune system, acting as PRRs for structurally-conserved molecules derived from microbes (Carpenter and O'Neill, 2009). TLR2 ligands, including constituents of microbial cell walls such as bacterial lipopeptides and lipoteichoic acid, signal via activation of NFκB and c-Jun N-terminal kinase (JNK) pathways ultimately resulting in the increased expression of pro-inflammatory cytokines and stimulation of phagocytosis (Palsson-McDermott and O'Neill, 2007).

SRs, such as CD36, are cell surface proteins that mediate adhesion to, and endocytosis of, various native and pathologically modified-substances. CD36 is thought to play an important role in CNS homeostasis acting as a mediator of the phagocytosis of apoptotic cells, lipid metabolism, and endocytosis of native, denatured, and chemically modified proteins and lipoproteins (Husemann *et al.*, 2002). CD47, also referred to as integrin-associated protein, is a ubiquitously-

expressed transmembrane protein that reportedly acts as a '*don't eat me*' signal for phagocytic cells (Willingham et al., 2012). Integrins are important receptors that mediate cell–extracellular matrix (ECM) and cell–cell adhesion events, thus playing an important role in passing information to the cell about its surroundings, resulting in the regulation of cell cycle, shape and motility (Wu *et al.*, 2011). A receptor complex comprising the integrin-associated protein CD47, CD36 and the α6β1 integrin has recently been described as a receptor for fibrillar Aβ on microglia (Bamberger *et al.*, 2003, Reed-Geaghan *et al.*, 2009).

RAGE is a multi-ligand member of the IgG super-family of cell surface molecules that is reported to act as an Aβ receptor on neurons, microglia and astrocytes (Lue *et al.*, 2001). Activation of RAGE by many of its ligands, including Aβ, results in the release of pro-inflammatory cytokines and ROS, chiefly mediated by activation of the transcription factor NFκB (Basta *et al.*, 2002, Berbaum *et al.*, 2008). In its inactivated state, NFκB is located in the cytosol complexed with its inhibitory protein, IκBα. Following activation of IκB kinase, IκBα becomes phosphorylated, leading to its ubiquitination, dissociation from NFκB and eventual degradation by the proteasome. NFκB is then free to translocate to the nucleus and participate in the transcriptional regulation of its target genes (Camandola and Mattson, 2007). Such genes in the CNS include numerous proteins associated with immune and inflammatory activities; although there is some evidence that NFκB also plays a role in processes such as neuronal plasticity and development (O'Neill and Kaltschmidt, 1997).

For the purpose of this study, wedelolactone was chosen to investigate the effect of NFκB inhibition on the Aβ-induced stimulation of astrocytes *in vitro*. Wedelolactone acts as a cell-permeable, selective and irreversible inhibitor of IκB kinase activity, blocking the phosphorylation and degradation of IκBα and thus preventing NFκB from translocating to the nucleus. A herbal medicine derived from *Eclipta prostrata*,

wedelolactone is associated with having anti-inflammatory and growth inhibitory properties in chronic diseases such as cancer (Lim *et al.*, 2012).

The aims of these studies were as follows:

1. To assess the effects of blocking the activity of RAGE, TLR2, CD36 and CD47 on the Aβ-induced release of pro-inflammatory cytokines and phagocytosis by primary astrocytes *in vitro*.
2. To assess the effects of NFκB inhibition on the Aβ-induced release of pro-inflammatory cytokines and phagocytosis by astrocytes *in vitro*.

4.2 Methods

Primary astrocytes, isolated from the brains of three neonatal rats as described in section 2.1.5, were incubated with a cocktail of aggregated Aβ, or reverse peptide $A\beta_{40\text{-}1}$ (10μM), for 24 hours in combination with anti-RAGE, anti-TLR2, anti-CD36 or anti-CD47 neutralising antibodies or their appropriate IgG controls (all at 2.5μg/ml). These neutralising antibodies reportedly block 50% of binding at the concentrations used. In a further set of experiments, astrocytes were incubated with Aβ or reverse peptide in combination with the NFκB inhibitor wedelolactone (25μM) or vehicle control for 24 hours. The data shown are from one of three independent experiments with similar results, performed on cells obtained from separate isolations.

After 24 hours, release of IL-1β, IL-6 and TNFα into the supernatant was assessed by ELISA as described in section 2.11. Phagocytosis of fluorescently-labelled latex beads was also assessed using flow cytometry as described in section 2.7.1.

4.3 Results

4.3.1 Analysis of the effect of TLR2 inhibition on the Aβ-induced release of pro-inflammatory cytokines and phagocytosis by astrocytes *in vitro*.

A 2-way ANOVA followed by *post-hoc* analysis revealed that incubation of isolated neonatal astrocytes with Aβ induced the release of IL-1β, IL-6 and TNFα ($p<0.01$), as shown in figure 4.1. The data further demonstrate that inhibition of TLR2 significantly attenuated the Aβ-induced release of these pro-inflammatory cytokines ($p<0.01$).

A 2-way ANOVA followed by *post-hoc* analysis revealed that Aβ enhanced the phagocytosis of fluorescently-labelled latex beads by astrocytes *in vitro* ($p<0.05$) as shown in figure 4.2. Inhibition of TLR2 had no effect on the phagocytosis of latex beads by control- or Aβ-stimulated astrocytes.

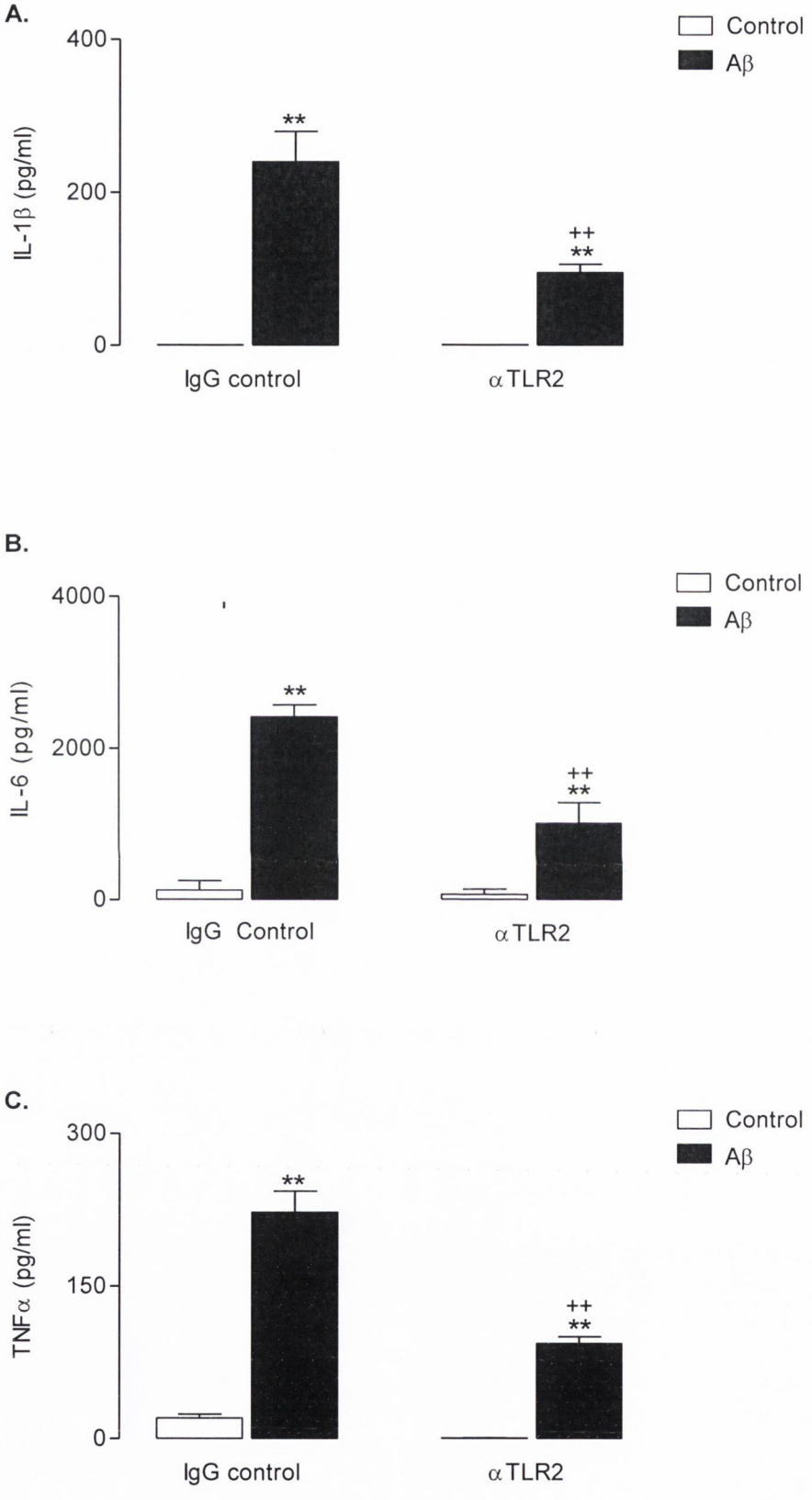
A.
400
200
0
IL-1β (pg/ml)
**
++
**
Control
Aβ
IgG control
αTLR2
B.
4000
2000
0
IL-6 (pg/ml)
**
++
**
Control
Aβ
IgG Control
αTLR2
C.
300
150
0
TNFα (pg/ml)
**
++
**
Control
Aβ
IgG control
αTLR2

Figure 4.1 Inhibition of TLR2 attenuated the Aβ-induced release of IL-1β, IL-6 and TNFα by isolated astrocytes.

Isolated neonatal astrocytes were co-incubated with Aβ or reverse peptide and anti-TLR2 or its IgG control for 24 hours *in vitro*. After 24 hours, supernatant concentrations of IL-1β (A), IL-6 (B) and TNFα (C) were determined by ELISA. Aβ induced the release of IL-1β, IL-6 and TNF-α by isolated astrocytes ($p<0.01$). Co-incubation with anti-TLR2 significantly attenuated the Aβ-induced release of IL-1β, IL-6 and TNFα ($p<0.01$). Data are expressed as means + SEM ($n=4$) from one of three independent experiments with similar results. $^{**}p<0.01$ versus vehicle control; $^{++}p<0.01$ versus IgG control (2-way ANOVA followed by Newman-Keuls *post-hoc* analysis).

A: $A\beta_{effect}$ [$F_{(1,12)}=67.16$, $p<0.0001$], $antibody_{effect}$ [$F_{(1,12)}=12.54$, $p=0.0041$], $interaction_{effect}$ [$F_{(1,12)}=12.54$, $p=0.0041$]. **B:** $A\beta_{effect}$ [$F_{(1,12)}=85.71$, $p<0.0001$], $antibody_{effect}$ [$F_{(1,12)}=17.64$, $p=0.0012$], $interaction_{effect}$ [$F_{(1,12)}=15.06$, $p=0.0022$]. **C:** $A\beta_{effect}$ [$F_{(1,12)}=178.23$, $p<0.0001$], $antibody_{effect}$ [$F_{(1,12)}=45.65$, $p=0.0004$], $interaction_{effect}$ [$F_{(1,12)}=24.1$, $p=0.0004$].

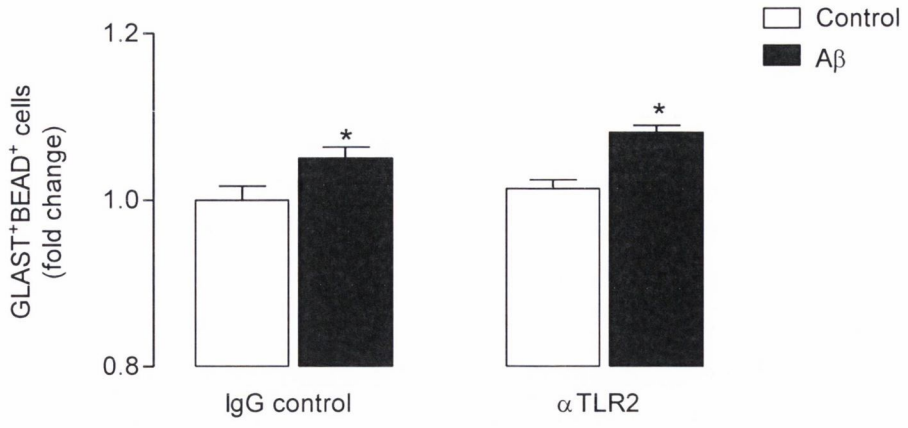

Figure 4.2 Inhibition of TLR2 had no effect on the phagocytosis of fluorescently-labelled latex beads by isolated astrocytes.

Isolated astrocytes were co-incubated with Aβ or reverse peptide and anti-TLR2 or its IgG control for 24 hours *in vitro* and phagocytosis of fluorescently-labelled latex beads was assessed using flow cytometry. Aβ increased the phagocytosis of fluorescently-labelled latex beads by control- and Aβ-stimulated astrocytes ($p<0.05$), but no effect of TLR2 inhibition was observed. Data are expressed as means + SEM ($n=4$) from one of three independent experiments with similar results. *$p<0.05$ versus vehicle control (2-way ANOVA followed by Newman-Keuls *post-hoc* analysis).

$A\beta_{effect}$ [$F_{(1,12)}=5.88$, $p=0.0197$], $antibody_{effect}$ [$F_{(1,12)}=0.88$, $p=0.354$], $interaction_{effect}$ [$F_{(1,12)}=0.13$, $p=0.7216$].

4.3.2 Analysis of the effect of CD36 inhibition on the Aβ-induced release of pro-inflammatory cytokines and phagocytosis by astrocytes *in vitro*.

A 2-way ANOVA followed by *post-hoc* analysis revealed that incubation of isolated neonatal astrocytes with Aβ induced the release of IL-1β, IL-6 and TNFα ($p<0.01$), as shown in figure 4.3. The data further demonstrate that co-incubation with anti-CD36 significantly enhanced the Aβ-induced release of these pro-inflammatory cytokines ($p<0.01$).

A 2-way ANOVA followed by *post-hoc* analysis revealed that Aβ enhanced the phagocytosis of fluorescently-labelled latex beads by astrocytes *in vitro* ($p<0.05$) as shown in figure 4.4. Inhibition of CD36 reduced the phagocytosis of latex beads by both control- and Aβ-stimulated astrocytes ($p<0.01$).

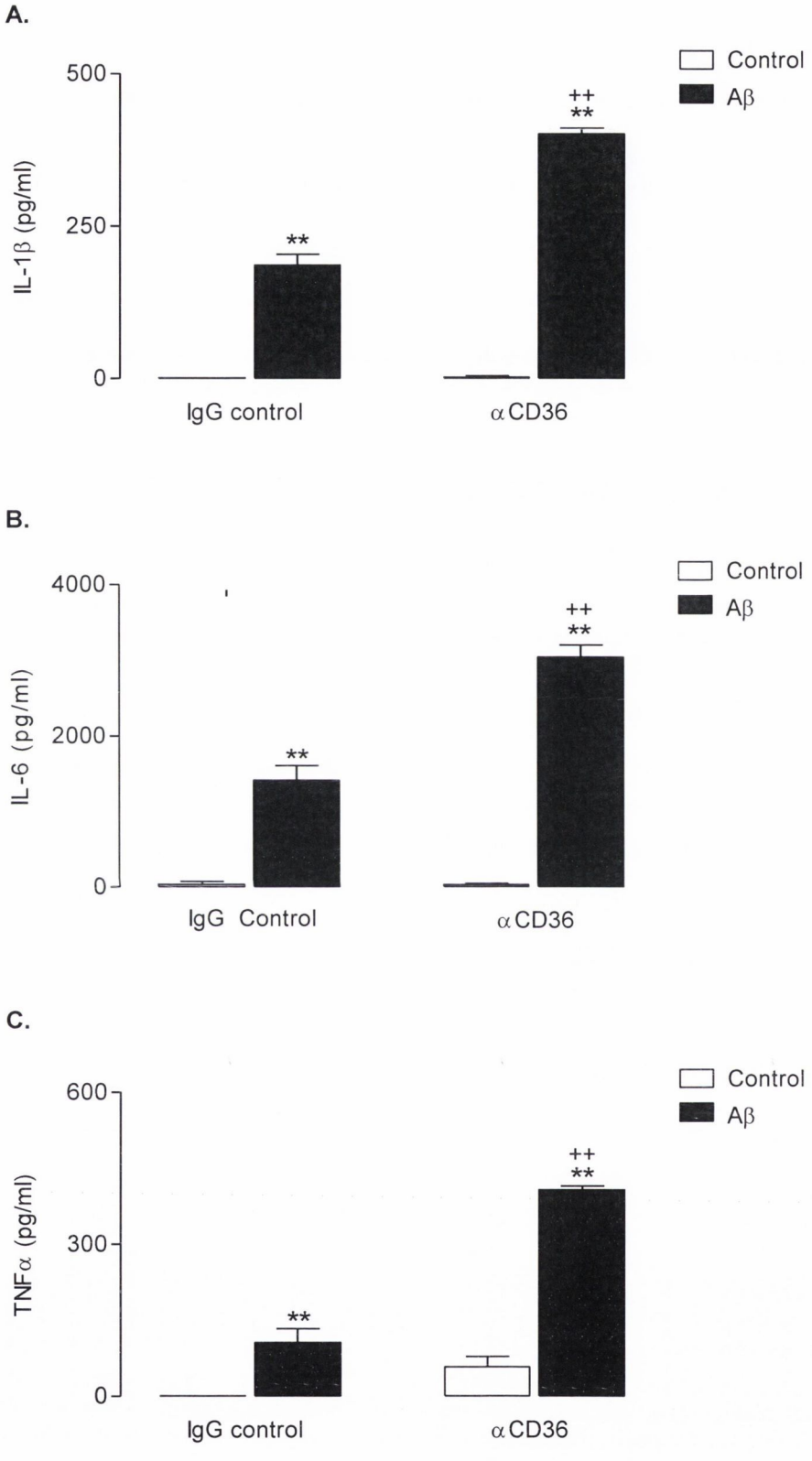
A.
Control
Aβ
500
250
0
IL-1β (pg/ml)
**
++
**
IgG control
αCD36
B.
Control
Aβ
4000
2000
0
IL-6 (pg/ml)
**
++
**
IgG Control
αCD36
C.
Control
Aβ
600
300
0
TNFα (pg/ml)
**
++
**
IgG control
αCD36

Figure 4.3 Inhibition of CD36 enhanced the Aβ-induced release of IL-1β, IL-6 and TNFα by isolated astrocytes.

Isolated astrocytes were co-incubated with Aβ or reverse peptide and anti-CD36 or its IgG control for 24 hours *in vitro*. After 24 hours, supernatant concentrations of IL-1β (A), IL-6 (B) and TNFα (C) were determined by ELISA. Aβ induced the release of IL-1β, IL-6 and TNF-α by isolated astrocytes ($p<0.01$). Co-incubation with anti-CD36 enhanced the Aβ-induced release of IL-1β, IL-6 and TNFα ($p<0.01$). Data are expressed as means + SEM ($n=4$) from one of three independent experiments with similar results. $^{**}p<0.01$ versus vehicle control; $^{++}p<0.01$ versus IgG control (2-way ANOVA followed by Newman-Keuls *post-hoc* analysis).

A: $A\beta_{effect}$ $[F_{(1,12)}=855.84,\ p<0.0001]$, $antibody_{effect}$ $[F_{(1,12)}=117.73,\ p<0.0001]$, $interaction_{effect}$ $[F_{(1,12)}=112.90,\ p<0.0001]$. **B:** $A\beta_{effect}$ $[F_{(1,12)}=303.33,\ p<0.0001]$, $antibody_{effect}$ $[F_{(1,12)}=41.39,\ p<0.0001]$, $interaction_{effect}$ $[F_{(1,12)}=42.13,\ p<0.0001]$. **C:** $A\beta_{effect}$ $[F_{(1,12)}=174.94,\ p<0.0001]$, $antibody_{effect}$ $[F_{(1,12)}=109.2,\ p<0.0001]$, $interaction_{effect}$ $[F_{(1,12)}=49.92,\ p<0.0001]$.

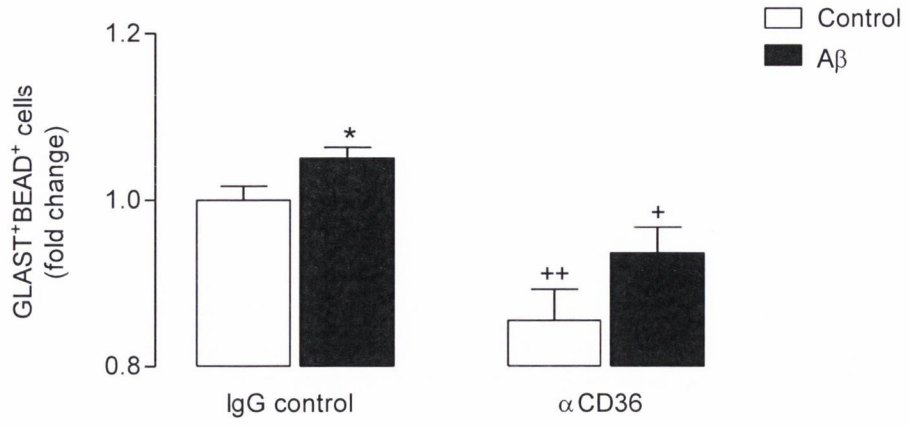

Figure 4.4 Inhibition of CD36 reduced the phagocytosis of fluorescently-labelled latex beads by control- and Aβ-stimulated astrocytes.

Isolated astrocytes were co-incubated with Aβ or reverse peptide and anti-CD36 or its IgG control for 24 hours *in vitro* and phagocytosis of fluorescently-labelled latex beads was assessed using flow cytometry. Aβ increased the phagocytosis of fluorescently-labelled latex beads by isolated astrocytes ($p<0.05$). Co-incubation with anti-CD36 reduced the phagocytosis of fluorescently-labelled latex beads by both control- ($p<0.01$) and Aβ-stimulated ($p<0.05$) cells. Data are expressed as means + SEM ($n=4$) from one of three independent experiments with similar results. $^{*}p<0.05$ versus vehicle control; $^{+}p<0.05$; $^{++}p<0.01$ versus IgG control (2-way ANOVA followed by Newman-Keuls *post-hoc* analysis).

$A\beta_{effect}$ [$F_{(1,12)}=6.25$, $p=0.0164$], $antibody_{effect}$ [$F_{(1,12)}=24.496$, $p<0.0001$], $interaction_{effect}$ [$F_{(1,12)}=0.342$, $p=0.5618$].

4.3.3 Analysis of the effect of CD47 inhibition on the Aβ-induced release of pro-inflammatory cytokines and phagocytosis by astrocytes *in vitro*.

A 2-way ANOVA followed by *post-hoc* analysis revealed that incubation of isolated neonatal astrocytes with Aβ induced the release of IL-1β, IL-6 and TNFα ($p<0.01$), as shown in figure 4.5. The data further demonstrate that co-incubation with anti-CD47 significantly attenuated the Aβ-induced release of IL-1β ($p<0.05$), TNFα ($p<0.01$) and IL-6 ($p<0.01$).

A 2-way ANOVA followed by *post-hoc* analysis revealed that Aβ enhanced the phagocytosis of fluorescently-labelled latex beads by astrocytes *in vitro* ($p<0.05$) as shown in figure 4.6. Inhibition of CD47 significantly reduced the phagocytosis of latex beads by control-treated cells only ($p<0.05$).

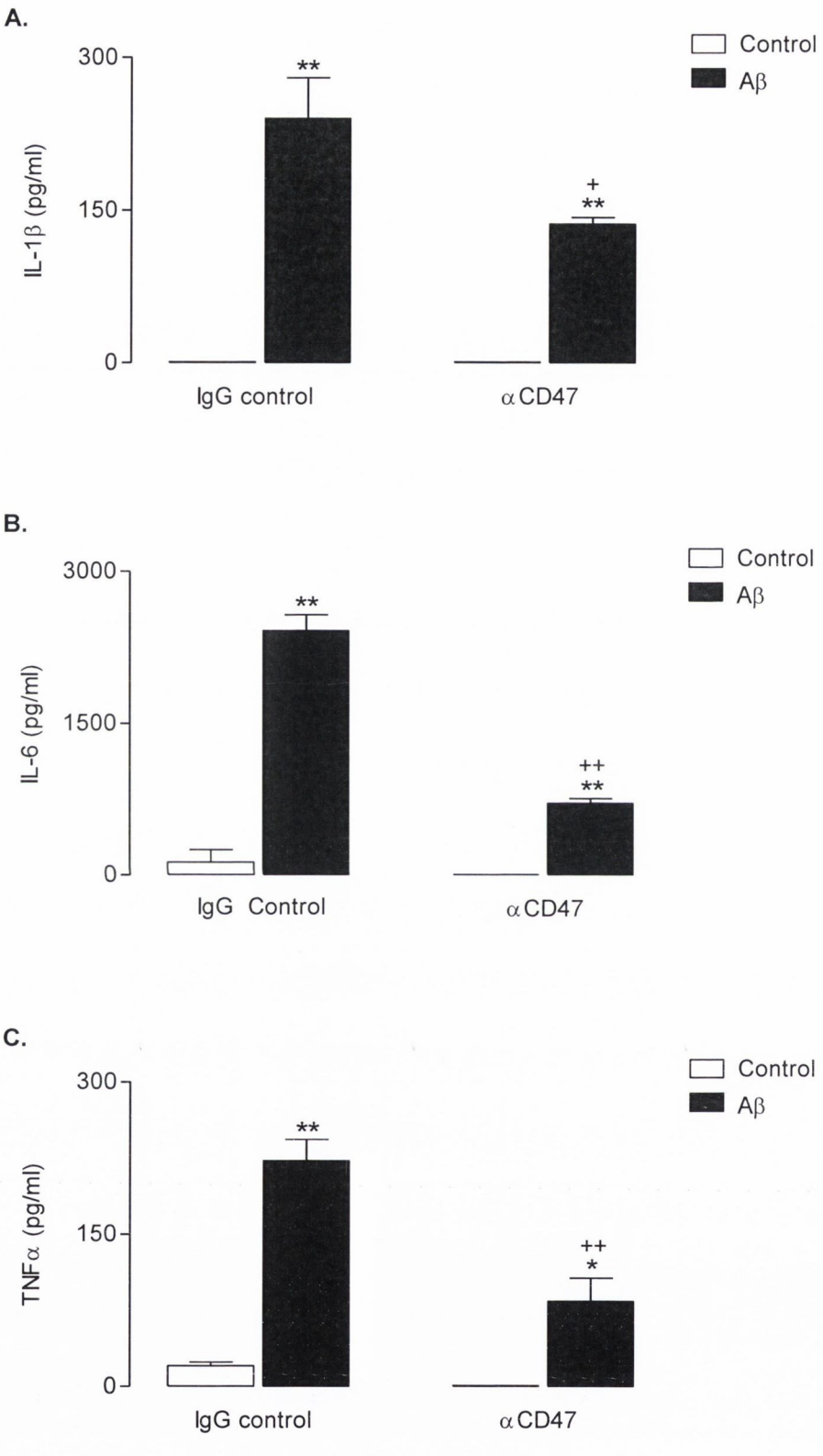
A.
Control
Aβ
IL-1β (pg/ml)
300
150
0
**
+
**
IgG control
αCD47
B.
Control
Aβ
IL-6 (pg/ml)
3000
1500
0
**
++
**
IgG Control
αCD47
C.
Control
Aβ
TNFα (pg/ml)
300
150
0
**
++
*
IgG control
αCD47

Figure 4.5 Inhibition of CD47 attenuated the Aβ-induced release of IL-1β, IL-6 and TNFα by isolated astrocytes.

Isolated astrocytes were co-incubated with Aβ or reverse peptide and anti-CD47 or its IgG control for 24 hours *in vitro*. After 24 hours, supernatant concentrations of IL-1β (A), IL-6 (B) and TNFα (C) were determined by ELISA. Aβ induced the release of IL-1β, IL-6 and TNF-α by isolated astrocytes ($p<0.01$). Inhibition of CD47 significantly attenuated the Aβ-induced release of IL-1β, IL-6 and TNFα ($p<0.01$). Data are expressed as means + SEM ($n=4$) from one of three independent experiments with similar results. *$p<0.05$, **$p<0.01$ versus vehicle control; $^{+}p<0.05$, $^{++}p<0.01$ versus IgG control (2-way ANOVA followed by Newman-Keuls *post-hoc* analysis).

A: $A\beta_{effect}$ [$F_{(1,12)}=64.22$, $p<0.0001$], $antibody_{effect}$ [$F_{(1,12)}=4.87$, $p=0.0518$], $interaction_{effect}$ [$F_{(1,12)}=4.87$, $p=0.0518$]. **B:** $A\beta_{effect}$ [$F_{(1,12)}=153.67$, $p<0.0001$], $antibody_{effect}$ [$F_{(1,12)}=57.24$, $p<0.0001$], $interaction_{effect}$ [$F_{(1,12)}=42.55$, $p<0.0001$]. **C:** $A\beta_{effect}$ [$F_{(1,12)}=82.58$, $p<0.0001$], $antibody_{effect}$ [$F_{(1,12)}=25.53$, $p=0.0005$], $interaction_{effect}$ [$F_{(1,12)}=14.04$, $p=0.0038$].

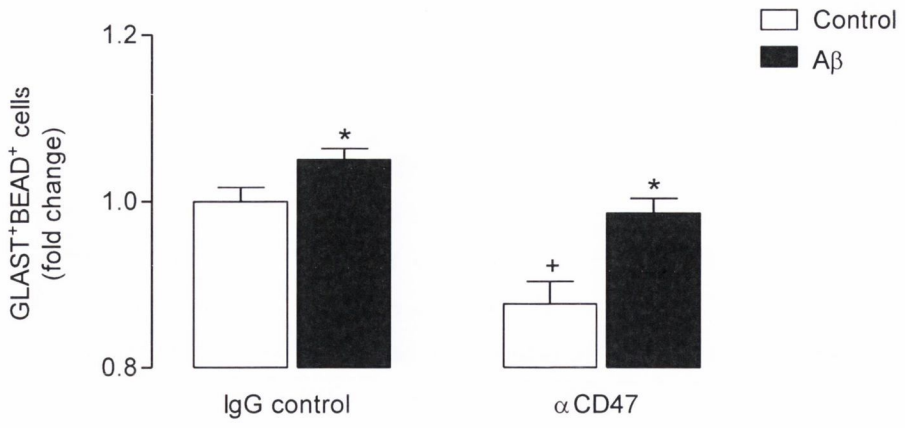

Figure 4.6 Blocking CD47 reduced the phagocytosis of fluorescently-labelled latex beads by isolated astrocytes.

Isolated astrocytes were co-incubated with Aβ or reverse peptide and anti-CD47 or its IgG control for 24 hours *in vitro* and phagocytosis of fluorescently-labelled latex beads was assessed using flow cytometry. Aβ increased the phagocytosis of fluorescently-labelled latex beads by isolated astrocytes ($p<0.05$). Inhibition of CD47 reduced the phagocytosis of fluorescently-labelled latex beads by control-treated cells ($p<0.05$). Data are expressed as means + SEM ($n=4$) from one of three independent experiments with similar results. *$p<0.05$ versus vehicle control; $^{+}p<0.05$ versus IgG control (2-way ANOVA followed by Newman-Keuls *post-hoc* analysis).

$A\beta_{effect}$ [$F_{(1,12)}=7.82$, $p=0.0079$], $antibody_{effect}$ [$F_{(1,12)}=10.88$, $p=0.0021$], $interaction_{effect}$ [$F_{(1,12)}=1.07$, $p=0.3079$].

4.3.4 Analysis of the effect of RAGE inhibition on the Aβ-induced release of pro inflammatory cytokines and phagocytosis by astrocytes in vitro.

A 2-way ANOVA followed by *post-hoc* analysis revealed that incubation of isolated neonatal astrocytes with Aβ induced the release of IL-1β, IL-6 and TNFα ($p<0.01$), as shown in figure 4.7. The data further demonstrate that co-incubation with anti-RAGE significantly enhanced the Aβ-induced release of IL-1β ($p<0.01$). While the release of IL-6 and TNFα was also exacerbated following inhibition of RAGE, this failed to reach statistical significance.

A 2-way ANOVA followed by *post-hoc* analysis revealed that Aβ enhanced the phagocytosis of fluorescently-labelled latex beads by astrocytes *in vitro* ($p<0.05$) as shown in figure 4.8. Inhibition of RAGE significantly reduced the phagocytosis of latex beads by control- and Aβ-stimulated cells ($p<0.01$).

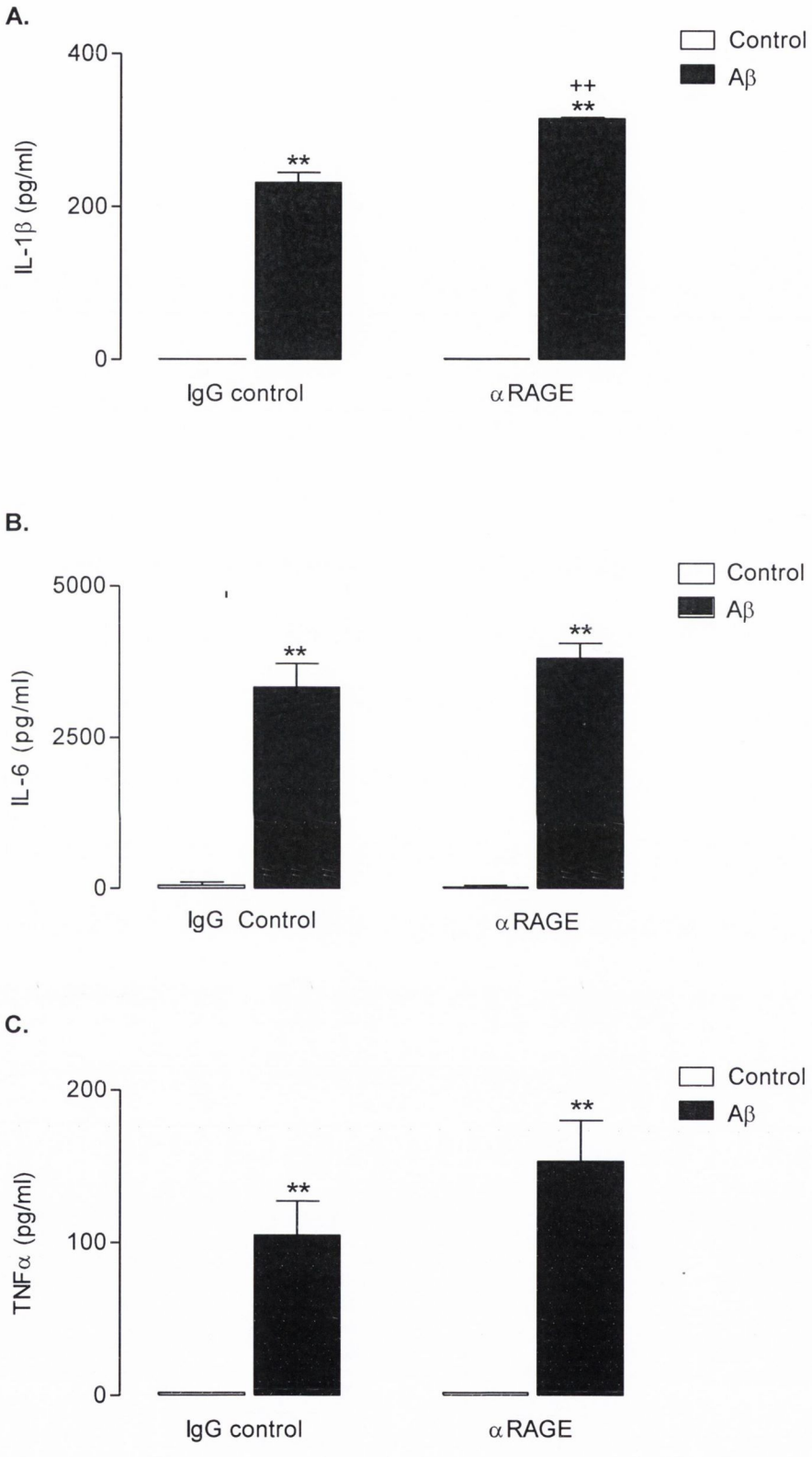
A.
Control
Aβ
400
200
0
IL-1β (pg/ml)
**
++
**
IgG control
αRAGE
B.
Control
Aβ
5000
2500
0
IL-6 (pg/ml)
**
**
IgG Control
αRAGE
C.
Control
Aβ
200
100
0
TNFα (pg/ml)
**
**
IgG control
αRAGE

Figure 4.7 Inhibition of RAGE enhanced the Aβ-induced release of IL-1β by isolated astrocytes.

Isolated astrocytes were co-incubated with Aβ or reverse peptide and anti-RAGE or its IgG control for 24 hours *in vitro*. After 24 hours, supernatant concentrations of IL-1β (A), IL-6 (B) and TNFα (C) were determined by ELISA. Aβ induced the release of IL-1β, IL-6 and TNF-α by isolated astrocytes ($p<0.01$). Inhibition of RAGE further enhanced the Aβ-induced release of IL-1β ($p<0.01$). Data are expressed as means + SEM ($n=3$-4) from one of three independent experiments with similar results. $^{**}p<0.01$ versus vehicle control; $^{++}p<0.01$ versus IgG control (2-way ANOVA followed by Newman-Keuls *post-hoc* analysis).

A: $A\beta_{effect}$ [$F_{(1,12)}=2899.44$, $p<0.0001$], $antibody_{effect}$ [$F_{(1,12)}=68.74$, $p<0.0001$], $interaction_{effect}$ [$F_{(1,12)}=67.52$, $p<0.0001$]. **B:** $A\beta_{effect}$ [$F_{(1,12)}=233.46$, $p<0.0001$], $antibody_{effect}$ [$F_{(1,12)}=0.94$, $p=0.35$], $interaction_{effect}$ [$F_{(1,12)}=1.2$, $p=0.29$]. **C:** $A\beta_{effect}$ [$F_{(1,12)}=55.35$, $p<0.0001$], $antibody_{effect}$ [$F_{(1,12)}=1.93$, $p=0.19$], $interaction_{effect}$ [$F_{(1,12)}=1.93$, $p=0.19$].

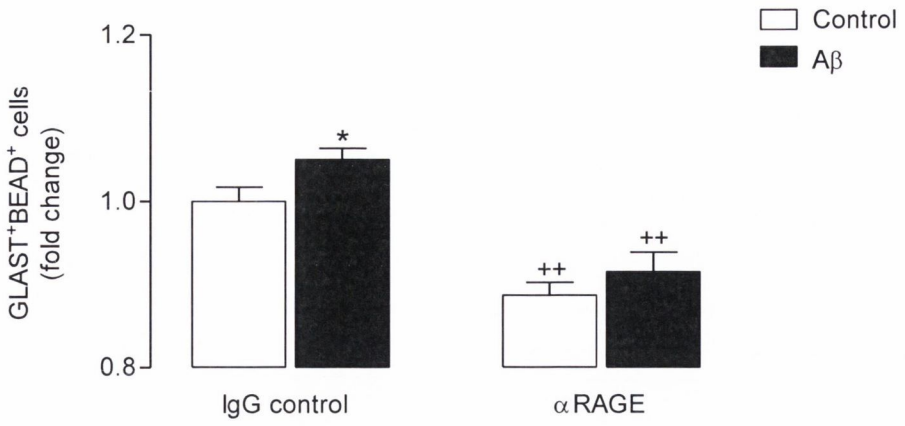

Figure 4.8 Inhibition of RAGE reduced the phagocytosis of fluorescently-labelled latex beads by control- and Aβ-stimulated astrocytes.

Isolated astrocytes were co-incubated with Aβ or reverse peptide and anti-RAGE or its IgG control for 24 hours *in vitro* and phagocytosis of fluorescently-labelled latex beads was assessed using flow cytometry. Aβ increased the phagocytosis of fluorescently-labelled latex beads by isolated astrocytes ($p<0.05$). Inhibition of RAGE reduced the phagocytosis of fluorescently-labelled latex beads by both control- and Aβ-stimulated cells ($p<0.01$). Data are expressed as means + SEM ($n=4$) from one of three independent experiments with similar results. *$p<0.05$ versus vehicle control; $^{++}p<0.01$ versus IgG control (2-way ANOVA followed by Newman-Keuls *post-hoc* analysis).

$A\beta_{effect}$ [$F_{(1,12)}=2.48$, $p=0.1226$], $antibody_{effect}$ [$F_{(1,12)}=24.99$, $p<0.0001$], $interaction_{effect}$ [$F_{(1,12)}=0.198$, $p=0.6582$].

4.3.5 Analysis of the effect of NFκB inhibition on the Aβ-induced release of pro-inflammatory cytokines and phagocytosis by astrocytes *in vitro*.

Primary cultures of isolated neonatal astrocytes were incubated with Aβ or reverse peptide in combination with wedelolactone (25μM) or its vehicle control for 24 hours *in vitro*. A 2-way ANOVA followed by *post-hoc* analysis revealed that incubation of isolated astrocytes with Aβ induced the release of IL-1β, IL-6 and TNFα ($p<0.01$), as shown in figure 4.9. The data demonstrate that co-incubation with wedelolactone significantly attenuated the Aβ-induced release of these pro-inflammatory cytokines ($p<0.01$), almost returning their concentrations to control levels.

A 2-way ANOVA followed by *post-hoc* analysis revealed that Aβ enhanced the phagocytosis of fluorescently-labelled latex beads by astrocytes *in vitro* ($p<0.01$) as shown in figure 4.10. Inhibition of NFκB activity following treatment with wedelolactone significantly reduced the phagocytosis of latex beads by control- and Aβ-stimulated astrocytes ($p<0.01$).

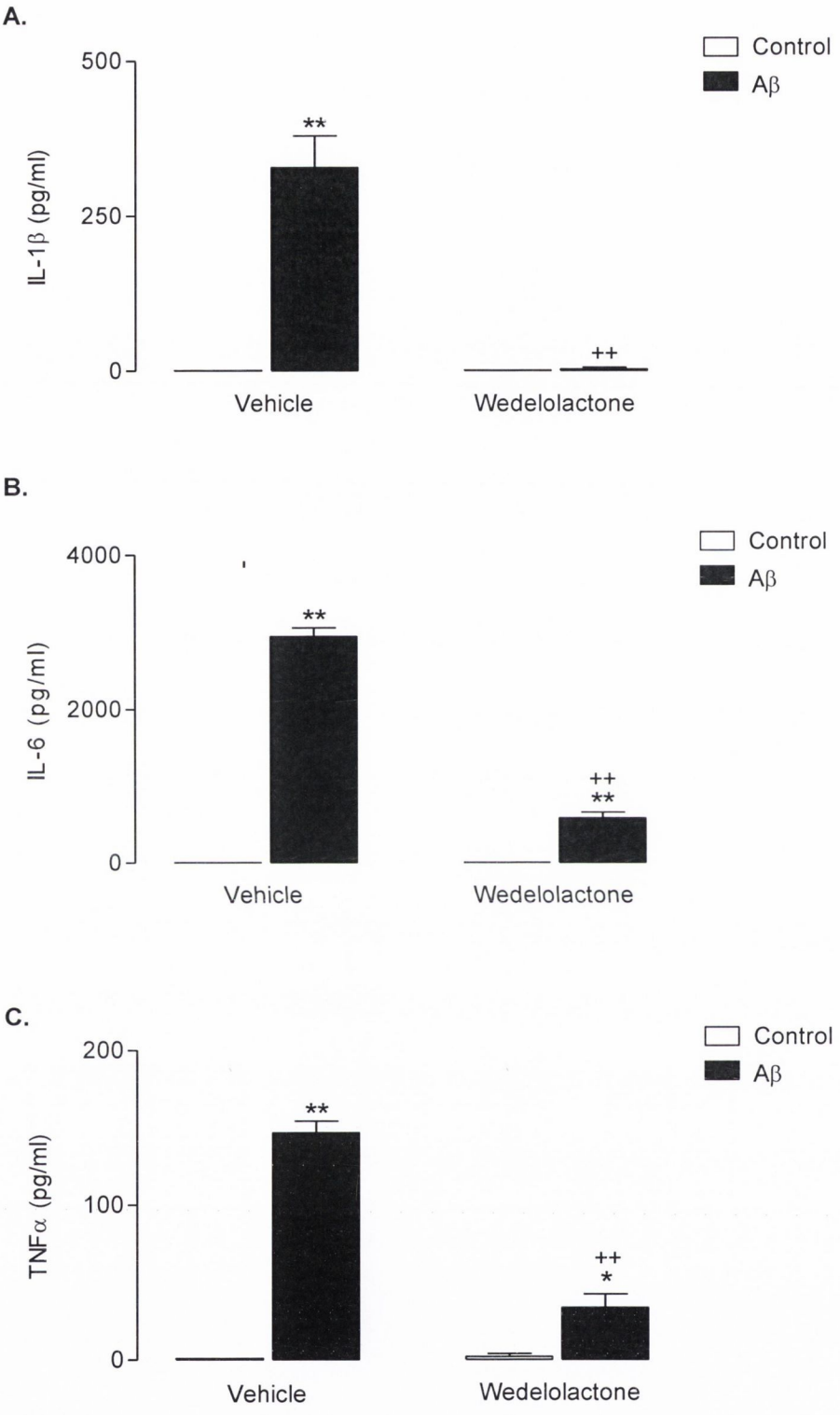
A.
Control
Aβ
500
250
0
IL-1β (pg/ml)
**
++
Vehicle
Wedelolactone
B.
Control
Aβ
4000
2000
0
IL-6 (pg/ml)
**
++
**
Vehicle
Wedelolactone
C.
Control
Aβ
200
100
0
TNFα (pg/ml)
**
++
*
Vehicle
Wedelolactone

Figure 4.9 Wedelolactone attenuated the Aβ-induced release of IL-1β, IL-6 and TNFα by isolated astrocytes.

Isolated astrocytes were co-incubated with Aβ or reverse peptide and wedelolactone or vehicle control for 24 hours *in vitro*. After 24 hours, supernatant concentrations of IL-1β (A), IL-6 (B) and TNFα (C) were determined by ELISA. Aβ induced the release of IL-1β, IL-6 and TNF-α by isolated astrocytes ($p<0.01$). Co-incubation with wedelolactone significantly attenuated the Aβ-induced release of IL-1β, IL-6 and TNFα ($p<0.01$). Data are expressed as means + SEM ($n=4$) from one of three independent experiments with similar results. *$p<0.01$, **$p<0.01$ versus vehicle control; $^{++}p<0.01$ versus wedelolactone control (2-way ANOVA followed by Newman-Keuls *post-hoc* analysis).

A: $A\beta_{effect}$ [$F_{(1,12)}=41.5$, $p<0.0001$], $wedelolactone_{effect}$ [$F_{(1,12)}=40.07$, $p<0.0001$], $interaction_{effect}$ [$F_{(1,12)}=40.07$, $p<0.0001$]. **B:** $A\beta_{effect}$ [$F_{(1,12)}=699.18$, $p<0.0001$], $wedelolactone_{effect}$ [$F_{(1,12)}=312.62$, $p<0.0001$], $interaction_{effect}$ [$F_{(1,12)}=312.62$, $p<0.0001$]. **C:** $A\beta_{effect}$ [$F_{(1,12)}=240.52$, $p<0.0001$], $wedelolactone_{effect}$ [$F_{(1,12)}=92.96$, $p<0.0001$], $interaction_{effect}$ [$F_{(1,12)}=100.11$, $p<0.0001$].

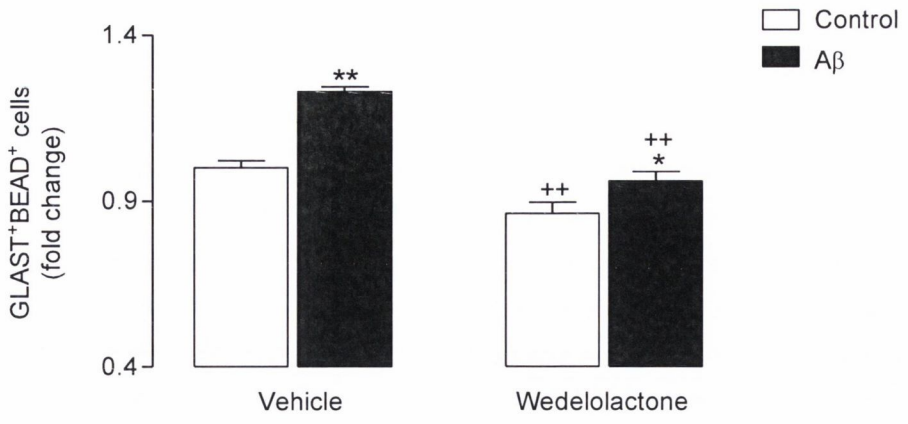

Figure 4.10 Wedelolactone reduced the phagocytosis of fluorescently-labelled latex beads by control- and Aβ-stimulated astrocytes.

Isolated astrocytes were co-incubated with Aβ or reverse peptide and wedelolactone or its vehicle control for 24 hours *in vitro* and phagocytosis of fluorescently-labelled latex beads was assessed using flow cytometry. Aβ increased the phagocytosis of fluorescently-labelled latex beads by isolated astrocytes ($p<0.01$). Co-incubation with wedelolactone reduced the phagocytosis of fluorescently-labelled latex beads by control- and Aβ-stimulated cells ($p<0.01$). Data are expressed as means + SEM ($n=4$) from one of three independent experiments with similar results. $^{*}p<0.05$ versus vehicle control; $^{++}p<0.01$ versus wedelolactone control (2-way ANOVA followed by Newman-Keuls *post-hoc* analysis).

$A\beta_{effect}$ [$F_{(1,12)}=41.42$, $p<0.0001$], $antibody_{effect}$ [$F_{(1,12)}=64.12$, $p<0.0001$], $interaction_{effect}$ [$F_{(1,12)}=6.78$, $p=0.0231$].

4.4 Discussion

The objective of the current study was to investigate a role for the putative Aβ-binding receptors TLR2, CD36, CD47 and RAGE, and the transcription factor NFκB in the activation of astrocytes by Aβ *in vitro*. The data demonstrate that incubation of primary astrocytes with Aβ for 24 hours induced release of the pro-inflammatory cytokines IL-1β, IL-6 and TNFα. Aβ also enhanced the uptake of fluorescently-labelled latex beads by these cells. This is in line with results observed in the previous chapter, which demonstrated that Aβ increased mRNA expression of IL-1β, IL-6, TNFα and iNOS. These results are consistent with others reporting the induction of a pro-inflammatory environment following stimulation of astrocytes with Aβ *in vitro* (White et al., 2005, Liu et al., 2011, LaDu et al., 2000).

While assessing the uptake of latex beads was the method chosen to estimate the phagocytic capacity of astrocytes in these experiments, it must be mentioned that these data may not reflect actual changes in the phagocytosis of Aβ. Although this could potentially have been evaluated by examining the uptake of fluorescently-labelled Aβ, this method also has its limitations, with the possibility that addition of a fluorescent tag to the peptide to make it visible using flow cytometry itself affects phagocytosis.

TLR2 is widely reported to be associated with Aβ-induced microglial activation and phagocytosis (Liu *et al.*, 2012). Recent studies carried out in microglia demonstrated that inhibition of TLR2 by antisense knockdown suppressed the Aβ-induced expression of pro-inflammatory cytokines and markers of activation (Udan *et al.*, 2008, Jana *et al.*, 2008). It has also been shown that microglia lacking TLR2 are unable to mount a phagocytic response or produce ROS following stimulation with fibrillar Aβ (Reed-Geaghan *et al.*, 2009). Further evidence for its role in disease pathogenesis comes from observations of increased expression of TLR2, along with

its co-receptor CD14, in animal models of AD and in the AD brain (Reed-Geaghan et al., 2010).

Although TLR2 is reported to be expressed by astrocytes (Trudler *et al.*, 2010), there is little evidence regarding its role in the response of these cells to Aβ. Results presented here demonstrate that inhibition of TLR2 using a neutralising antibody attenuated the Aβ-induced release of IL-1β, IL-6 and TNFα by astrocytes *in vitro*. This suggests that TLR2 plays a similar role in astrocytes as it does in microglia, stimulating cells to release of a host of pro-inflammatory cytokines in response to Aβ, potentially via activation of NFκB signalling pathways. In contrast to its effect on cytokine release, inhibition of TLR2 exerted no effect on the phagocytosis of fluorescently-labelled latex beads, suggesting that TLR2 may be less involved in the phagocytic response of these cells.

CD47 is reported to act as a '*don't eat me*' signal for phagocytic cells (Willingham et al., 2012). A ligand for signal regulatory protein-α (SIRPα), communication between the two proteins is important in regulation of cell migration and phagocytosis, with recent studies implicating a role for CD47-SIRPα interactions in immune homeostasis and regulation of neuronal networks (Matozaki et al., 2009). Only a limited number of studies have reported the expression of CD47 on astrocytes, with one recently describing immunoreactivity on astrocytes within active lesions during multiple sclerosis (Han *et al.*, 2012). Results from the current study indicate that inhibition of CD47 attenuated the Aβ-induced release of IL-1β, IL-6 and TNFα. Furthermore, blocking CD47 resulted in decreased uptake of fluorescently-labelled latex beads by both control- and Aβ-stimulated astrocytes. This is in agreement with studies carried out on THP-1 monocytes, which demonstrated that antagonists of CD47 inhibited adhesion of these cells to Aβ fibrils, thus resulting in decreased production of cytokines such as IL-1β (Bamberger et al., 2003).

Microglial Aβ-CD36 interaction is reported to signal via activation of the mitogen-activated protein kinase (MAPK) pathway, resulting in production of chemokine and ROS (Wilkinson and El Khoury, 2012). CD36 is also thought to be involved in a second heterotrimeric complex involving TLR4 and TLR6 that signals through NFκB, as has been demonstrated in Aβ-induced pro-inflammatory responses in macrophages (Stewart et al., 2010). Again, only a limited number of studies report the expression of CD36 on astrocytes, including one describing its role in glial scar formation during stroke (Bao *et al.*, 2012). Results from the current study indicate that inhibition of CD36 in astrocytes resulted in decreased uptake of fluorescently-labelled latex beads, but also led to the enhanced release of IL-1β, IL-6 and TNFα following stimulation with Aβ. Studies carried out in microglia have shown that CD36 antagonists block Aβ-induced phagocytosis, but also decrease the Aβ-induced generation of ROS and inflammatory cytokines (Bamberger *et al.*, 2003). The latter is in contrast to results observed here, suggesting differential roles with regard to the role of CD36 in the Aβ-induced release of pro-inflammatory cytokines by microglia and astrocytes *in vitro*.

Interestingly, a receptor complex comprised of CD47, CD36 and the α6β1 integrin is reported to be involved in the response of microglia to Aβ (Koenigsknecht and Landreth, 2004). Binding of Aβ to this receptor complex has been shown to drive a tyrosine kinase-based signalling cascade (Wilkinson et al., 2006). It could be speculated that, in astrocytes, CD47 is important in binding Aβ, while CD36 plays a role in modulating signalling events. Therefore it is possible that if the effect of CD36 regulation on CD47 is removed, a heightened response of astrocytes to Aβ occurs, as was observed following inhibition of CD36 in these experiments. Studies have shown that inhibition of CD36 in primary astrocytes increases the expression of CD47 (Rodrigo Gonzales-Reyes, unpublished data), something which is consistent with this suggestion.

RAGE is a multi-ligand receptor that engages structurally dissimilar molecules resulting in the activation of diverse signalling pathways depending on ligand and/or cell type. Advanced glycation endproducts (AGEs) were originally described as the primary ligand for RAGE, consisting of non-enzymatically modified proteins, lipids and nucleic acids (Han *et al.*, 2011). Other ligands have subsequently been described, including high-mobility group box 1 (HMGB1) and the S100 proteins. Microglial RAGE is reported to bind diverse forms of Aβ, including oligomeric and fibrillar species (Sturchler *et al.*, 2008, Verdier *et al.*, 2004). There is a good deal of evidence indicating that RAGE is involved in AD. A comparison of brains from non-demented and AD individuals indicates that RAGE expression parallels disease severity, with AD patients showing higher microglial RAGE immunoreactivity in the dentate gyrus, CA and subiculum regions of the hippocampus compared with age-matched controls (Lue *et al.*, 2001). Interestingly, a RAGE-specific inhibitor has recently been shown to reduce Aβ-induced cellular stress in a mouse model of AD (Deane *et al.*, 2012).

Results from the current study demonstrate that while RAGE inhibition decreased the phagocytosis of fluorescently-labelled latex beads, it also, perhaps unexpectedly, exacerbated the Aβ-induced release of pro-inflammatory cytokines. While there is little evidence describing a role for RAGE in phagocytosis by microglia and astrocytes, a limited number of studies detail its involvement in phagocytosis by peripheral cells. For example, macrophages from RAGE-knockout mice display a decreased ability to phagocytose apoptotic cells, while overexpression of RAGE resulted in enhanced uptake of these cells (Friggeri *et al.*, 2011).

Results from the current study perhaps suggest that the role of RAGE in astrocytes is more important in the phagocytosis and clearance of Aβ, thus terminating the signal and preventing it from continuing to elicit a pro-inflammatory response. A role for matrix-metalloproteinases (MMPs) may provide further support for the importance of

an interaction between RAGE and Aβ in astrocytes in the degradation and removal of Aβ from the external milieu. MMPs are a family of zinc-dependent endopeptidases, known to be expressed and secreted by astrocytes, that are capable of degrading proteins present in the extracellular matrix, including Aβ (Liao *et al.*, 2009). Astrocytes surrounding amyloid plaques show enhanced expression of MMP2 and MMP9 in APP/PS1 mice, and astrocyte-conditioned medium alone can degrade Aβ (Yin *et al.*, 2006). Engagement of RAGE has been shown to trigger pathways linked to MMP expression via activation of p44/p42, p38 and JNK (Taguchi *et al.*, 2000). This provides one possible explanation as to why blocking the RAGE-Aβ interaction in astrocytes has, what can presumably be described as, deleterious effects. If inhibition of RAGE results in decreased stimulation of MMPs by astrocytes, this may inhibit the processing, degradation and removal of Aβ and thus enhance the release of pro-inflammatory mediators. Additional experiments using zymography to assess MMP activity could be carried out following RAGE inhibition in order to further investigate this theory.

Wedelolactone acts as an irreversible inhibitor of IκB kinase activity, blocking the phosphorylation and degradation of IκBα and thus preventing NFκB from translocating to the nucleus to exert its inflammatory effects. Studies of postmortem AD brain tissue has revealed that NFκB activity is increased in neurons and astrocytes adjacent to amyloid plaques (O'Neill and Kaltschmidt, 1997). When translocation of NFκB to the nucleus is inhibited, for example by lipoxin A(4), the Aβ-induced production of IL-1β and TNF *in vitro* and *in vivo* is decreased (Wu *et al.*, 2011).

Considering that many of these putative Aβ binding receptors, including TLR2, RAGE, and potentially CD36, exert their effects through activation of NFκB signalling pathways, it might be predicted that wedelolactone would influence the Aβ-induced release of pro-inflammatory cytokines and phagocytosis. The data confirm this

prediction and demonstrate that wedelolactone significantly attenuated the release of IL-1β, IL-6 and TNFα, in addition to reducing phagocytosis of fluorescently-labelled latex beads.

In terms of cytokine release, these results are similar to those observed following inhibition of TLR2, suggesting that Aβ-TLR2 interactions in astrocytes result in stimulation of NFκB signalling pathways. In contrast, results observed following RAGE inhibition suggest that Aβ-RAGE interaction activates astrocytes via an alternative signalling pathway; one possibility is activation of the MAPK pathway that leads to MMP expression (Taguchi et al., 2000). CD36 is reported to act through two alternative pathways in macrophages, one involving MAPK, and a second that signals through activation of NFκB. As inhibition of NFκB and CD36 resulted in opposing effects on the production of Aβ-induced cytokines by astrocytes, it can be inferred that stimulation of CD36 does not exert its effects through activation of the complex involving TLR4 and TLR6 that ultimately leads to NFκB activation.

The objective of the current study was to investigate if TLR2, CD36, CD47, RAGE and NFκB signalling have a role to play in the Aβ-induced activation of astrocytes *in vitro*. The most significant finding is that each of these molecules appears to have some part to play in the complex response of astrocytes to Aβ. Inhibition of TLR2, CD47 and NFκB attenuated the Aβ-induced release of IL-1β, IL-6 and TNFα. In contrast, blocking CD36 and RAGE exacerbated the pro-inflammatory response to Aβ. While inhibition of TLR2 had no effect on phagocytosis, blocking CD36, CD47, RAGE and NFκB all resulted in decreased phagocytosis of fluorescently-labelled latex beads. While further experiments are required to fully elucidate the precise pathways elicited following stimulation of each of these receptors, it can be concluded that activation of NFκB undoubtedly plays a role. While a function for these proteins in the response of microglia to Aβ has been reported (Matozaki *et al.*, 2009, Greenberg *et al.*, 2006, Friggeri *et al.*, 2011, Bao *et al.*, 2012, Gitik *et al.*, 2011), to our knowledge, there is no previous evidence that they play a role in the

response of astrocytes to Aβ. The present data highlights this as a further area to explore in an effort to clear Aβ from the AD brain.

5: The effect of endogenous Aβ accumulation on glial activation and phagocytosis in a mouse model of AD

5.1 Introduction

AD is an age-related, progressive neurodegenerative disorder that affects over 35.6 million people worldwide (Ittner and Gotz, 2011). Clinically, patients present with short-term memory loss followed by a progressive decline in cognitive and executive functioning (Bekris *et al.*, 2010). In addition to extensive neuron and synapse loss, the post-mortem AD brain is characterised by the presence of two hallmark proteins, Aβ, which accumulates in extracellular senile plaques, and microtubule-associated tau, which localises to intracellular neurofibrillary tangles. These abnormal protein accumulations are believed to act in concert to cause the progressive inflammation and neuronal degradation that lead to subsequent symptoms of the disease.

The most commonly used animal models of AD are mice genetically modified to express genes associated with familial AD, namely PS1, PS2, APP or tau protein (Johnston *et al.*, 2011). The mouse model used in this study was the double transgenic APPSwe/PS1dE9 strain containing one transgene encoding a chimeric Aβ (A4) precursor protein (APPswe), and a second encoding the 'DeltaE9' mutation of human PS1, linked to increased Aβ plaque formation and early-onset AD respectively (Vincent and Smith, 2000). Both transgenes are inserted at a single locus and thus are inherited together.

In terms of phenotype, APP/PS1 mice develop sparse cortical and hippocampal Aβ deposits as early as 5 months of age, with evidence of substantial plaque burden by 12 months of age (Jankowsky *et al.*, 2004). Female APP/PS1 mice accumulate significantly higher levels of Aβ compared with males (Burgess *et al.*, 2006). Confocal microscopy has demonstrated that deposition of $CD11b^+$ microglia and $GFAP^+$ astrocytes with associated with Aβ plaques increases over time (Ruan *et al.*, 2009). There is evidence of synapse loss, with reduced expression of synaptophysin, a pre-synaptic marker, and PSD-95, a post-synaptic marker, in the cortex of these animals (Gimbel *et al.*, 2010). The number of neurons in the striatum of 12 month-old, but not

6 month-old, APP/PS1 mice was also marginally decreased, implying that that plaque development in the brains of these animals is related to neuronal loss (Richner *et al.*, 2009). Behaviourally, APP/PS1 mice display an age-dependent impairment in spatial learning, memory deficits in the Morris water maze and long-term contextual memory deficits in the step-down passive avoidance test (Gimbel *et al.*, 2010). The ability to sustain transient long term potentiation (LTP) is also impaired in APP/PS1 animals compared with WT controls (Volianskis *et al.*, 2010).

Although transgenic mice undoubtedly show some features of AD they, by no means, recapitulate all aspects of the disease, in particular showing only moderate neuronal loss (Johnston *et al.*, 2011). While one has to exercise caution in interpreting the findings from transgenic models, they still present key features of the human disease and thus are a valuable tool in attempting to elucidate the molecular basis of cognitive impairment that occurs during the course of this debilitating disease.

The aims of these studies were as follows:

1. To assess the concentrations of soluble and insoluble $A\beta_{1-38}$, $A\beta_{1-40}$ and $A\beta_{1-42}$ in the hippocampus of middle-aged (13-14 months) and aged (22-24 months) APP/PS1 mice compared with WT controls.
2. To examine the mRNA expression of some markers of glial activation in the cortex and hippocampus of APP/PS1 mice of both ages.
3. To evaluate the *ex vivo* phagocytosis of fluorescently-labelled latex beads by microglia and astrocytes isolated from the brains of APP/PS1 mice compared with WT controls.
4. To assess the effect of endogenous Aβ accumulation on mRNA expression of the putative Aβ receptors TLR2 and TLR4.

5.2 Methods

Groups of middle-aged (13-14 months) and aged (22-24 months) APP/PS1 mice and their WT littermate controls were used in this study. Middle-aged WT mice consisted of 5 females and 2 males, and APP/PS1 mice of 7 females and 2 males. Aged WT mice consisted of 4 males, and APP/PS1 mice of 6 males and 2 females.

Mice were sacrificed by decapitation whilst under anaesthesia induced by inhalation of isofluorane. Brains were dissected free and placed on a Petri dish containing dry ice, the cerebellum was removed and the cortex and hippocampus dissected out. Portions of cortex and hippocampus were snap-frozen in liquid nitrogen and stored at -80°C in nuclease-free tubes for mRNA analysis as described in section 2.8 and assessment of levels of soluble and insoluble Aβ by multiplex ELISA as described in section 2.9.

The remaining cortical tissue was used for the isolation of microglia and astrocytes as described in section 2.6, in order to assess the phagocytosis of fluorescently-labelled latex beads as described in section 2.7.1.

5.3 Results

5.3.1 The effect of age on the deposition of soluble and insoluble Aβ in the hippocampus of APP/PS1 mice

A 2-way ANOVA followed by *post-hoc* analysis demonstrated a genotype-related increase in the concentration of soluble $A\beta_{1-38}$ in the hippocampus of APP/PS1 mice compared with WT controls ($p<0.01$) as shown in figure 5.1, this increase was further enhanced in older animals ($p<0.01$). A similar trend in the concentration of insoluble $A\beta_{1-38}$ failed to meet statistical significance. A 2-way ANOVA followed by *post-hoc* analysis also revealed a genotype-related increase in the concentrations of soluble ($p<0.01$) and insoluble ($p<0.05$) $A\beta_{1-40}$ in the hippocampus of APP/PS1 mice as shown in figure 5.2, in both cases this was further enhanced in older animals ($p<0.05$; $p<0.01$). Statistical analysis revealed a genotype-related increase in the concentration of soluble $A\beta_{1-42}$ in the hippocampus of APP/PS1 mice compared with WT controls ($p<0.01$) as shown in figure 5.3, this was further enhanced in older animals ($p<0.01$). While a genotype-related increase in the concentration of insoluble $A\beta_{1-42}$ was also observed in the hippocampus ($p<0.05$), this was not further enhanced in older animals.

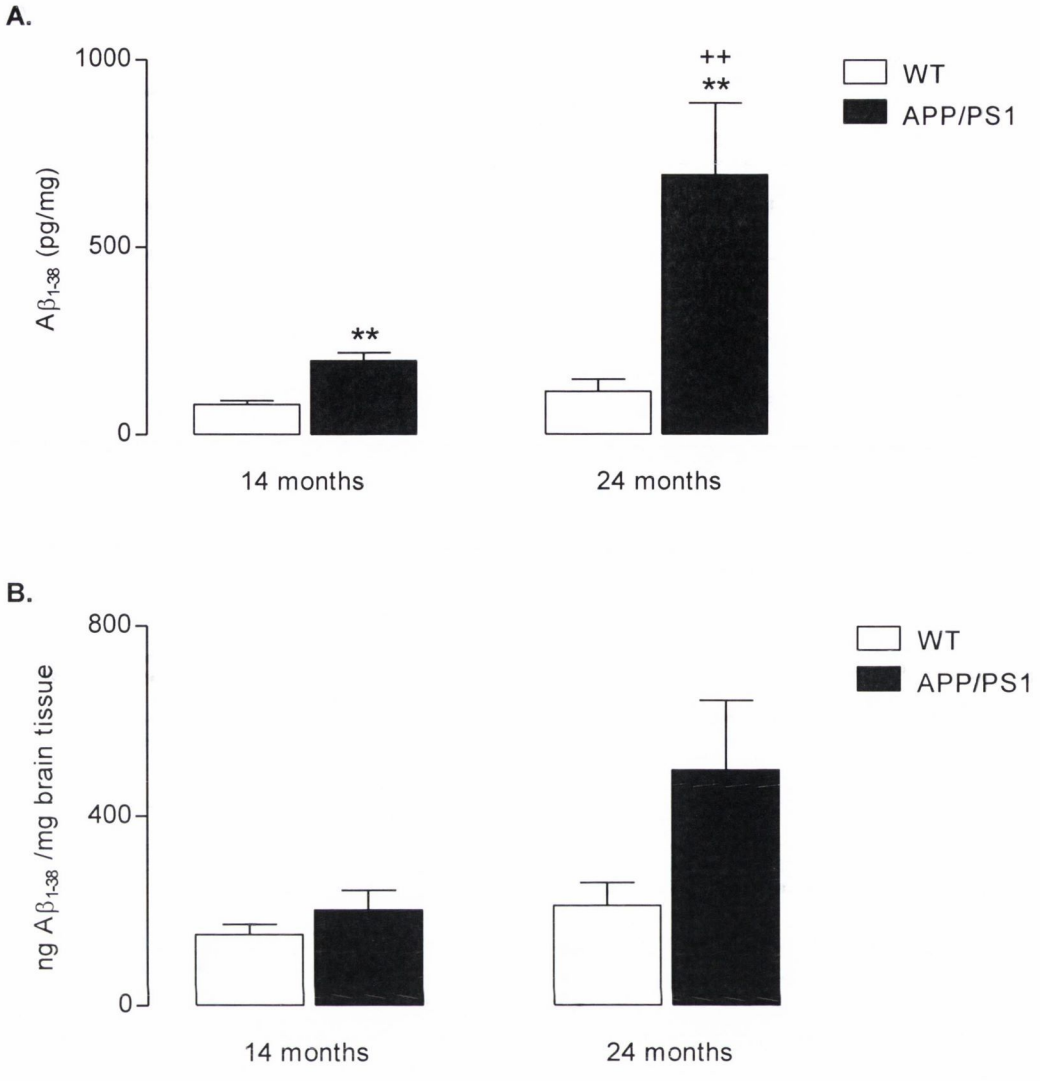

Figure 5.1 Soluble $A\beta_{1-38}$ was increased in the hippocampus of middle-aged APP/PS1 mice and this was further enhanced in older animals.

Groups of middle-aged (13-14 months) and aged (22-24 months) WT and APP/PS1 mice were sacrificed and the presence of soluble (A) and insoluble (B) $A\beta_{1-38}$ was assessed in the hippocampus by multiplex ELISA. The data show a genotype-related increase in the concentraion of soluble $A\beta_{1-38}$ in the hippocampus of APP/PS1 mice compared with WT controls ($p<0.01$), this increase was further enhanced in older animals ($p<0.01$). A similar trend in the concentration of insoluble $A\beta_{1-38}$ failed to reach statistical significance. Data are expressed as means + SEM (n=4-8). $^{**}p<0.01$ versus WT controls; $^{++}p<0.01$ versus middle-aged APP/PS1 mice (2-way ANOVA followed by Newman-Keuls *post-hoc* analysis).

A: $Genotype_{effect}$ [$F_{(1,23)}$=8.797, p=0.0076], age_{effect} [$F_{(1,23)}$=5.166, p=0.0342], $interaction_{effect}$ [$F_{(1,23)}$=3.907, p=0.062]. **B:** $Genotype_{effect}$ [$F_{(1,23)}$=2.819, p=0.1073], age_{effect} [$F_{(1,23)}$=3.138, p=0.0903], $interaction_{effect}$ [$F_{(1,23)}$=1.36, p=0.256].

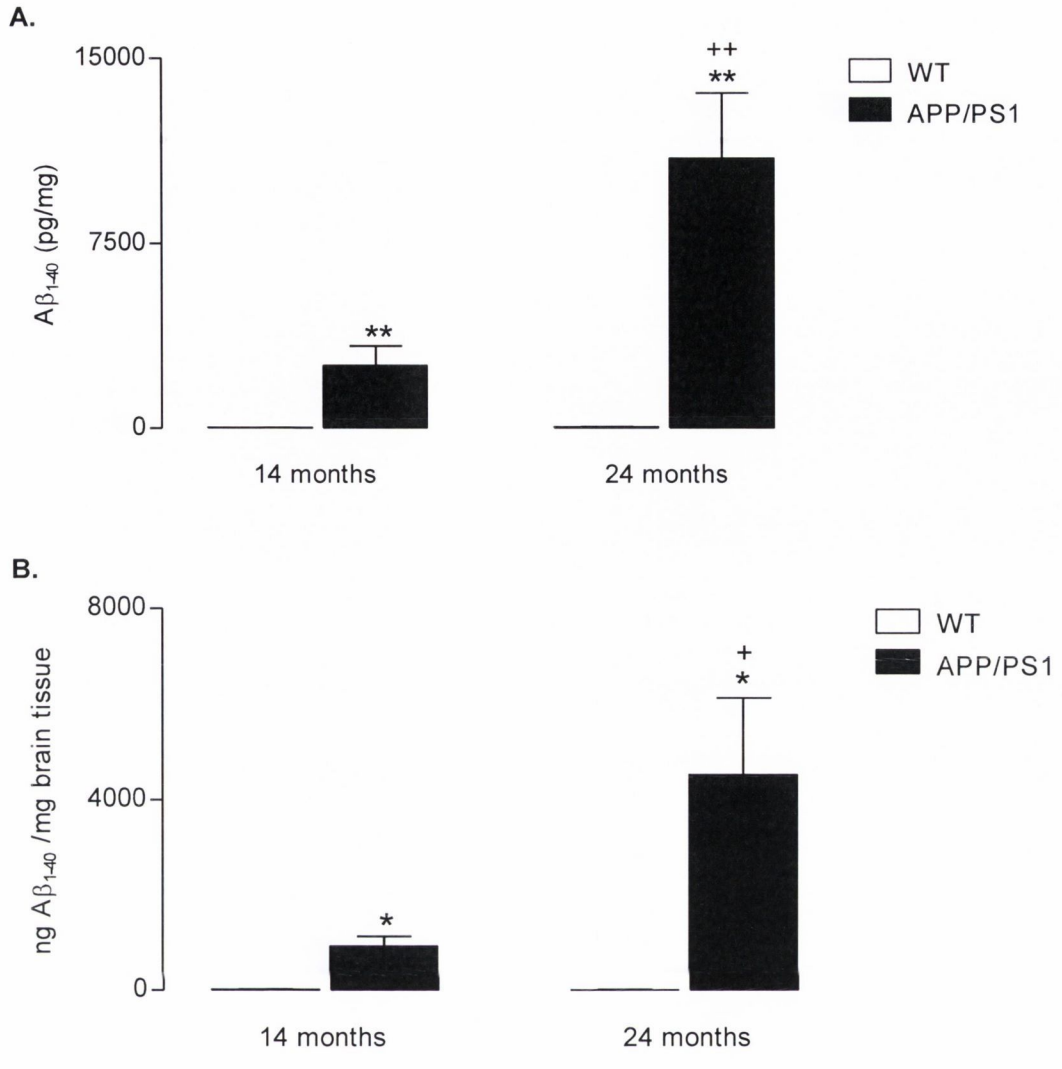

Figure 5.2 Soluble and insoluble $A\beta_{1-40}$ were increased in the hippocampus of middle-aged APP/PS1 mice and this was further enhanced in older animals.

Groups of middle-aged (13-14 months) and aged (22-24 months) WT and APP/PS1 mice were sacrificed and the presence of soluble (A) and insoluble (B) $A\beta_{1-40}$ was assessed in the hippocampus by multiplex ELISA. The data show a genotype-related increase in the concentration of soluble ($p<0.01$) and insoluble ($p<0.05$) $A\beta_{1-40}$ in the hippocampus of APP/PS1 mice compared with WT controls, and this was further enhanced in older animals ($p<0.05$, $p<0.01$). Data are expressed as means + SEM (n=4-8). *$p<0.05$, **$p<0.01$ versus WT controls; $^{+}p<0.05$, $^{++}p<0.01$ versus middle-aged APP/PS1 mice (2-way ANOVA followed by Newman-Keuls *post-hoc* analysis).

A: $Genotype_{effect}$ [$F_{(1,23)}$=13.92, p=0.0012], age_{effect} [$F_{(1,23)}$=5.482, p=0.0287], $interaction_{effect}$ [$F_{(1,23)}$=5.424, p=0.0294]. **B:** $Genotype_{effect}$ [$F_{(1,23)}$=6.641, p=0.0172], age_{effect} [$F_{(1,23)}$=2.935, p=0.1007], $interaction_{effect}$ [$F_{(1,23)}$=2.945, p=0.1002].

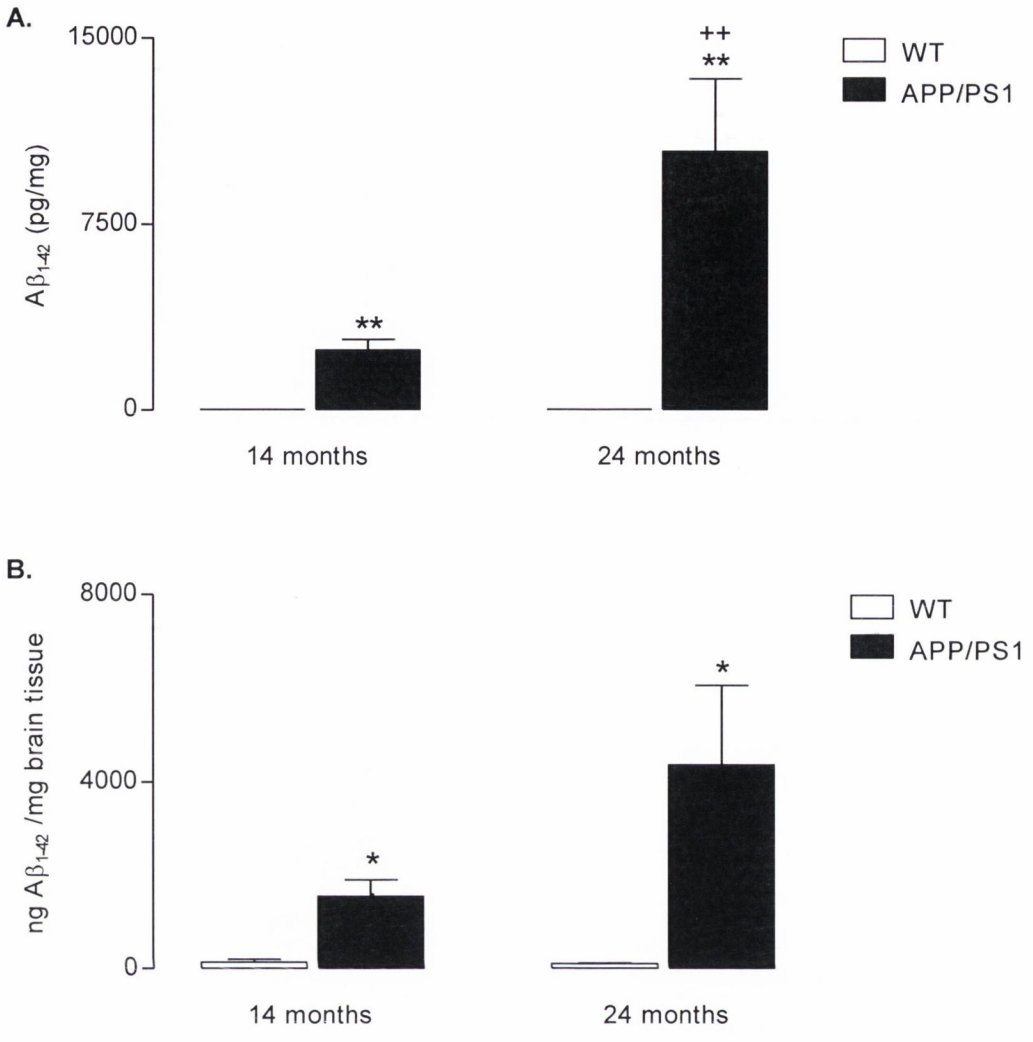

Figure 5.3 Soluble $A\beta_{1-42}$ was increased in the hippocampus of middle-aged APP/PS1 mice and this was further enhanced in older animals.

Groups of middle-aged (13-14 months) and aged (22-24 months) WT and APP/PS1 mice were sacrificed and the presence of soluble (A) and insoluble (B) $A\beta_{1-42}$ was assessed in the hippocampus by multiplex ELISA. The data show a genotype-related increase in the concentration of soluble ($p<0.01$) and insoluble ($p<0.05$) $A\beta_{1-42}$ in the hippocampus of APP/PS1 mice compared with WT controls. In the case of soluble $A\beta_{1-42}$, this was further enhanced in older animals ($p<0.01$). Data are expressed as means + SEM (n=4-8). *$p<0.05$, **$p<0.01$ versus WT controls; $^{++}p<0.01$ versus middle-aged APP/PS1 mice (2-way ANOVA followed by Newman-Keuls *post-hoc* analysis).

A: $Genotype_{effect}$ [$F_{(1,23)}$=11.3, p=0.0028], age_{effect} [$F_{(1,23)}$=4.416, p=0.0473], $interaction_{effect}$ [$F_{(1,23)}$=4.413, p=0.0474]. **B:** $Genotype_{effect}$ [$F_{(1,23)}$=6.436, p=0.0688], age_{effect} [$F_{(1,23)}$=1.581, p=0.2218], $interaction_{effect}$ [$F_{(1,23)}$=1.515, p=0.2314].

5.3.2 The effect of age and genotype on microglial activation

A 2-way ANOVA followed by *post-hoc* analysis demonstrated a genotype-related increase in mRNA expression of CD11b in the cortex and hippocampus of APP/PS1 mice compared with WT controls ($p<0.01$) as shown in figure 5.4. This increase was exacerbated in the hippocampus of aged APP/PS1 animals compared with their middle-aged counterparts ($p<0.05$).

A similar genotype-related increase was observed in mRNA expression of CD68 in the cortex of APP/PS1 mice compared with WT controls ($p<0.01$), as shown in figure 5.5. This increase was further exacerbated in aged APP/PS1 mice compared with their middle-aged counterparts ($p<0.01$).

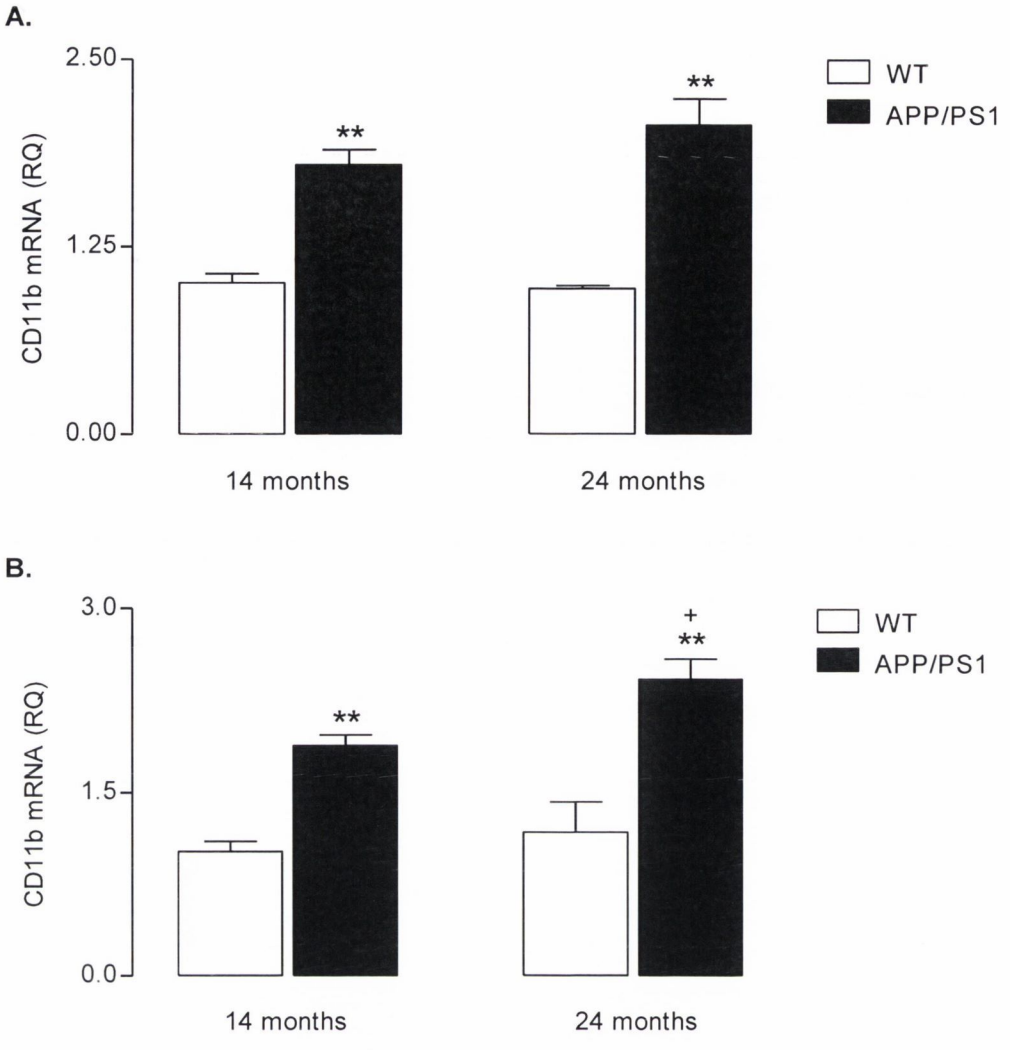

Figure 5.4 CD11b mRNA expression was increased in the cortex and hippocampus of middle-aged APP/PS1 mice and this was further enhanced in older animals.

Groups of middle-aged (13-14 months) and aged (22-24 months) WT and APP/PS1 mice were sacrificed and CD11b mRNA expression was assessed in the cortex (A) and hippocampus (B) using RT-PCR. The data show a genotype-related increase in CD11b mRNA expression in the cortex and hippocampus of APP/PS1 mice compared with WT controls ($p<0.01$). In the hippocampus, this increase was further enhanced in older animals ($p<0.05$). Data are expressed as means + SEM (n=4-8). $^{**}p<0.01$ versus WT controls; $^{+}p<0.05$ versus middle-aged APP/PS1 mice (2-way ANOVA followed by Newman-Keuls *post-hoc* analysis).

A: $\text{Genotype}_{\text{effect}}$ [$F_{(1,23)}=51.01$, $p<0.0001$], $\text{age}_{\text{effect}}$ [$F_{(1,23)}=0.7294$, $p=0.4027$], $\text{interaction}_{\text{effect}}$ [$F_{(1,23)}=1.343$, $p=0.2595$]. **B:** $\text{Genotype}_{\text{effect}}$ [$F_{(1,23)}=50.57$, $p<0.0001$], $\text{age}_{\text{effect}}$ [$F_{(1,23)}=5.531$, $p=0.028$], $\text{interaction}_{\text{effect}}$ [$F_{(1,23)}=1.666$, $p=0.2102$].

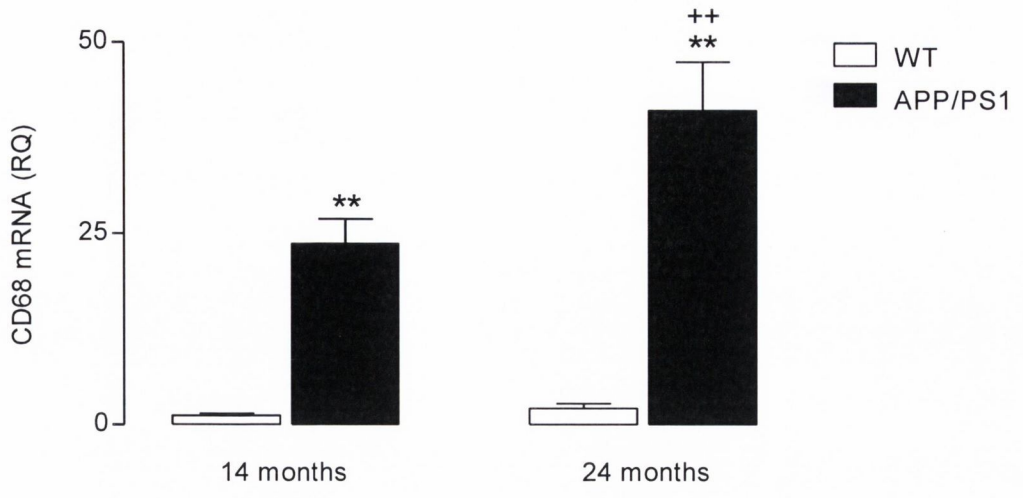

Figure 5.5 CD68 mRNA expression was increased in the cortex of middle-aged APP/PS1 mice and this was further enhanced in older animals.

Groups of middle-aged (13-14 months) and aged (22-24 months) WT and APP/PS1 mice were sacrificed and CD68 mRNA expression was assessed in the cortex using RT-PCR. The data show a genotype-related increase in CD68 mRNA expression in the cortex of APP/PS1 mice compared with WT controls ($p<0.01$). This increase was further enhanced in older APP/PS1 animals ($p<0.01$). Data are expressed as means + SEM ($n=4$-8). $^{**}p<0.01$ versus WT controls; $^{++}p<0.01$ versus middle-aged APP/PS1 mice (2-way ANOVA followed by Newman-Keuls *post-hoc* analysis).

$\text{Genotype}_{\text{effect}}$ [$F_{(1,23)}=46.72$, $p<0.0001$], $\text{age}_{\text{effect}}$ [$F_{(1,23)}=4.178$, $p=0.0537$], $\text{interaction}_{\text{effect}}$ [$F_{(1,23)}=3.374$, $p=0.0804$].

5.3.3 The effect of age and genotype on astrocytic activation

A 2-way ANOVA followed by *post-hoc* analysis demonstrated a genotype-related increase in mRNA expression of GFAP in the cortex and hippocampus of APP/PS1 mice compared with WT controls ($p<0.01$) as shown in figure 5.6. This increase was exacerbated in aged APP/PS1 animals compared with their middle-aged counterparts in both brain regions examined ($p<0.01$).

Neither age nor genotype had an effect on mRNA expression of GLAST or glutamine synthetase in the cortex or hippocampus of APP/PS1 mice compared with WT controls as shown in figure 5.7 and 5.8 respectively.

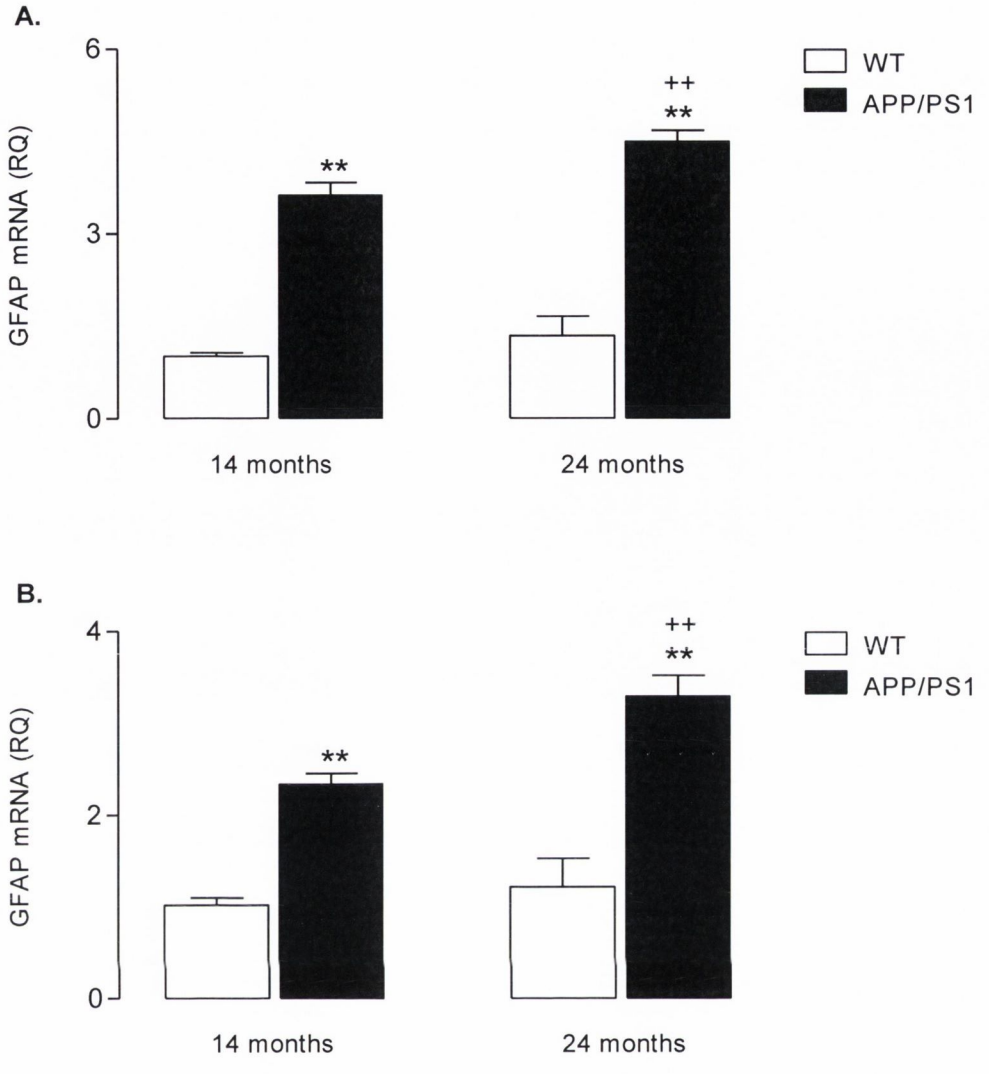

Figure 5.6 GFAP mRNA expression was increased in the cortex and hippocampus of middle-aged APP/PS1 mice and this was further enhanced in older animals.

Groups of middle-aged (13-14 months) and aged (22-24 months) WT and APP/PS1 mice were sacrificed and GFAP mRNA expression was assessed in the cortex (A) and hippocampus (B) using RT-PCR. The data show a genotype-related increase in GFAP mRNA expression in the cortex and hippocampus of APP/PS1 mice compared with WT controls ($p<0.01$). This increase was further enhanced in older animals ($p<0.01$) in both brain regions examined. Data are expressed as means + SEM (n=4-8). $^{**}p<0.01$ versus WT controls; $^{++}p<0.01$ versus middle-aged APP/PS1 mice (2-way ANOVA followed by Newman-Keuls *post-hoc* analysis).

A: $\text{Genotype}_{\text{effect}}$ [$F_{(1,23)}=213.1$, $p<0.0001$], $\text{age}_{\text{effect}}$ [$F_{(1,23)}=9.4$, $p=0.0057$], $\text{interaction}_{\text{effect}}$ [$F_{(1,23)}=1.888$, $p=0.1832$]. **B:** $\text{Genotype}_{\text{effect}}$ [$F_{(1,23)}=82.16$, $p<0.0001$], $\text{age}_{\text{effect}}$ [$F_{(1,23)}=9.63$, $p=0.005$], $\text{interaction}_{\text{effect}}$ [$F_{(1,23)}=4.136$, $p=0.0537$].

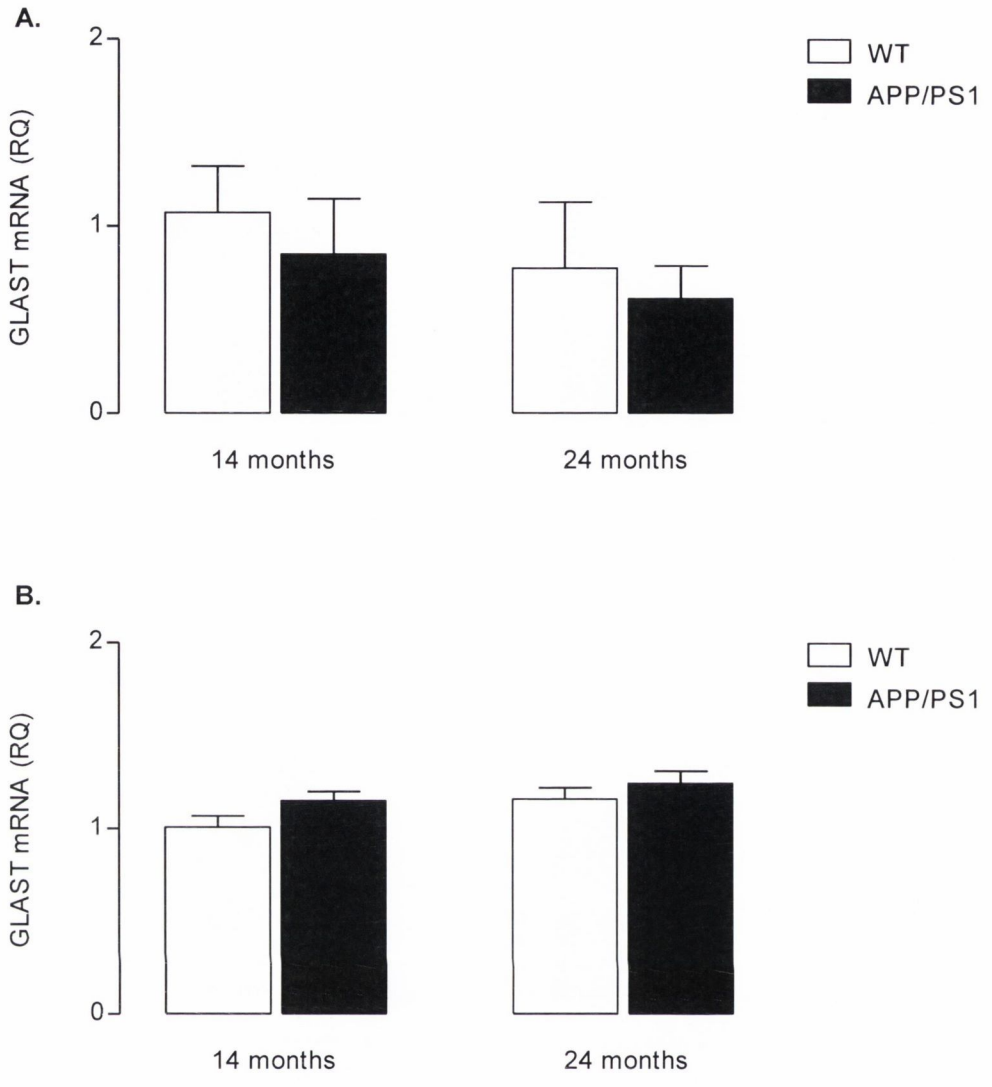

Figure 5.7 Neither age nor genotype had an effect on GLAST mRNA expression in the cortex or hippocampus of APP/PS1 mice.

Groups of middle-aged (13-14 months) and aged (22-24 months) WT and APP/PS1 mice were sacrificed and GLAST mRNA expression was assessed in the cortex (A) and hippocampus (B) using RT-PCR. The data show that GLAST mRNA expression was unchanged in either brain region of APP/PS1 mice compared with WT controls. Data are expressed as means + SEM (n=4-8).

A: $Genotype_{effect}$ [$F_{(1,23)}$=0.4808, p=0.4987], age_{effect} [$F_{(1,23)}$=0.9484, p=0.3456], $interaction_{effect}$ [$F_{(1,23)}$=0.012, p=0.9146]. **B:** $Genotype_{effect}$ [$F_{(1,23)}$=3.185, p<0.0875], age_{effect} [$F_{(1,23)}$=3.751, p=0.0651], $interaction_{effect}$ [$F_{(1,23)}$=0.1849, p=0.6712].

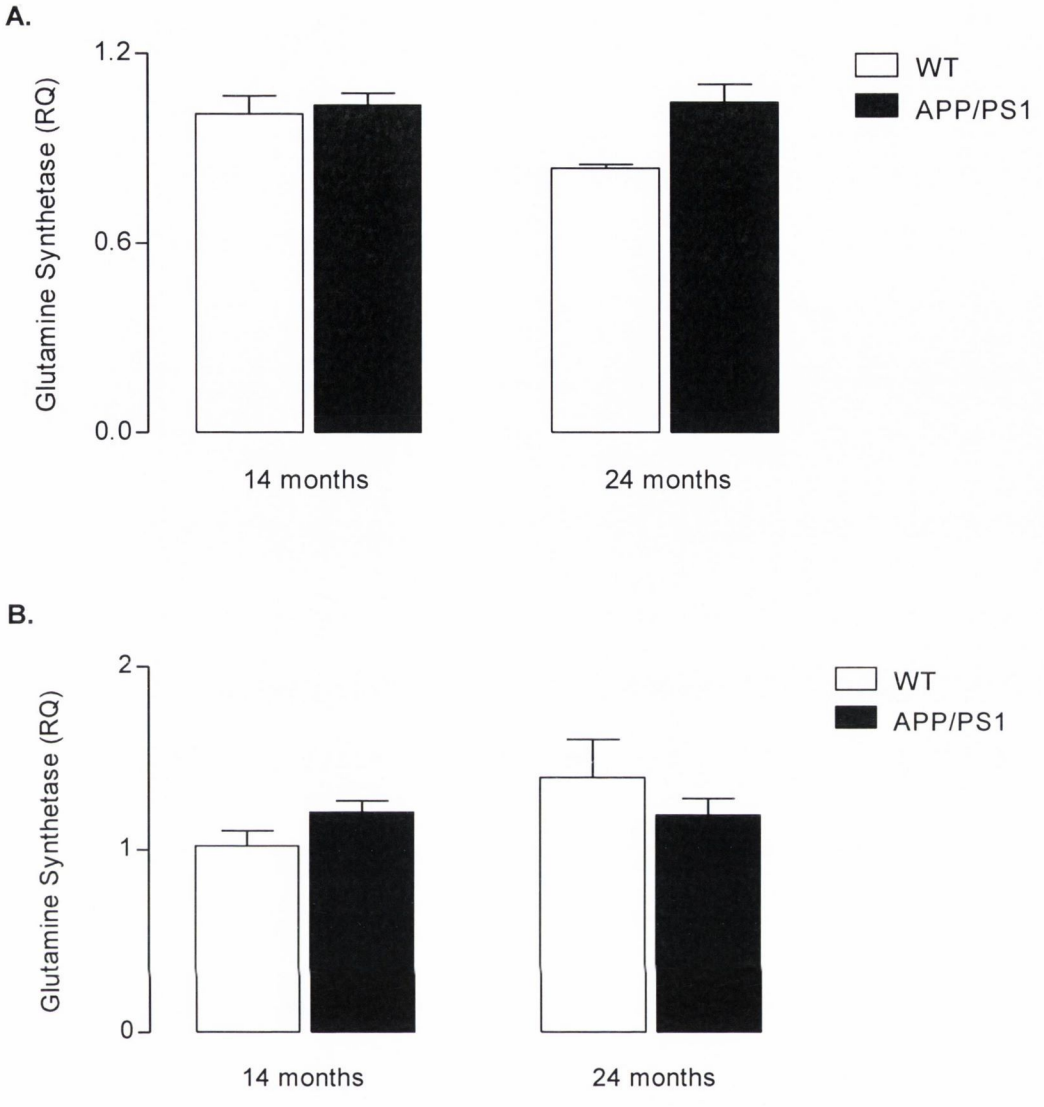

Figure 5.8 Neither age nor genotype had an effect on glutamine synthethase mRNA expression in the cortex or hippocampus of APP/PS1 mice.

Groups of middle-aged (13-14 months) and aged (22-24 months) WT and APP/PS1 mice were sacrificed and glutamine synthetase mRNA expression was assessed in the cortex (A) and hippocampus (B) using RT-PCR. The data show that mRNA expression of glutamine synthetase was unchanged in either brain region of APP/PS1 mice compared with WT controls. Data are expressed as means + SEM (n=4-8).

A: $Genotype_{effect}$ [$F_{(1,23)}$=4.337, p=0.0597], age_{effect} [$F_{(1,23)}$=2.113, p=0.1608], $interaction_{effect}$ [$F_{(1,23)}$=2.618, p=0.1206]. **B:** $Genotype_{effect}$ [$F_{(1,23)}$=0.013, p=0.911], age_{effect} [$F_{(1,23)}$=3.102, p=0.0915], $interaction_{effect}$ [$F_{(1,23)}$=3.701, p=0.0669].

5.3.4 The effect of age and genotype on the *ex vivo* phagocytosis by microglia and astrocytes

A 2-way ANOVA followed by *post-hoc* analysis revealed no effect of genotype on the *ex vivo* phagocytosis of fluorescently-labelled latex beads by $CD11b^+$ microglia or $GLAST^+$ astrocytes as shown in figures 5.9 and 5.10 respectively. However, an age-related increase ($p<0.01$) in phagocytosis was observed in both cell types isolated from the cortex of aged WT and APP/PS1 mice.

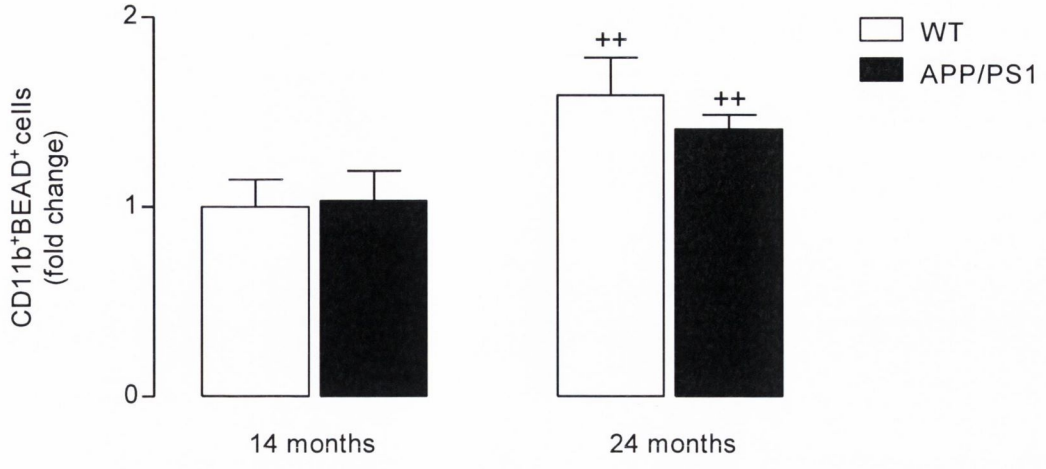

Figure 5.9 *Ex vivo* phagocytosis by microglia was increased in aged animals.

Microglia were isolated from the cortex of middle-aged (13-14 months) and aged (22-24 months) WT and APP/PS1 mice and the *ex vivo* phagocytosis of fluorescently-labelled latex beads was assessed using flow cytometry. The data demonstrate an age-related increase in phagocytosis by $CD11b^+$ microglia isolated from older WT and APP/PS1 animals ($p<0.01$) but no effect of genotype was observed. Data are expressed as means + SEM (n=4-8). $^{++}p<0.01$ versus middle-aged animals (2-way ANOVA followed by Newman-Keuls *post-hoc* analysis).

$Genotype_{effect}$ [$F_{(1,23)}=0.2656$, $p=0.6117$], age_{effect} [$F_{(1,23)}=11.56$, $p=0.0027$], $interaction_{effect}$ [$F_{(1,23)}=0.551$, $p=0.4661$].

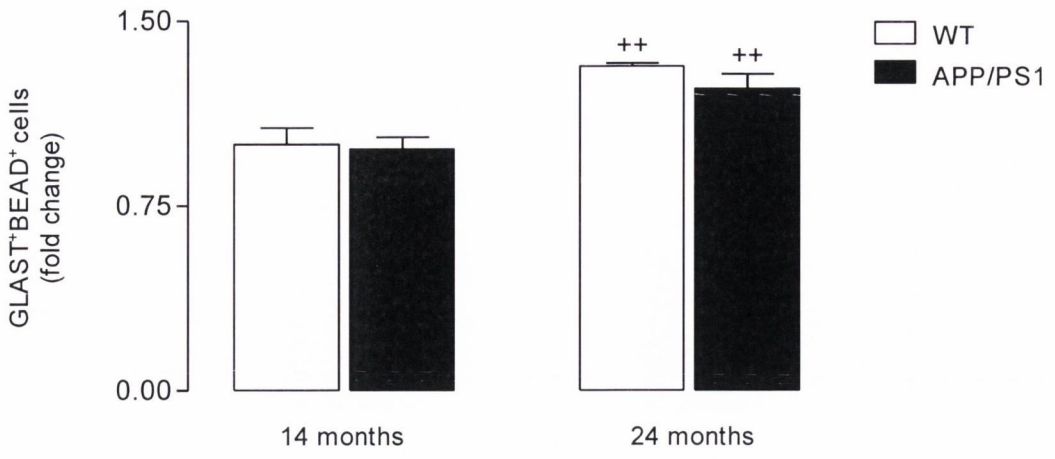

Figure 5.10 *Ex vivo* phagocytosis by astrocytes was increased in aged animals.

Astrocytes were isolated from the cortex of middle-aged (13-14 months) and aged (22-24 months) WT and APP/PS1 mice and the *ex vivo* phagocytosis of fluorescently-labelled latex beads was assessed using flow cytometry. The data demonstrate an age-related increase in phagocytosis by $GLAST^+$ astrocytes isolated from older WT and APP/PS1 animals ($p<0.01$) but no effect of genotype was observed. Data are expressed as means + SEM (n=4-8). $^{++}p<0.01$ versus middle-aged animals (2-way ANOVA followed by Newman-Keuls *post-hoc* analysis).

$Genotype_{effect}$ [$F_{(1,23)}=0.9332$, $p=0.3462$], age_{effect} [$F_{(1,23)}=24.48$, $p<0.0001$], $interaction_{effect}$ [$F_{(1,23)}=0.4156$, $p=0.5268$].

5.3.5 The effect of age and genotype on putative Aβ receptors

A 2-way ANOVA followed by *post-hoc* analysis demonstrated a genotype-related increase in mRNA expression of TLR2 in the cortex and hippocampus of APP/PS1 mice compared with WT controls ($p<0.01$) as shown in figure 5.11. This increase was further exacerbated in the hippocampus of aged APP/PS1 animals compared with their middle-aged counterparts ($p<0.05$).

A genotype-related increase in mRNA expression of TLR4 was also observed in the cortex ($p<0.05$) and hippocampus ($p<0.01$) of APP/PS1 mice compared with WT controls as shown in figure 5.12. No further effect of age was observed in either brain region examined.

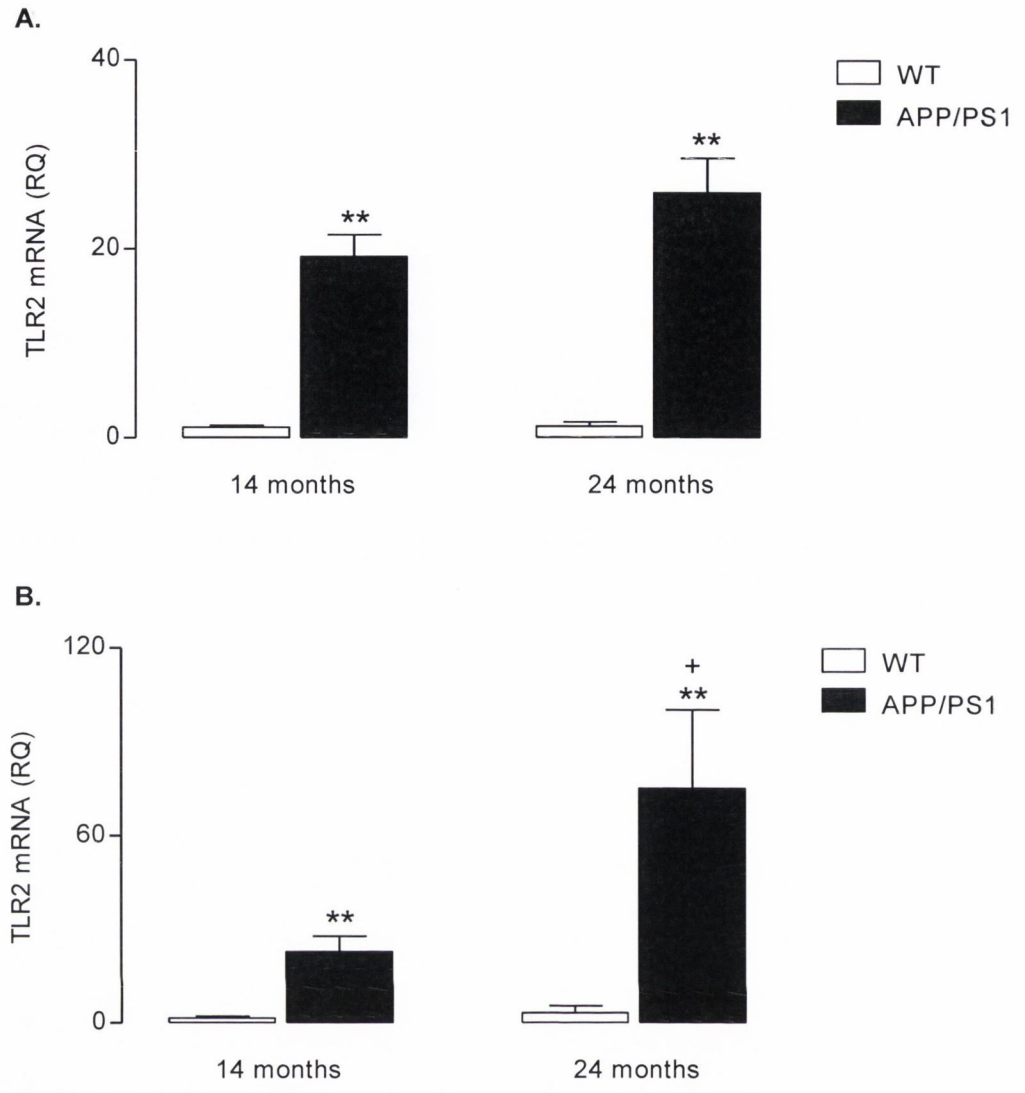

Figure 5.11 TLR2 mRNA expression was increased in the cortex and hippocampus of middle-aged APP/PS1 mice and this was further enhanced in older animals.

Groups of middle-aged (13-14 months) and aged (22-24 months) WT and APP/PS1 mice were sacrificed and TLR2 mRNA expression was assessed in the cortex (A) and hippocampus (B) using RT-PCR. The data show a genotype-related increase in TLR2 mRNA expression in the cortex and hippocampus of APP/PS1 mice compared with WT controls ($p<0.01$). In the hippocampus, this increase was further enhanced in older animals ($p<0.05$). Data are expressed as means + SEM (n=4-8). $^{**}p<0.01$ versus WT controls; $^{+}p<0.05$ versus middle-aged APP/PS1 mice (2-way ANOVA followed by Newman-Keuls *post-hoc* analysis).

A: $\text{Genotype}_{\text{effect}}$ [$F_{(1,23)}=60.83$, $p<0.0001$], $\text{age}_{\text{effect}}$ [$F_{(1,23)}=1.526$, $p=0.2310$], $\text{interaction}_{\text{effect}}$ [$F_{(1,23)}=1.477$, $p=0.2384$]. **B:** $\text{Genotype}_{\text{effect}}$ [$F_{(1,23)}=12.23$, $p=0.0019$], $\text{age}_{\text{effect}}$ [$F_{(1,23)}=3.506$, $p=0.0739$], $\text{interaction}_{\text{effect}}$ [$F_{(1,23)}=2.865$, $p=0.104$].

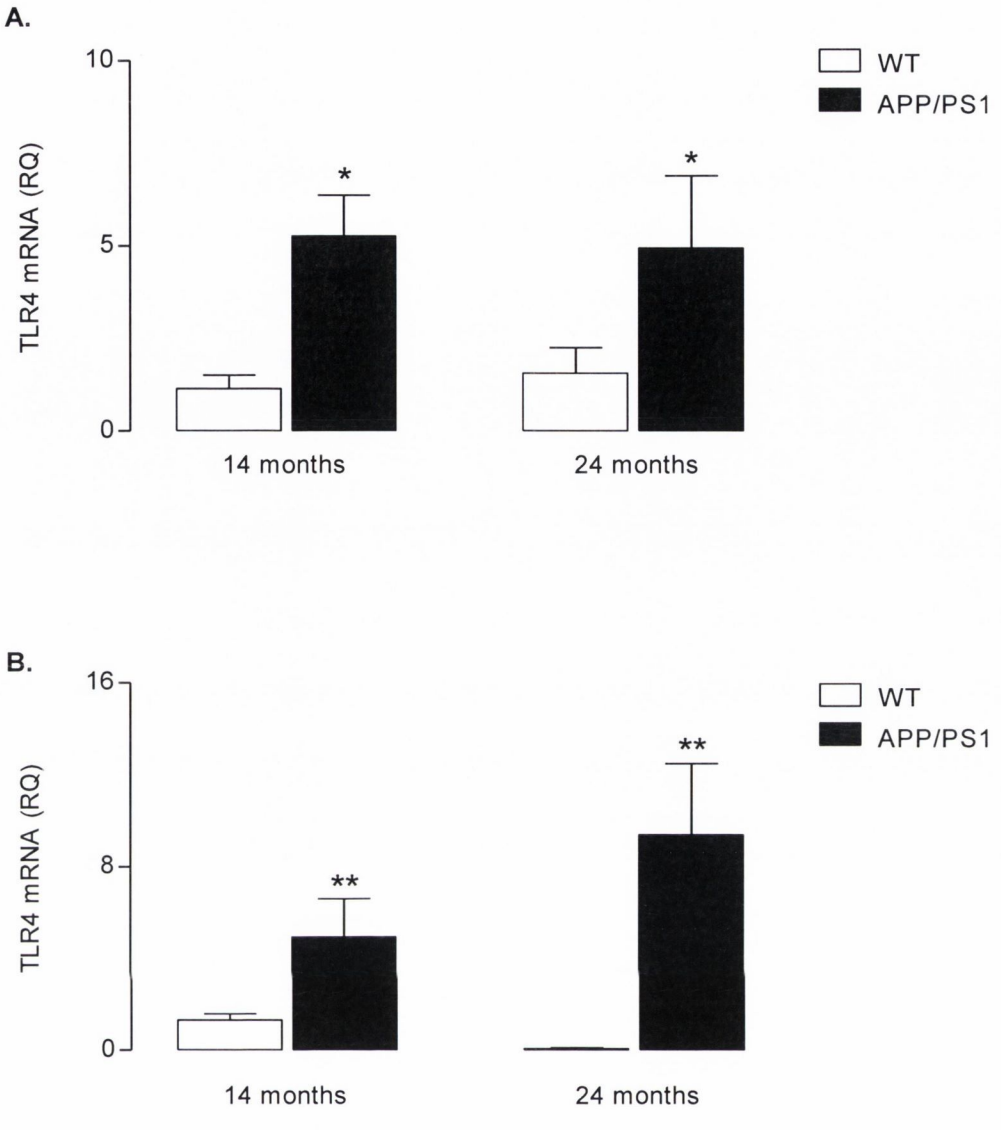

Figure 5.12 TLR4 mRNA expression was increased in the cortex of middle-aged and aged APP/PS1 mice.

Groups of middle-aged (13-14 months) and aged (22-24 months) WT and APP/PS1 mice were sacrificed and TLR4 mRNA expression was assessed in the cortex (A) and hippocampus (B) using RT-PCR. The data show a genotype-related increase in TLR4 mRNA expression in the cortex ($p<0.01$) and hippocampus ($p<0.05$) of APP/PS1 mice compared with WT controls. Data are expressed as means + SEM (n=4-8). *$p<0.05$, **$p<0.01$ versus WT controls (2-way ANOVA followed by Newman-Keuls *post-hoc* analysis).

A: $Genotype_{effect}$ [$F_{(1,23)}=5.678$, $p=0.0284$], age_{effect} [$F_{(1,23)}=0.0008$, $p=0.9783$], $interaction_{effect}$ [$F_{(1,23)}=0.056$, $p=0.8157$]. **B:** $Genotype_{effect}$ [$F_{(1,23)}=8.354$, $p=0.0090$], age_{effect} [$F_{(1,23)}=0.5211$, $p=0.4787$], $interaction_{effect}$ [$F_{(1,23)}=1.622$, $p=0.2174$].

5.4 Discussion

The main aim of this study was to investigate if there was an increase in the presence of soluble and insoluble Aβ in the brains of APP/PS1 mice as they aged from 12-24 months, and to evaluate whether this was paralleled by changes in glial activation. With this in mind, the first objective was to quantify soluble and insoluble Aβ in the brains of middle-aged (13-14 months) compared with aged (22-24 months) APP/PS1 mice. Accumulation of Aβ has been shown to begin in these mice as early as 5 months of age, with evidence of substantial plaque burden by 12 months of age (Jankowsky *et al.*, 2004).

As would be expected, the present data indicate that concentrations of both soluble and insoluble $A\beta_{1-38}$, $A\beta_{1-40}$ and $A\beta_{1-42}$ were markedly increased in the hippocampus of middle-aged APP/PS1 mice compared with WT controls. Interestingly, increases in the presence of all three forms of soluble Aβ were significantly enhanced in older APP/PS1 animals. While a similar trend was observed in concentrations of insoluble Aβ, with further increased deposition in older animals, this only reached statistical significance in the case of $A\beta_{1-40}$. These results are in agreement and extend others detailing increasing amyloid burden and plaque numbers in 4, 12 and 17 month old APP/PS1 animals (Wang *et al.*, 2003). This could, in part, be due to decreased phagocytosis and expression of Aβ degrading enzymes and/or enhanced processing of APP as a result of inflammation or vice versa, thus enforcing a positive feedback loop. The precise mechanisms for the observed increase in deposition of Aβ with age remain to be fully elucidated.

A gender-related difference in the development of pathology in APP/PS1 mice has been reported. The evidence indicates that female mice display increased numbers of senile plaques and concentrations of insoluble $A\beta_{1-42}$ in both cortex and hippocampus compared with male mice (Gallagher *et al.*, 2012). Epidemiological studies suggest that this phenomenon may also be present in humans, as the risk of AD is higher in

women even when data are adjusted for age (Brookmeyer *et al.*, 1998). The cohort of animals in this study consisted predominantly of females in the middle-aged group and males in the older age group, therefore it is possible that the full extent of enhanced Aβ deposition with age may have been underestimated.

In parallel with findings of increased Aβ accumulation with age, mRNA expression of several activation makers of microglia and astrocytes were increased in tissue prepared from middle-aged APP/PS1 mice compared with WT controls. In many cases, these changes were further exacerbated in older animals. The presence of large numbers of activated glial cells in the AD brain, specifically surrounding Aβ plaques, has been interpreted as an indication that they play a significant role in disease progression.

CD11b is a β-integrin receptor that pairs with CD18 to form the CR3 heterodimer, functioning in cell-mediated cytotoxicity, chemotaxis and phagocytosis (Kawai *et al.*, 2005). It is expressed on the surface of monocytes, macrophages and granulocytes, functionally regulating cellular adhesion and migration to mediate an inflammatory response. CD11b is considered a phenotypic marker of microglia within the CNS (Nagai *et al.*, 2005). Results presented here demonstrate a 2-fold increase in CD11b mRNA expression in the cortex and hippocampus of middle-aged APP/PS1 mice compared with WT controls, and this was further enhanced in the hippocampus of older animals. It is reported that CD11b expression corresponds with the severity of microglial activation in several neuroinflammatory diseases, including AD (Akiyama and McGeer, 1990). It can thus be inferred that microglia have become more activated corresponding with increased Aβ deposition in the brains of older APP/PS1 compared with their middle-aged counterparts. It is suggested that the phenotypic changes that occur when microglia respond to increased Aβ deposition are an important component of disease progression, as the presence of increased numbers of activated microglia likely leads to enhanced expression of pro-inflammatory mediators (Combs, 2009).

CD68, a lysosome-associated marker widely expressed on mononuclear phagocytes, including microglia, is reported to play an important role in phagocytosis by these cells (da Silva and Gordon, 1999). It is predominantly found localised to late endosomal and lysosomal compartments, with modest cell surface expression (Kurushima *et al.*, 2000), and its profile is reported to correspond to activation of the cells on which it is expressed (Song *et al.*, 2011). CD68 mRNA expression was increased over 24-fold in the cortex of middle-aged APP/PS1 compared with WT mice, and this was further enhanced in the hippocampus of older animals. Increased CD68 expression could be a compensatory mechanism whereby microglia are attempting, but failing, to upregulate their phagocytic capacity in order to clear the accumulating Aβ in the brains of these mice. Alongside the observed increase in CD11b expression, the data further corroborates evidence that microglia are changing phenotype and becoming increasingly activated in parallel with Aβ deposition over time.

The presence of reactive astrocytes and astrocytosis is a further pathological hallmark of AD. The domain of a single astrocyte in the rodent brain is reported to have a volume of ~66,000μm^3 with its membrane covering around 90,000 synapses (Oberheim *et al.*, 2006). The general housekeeping roles of astrocytes, including metabolic support, nutrition and regulation of the BBB are believed to be disrupted in AD, resulting in astrocyte-specific pathologies that contribute to the disease. Several markers of astrocytic activation were examined in the course of this study, including GFAP, GLAST and glutamine synthetase.

GFAP, a member of the cytoskeletal protein family, is important in modulating astrocyte motility and shape by providing structural stability to astrocytic processes (Eng *et al.*, 2000). Results from the current study indicate that GFAP mRNA expression was increased almost 3-fold in the hippocampus and cortex of middle-aged APP/PS1 mice, and this was further enhanced in older animals. Astrogliosis in the CNS is characterised by rapid synthesis of GFAP, and is shown to occur as a result of trauma, disease and chemical insult (Eng and Ghirnikar, 1994). Studies have shown

robust astrogliosis in the hippocampus and amygdala of 15-23 month old APP/PS1 mice compared with WT controls (Manaye *et al.*, 2007). In humans, prominent astrogliosis has been observed in cells surrounding amyloid plaques, and these activated astrocytes were shown to internalise large amounts of Aβ immunoreactive material (Nagele *et al.*, 2003). It is interesting to note that while astrocytes undergo reactive hypertrophy surrounding neuritic plaques, they are reported to undergo atrophy throughout the rest of the brain parenchyma (Olabarria *et al.*, 2010). This is thought to result in disruptions in synaptic connectivity, imbalance in neurotransmitter homeostasis, and neuronal death through increased excitotoxicity (Rodriguez *et al.*, 2009).

The amino acid L-glutamate is the main excitatory neurotransmitter in CNS, with important roles in normal brain function, cognition and memory (Nakanishi *et al.*, 1998). In order to prevent excitotoxicity, extracellular glutamate concentrations are kept below threshold levels being rapidly removed via Na^+-dependent glutamate transporters such as GLAST and GLT-1. Astrocytes are considered the main glutamate scavengers in the brain (Persson and Ronnback, 2012), with evidence indicating increased levels of extracellular glutamate and down-regulation of glutamate transporters in AD (Liang *et al.*, 2002). Expression of GLAST was unchanged with age or genotype in the course of this study. Interestingly, work carried out on post-mortem tissue comparing levels of GLAST and GLT-1 in AD brains with age-matched controls, revealed an individual variation in levels of both markers, but no significant correlation with AD, results which are consistent with those observed in the current study (Beckstrom *et al.*, 1999).

Glutamine synthetase is a key enzyme responsible for the metabolic conversion of glutamate to glutamine. In the brain, glutamine synthetase is generally located in astrocytes, and plays a key role in the detoxification of ammonia and regulation of neuronal glutamate levels (Finch and Cohen, 1997). During normal ageing, rodent and human brains reportedly show a distinct loss in activity of this enzyme, with human

brains displaying a 45% reduction between young and aged adults (Lai and Cooper, 1986). AD brains show a further reduction in activity of this oxidative-sensitive enzyme (Markesbery and Carney, 1999). This decrease is thought to occur as a result of oxidative damage, with Aβ accumulation in AD shown to induce major oxidative stress and subsequently diminish glutamine synthetase activity *in vitro* and *in vivo* (Finch and Cohen, 1997).

Expression of glutamine synthetase was found to be unchanged by age or genotype in the course of this study, however, a limitation of the data is that it was only investigated at the mRNA level. As an enzyme, it may have been more appropriate to assess its biological activity using a widely reported biosynthetic assay that relies on the formation of γ-glutamylhydroxamate from hydroxyl amine and either glutamine or glutamate (Gawronski and Benson, 2004). As this assay is considered a functional metabolic test for astrocytes, it may have yielded more information on the activity of these cells in the brains of APP/PS1 mice compared with WT controls.

According to the amyloid hypothesis, accumulation of Aβ in the brain is the primary driving force in AD pathogenesis, with subsequent disease processes resulting from an imbalance between Aβ production and clearance (Hardy and Selkoe, 2002). Enhanced Aβ deposition in aged APP/PS1 mice paralleled with increased activation markers of microglia and astrocytes is consistent with this theory and also with numerous reports in the literature indicating the presence of an increased neuroinflammatory profile in AD.

Results presented in the previous chapters demonstrate that phagocytosis of fluorescently-labelled latex beads by microglia and astrocytes was enhanced following stimulation with Aβ *in vitro,* and that this was dependent on actin polymerisation. Interestingly intracerebroventricular infusion of Aβ for 28 days increased phagocytosis of latex beads by astrocytes but not microglia, indicating differential effects of Aβ *in vitro* and *in vivo*. A further aim of this study was to assess the effect of endogenous Aβ

accumulation on phagocytosis by glial cells. Ultrastructural studies have identified intra-cytoplasmic fragments of Aβ within microglia in animal models of AD (Mandrekar-Colucci *et al.*, 2012), and in post-mortem tissue derived from AD patients (Lewandowska *et al.*, 2004). Despite local recruitment of glial cells to sites of Aβ deposition in the AD brain, it is obvious that clearance attempts by these cells ultimately fails to restrict the formation of senile plaques.

An age-related decline in adherence, opsonisation and phagocytosis by macrophages has been reported, although this was not observed in the case of all studies carried out (Plowden *et al.*, 2004). Results have demonstrated AD macrophages to be poor in transporting Aβ to endosomes and lysosomes, and AD monocytes to be deficient in clearing Aβ from AD brain sections, although they still had the capacity to phagocytose bacteria (Fiala and Veerhuis, 2010, Mizwicki *et al.*, 2012). A recent study has reported that phagocytosis by PBMCs was significantly depressed in AD patients compared with controls (which in this case were university professors), in addition to AD monocytes showing lower expression of cell-surface proteins important for phagocytosis (Avagyan *et al.*, 2009).

In comparison, little has been described with regard to the phagocytic capacity of microglia in AD, and even less has been documented in relation to the role of astrocytes in this process. While the current study demonstrates an age-related increase in the phagocytosis of fluorescently-labelled latex beads by microglia and astrocytes *ex vivo*, no genotype-related change was observed. It is worth noting that the phagocytosis of latex beads and Aβ may not be directly comparable, and this is a possible explanation for the somewhat unexpected lack of genotype effect compared with studies detailed previously. The fact that macrophages were shown to be inefficient in clearing Aβ from brain sections but still had the capacity to phagocytose bacteria (i.e. comparable to the ability to phagocytose beads in the current study) perhaps goes some way towards explaining this result, and might hold true for microglia in the AD brain. An age-related increase in uptake of quantum dots by

microglia has been previously been described (Lynch *et al.*, 2010), but to our knowledge, no age-related effect on phagocytosis by astrocytes had been reported to date.

Multiple Aβ binding receptors have been identified within the CNS, including TLR2, TLR4, RAGE, CD36 and CD47, engagement of which results in the activation of numerous parallel signalling cascades (Lucin and Wyss-Coray, 2009). While it was outside the remit of this study to investigate all of the receptors listed above, analysis of mRNA expression of TLR2 and TLR4 was carried out.

TLRs are widely reported to be associated in Aβ-induced inflammatory activation, with TLR2 and TLR4 in particular continuing to emerge as key players in CNS diseases and much data linking them to AD pathology (Wang *et al.*, 2011). Increased expression of TLR2, TLR4 and their co-receptor CD14 are observed in the brains of AD patients and in animal models of AD (Reed-Geaghan *et al.*, 2010). Data presented in the first two chapters of this thesis support a role for the involvement of TLR2 and TLR4 in Aβ-induced inflammatory responses by microglia and astrocytes *in vitro*. In the current study, TLR2 mRNA was increased in the cortex and hippocampus of middle-aged APP/PS1 mice compared with WT controls, and this was significantly enhanced in older animals. TLR4 mRNA expression was also increased in the cortex of APP/PS1 mice, but no further age-related effect was observed. These results are consistent with the evidence that TLRs have a role to play with regard to Aβ accumulation *in vivo*, and also indicate that, in the case of TLR2, heightened expression mimics the age-related increase in glial activation in the brains of APP/PS1 mice.

This study set out to assess the effect of age on Aβ accumulation in the brains of middle-aged compared with aged APP/PS1 mice, and to investigate if this was associated with an increased neuroinflammatory profile. Concentrations of soluble and insoluble Aβ were greater in aged APP/PS1 mice compared with their middle-aged counterparts, and this was accompanied by enhanced activation of microglia and

astrocytes as assessed by expression of CD11b, CD68 and GFAP respectively. While *ex vivo* phagocytosis by glial cells was unaffected by genotype, an age-related increase in the uptake of latex beads was observed by both cell types. In addition, expression of the putative Aβ receptors TLR2 and TLR4 were increased in APP/PS1 mice, and in the case of TLR2, this was further enhanced in older animals. Taken together, these results support the idea that deposition of soluble and/or insoluble Aβ in the brain is an important event in AD, and enhancing its clearance may be of benefit in halting disease progression.

6: Delineating activation states, leukocyte infiltration & chemokine expression in a mouse model of AD

6.1 Introduction

Results presented in the previous chapter described an age-related increase in hippocampal Aβ concentrations in APP/PS1 mice, associated with enhanced expression of markers of glial activation, CD11b, CD68 and GFAP. Glial cells play a pleiotropic role in physiological and pathological conditions, aggravating injury and adding to subsequent neurodegeneration, but also helping to restore CNS integrity through their actions underlying tissue repair and regeneration (Czeh *et al.*, 2011).

Similar to tissue macrophages, microglia respond to inflammatory stimuli in the CNS in a pre-programmed manner designed to kill but also to initiate repair and resolution of the disease (Czeh *et al.*, 2011). Macrophages/microglia can be classified into two major subsets, and further intermediate ones, with discrete molecular phenotypes and effector functions depending on the activation pathways elicited. Classical activation involves pro-inflammatory Th1 cytokines such as IFNγ, TNFα and IL-1β, inflammation, ECM destruction and apoptosis (Mosser and Edwards, 2008). In contrast, alternative activation and acquired deactivation involves anti-inflammatory Th2 cytokines such as IL-4, IL-10 and IL-13, ECM construction and cell proliferation (Mosser, 2003).

While reports detailing the role of classical activation in AD are numerous, less work has been carried out investigating the role of alternative action and acquired deactivation in the disease process. One recent study, however, has suggested there is increased expression of markers of alternative activation and acquired deactivation, such as mannose receptor (MR) and arginase-1, in Tg2576 mice (Colton *et al.*, 2006). As such, a hybrid activation state incorporating characteristics of both classical and alternative activation has been hypothesised to play a role in AD.

The BBB functions to protect the brain from toxic substances in the blood, while at the same time supplying it with all the nutrients it needs to maintain an appropriate 'milieu' for neuronal circuits to function correctly (Zlokovic, 2002). A number of

neuroinflammatory conditions, including AD, are associated with BBB disruption and the subsequent opening of tight junctions (Avison *et al.*, 2004). As a result, trans-endothelial migration of peripheral leukocytes across the BBB is reported to be a pathological process in AD (Togo *et al.*, 2002). It is of interest to further investigate the presence of these cells and assess their effect on the expression profile of classical and alternative activation in APP/PS1 mice. Understanding the complex process behind leukocyte infiltration into the brain parenchyma is crucial in elucidating the chronic inflammatory processes that are apparent in AD.

The aims of these studies were as follows:

1. To assess the expression profile of markers of alternative activation, acquired deactivation and classical activation in the cortex and hippocampus of middle-aged and aged APP/PS1 mice compared with WT controls.
2. To determine whether changes in microglial activation state were associated with increased numbers of infiltrating monocytes/macrophages, neutrophils and $CD4^+$ T cells in the cortex of APP/PS1 mice.
3. To analyse expression of the chemokines CXCL1, MIP-1, RANTES, IP-10, MCP-1 and their association with leukocyte infiltration in the cortex of middle-aged and aged APP/PS1 mice.

6.2 Methods

Groups of middle-aged (13-14 months) and aged (22-24 months) APP/PS1 mice and their WT littermate controls were used in this study. Middle-aged WT mice consisted of 5 females and 2 males, and APP/PS1 mice of 7 females and 2 males. Aged WT mice consisted of 4 males, and APP/PS1 mice of 6 males and 2 females.

Mice were sacrificed by decapitation whilst under anaesthesia induced by inhalation of isofluorane. Brains were placed on a Petri dish containing dry ice, the cerebellum removed and cortex and hippocampus dissected out. Portions of cortex and hippocampus were snap-frozen in liquid nitrogen and stored at -80°C in nuclease-free tubes for mRNA and protein analysis.

In a separate series of experiments, a cohort of APP/PS1 mice (17-19 months) and their WT littermate controls were used to assess the presence of infiltrating $CD11b^{+}CD45^{hi}$ monocytes/macrophages, $CD11b^{+}Ly6G^{+}$ neutrophils and $CD3^{+}CD4^{+}$ T cells in the brain parenchyma. WT mice consisted of 5 females and 3 males, and APP/PS1 mice of 4 females and 4 males. Following sacrifice, a portion of the hippocampus was taken for mRNA analysis while the rest of the brain was used to isolate mononuclear cells as described in section 2.6.3. Further analysis of $CD3^{+}CD4^{+}$ T cell subtypes was carried out as described in section 2.7.3.

6.3 Results

6.3.1 The effect of age and genotype on markers of alternative activation and acquired deactivation

A 2-way ANOVA followed by *post-hoc* analysis demonstrated a genotype-related increase in IL-4Rα mRNA expression in cortical and hippocampal tissue prepared from middle-aged (13-14 months) and aged (22-24 months) APP/PS1 mice as shown in figure 6.1 ($p<0.05$). However, protein expression of IL-4Rα on $CD11b^+$ microglia was decreased in middle-aged APP/PS1 mice compared with WT controls ($p<0.05$) as shown in figure 6.2. While a genotype-related increase in IL-10 protein expression was observed in hippocampal tissue prepared from middle-aged and aged APP/PS1 mice compared with WT controls as shown in figure 6.3 ($p<0.05$), an age-related decrease in protein expression of IL-10R was observed on $CD11b^+$ microglia ($p<0.05$) as shown in figure 6.4.

Expression of MR, arginase-1 and 'found in inflammatory zone' (FIZZ)-1 mRNA was assessed in cortical tissue prepared from middle-aged and aged WT and APP/PS1 mice. Figure 6.5 illustrates that neither age nor genotype had an effect on expression of any of these markers of alternative activation.

Nerve-growth factor (NGF) mRNA was decreased in the cortex ($p<0.01$) and hippocampus ($p<0.05$) of middle-aged and aged APP/PS1 mice compared with WT controls as shown in figure 6.6. A genotype-related decrease in brain-derived neurotrophic factor (BDNF) mRNA was observed in the cortex of APP/PS1 mice at both ages ($p<0.05$), while its expression was only significantly decreased in the hippocampus of older animals ($p<0.05$) as shown in figure 6.7.

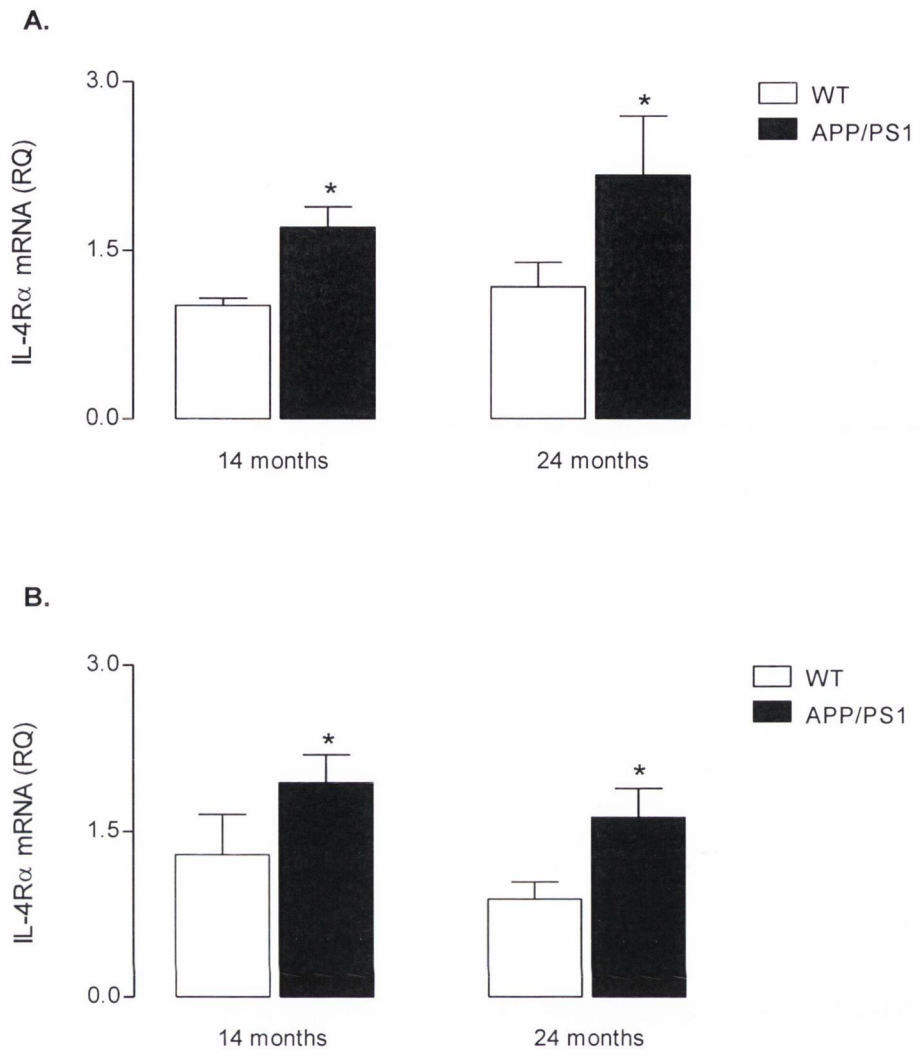

Figure 6.1 IL-4Rα mRNA expression was increased in the cortex and hippocampus of middle-aged and aged APP/PS1 mice compared with WT controls.

Groups of middle-aged (13-14 months) and aged (22-24 months) WT and APP/PS1 mice were sacrificed and IL-4Rα mRNA expression was assessed in the cortex (A) and hippocampus (B) using RT-PCR. The data show that IL-4Rα was increased in the cortex and hippocampus ($p<0.05$) of middle-aged and aged APP/PS1 mice compared with WT controls. Data are expressed as means + SEM (n=4-8). *$p<0.05$ versus WT controls (2-way ANOVA followed by Newman-Keuls *post-hoc* analysis).

A: $Genotype_{effect}$ [$F_{(1,23)}=5.72$, $p=0.03$], age_{effect} [$F_{(1,23)}=0.79$, $p=0.38$], $interaction_{effect}$ [$F_{(1,23)}=0.18$, $p=0.68$]. **B:** $Genotype_{effect}$ [$F_{(1,23)}=4.686$, $p=0.0421$], age_{effect} [$F_{(1,23)}=1.249$, $p=0.276$], $interaction_{effect}$ [$F_{(1,23)}=0.02$, $p=0.885$].

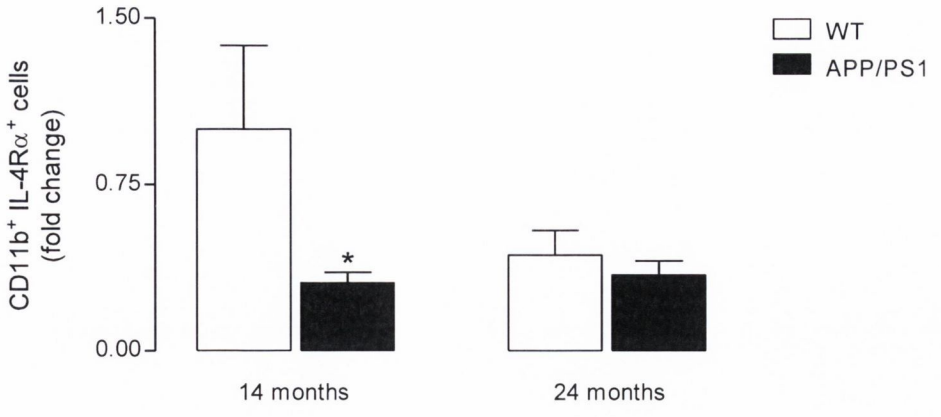

Figure 6.2 IL-4Rα protein expression on microglia isolated from the cortex of middle-aged APP/PS1 mice was decreased compared with WT controls.

Groups of middle-aged (13-14 months) and aged (22-24 months) WT and APP/PS1 mice were sacrificed and IL-4Rα expression on $CD11b^+$ microglia was assessed using flow cytometry. The data show that IL-4Rα expression on microglia isolated from middle-aged APP/PS1 mice was decreased compared with WT controls ($p<0.05$). Data are expressed as means + SEM ($n=4$-8). *$p<0.05$ versus WT controls (2-way ANOVA followed by Newman-Keuls *post-hoc* analysis).

$Genotype_{effect}$ [$F_{(1,22)}=5.598$, $p=0.031$], age_{effect} [$F_{(1,22)}=2.604$, $p=0.126$], $interaction_{effect}$ [$F_{(1,22)}=3.324$, $p=0.087$].

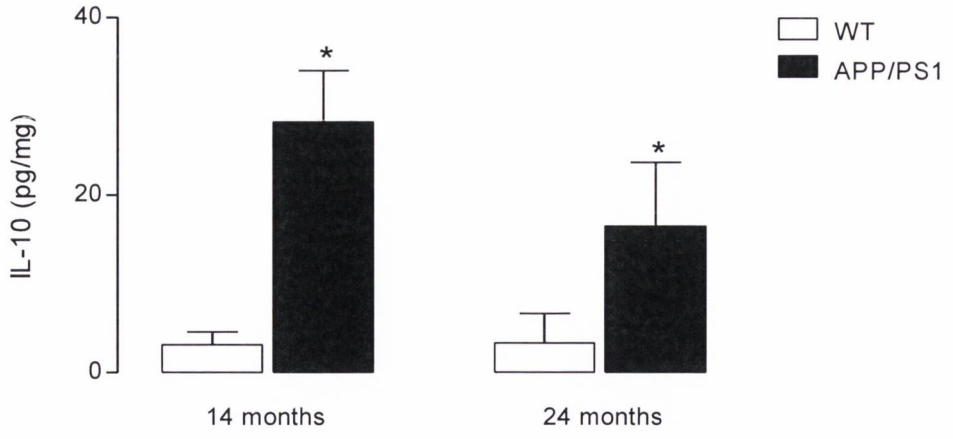

Figure 6.3 IL-10 protein expression was increased in the hippocampus of middle-aged and aged APP/PS1 mice compared with WT controls.

Groups of middle-aged (13-14 months) and aged (22-24 months) WT and APP/PS1 mice were sacrificed and IL-10 protein expression was assessed in the hippocampus by multiplex ELISA. The data show that IL-10 was increased in the hippocampus of middle-aged and aged animals compared with WT controls ($p<0.05$). Data are expressed as means + SEM ($n=4$-8). *$p<0.05$ versus WT controls (2-way ANOVA followed by Newman-Keuls *post-hoc* analysis).

$Genotype_{effect}$ [$F_{(1,23)}=6.339$, $p=0.0246$], age_{effect} [$F_{(1,23)}=0.003$, $p=0.9602$], $interaction_{effect}$ [$F_{(1,23)}=2.414$, $p=0.1425$].

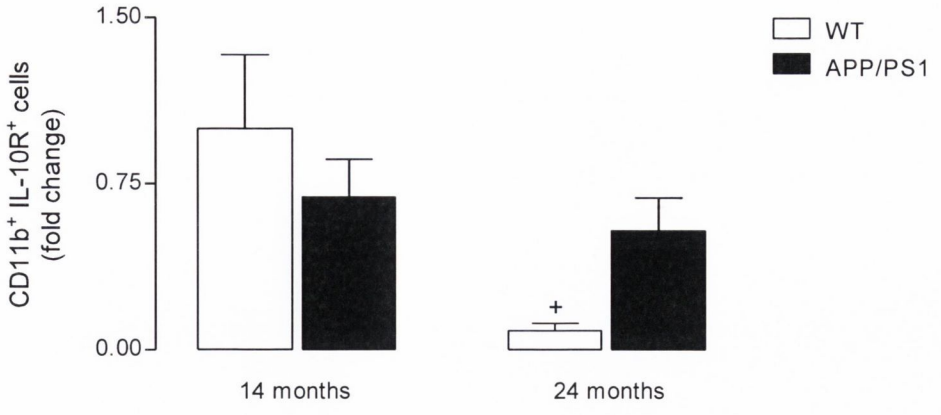

Figure 6.4 IL-10R protein expression on microglia isolated from the cortex of WT mice was decreased between middle-aged and aged animals.

Groups of middle-aged (13-14 months) and aged (22-24 months) WT and APP/PS1 mice were sacrificed and IL-10R expression was assessed on $CD11b^+$ microglia using flow cytometry. The data show there was an age related decrease in IL-10R expression between middle-aged and aged WT mice ($p<0.05$). No further effect of genotype was observed. Data are expressed as means + SEM (n=4-8). $^+p<0.05$ versus middle-aged WT mice (2-way ANOVA followed by Newman-Keuls *post-hoc* analysis).

$Genotype_{effect}$ [$F_{(1,22)}$=0.1056, p=0.7485], age_{effect} [$F_{(1,22)}$=6.022, p=0.0229], $interaction_{effect}$ [$F_{(1,22)}$=3.07, p=0.0943].

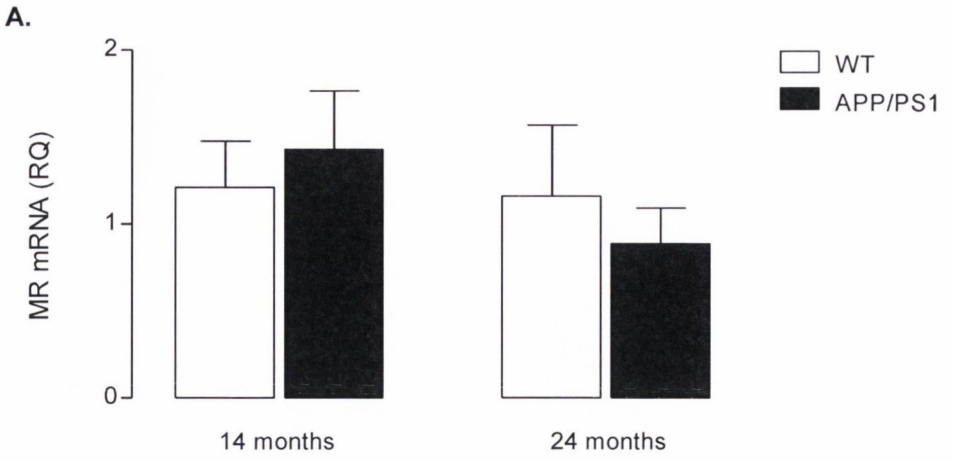
A.
MR mRNA (RQ)
2
1
0
WT
APP/PS1
14 months
24 months

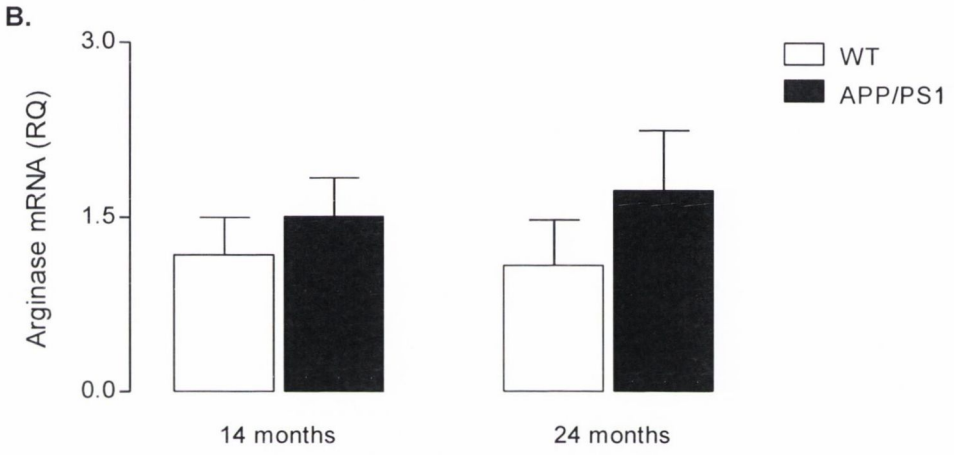
B.
Arginase mRNA (RQ)
3.0
1.5
0.0
WT
APP/PS1
14 months
24 months

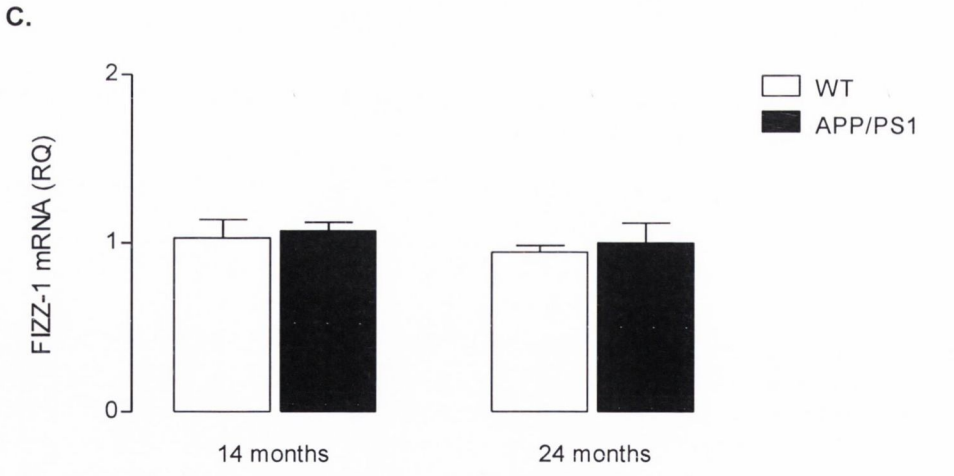
C.
FIZZ-1 mRNA (RQ)
2
1
0
WT
APP/PS1
14 months
24 months

Figure 6.5 Neither age nor genotype had an effect on mRNA expression of MR, arginase-1 or FIZZ-1 in the cortex of APP/PS1 mice.

Groups of middle-aged (13-14 months) and aged (22-24 months) WT and APP/PS1 mice were sacrificed and MR (A), arginase-1 (B) and FIZZ-1 (C) mRNA expression were assessed in the cortex using RT-PCR. The data demonstrate that mRNA expression of all three markers of alternative activation were unchanged in the cortex of middle-aged or aged APP/PS1 mice compared with WT controls. Data are expressed as means + SEM (n=4-8).

A: $Genotype_{effect}$ [$F_{(1,23)}$=0.0074, p=0.9322], age_{effect} [$F_{(1,23)}$=0.8269, p=0.3735], $interaction_{effect}$ [$F_{(1,23)}$=0.5658, p=0.4603]. **B:** $Genotype_{effect}$ [$F_{(1,23)}$=2.29, p=0.1445], age_{effect} [$F_{(1,23)}$=2.798, p=0.1085], $interaction_{effect}$ [$F_{(1,23)}$=2.589, p=0.1219]. **C:** $Genotype_{effect}$ [$F_{(1,23)}$=0.1978, p=0.661], age_{effect} [$F_{(1,23)}$=0.5292, p=0.475], $interaction_{effect}$ [$F_{(1,23)}$=0.002, p=0.961].

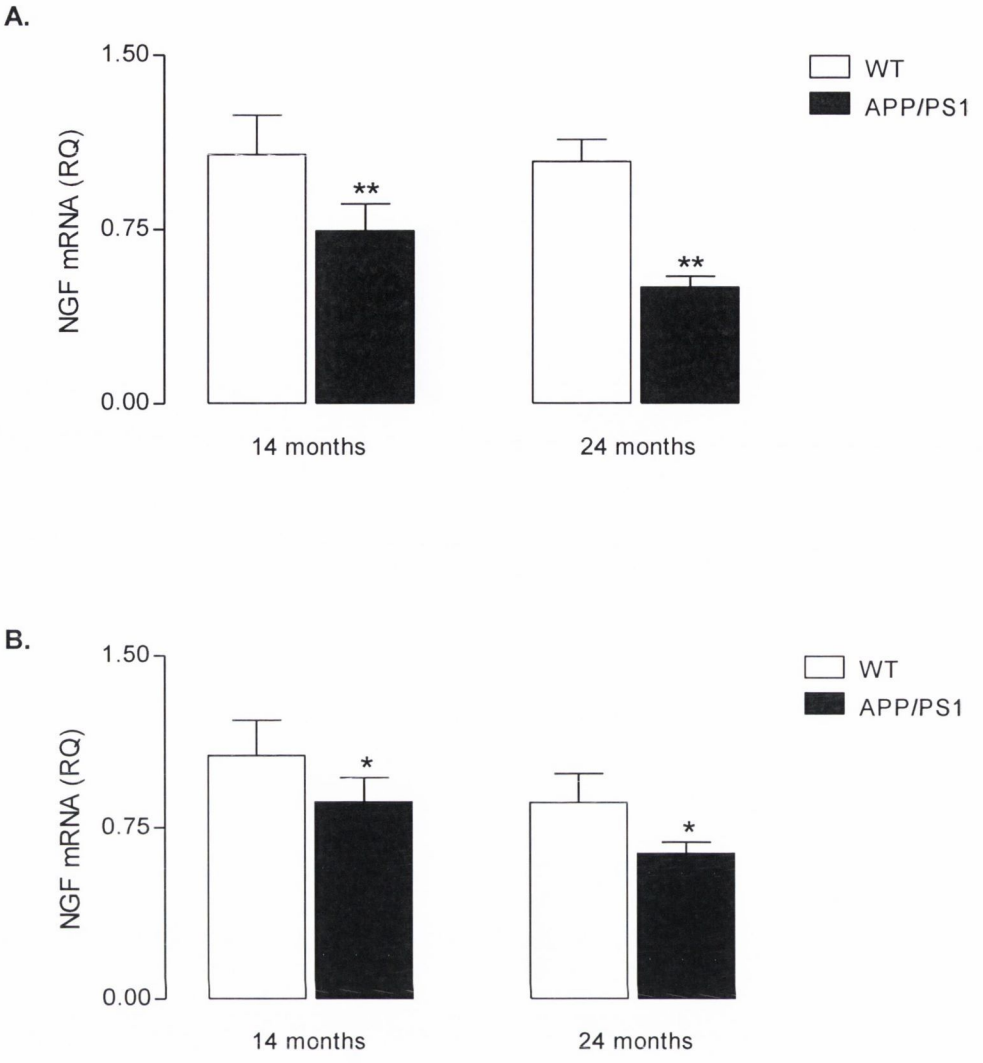

Figure 6.6 NGF mRNA expression was decreased in the cortex and hippocampus of middle-aged and aged APP/PS1 mice compared with WT controls.

Groups of middle-aged (13-14 months) and aged (22-24 months) WT and APP/PS1 mice were sacrificed and NGF mRNA expression was assessed in the cortex (A) and hippocampus (B) using RT-PCR. The data show that NGF was decreased in the cortex ($p<0.01$) and hippocampus ($p<0.05$) of APP/PS1 mice compared with WT controls. Data are expressed as means + SEM ($n=4$-8). *$p<0.05$, *$p<0.01$ versus WT controls (2-way ANOVA followed by Newman-Keuls *post-hoc* analysis).

A: $\text{Genotype}_{\text{effect}}$ [$F_{(1,23)}=10.09$, $p=0.0046$], $\text{age}_{\text{effect}}$ [$F_{(1,23)}=0.9912$, $p=0.3308$], $\text{interaction}_{\text{effect}}$ [$F_{(1,23)}=0.5949$, $p=0.4491$]. **B:** $\text{Genotype}_{\text{effect}}$ [$F_{(1,23)}=4.994$, $p=0.036$], $\text{age}_{\text{effect}}$ [$F_{(1,23)}=1.693$, $p=0.2067$], $\text{interaction}_{\text{effect}}$ [$F_{(1,23)}=0.3085$, $p=0.5842$].

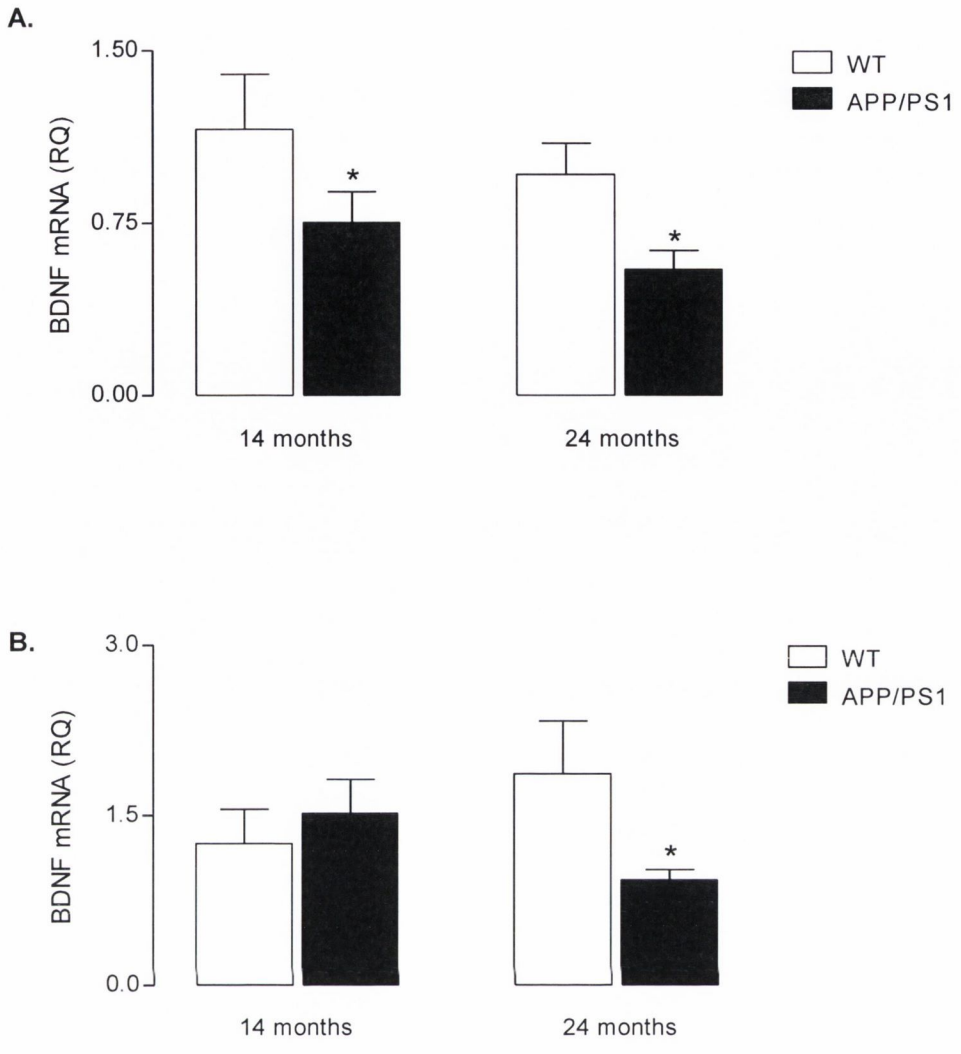

Figure 6.7 BDNF mRNA expression was decreased in the cortex of middle-aged and aged APP/PS1 mice compared with WT controls.

Groups of middle-aged (13-14 months) and aged (22-24 months) WT and APP/PS1 mice were sacrificed and BDNF mRNA expression was assessed in the cortex (A) and hippocampus (B) using RT-PCR. The data show that BDNF was decreased in the cortex ($p<0.05$) of middle-aged and aged APP/PS1 mice compared with WT controls, and in the hippocampus ($p<0.05$) of aged APP/PS1 animals only. Data are expressed as means + SEM (n=4-8). *$p<0.05$, *$p<0.01$ versus WT controls (2-way ANOVA followed by Newman-Keuls *post-hoc* analysis).

A: $\text{Genotype}_{\text{effect}}$ [$F_{(1,22)}=5.21$, $p=0.0325$], $\text{age}_{\text{effect}}$ [$F_{(1,22)}=1.232$, $p=0.2790$], $\text{interaction}_{\text{effect}}$ [$F_{(1,22)}=0.0005$, $p=0.9825$]. **B:** $\text{Genotype}_{\text{effect}}$ [$F_{(1,22)}=1.342$, $p=0.2586$], $\text{age}_{\text{effect}}$ [$F_{(1,22)}=0.002$, $p=0.9628$], $\text{interaction}_{\text{effect}}$ [$F_{(1,22)}=4.342$, $p=0.0485$]

6.3.2 The effect of age and genotype on markers of classical activation

A 2-way ANOVA followed by *post-hoc* analysis demonstrated a genotype-related increase in TNFα mRNA expression in the cortex of APP/PS1 mice compared with WT controls ($p<0.01$) as shown in figure 6.8, and this was further enhanced in older animals ($p<0.05$). A similar trend in the hippocampus failed to reach statistical significance. A genotype-related increase in TNFα protein expression was also observed in the hippocampus of APP/PS1 mice compared with WT controls ($p<0.01$) as shown in figure 6.9. This figure also demonstrates that IL-1β protein expression was increased in the hippocampus of middle-aged APP/PS1 mice ($p<0.01$), and this was further enhanced in older animals ($p<0.01$). Neither age nor genotype had an effect on iNOS mRNA expression in either brain region examined as shown in figure 6.10.

While neither age nor genotype had an effect on mRNA expression of IFNγR in the cortex of APP/PS1 mice as demonstrated in figure 6.11, protein expression of IFNγR was increased on microglia isolated from the cortex of middle-aged and aged transgenic mice compared with WT controls ($p<0.01$) as shown in figure 6.12.

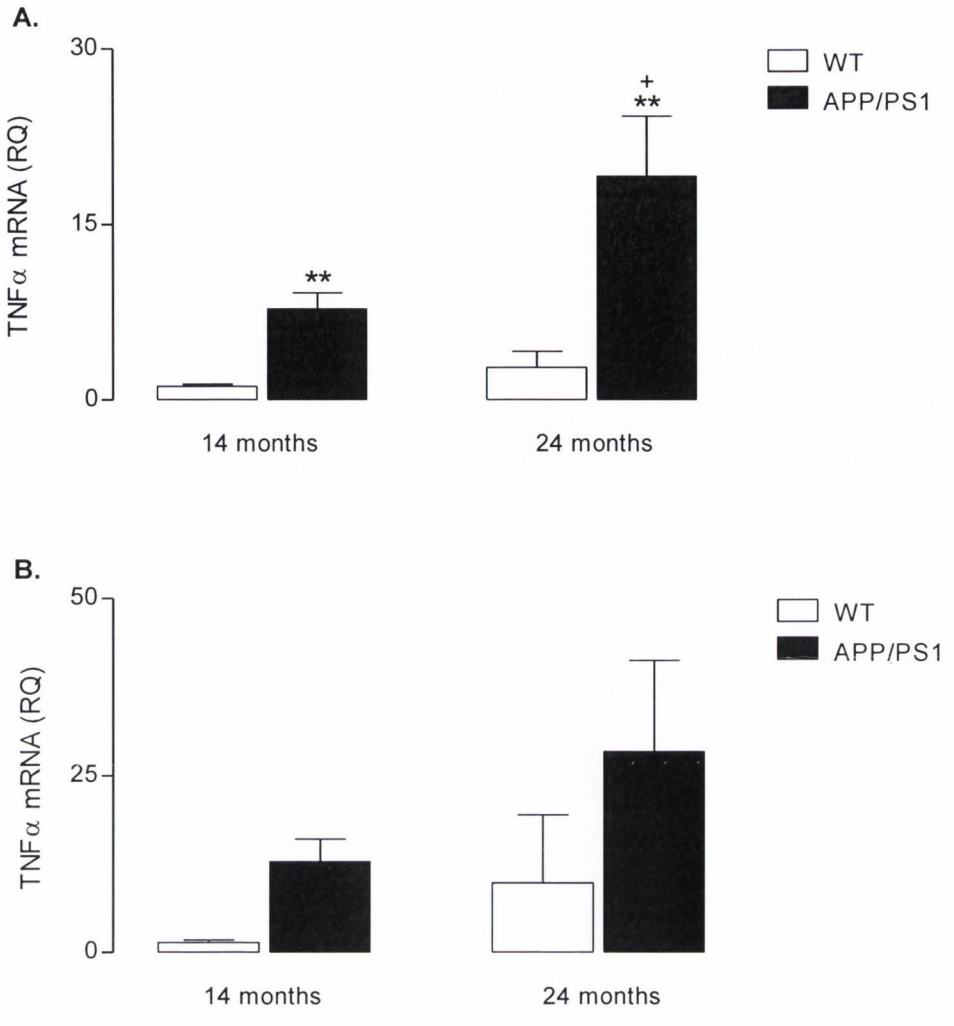

Figure 6.8 TNFα mRNA expression was increased in the cortex of middle-aged APP/PS1 mice and this was further enhanced in older animals.

Groups of middle-aged (13-14 months) and aged (22-24 months) WT and APP/PS1 mice were sacrificed and TNFα mRNA expression was assessed in the cortex (A) and hippocampus (B) using RT-PCR. The data demonstrate a genotype-related increase in TNFα mRNA expression in the cortex of APP/PS1 mice compared with WT controls ($p<0.01$), and this was further enhanced in older animals ($p<0.05$). Data are expressed as means + SEM (n=4-8). $^{**}p<0.01$ versus WT controls; $^{+}p<0.05$ versus middle-aged APP/PS1 mice (2-way ANOVA followed by Newman-Keuls *post-hoc* analysis).

A: $Genotype_{effect}$ [$F_{(1,23)}=10.05$, $p=0.0044$], age_{effect} [$F_{(1,23)}=3.2$, $p=0.0874$], $interaction_{effect}$ [$F_{(1,23)}=1.784$, $p=0.1953$]. **B:** $Genotype_{effect}$ [$F_{(1,23)}=2.727$, $p=0.1151$], age_{effect} [$F_{(1,23)}=1.763$, $p=0.2$], $interaction_{effect}$ [$F_{(1,23)}=0.1545$, $p=0.6986$].

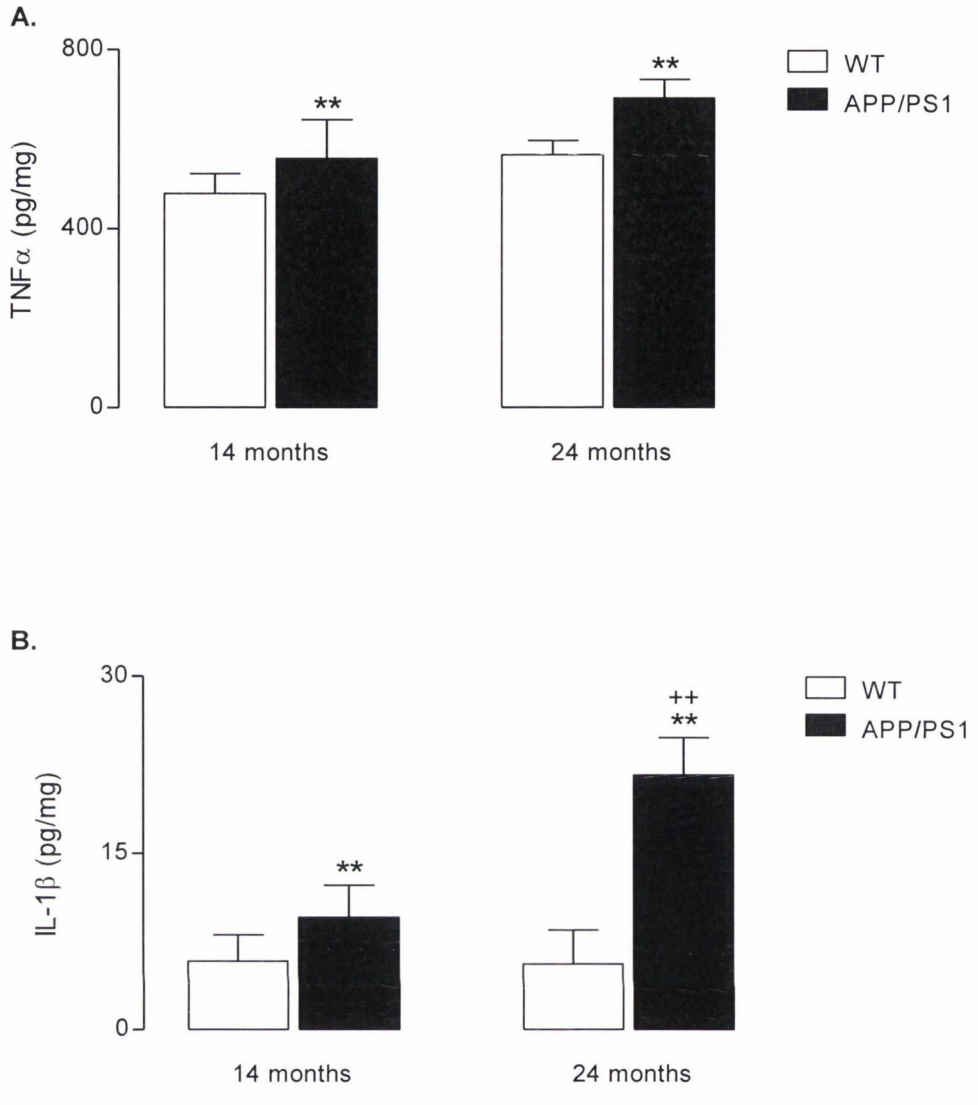

Figure 6.9 TNFα and IL-1β were increased in the hippocampus of middle-aged and aged APP/PS1 mice.

Groups of middle-aged (13-14 months) and aged (22-24 months) WT and APP/PS1 mice were sacrificed and protein expression of TNFα (A) and IL-1β (B) were assessed in the hippocampus by multiplex ELISA. The data demonstrate a genotype-related increase in TNFα in the hippocampus of APP/PS1 mice ($p<0.01$). IL-1β was also increased in the hippocampus of middle-aged APP/PS1 mice ($p<0.01$) and this was further enhanced in older animals ($p<0.01$). Data are expressed as means + SEM (n=4-8). $^{**}p<0.01$ versus WT controls; $^{+}p<0.05$ versus middle-aged APP/PS1 mice (2-way ANOVA followed by Newman-Keuls *post-hoc* analysis).

A: $\text{Genotype}_{\text{effect}}$ [$F_{(1,22)}=10.27$, $p=0.0047$], $\text{age}_{\text{effect}}$ [$F_{(1,22)}=2.417$, $p=0.1365$], $\text{interaction}_{\text{effect}}$ [$F_{(1,22)}=0.1426$, $p=0.7099$]. **B:** $\text{Genotype}_{\text{effect}}$ [$F_{(1,22)}=9.397$, $p=0.0059$], $\text{age}_{\text{effect}}$ [$F_{(1,22)}=3.352$, $p=0.0814$], $\text{interaction}_{\text{effect}}$ [$F_{(1,22)}=3.652$, $p=0.0697$].

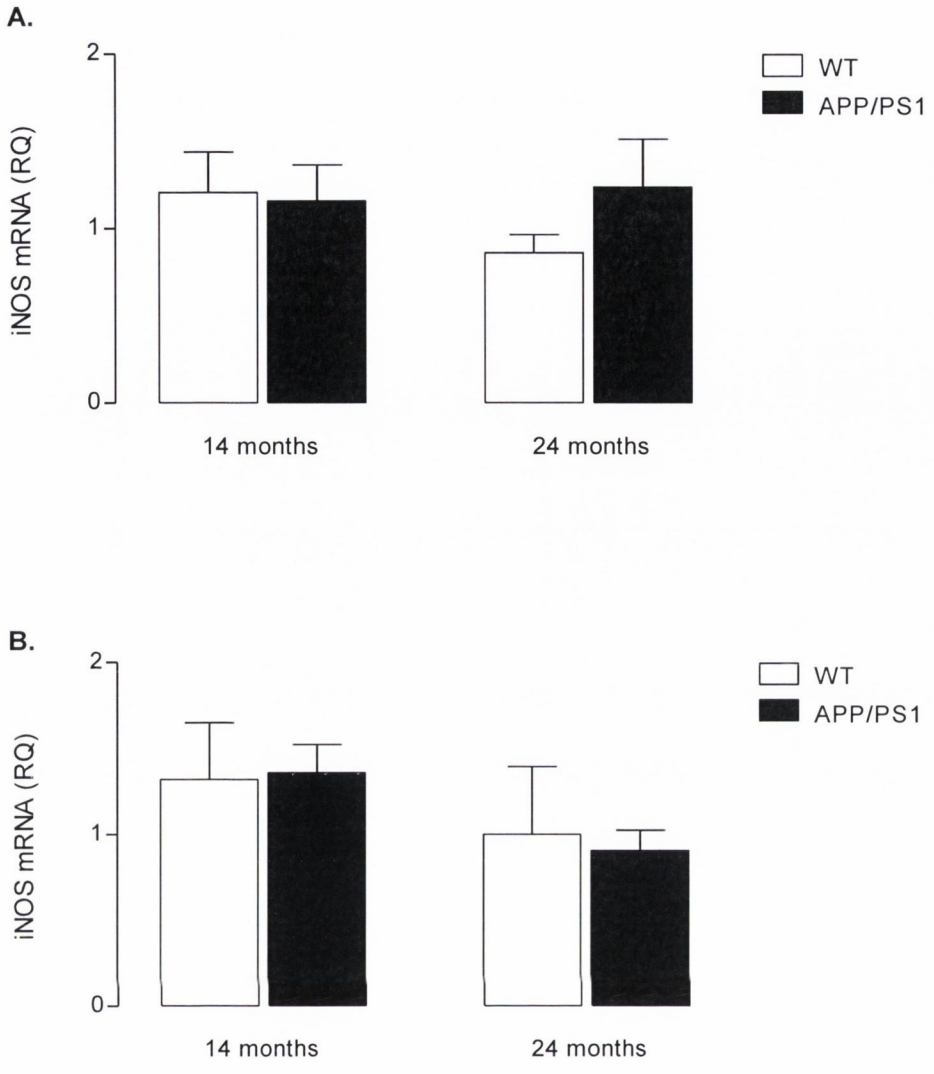

Figure 6.10 Neither age nor genotype had an effect on iNOS mRNA expression in the cortex or hippocampus of APP/PS1 mice.

Groups of middle-aged (13-14 months) and aged (22-24 months) WT and APP/PS1 mice were sacrificed and iNOS mRNA expression was assessed in the cortex (A) and hippocampus (B) using RT-PCR. The data show that iNOS mRNA expression was unchanged by age or genotype in either brain region examined. Data are expressed as means + SEM (n=4-8).

A: $Genotype_{effect}$ [$F_{(1,22)}$=0.3603, p=0.5545], age_{effect} [$F_{(1,22)}$=0.2433, p=0.6267], $interaction_{effect}$ [$F_{(1,22)}$=0.6117, p=0.4425]. **B:** $Genotype_{effect}$ [$F_{(1,22)}$=0.013, p=0.9112], age_{effect} [$F_{(1,22)}$=2.622, p=0.1203], $interaction_{effect}$ [$F_{(1,22)}$=0.013, p=0.9112].

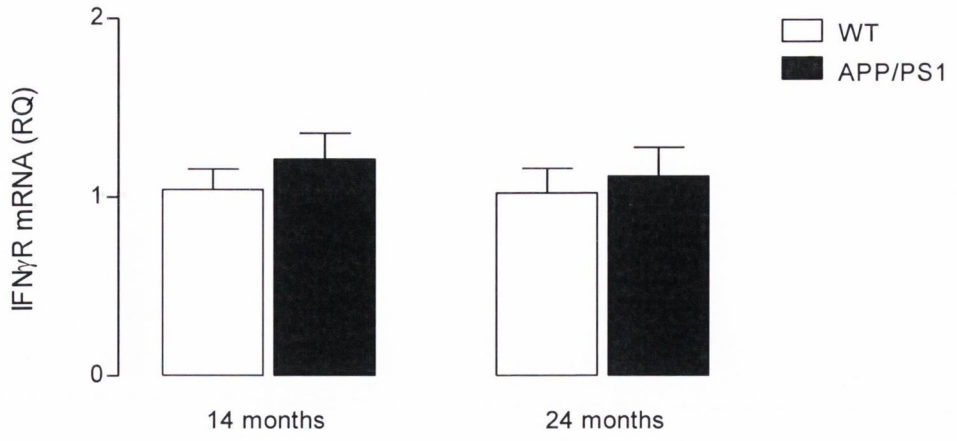

Figure 6.11 Neither age nor genotype had an effect on IFNγR mRNA expression in the cortex of APP/PS1 mice.

Groups of middle-aged (13-14 months) and aged (22-24 months) WT and APP/PS1 mice were sacrificed and IFNγR mRNA expression was assessed in the cortex using RT-PCR. The data demonstrate that IFNγR mRNA expression was unchanged in the cortex of middle-aged or aged APP/PS1 mice compared with WT controls. Data are expressed as means + SEM (n=4-8).

$Genotype_{effect}$ [$F_{(1,23)}$=0.667, p=0.4232], age_{effect} [$F_{(1,23)}$=0.128, p=0.7241], $interaction_{effect}$ [$F_{(1,23)}$=0.06, p=0.8093].

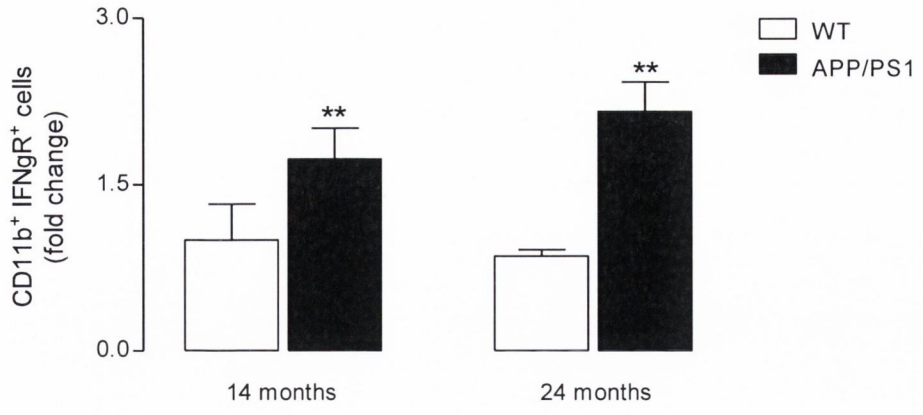

Figure 6.12 IFNγR protein expression was increased on microglia isolated from the cortex of middle-aged and aged APP/PS1 mice.

Groups of middle-aged (13-14 months) and aged (22-24 months) WT and APP/PS1 mice were sacrificed and IFNγR expression was assessed on $CD11b^+$ microglia using flow cytometry. The data show that IFNγR expression on microglia isolated from APP/PS1 mice was increased in middle-aged and aged mice ($p<0.01$). Data are expressed as means + SEM (n=4-8). $^{**}p<0.01$ versus WT controls (2-way ANOVA followed by Newman-Keuls *post-hoc* analysis).

$Genotype_{effect}$ [$F_{(1,23)}$=12.12, p=0.0022], age_{effect} [$F_{(1,23)}$=0.2388, p=0.6301], $interaction_{effect}$ [$F_{(1,23)}$=0.9553, p=0.3395].

6.3.3 The effect of genotype on the presence of infiltrating T cells, monocytes/macrophages and neutrophils in the cortex of APP/PS1 mice

The presence of infiltrating leukocytes was assessed in the cortex of 18-month old WT and APP/PS1 mice using flow cytometry. A 2-fold increase in the presence of $CD3^+CD4^+$ T cells ($p<0.05$) and $CD11b^+CD45^+$ ($p<0.01$) monocytes/macrophages, and a 4-fold increase in $CD11b^+Ly6G^+$ neutrophils ($p<0.01$) was observed in tissue prepared from APP/PS1 mice compared with WT controls as shown in figure 6.13.

T cell subtypes were identified by intracellularly staining $CD3^+CD4^+$ T cells for the presence of IFNγ (Th1), IL-4 (Th2) or IL-17 (Th17). The number of Th1 cells was significantly increased ($p<0.05$), while Th2 cells were significantly decreased ($p<0.05$) in tissue prepared from APP/PS1 mice compared with WT controls as shown in figure 6.14. A similar increase in the presence of Th17 cells ($p=0.1138$) cells failed to reach statistical significance.

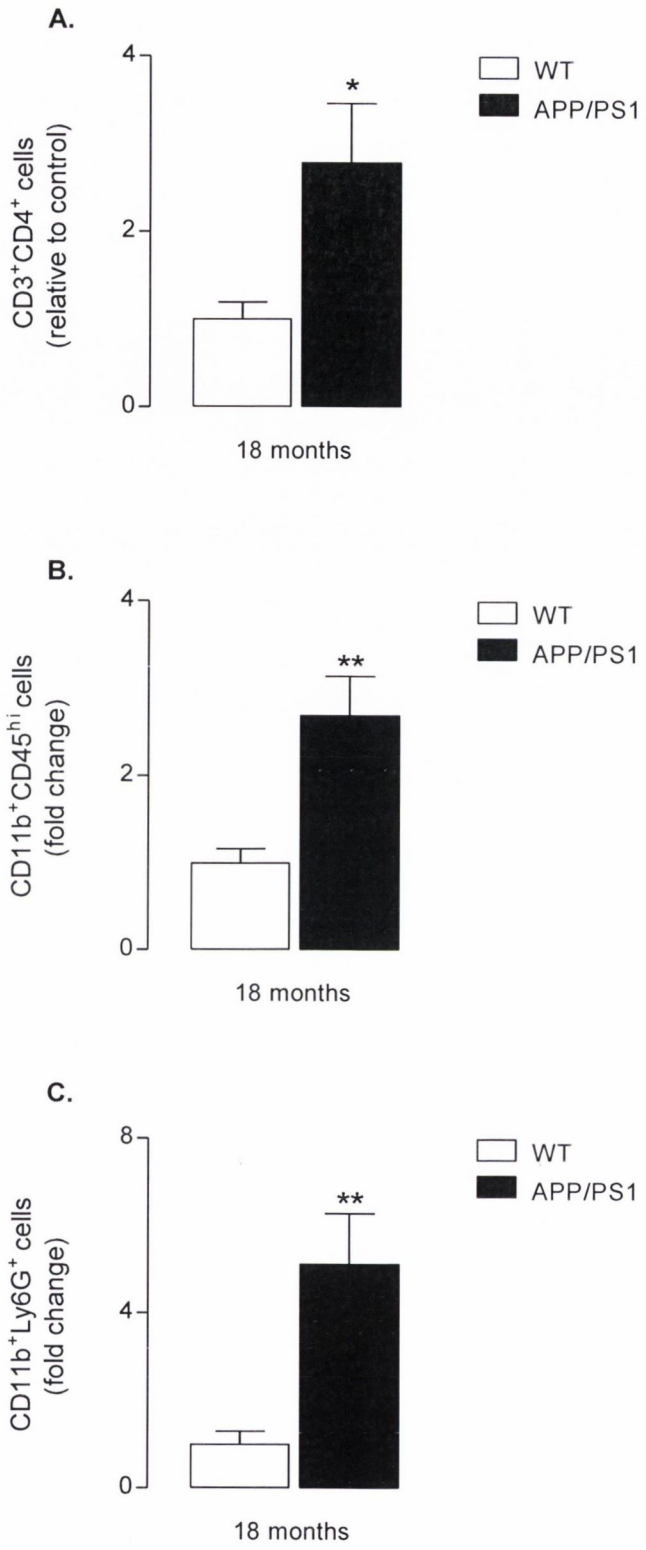
A.
CD3+CD4+ cells
(relative to control)
4
2
0
*
WT
APP/PS1
18 months
B.
CD11b+CD45hi cells
(fold change)
4
2
0
**
WT
APP/PS1
18 months
C.
CD11b+Ly6G+ cells
(fold change)
8
4
0
**
WT
APP/PS1
18 months

Figure 6.13 T cell, monoctye/macrophage and neutrophil cell numbers were increased in the cortex of APP/PS1 mice.

WT and APP/PS1 mice (18 months) were sacrificed and the presence of $CD11b^{+}CD5^{hi}$ macrophages (A), $CD11b^{+}Ly6G^{+}$ neutrophils (B) and $CD3^{+}CD4^{+}$ T cells (C) was assessed in the cortex using flow cytometry. The data show the presence of T cells ($p<0.05$), monocytes/macrophages ($p<0.01$) and neutrophils ($p<0.01$) was increased in tissue prepared from APP/PS1 mice compared with WT controls. Data are expressed as means + SEM (n=4-8). *$p<0.05$, **$p<0.01$ versus WT controls (Student's t-test for independent means).

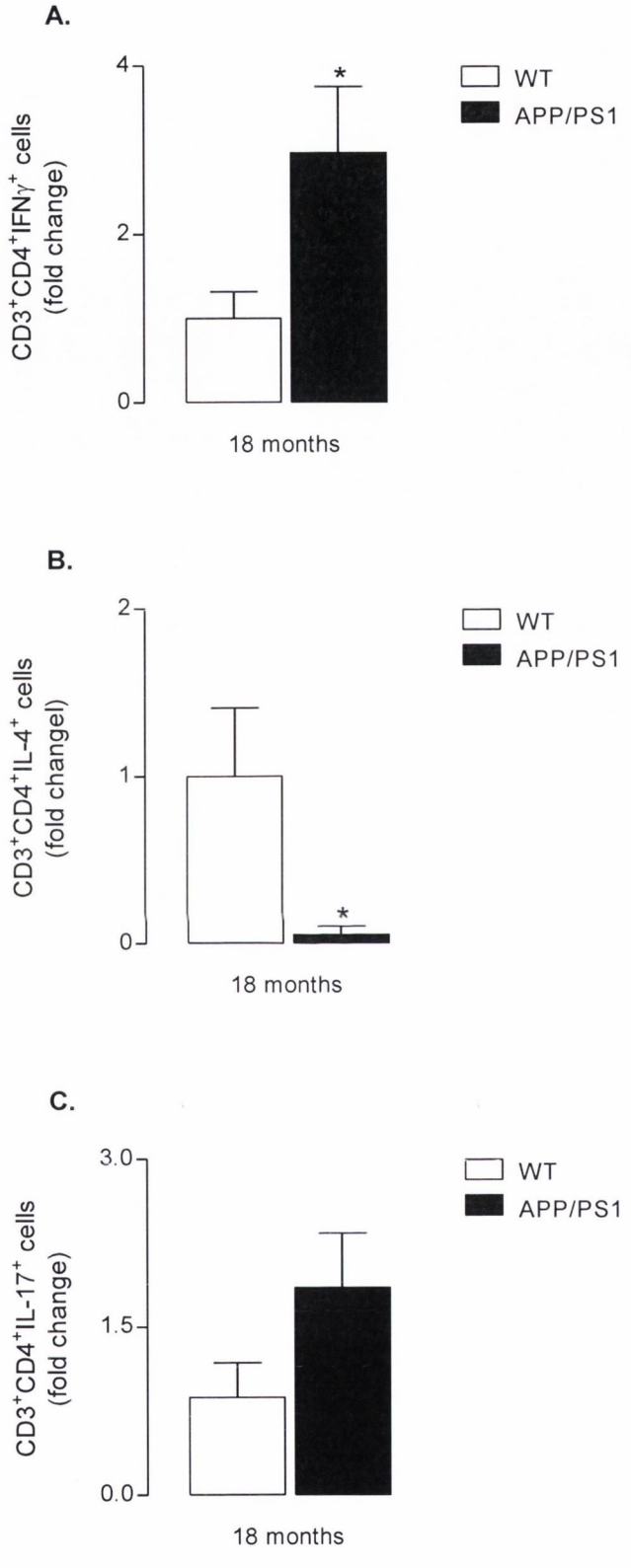
A.
4
2
0
*
WT
APP/PS1
CD3+CD4+IFNγ+ cells
(fold change)
18 months
B.
2
1
0
*
WT
APP/PS1
CD3+CD4+IL-4+ cells
(fold changel)
18 months
C.
3.0
1.5
0.0
WT
APP/PS1
CD3+CD4+IL-17+ cells
(fold change)
18 months

Figure 6.14 Th1 cell numbers were increased and Th2 cell numbers decreased in the cortex of APP/PS1 mice.

WT and APP/PS1 mice (18 months) were sacrificed and the presence of Th1 (A), Th2 (B) and Th17 (C) T cells was assessed in the cortex using flow cytometry. Mononuclear cells were isolated from cortical tissue by density separation over Percoll and incubated with PMA (10ng/ml), ionomycin (1µg/ml) and BFA (5µg/ml) at 37°C for 5 hours. The data show that Th1 cell numbers were increased ($p<0.05$), while Th2 cell numbers were decreased ($p<0.05$) in tissue prepared from APP/PS1 mice compared with WT controls. Increased numbers of Th17 cells cells failed to reach statistical significance. Data are expressed as means + SEM (n=4-8). *$p<0.05$ versus WT controls (Student's t-test for independent means).

6.3.4 The effect of age and genotype on chemokine expression

A 2-way ANOVA followed by *post-hoc* analysis demonstrated an increase in CXCL1 protein expression in hippocampal tissue prepared from aged APP/PS1 mice compared with WT controls ($p<0.05$) and also compared with middle-aged transgenic animals ($p<0.01$) as shown in figure 6.15.

An increase in MIP-1α mRNA expression was observed in the hippocampus of aged APP/PS1 mice compared with WT controls ($p<0.01$) and also with middle-aged APP/PS1 animals ($p<0.01$) as demonstrated in figure 6.16. A similar trend in the expression of RANTES, IP-10 and MCP-1 failed to reach statistical significance.

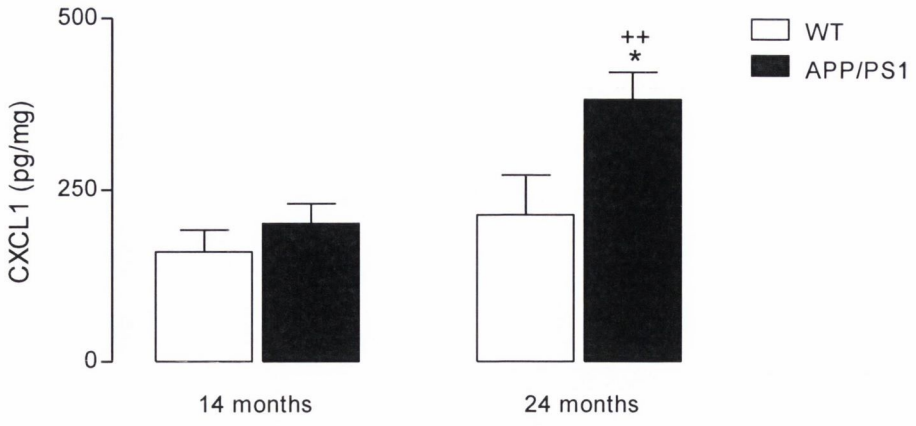

Figure 6.15 CXCL1 protein expression was increased in the hippocampus of aged APP/PS1 mice compared with WT controls.

Groups of middle-aged (13-14 months) and aged (22-24 months) WT and APP/PS1 mice were sacrificed and CXCL1 protein was assessed in the hippocampus by multiplex ELISA. The data show that the presence of CXCL1 was increased in the hippocampus of aged APP/PS1 animals compared with WT controls ($p<0.05$), and also compared with middle-aged APP/PS1 mice ($p<0.01$). Data are expressed as means + SEM ($n=4$-8). $^{*}p<0.05$ versus WT controls; $^{++}p<0.01$ versus middle-aged APP/PS1 mice (2-way ANOVA followed by Newman-Keuls *post-hoc* analysis).

$Genotype_{effect}$ [$F_{(1,23)}=7.163$, $p=0.0315$], age_{effect} [$F_{(1,23)}=9.001$, $p=0.0065$], $interaction_{effect}$ [$F_{(1,23)}=2.619$, $p=0.1192$].

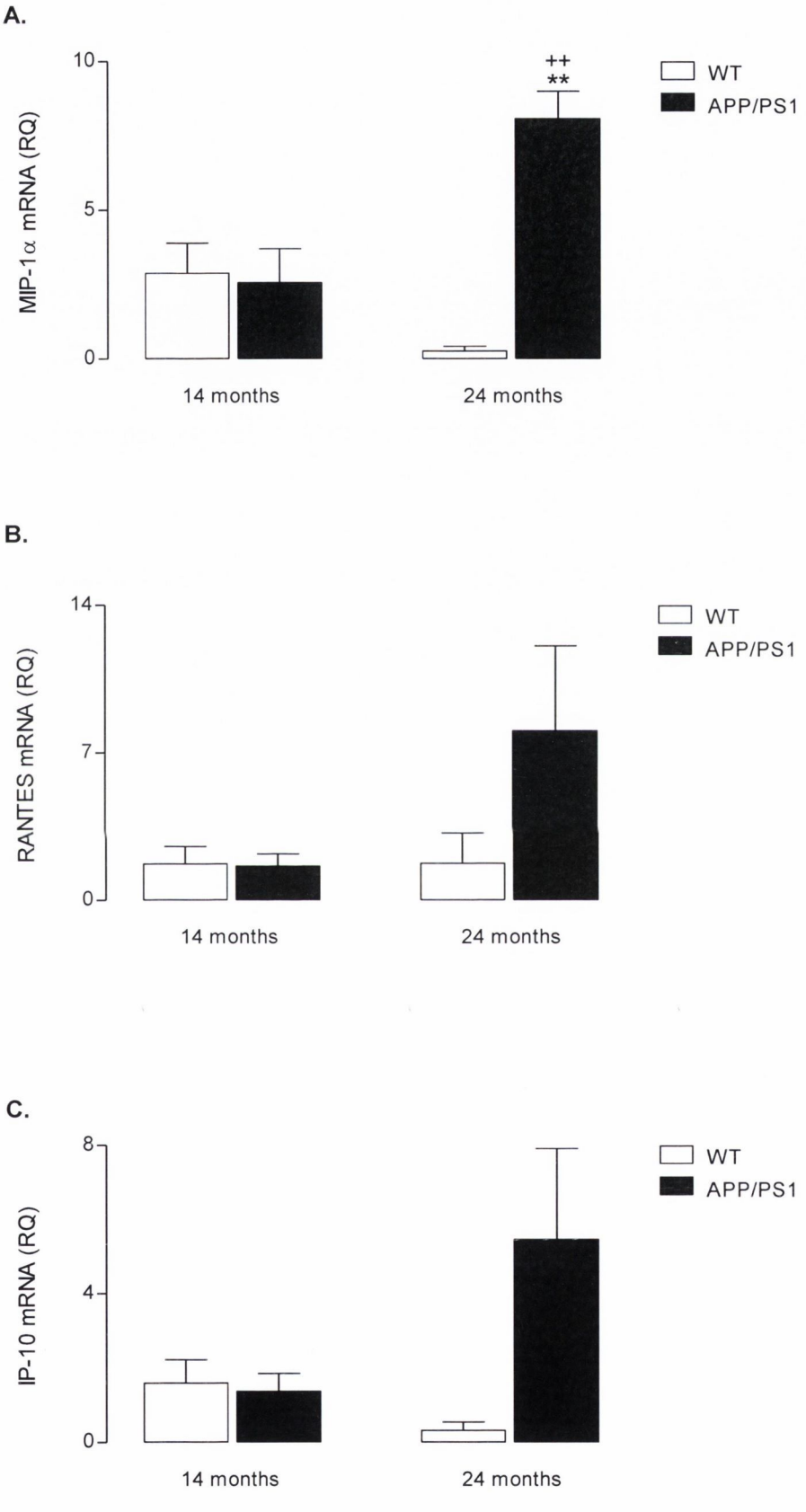
A.
MIP-1α mRNA (RQ)
10
5
0
++
**
WT
APP/PS1
14 months
24 months
B.
RANTES mRNA (RQ)
14
7
0
WT
APP/PS1
14 months
24 months
C.
IP-10 mRNA (RQ)
8
4
0
WT
APP/PS1
14 months
24 months

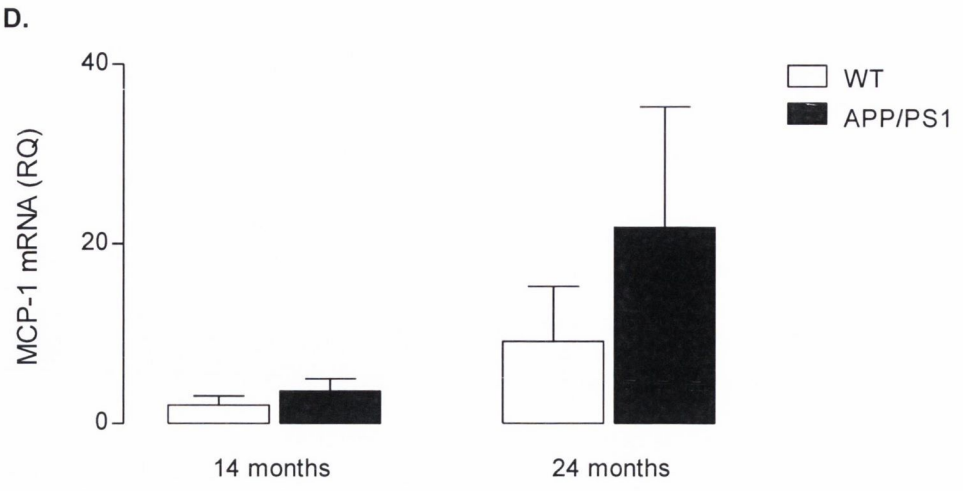

Figure 6.16 MIP-1α mRNA expression was increased in the hippocampus of aged APP/PS1 mice compared with WT controls.

Groups of middle-aged (13-14 months) and aged (22-24 months) WT and APP/PS1 mice were sacrificed and MIP-1α (A), RANTES (B), IP-10 (C) and MCP-1 (D) mRNA expression was assessed in the cortex and hippocampus using RT-PCR. The data show that MIP-1α mRNA was significantly increased in the hippocampus of aged APP/PS1 animals compared with WT controls ($p<0.01$) and also with their middle-aged counterparts ($p<0.01$). A similar trend in the expression of RANTES, IP-10 and MCP-1 failed to reach statistical significance. Data are expressed as means + SEM (n=4-8). $^{**}p<0.01$ versus WT controls; $^{++}p<0.01$ versus middle-aged APP/PS1 mice (2-way ANOVA followed by Newman-Keuls *post-hoc* analysis).

A: $Genotype_{effect}$ [$F_{(1,22)}$=12.24, p=0.0019], age_{effect} [$F_{(1,22)}$=1.827, p=0.1896], $interaction_{effect}$ [$F_{(1,22)}$=14.41, p=0.0009]. **B:** $Genotype_{effect}$ [$F_{(1,23)}$=1.368, p=0.2457], age_{effect} [$F_{(1,23)}$=1.514, p=0.2309], $interaction_{effect}$ [$F_{(1,23)}$=1.489, p=0.2347]. **C:** $Genotype_{effect}$ [$F_{(1,23)}$=2.361, p=0.1381], age_{effect} [$F_{(1,23)}$=0.7761, p=0.3874], $interaction_{effect}$ [$F_{(1,23)}$=2.812, p=0.1071]. **D:** $Genotype_{effect}$ [$F_{(1,23)}$=0.713, p=0.4084], age_{effect} [$F_{(1,23)}$=2.247, p=0.1495], $interaction_{effect}$ [$F_{(1,23)}$=0.4378, p=0.5157].

6.4 Discussion

This study set out to assess the expression profile of markers of classical activation, alternative activation and acquired deactivation in the brains of APP/PS1 mice and to assess whether results could be correlated with the presence of infiltrating peripheral leukocytes and enhanced chemokine expression. Macrophages/microglia are stimulated to become classically active in the presence of IFNγ, resulting in the production of oxidative metabolites and the release of pro-inflammatory cytokines such as TNFα, IL-1β, IL-6 and IL-12p40 (Colton, 2009). In contrast, markers of alternative activation and acquired deactivation are induced by IL-4 and IL-13, and stimulate release of IL-10 and TGFβ in order to promote tissue repair and recovery (Mosser, 2003).

Results presented here suggest that IL-4Rα mRNA expression was increased in the cortex and hippocampus of APP/PS1 mice compared with WT controls. However, although its mRNA was increased, this did not translate to enhanced protein expression of IL-4Rα on microglia, where a reduction was observed in middle-aged APP/PS1 mice compared with WT controls. Stimulation of peripheral macrophages with IL-4 has been shown to antagonise classical activation pathways and induce the expression of proteins involved in tissue repair and reconstruction (Colton, 2009). Although they share only ~25% sequence homology, IL-4 and IL-13 are ligands for the same functional IL-4Rα receptor subunit, explaining the overlap in their biological effects (Vita *et al.*, 1995).

Treatment of primary rat glia with IL-4 has been shown to enhance the uptake and degradation of oligomeric Aβ, in addition to inducing expression of CD36 and the Aβ-degrading enzymes neprilysin and insulin-degrading enzyme (Shimizu *et al.*, 2008). Interestingly, enhanced expression of IL-4 in APP/PS1 mice has also been shown to attenuate AD pathogenesis by reducing gliosis and Aβ deposition, while

simultaneously enhancing neurogenesis and spatial learning (Kiyota *et al.*, 2010). The current data suggest that IL-4, and indeed IL-13, may not be able to exert their full repertoire of anti-inflammatory effects due to decreased expression of their cognate binding receptor on microglia in APP/PS1 mice. It could be speculated that the observed increase in mRNA expression was a compensatory measure in order to enhance protein expression of IL-4Rα, thus attempting to allow the cells to better respond to IL-4 and assist in the promotion of tissue repair and recovery.

Results from the current study demonstrate that expression of IL-10 was increased in the hippocampus of middle-aged and aged APP/PS1 mice compared with WT controls. While IL-10R was unaffected by genotype, an age-related reduction in its expression was also observed. These results indicate an attempt to mount an anti-inflammatory response in the cortex of APP/PS1 animals compared with WT controls. IL-10 is a Th2-type cytokine, elevated during the course of most major CNS diseases, that acts to downregulate expression of pro-inflammatory cytokines, thus promoting the survival of neurons and glia (Strle *et al.*, 2001). Expression of IL-10 is detectable in the frontal and parietal lobe of the healthy brain, and has been suggested to play a role in neuronal homeostasis and cell survival (Rubio-Perez and Morillas-Ruiz, 2012). While Aβ does not appear to stimulate production of IL-10 by glial cells *in vitro*, pre-treatment with IL-10 inhibits the Aβ-induced production of pro-inflammatory cytokines (Szczepanik *et al.*, 2001). Results from the current study are in agreement with previous findings of reactive astrocytes demonstrating increased IL-10 immunoreactivity in the brains of 13 month transgenic Tg2576 mice compared with non-transgenic controls (Apelt and Schliebs, 2001).

With regard to some further markers of alternative activation, results demonstrate that neither age nor genotype had an effect on mRNA expression of MR, arginase-1 or FIZZ-1 in APP/PS1 mice compared with WT controls. Engagement of MR with its ligand is generally reported to initiate phagocytosis, with subsequent activation of anti-inflammatory signalling pathways resulting in increased expression of IL-10 and

decreased expression of IL-12 and TNFα (Chieppa *et al.*, 2003). MR expression in the brain is found primarily on perivascular microglia (Perry and Gordon, 1988). Arginase-1, a manganese-containing enzyme that provides a cell specific system for arginine metabolism, is robustly expressed in the cerebellum, pons, medulla, and spinal cord with lower expression in the hippocampus and the entorhinal and temporal cortices (Yu *et al.*, 2001). FIZZ-1, a cysteine-rich protein that shares significant homology with IL-4, is a member of a family of resistin-like molecules reported to regulate pro-inflammatory cytokine expression (Dong *et al.*, 2010). Reports regarding the role of MR, arginase-1 and FIZZ-1 in the brain, and indeed in AD, are extremely limited. A recent study demonstrated increased mRNA expression of MR and arginase-1 in the brains of Tg2576 mice at 15 months of age (Colton *et al.*, 2006). Although these results are of interest, the different transgenic model used must be noted, and so a direct comparison with results from the current study may not be appropriate.

Results presented here demonstrate that both NGF and BDNF mRNA expression were decreased in the cortex and hippocampus of APP/PS1 mice compared with WT controls. While neurotrophins have been shown to control many aspects of neuronal function, survival and development throughout the CNS (Skaper, 2008), it must also be noted that increased expression of NGF has been reported as a marker of acquired deactivation (Wei and Jonakait, 1999). Studies have demonstrated that IL-4 induces the secretion of NGF by cortical and cerebellar astrocytes (Awatsuji *et al.*, 1993, Brodie *et al.*, 1998). A recent study has also demonstrated that IL-4 directly induces BDNF mRNA in cultured astrocytes, in addition to reversing the decreased production of BDNF following incubation of astrocytes with pro-inflammatory cytokines (Derecki *et al.*, 2010). Although IL-4 and IL-10 are both associated with increased expression of neurotrophins (Colton and Wilcock, 2010), the opposite was observed in the current study, something which could have, in part, been due to decreased expression of IL-4Rα.

It must also be noted that reduced levels of neurotrophins are linked with AD progression in terms of a loss of trophic support for neurons, specifically basal forebrain cholinergic neurons (Davies and Maloney, 1976). A reduction in NGF-containing neurons has been reported in AD (Mufson *et al.*, 1989), and BDNF mRNA is also decreased in the post-mortem hippocampus of AD patients as assessed by *in situ* hybridization (Phillips *et al.*, 1991). It has been suggested that NGF and BDNF may be useful in halting, reversing or at least slowing the progression of AD related symptoms. A small study which implanted autologous fibroblasts genetically modified to express human NGF into the forebrain of humans suffering from mild AD, reported an improvement in the rate of cognitive decline concomitant with robust growth responses to NGF, suggesting a role for the application of neurotrophins in counteracting the observed neuronal loss that occurs in AD (Tuszynski *et al.*, 2005).

To investigate whether there were age- or genotype-related changes in markers of classical activation, the hallmarks of this phenotype, TNFα and iNOS were assessed in cortical tissue prepared from middle-aged and aged WT and APP/PS1 mice. The data demonstrate that TNFα mRNA expression was significantly increased in the cortex of middle-aged and aged APP/PS1 mice compared with WT controls. TNFα mRNA expression was further increased in cortical tissue prepared from aged compared with middle-aged APP/PS1 mice. Similar changes were observed in the hippocampus, however these did not reach statistical significance. In addition, TNFα protein expression was increased in the hippocampus of middle-aged and aged APP/PS1 mice. These results are in agreement with findings that increased TNFα expression in APP/PS1 mice can be correlated with disease severity (Ruan *et al.*, 2009). Examination of post-mortem human AD brains has revealed that TNFα co-localises with senile plaques, and is enhanced in both CSF and plasma (Montgomery and Bowers, 2012).

TNFα has been shown to upregulate activity of β-secretase, and as such APP mice lacking the TNF receptor show reduced Aβ generation and plaque formation, attributed to decreased activity of β-secretase (He *et al.*, 2007). Intracerebroventricular injection of anti-TNF antibody into the brains of APP/PS1 mice was shown to result in reduced plaque deposition and tau hyperphosphorylation as early as 3 days following initiation of the injection protocol (Shi *et al.*, 2011). While these results hold promise, it must be pointed out that the effect of long-term abrogation of TNFα receptor expression is, as of yet, unknown. As such, triple transgenic AD mice lacking the receptor for TNF were shown to exhibit enhanced amyloid and tau-related pathological features by the age of 15 months, attributed, in part, to impaired phagocytosis (Montgomery *et al.*, 2011).

Classical activation of microglia is associated with an inflammatory phenotype and, consistent with this, hippocampal concentrations of IL-1β were increased in middle-aged APP/PS1 mice, and this was further enhanced in older animals. Binding of IL-1β to its cognate receptor elicits signal transduction pathways resulting in activation of NFκB and MAPK (Malinin *et al.*, 1997). IL-1β, classified as an early and dominant injury signal, is shown to induce expression of TNFα and IL-6 by astrocytes and microglia (Basu *et al.*, 2004). Although IL-1β expression is barely detectable within the normal CNS, it is rapidly induced following experimental injury (Allan *et al.*, 2005) and increased IL-1β has been reported in the post-mortem brain of patients suffering from AD (Griffin *et al.*, 1989, Sheng *et al.*, 1998). In addition, unilateral hippocampal overexpression of IL-1β is a powerful stimulus for recruitment of leukocytes, such as neutrophils, T cells, dendritic cells and monocytes, to the brain parenchyma (Shaftel *et al.*, 2007).

Although increased iNOS activity is often associated with that of TNFα (Mosser, 2003), no effect of age or genotype on its mRNA expression was observed in the course of this study. iNOS is an inducible nitric oxide-synthesizing enzyme that catalyses the production of NO from L-argninine. Although NO is an important

atypical messenger mediating synaptic transmission and LTP, its presence in large amounts results in the death of neurons and glia (Amitai, 2010). Analysis of iNOS in patients with sporadic AD, and in a transgenic mouse model of AD revealed its presence was increased, specifically associated with astrocytes colocalised with Aβ deposits (Luth *et al.*, 2001). In future studies, it may be beneficial to carry out an assay to assess the enzymatic activity of iNOS rather than simply relying on mRNA expression as an indicator of its biological activity.

IFNγ is a pro-inflammatory cytokine that exerts its effects by binding to the IFNγR, consisting of IFNγRI and IFNγRII subunits, and activating JAK/STAT signalling pathways (Zaidi and Merlino, 2011). IFNγ, acting on its receptor, is known to act as the primary trigger of classical activation and thus, in an effort to understand the underlying cause of the observed inflammatory changes, IFNγR mRNA and cell surface expression were assessed. While there was no effect of age or genotype on mRNA expression of IFNγR in cortical tissue, flow cytometric analysis revealed an increase in IFNγR expression on microglia prepared from middle-aged and aged APP/PS1 mice compared with WT controls.

IFNγ is produced most predominantly by activated NK-cells and T cells, and as these cells do not cross the BBB under normal conditions, IFNγ expression in the healthy CNS is undetectable (Hashioka *et al.*, 2010). Increased numbers of infiltrating T cells in AD (Itagaki *et al.*, 1988) paralleled with increased IFNγ expression (Popko *et al.*, 1997), suggests these cells to be a source of this pro-inflammatory cytokine (Benveniste and Benos, 1995). To examine the possibility that increased IFNγR expression in the brain was a consequence of infiltrating IFNγ-producing cells, a single cell suspension was prepared from APP/PS1 and WT mice for flow cytometric analysis. The data demonstrate a 2-fold increase in the presence of infiltrating T cells and monocytes/macrophages, and a 4-fold increase in neutrophils in tissue prepared from APP/PS1 mice compared with WT controls.

Following activation, naïve $CD4^+$ T cells, or helper T cells, undergo clonal expansion to differentiate into subtypes that can be further classified by their cytokine profiles and effector functions. These cells have no purported phagocytic activity and do not kill pathogens directly, instead they serve to activate and direct the functions of other immune cells (Zhu and Paul, 2008). Th1 and Th17 cells produce pro-inflammatory cytokines such as IL-1, IL-6, IL-17, TNFα and IFNγ, and are involved in inflammation and gliosis by upregulating the release of ROS and NO (Huang *et al.*, 2009). In contrast, Th2 cells produce anti-inflammatory cytokines, such as IL-4 and IL-10, that enhance glial-mediated neuroprotection (Huang *et al.*, 2009).

Several studies have examined T cell populations in the blood of AD patients and shown alterations in the function, differentiation and subset distribution of these cells (Town *et al.*, 2005). One such study demonstrated increased numbers of $CD4^+$ Th and $CD25^+$ Treg cells in blood from AD subjects compared with age-matched controls (Lombardi *et al.*, 1999). Studies have further indicated that increased numbers of T cells are present in post-mortem AD brains, although the subset distribution of these cells was not further characterised (Togo *et al.*, 2002, Itagaki *et al.*, 1988, Rogers *et al.*, 1988).

Although these cells undoubtedly have a role to play in disease progression, their presence is relatively low compared with other neurodegenerative diseases. In MS, for example, autoreactive Th1 and Th17 cells cross the BBB and are believed to be primarily responsible for causing the demyelination that results in subsequent disease symptoms (Jadidi-Niaragh and Mirshafiey, 2011). The potentially damaging and overwhelming results of excessive T cell infiltration into the CNS have also been observed in a clinical trial where humans were immunised with synthetic Aβ (as reviewed by Pfeifer *et al.*, 2002). This trial had to be halted when a small percentage of patients developed aseptic T cell meningoencephalitis, assumed to be mediated by the increased numbers of infiltrating T cells. It is important to note, however, that

this was the effect of a full-blown autoimmune response that does not normally occur in AD.

Results from the current study demonstrate that increased numbers of Th1 and Th17 cells were present in the brains of APP/PS1 mice, concomitant with decreased numbers of Th2 cells. There is some evidence that Th2 cells play a beneficial role in AD, for example recent findings indicate that the Aβ-induced release of inflammatory cytokines by mixed glia is exacerbated in the presence of Th1 and Th17 cells, and attenuated following the addition of Th2 cells (McQuillan *et al.*, 2010). More recently, Aβ-specific Th1, Th2, or IL-17-producing $CD4^+$ T cells were adoptively transferred to 6 month old APP/PS1 mice, where the presence of Th1 cells was found to increase Aβ deposition and microglial activation and negatively impact upon spatial learning following a 5-week period (Browne *et al.*, 2013). In a somewhat similar study, tail-vein infusion of Aβ-sensitised Th2 cells into APP/PS1 mice resulted in cognitively-impaired mice performing significantly better in working memory tasks, something which correlated with higher plasma levels of soluble Aβ (Cao *et al.*, 2009).

Numerous investigations, including one carried out in Tg2576 mice, have demonstrated reduced Th1 and enhanced Th2 responses following immunisation with Aβ, something which is associated with a strong antibody response (Town *et al.*, 2002). These results suggest that enhanced Th2 and down-regulated Th1 immunity may be beneficial in AD as they were associated with dramatically reduced Aβ deposition following the immunisation protocol (Town *et al.*, 2002). While the precise role of T cells in AD needs further clarification, it is perhaps the case that an imbalanced Th1/Th2 ratio is contributing to the classical pro-inflammatory cytokine microenvironment in the brains of APP/PS1 mice.

Although the number of infiltrating macrophages and neutrophils in AD is relatively small, it is still controversial as to whether these cells are beneficial or detrimental in disease pathogenesis. On one hand, it has been postulated that macrophages are

more efficient phagocytes than microglia (Wisniewski *et al.*, 1991), with recent evidence from Tg2576 mice supporting the idea that infiltration of peripheral mononuclear phagocytes limits the progression of AD pathology (Town *et al.*, 2008). On the other hand such cells could be provoking deleterious brain inflammation and causing tissue damage (Gate *et al.*, 2010). Interestingly, recent work has demonstrated that while sustained recruitment of peripheral leukocytes into the CNS was associated with neuroinflammation, it also helped to decrease cerebral amyloid burden (Shaftel *et al.*, 2007).

An intact BBB provides one of the most important protective strategies for the brain, however multiple lines of evidence suggest that its permeability is increased in AD. Levels of many tight junction proteins and their adaptor molecules are found to be decreased in AD (Zlokovic, 2008). Studies carried out in Tg2576 mice showed that animals as young as 4-months of age have a compromised BBB in several areas of the cortex (Ujiie *et al.*, 2003). It has been proposed that Aβ accumulation around blood vessels promotes extensive neoangiogenesis leading to increased vascular permeability in AD (Biron *et al.*, 2011). Results from animals used in the current study demonstrate that BBB permeability, as assessed using gadolinium-enhanced magnetic resonance imaging, was increased in the hippocampus of middle-aged APP/PS1 mice, and this was further enhanced in older animals (Dr. Ronan Kelly, unpublished data), providing a route by which to allow the observed increase in infiltrating leukocytes.

It has been shown that chemokines, released from resident cells in the brain act as chemoattractant molecules for peripheral leukocytes (Holman *et al*, 2011), by binding to G-protein-coupled receptors on target cells. Results from the current study demonstrate that CXCL1 protein expression was increased in the hippocampus of older APP/PS1 mice compared both with WT controls and their middle-aged transgenic counterparts. While reports of the role of CXCL1 in AD are few, unilateral overexpression of IL-1β in the mouse brain had been shown to induce leakage of the

BBB associated with dramatic infiltration of neutrophils, T cells, macrophages and dendritic cells into the CNS; neutrophils were observed in the hippocampal parenchyma as late as 1 year following transgene induction, and these findings correlated with upregulation of CXCL1 (Shaftel *et al.*, 2007).

MIP-1α is one of the chemokines most commonly expressed during CNS inflammation (Passos *et al.*, 2009). The data demonstrates that MIP-1α mRNA expression was increased in the cortex of older APP/PS1 mice compared both with WT controls and their middle-aged transgenic counterparts. A recent study has shown that injection of Aβ into the rat hippocampus induces MIP-1α overexpression accompanied by an increased presence of T cells in the cortex of these animals (Man *et al.*, 2007). Studies have shown that microglia from AD patients display increased expression of MIP-1α following exposure to Aβ (Lue *et al.*, 2001) and that MIP-1α expression in peripheral T cells of AD patients is significantly higher compared with age-matched controls (Man *et al.*, 2007). Recent studies have been demonstrated that AD-derived microvessels express and release higher levels of MIP-1α compared with those from age-matched controls (Tripathy *et al.*, 2007).

While a similar pattern in mRNA expression of RANTES, IP-10 and MCP-1 was observed, these results fell short of statistical significance. Briefly, evidence for increased expression of MCP-1, RANTES and IP-10 in AD has also been described. Exposure of astrocytes to Aβ results in increased concentrations of RANTES (Johnstone *et al.*, 1999), and elevated concentrations of the chemokine and its CCR5 receptor are reported in AD (Tripathy *et al.*, 2010). Enhanced expression of IP-10 has been demonstrated in the cortex and hippocampus of 17-month old Tg2576 mice compared with age-matched controls (Duan *et al.*, 2008). IP-10 expression in a subpopulation of cortical astrocytes was markedly increased in the AD brain, many of which were associated with senile plaques (Xia *et al.*, 2000). MCP-1 was also found to be increased in the cortex of Tg2576 mice compared with non-transgenic animals (Sly *et al.*, 2001), and its expression was upregulated in the AD brain (Grammas and

Ovase, 2001, Ishizuka *et al.*, 1997, Sokolova *et al.*, 2009). Interaction of MCP-1 with its receptor CCR2 is reported to regulate mononuclear phagocyte accumulation in AD, and CCR2 deficiency has been shown to result in increased amyloid pathology in association with aggregated amnesic deficits APP/PS1 mice (Naert and Rivest, 2011).

The most significant data presented in this study describes enhanced expression of markers of classical activation, such as TNFα and IL-1β, in the brains of aged APP/PS1 animals compared with WT controls. Although some markers of alternative activation, including IL-10, were increased, there was no change in the expression of MR, arginase-1 or FIZZ-1 and furthermore, decreased expression of IL-4Rα, NGF and BDNF was observed. Increased markers of classical activation were accompanied by breakdown of the BBB and infiltration of T cells, monocytes/macrophages and neutrophils into the brain parenchyma. It is therefore proposed that accumulation of Aβ and infiltration of peripheral leukocytes combine to induce an age-related shift towards a classical pro-inflammatory phenotype in APP/PS1 mice.

7: Identifying early inflammatory changes in monocyte-derived macrophages from a population with IQ-discrepant episodic memory

7.1 Introduction

Over the past two decades, significant progress has been made in identifying the structural and molecular changes, along with their biochemical footprints, that occur in the brain as a result of AD. This has led to the identification of several biomarkers of disease pathology, including decreased $A\beta_{1-42}$ and increased tau in CSF, decreased brain metabolism via fluorodeoxyglucose (FDG) uptake on positron emission tomography (PET), PET imaging of amyloid burden and MRI measures of cerebral atrophy (Jack, 2012). However, such advances in CSF and imaging biomarkers have only recently been incorporated into the revised Diagnostic and Statistical Manual of Mental Disorders (DSM-IV) guidelines for AD, which were updated for the first time since their original formulation in 1984 (Jack *et al.*, 2010).

Three stages of AD are proposed by these new criteria, namely preclinical AD, mild cognitive impairment (MCI) and AD proper. Preclinical AD involves measureable changes in brain and CSF biomarkers that indicate early signs of the disease, however no symptoms of memory loss accompany these changes. MCI incorporates mild but measurable changes in thinking abilities, noticeable to the person affected and to the people around them, but not sufficient to impact upon daily routine. In contrast, fully-fledged AD is characterised by memory, thinking and behavioural symptoms that greatly impair a person's ability to function in daily life.

This new classification system of AD reflects the current thinking that AD-related changes begin in the brain as early as 20 years prior to the onset of symptoms. While progress in research has gone a long way in understanding the pathogenesis of AD, disease-modifying treatments would undoubtedly be more effective at earlier stages of the disease before plaque load and neurodegeneration have become too far advanced (Blennow *et al.*, 2006). Thus, these treatments should be administered in the pre-dementia stage, or potentially even in pre-symptomatic individuals.

While some of the biomarkers used for AD have diagnostic potential that has been extended to pre-clinical stages of AD, in reality there is a distinct lack of diagnostic tools to enable early disease intervention. The objective of this study was to establish whether functional or phenotypic changes in monocyte-derived macrophages (MDMs) accompany IQ-discrepant episodic memory deficits in older individuals and thus have potential to provide a biomarker of early disease.

The aims of these studies were as follows:

1. To assess plasma concentrations of Aβ in a cohort of human subjects with IQ-discrepant memory compared with age-matched controls.
2. To isolate PBMCs from the whole blood of high-memory performers (HP) and low-memory performers (LP) and assess the phagocytosis of fluorescently-labelled latex beads and cell surface expression of CD11b, TLR2, TLR4, and IFNγR in monocytes/macrophages.
3. To differentiate $CD14^+$ monocytes into monocyte-derived macrophages (MDMs) and assess mRNA and cell surface expression of CD11b, TLR2, TLR4, IFNγR and IL-4Rα.
4. To stimulate MDMs derived from HP and LP subjects with LPS and determine their sensitivity as assessed by release of IL-1β, IFNγ, TNFα, IL-6, IL-12p70 and IL-10.

7.2 Methods

Forty-seven healthy elderly adults with a mean age of 71.5 years were recruited from the older adult participant panel of the Trinity College Institute of Neuroscience. Participants were defined as LP if they scored more than 0.75 standard deviations below their NART-estimated IQ on the WMS as described in section 2.11.1. All other participants were classified as HP. No significant difference was observed in MMSE scores between the two groups. This work was carried out by Ms. Eleonora Greco and Dr. Sabina Brennan.

Roughly 50ml venous blood per subject was collected in a heparin-coated syringe and PBMCs and plasma were isolated using a method of density separation over Lymphoprep as described in section 2.11.2. Phlebotomy was carried out by Ms. Lesley Penney and cell isolation by Dr. Eric Downer. Following isolation, PBMCs were taken for immediate analysis of phagocytic activity and cell surface analysis by flow cytometry as described in sections 2.7.1 and 2.7.2.

$CD14^+$ monocytes were isolated from the remaining PBMCs and cultured for 7 days with GM-CSF (10ng/ml) to generate MDMs as described in section 2.11.4. After 7 days, MDMs were assessed for differences in mRNA expression and cell surface immunofluorescence by RT-PCR and flow cytometry respectively. In another series of experiments, MDMs were stimulated with LPS (100ng/ml) for 24 hours, as described in section 2.11.5, and supernatants were assessed for the release of IL-1β, IFNγ, TNFα, IL-6, IL-12p70 and IL-10 by multiplex ELISA as described in section 2.11.6.

7.3 Results

7.3.1 Demographic of subjects

	High-performing (HP)	Low-performing (LP)
n	35	12
Age (years; mean + SD)	71.9 + 4.7	71.1 + 4.8
Sex (F/M)	26/9	9/3
MMSE	27.4 + 2.8	26.9 + 2.6
Premorbid IQ	1.13 + 0.37	1.2 + 0.29
Delayed verbal memory	1.43 + 0.82	-0.06 + 0.72*

General intellectual status was measured using the NART. Delayed verbal memory was determined by the Logical Memory subtest of the WMS.

*Participants were defined as LP if they scored more than 0.75 standard deviations below their NART-estimated IQ on the WMS. All other participants were classified as HP.

Table 7.1 Demographic of subjects

7.3.2 Analysis of Aβ concentrations in plasma isolated from LP and HP subjects.

Plasma was isolated from whole blood by density separation over Lymphoprep and assessed for the presence of $A\beta_{1-38}$, $A\beta_{1-40}$ and $A\beta_{1-42}$ by multiplex ELISA.

Plasma concentrations of $A\beta_{1-38}$ (p=0.67) and $A\beta_{1-40}$ (p=0.44) were unchanged between HP and LP subjects as shown in figure 7.1. The presence of $A\beta_{1-42}$ was below the limit of detection in plasma isolated from either group.

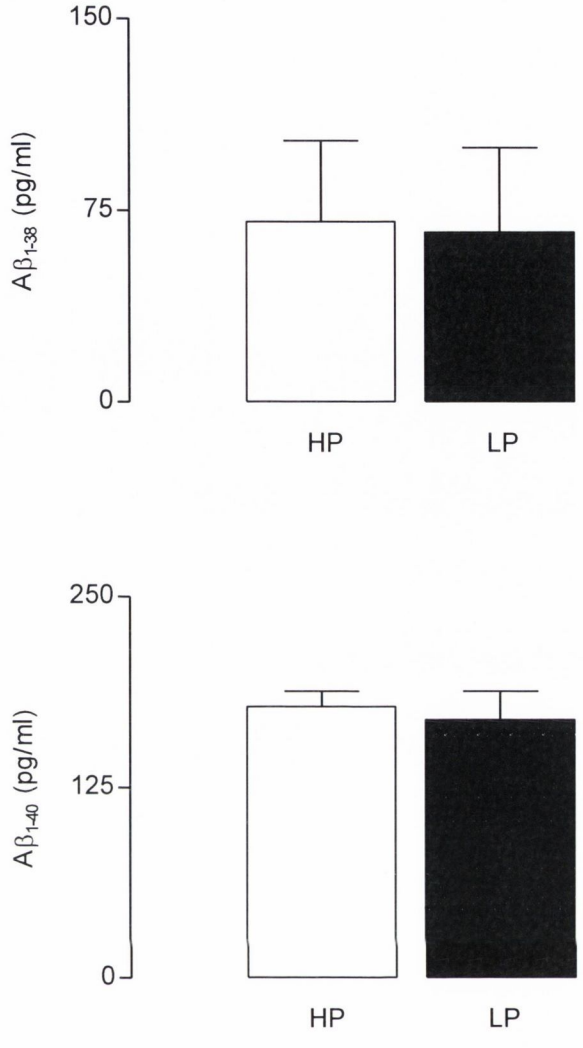

Figure 7.1 Plasma concentrations of $A\beta_{1-38}$ and $A\beta_{1-40}$ were unchanged between LP and HP subjects.

Plasma was isolated from whole blood by density separation over Lymphoprep and assessed for the presence of $A\beta_{1-38}$ (A), $A\beta_{1-40}$ (B) and $A\beta_{1-42}$ by multiplex ELISA. Concentrations of $A\beta_{1-38}$ and $A\beta_{1-40}$ were unchanged between HP and LP subjects. $A\beta_{1-42}$ was below the limit of detection in plasma isolated from either group. Data are expressed as means + SEM (*n*=12-35).

7.3.3 Analysis of receptor expression and phagocytosis by monocytes/macrophages isolated from the PBMCs of LP and HP subjects.

PBMCs were isolated from whole blood by density separation over Lymphoprep and assessed for CD11b expression using flow cytometry as shown in figure 7.2. No change in CD11b expression was observed between HP and LP subjects (p=0.26). The expression of TLR2 (p=0.21), TLR4 (p=0.08) and IFNγR (p=0.93) on $CD11b^+$ cells was also unchanged in PBMCs isolated from HP and LP subjects. A representative FACS plot is demonstrated in the case of each receptor examined.

$CD45^+CD11b^+$ monocytes/macrophages were more phagocytic than $CD45^+CD11b^-$ cells as assessed using the uptake of fluorescently-labelled latex beads as a readout and shown in figure 7.3. A representative FACS plot demonstrates the greater percentage of $BEAD^+$ $CD45^+CD11b^+$ monocytes/macrophages (~82%) in comparison to $BEAD^+$ $CD45^+CD11b^-$ cells (~22%). No change in the phagocytosis of fluorescently-labelled latex beads by $CD45^+CD11b^+$ monocytes/macrophages was observed between HP and LP subjects (p=0.35) as shown in figure 7.4.

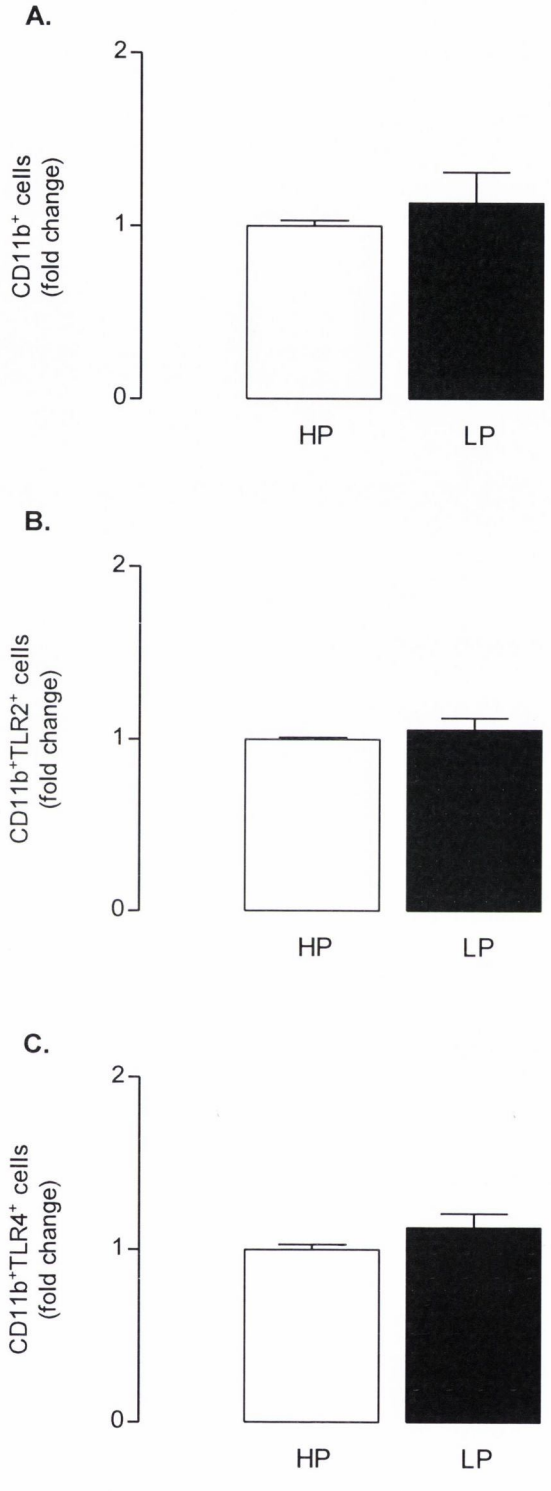
A.
CD11b+ cells
(fold change)
2
1
0
HP
LP
B.
CD11b+TLR2+ cells
(fold change)
2
1
0
HP
LP
C.
CD11b+TLR4+ cells
(fold change)
2
1
0
HP
LP

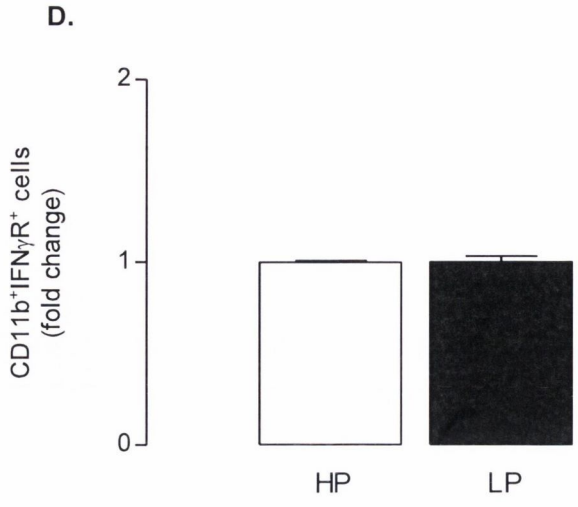

Figure 7.2 CD11b, TLR2, TLR2 and IFNγR expression on PBMCs was unchanged between LP and HP subjects.

PBMCs were isolated from the whole blood of HP and LP subjects and assessed for CD11b (A), TLR2 (B), TLR4 (C) and IFNγR (D) expression using flow cytometry. Debris and non-cellular events were initially excluded using forward/side scatter, with all further analysis gated on $CD11b^+$ PBMCs identified by the appropriate FMO. CD11b expression on PBMCs was unchanged between HP and LP subjects. No change was observed in the expression of TLR2, TLR4 or IFNγR (B-D) on $CD11b^+$ cells between HP and LP subjects. Data are expressed as means + SEM (*n*=5-14).

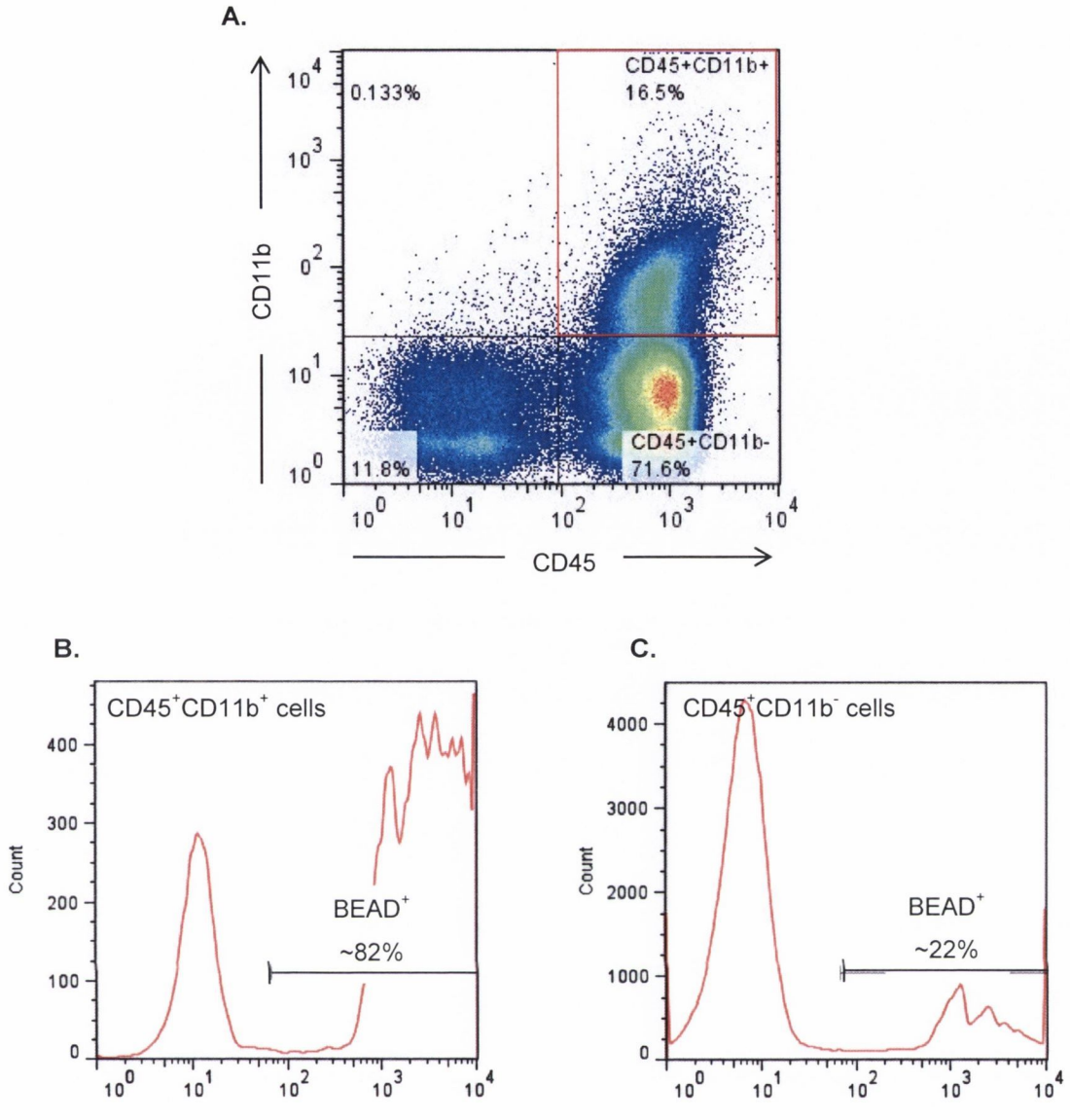

Figure 7.3 $CD45^+CD11b^+$ monocytes/macrophages were more phagocytic than $CD45^+CD11b^-$ cells.

PBMCs were isolated from the whole blood of HP and LP subjects and phagocytosis of fluorescently-labelled latex beads by $CD45^+CD11b^+$ monocytes/macrophages was assessed using flow cytometry. Debris and non-cellular events were initially excluded using forward/side scatter, with $CD45^+CD11b^+$ cells identified by the appropriate FMOs. A representative FACS plot (A) demonstrates the percentage of $CD45^+CD11b^+$ monocytes/macrophages (~16.5%) in comparison to $CD45^+CD11b^-$ cells (~71.6%). $CD45^+CD11b^+$ cells (B) were significantly more phagocytic, being ~82% positive for the uptake of fluorescently-labelled latex beads in comparison to $CD45^+CD11b^-$ cells, which were only ~22% positive (C).

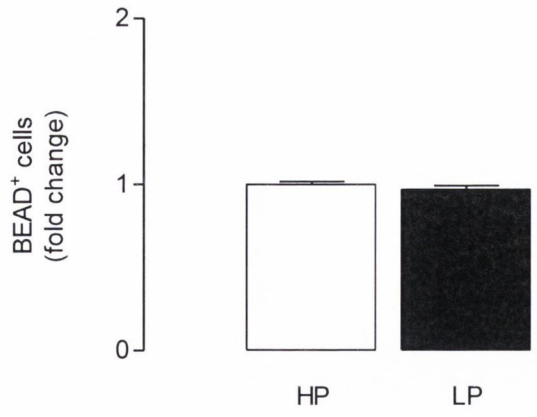

Figure 7.4 Phagocytosis by $CD45^+CD11b^+$ monocytes/macrophages was unchanged between LP and HP subjects.

PBMCs were isolated from the whole blood of HP and LP subjects and phagocytosis of fluorescently-labelled latex beads by $CD45^+CD11b^+$ monocytes/macrophages was assessed using flow cytometry. Debris and non-cellular events were initially excluded using forward/side scatter, with $CD45^+CD11b^+$ cells identified by the appropriate FMOs. The uptake of beads by $CD45^+CD11b^+$ cells was unchanged between HP and LP subjects. Data are expressed as means + SEM (*n*=12-35).

7.3.4 Analysis of CD11b, TLR2, TLR4, IFNγR and IL-4Rα expression on MDMs derived from LP and HP subjects.

Monocytes, isolated from the PBMCs of HP and LP subjects, were cultured for 7 days with GM-CSF to generate MDMs. After 7 days, MDMs were assessed for mRNA and protein expression of CD11b, TLR2 and TLR4, and protein expression only of IFNγR and IL-4Rα using flow cytometry. RT-PCR was carried out by Dr. Eric Downer.

MDMs derived from LP subjects displayed higher protein ($p<0.01$) but not mRNA ($p=0.31$) expression of CD11b compared with those derived from HP subjects as shown in figure 7.5. TLR2 mRNA ($p<0.05$) but not protein ($p=0.09$) expression was enhanced in MDMs derived from LP subjects, while both mRNA and protein ($p<0.01$) expression of TLR4 were increased in MDMs derived from LP subjects as shown in figures 7.6 and 7.7 respectively.

MDMs derived from LP subjects also displayed higher IFNγR ($p<0.05$) expression as shown in figure 7.8. In addition, no significant change was observed in the expression of IL-4Rα ($p=0.16$) as shown in figure 7.9.

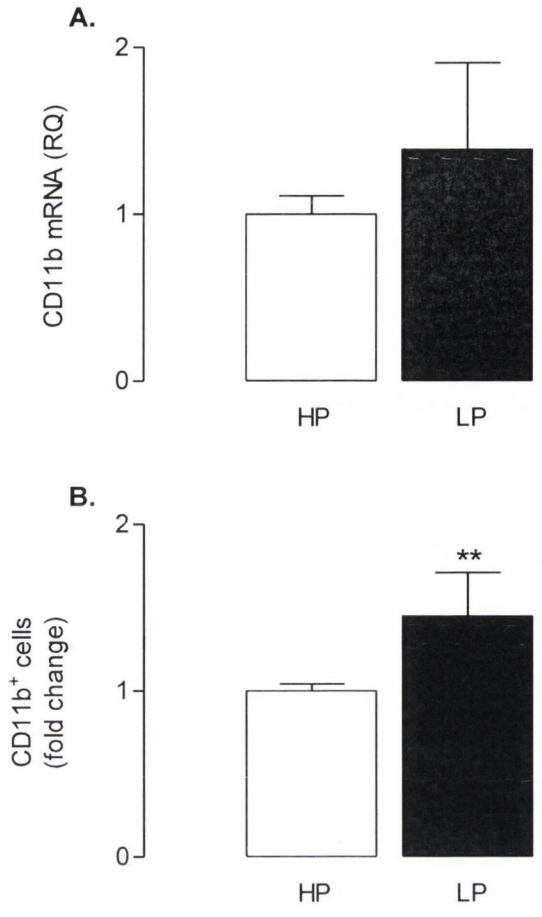

Figure 7.5a CD11b expression was enhanced in MDMs derived from LP compared with HP subjects.

Monocytes, isolated from the PBMCs of HP and LP subjects were cultured for 7 days with GM-CSF to generate MDMs. After 7 days, MDMs were assessed for expression of CD11b mRNA (A) using RT-PCR and protein (B) using flow cytometry (gating strategy described in figure 7.5b). MDMs derived from LP subjects expressed higher protein ($p<0.01$) but not mRNA expression of CD11b. Data are expressed as means + SEM (n=12-35). **$p<0.01$ versus HP group (Student's t-test for independent means).

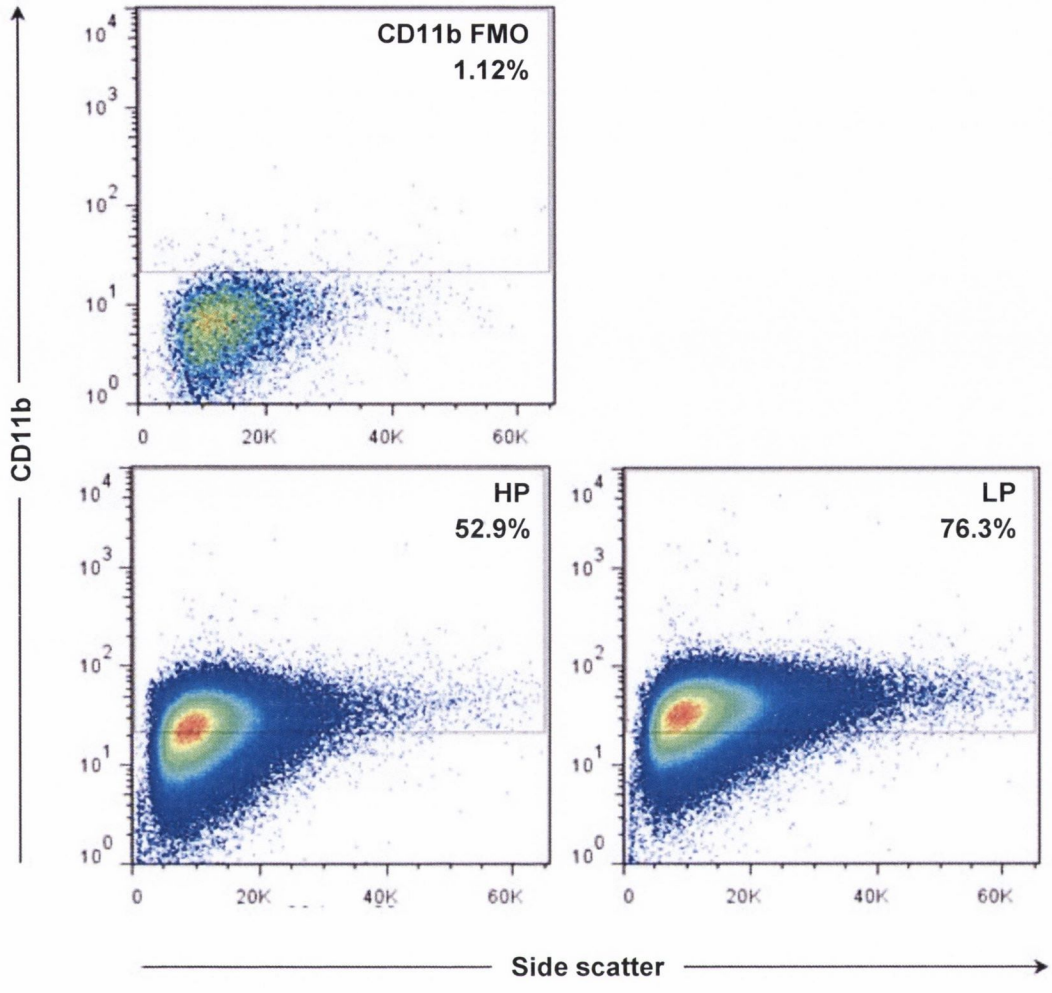

Figure 7.5b Gating strategy for the analysis of CD11b expression in MDMs.

Debris and non-cellular events were initially excluded using forward/side scatter, with all further analysis gated on $CD11b^+$ MDMs identified by the appropriate FMO. Representative dot plots from HP and LP subjects are presented plotting side scatter log versus CD11b with a gate placed around the $CD11b^+$ MDM population.

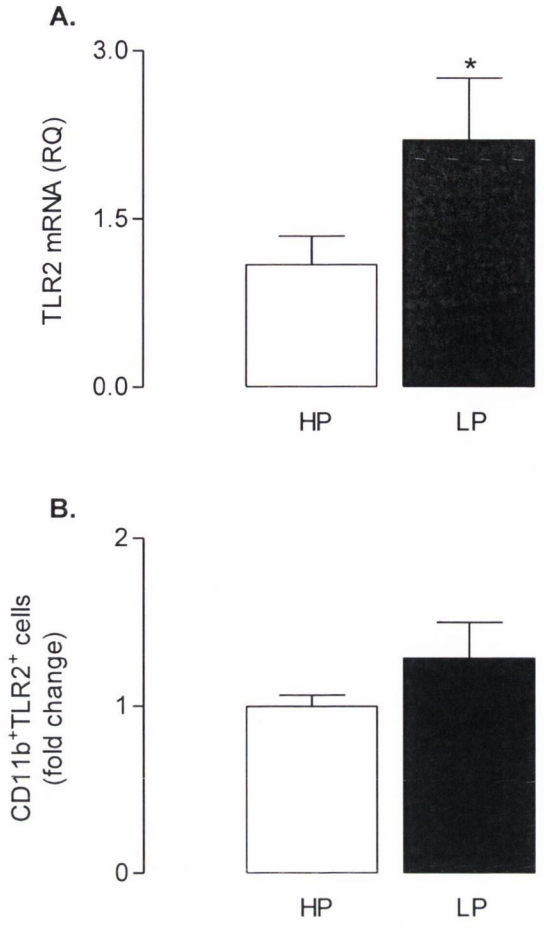

Figure 7.6a TLR2 mRNA expression was enhanced in MDMs derived from LP compared with HP subjects.

Monocytes, isolated from the PBMCs of HP and LP subjects were cultured for 7 days with GM-CSF to generate MDMs. After 7 days, MDMs were assessed for expression of TLR2 mRNA (A) using RT-PCR and protein (B) using flow cytometry cytometry (gating strategy described in figure 7.6b). TLR2 mRNA ($p<0.05$) but not protein expression was enhanced in MDMs derived from HP compared with LP subjects. Data are expressed as means + SEM (n=12-35). *$p<0.05$ versus HP group (Student's t-test for independent means).

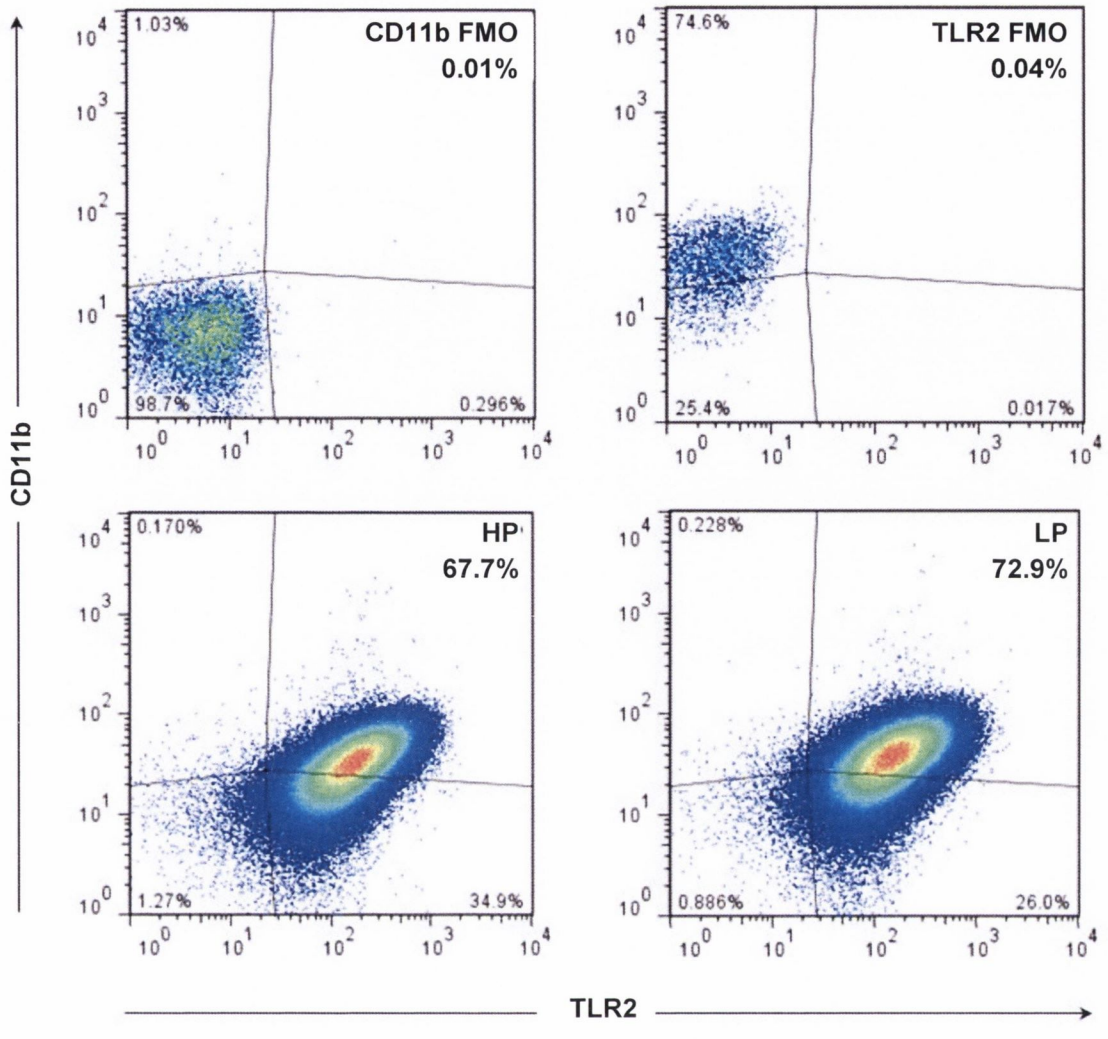

Figure 7.6b Gating strategy for the analysis of TLR2 expression in MDMs.

Debris and non-cellular events were initially excluded using forward/side scatter, with all further analysis gated on $CD11b^+$ MDMs identified by the appropriate FMO. Representative dot plots from HP and LP subjects are presented plotting CD11b versus TLR2, with the percentage of $CD11b^+TLR2^+$ cells in the top right-hand quadrant.

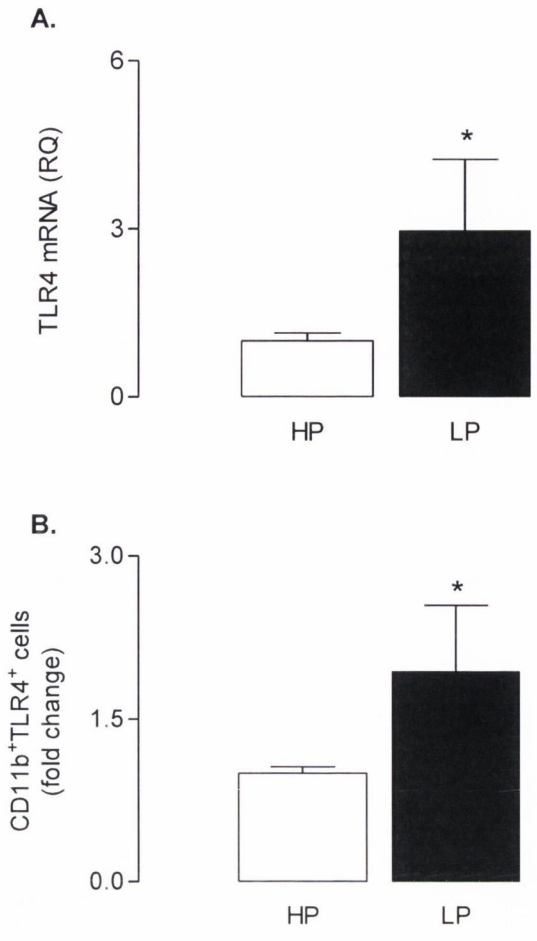

Figure 7.7a TLR4 expression was enhanced in MDMs derived from LP compared with HP subjects.

Monocytes, isolated from the PBMCs of HP and LP subjects, were cultured for 7 days with GM-CSF to generate MDMs. After 7 days, MDMs were assessed for expression of TLR4 mRNA (A) using RT-PCR and protein (B) using flow cytometry cytometry (gating strategy described in figure 7.7b). Both mRNA ($p<0.05$) and protein ($p<0.05$) expression of TLR4 were enhanced in MDMs derived from HP compared with LP subjects. Data are expressed as means + SEM (n=12-35). *$p<0.05$ versus HP group (Student's t-test for independent means).

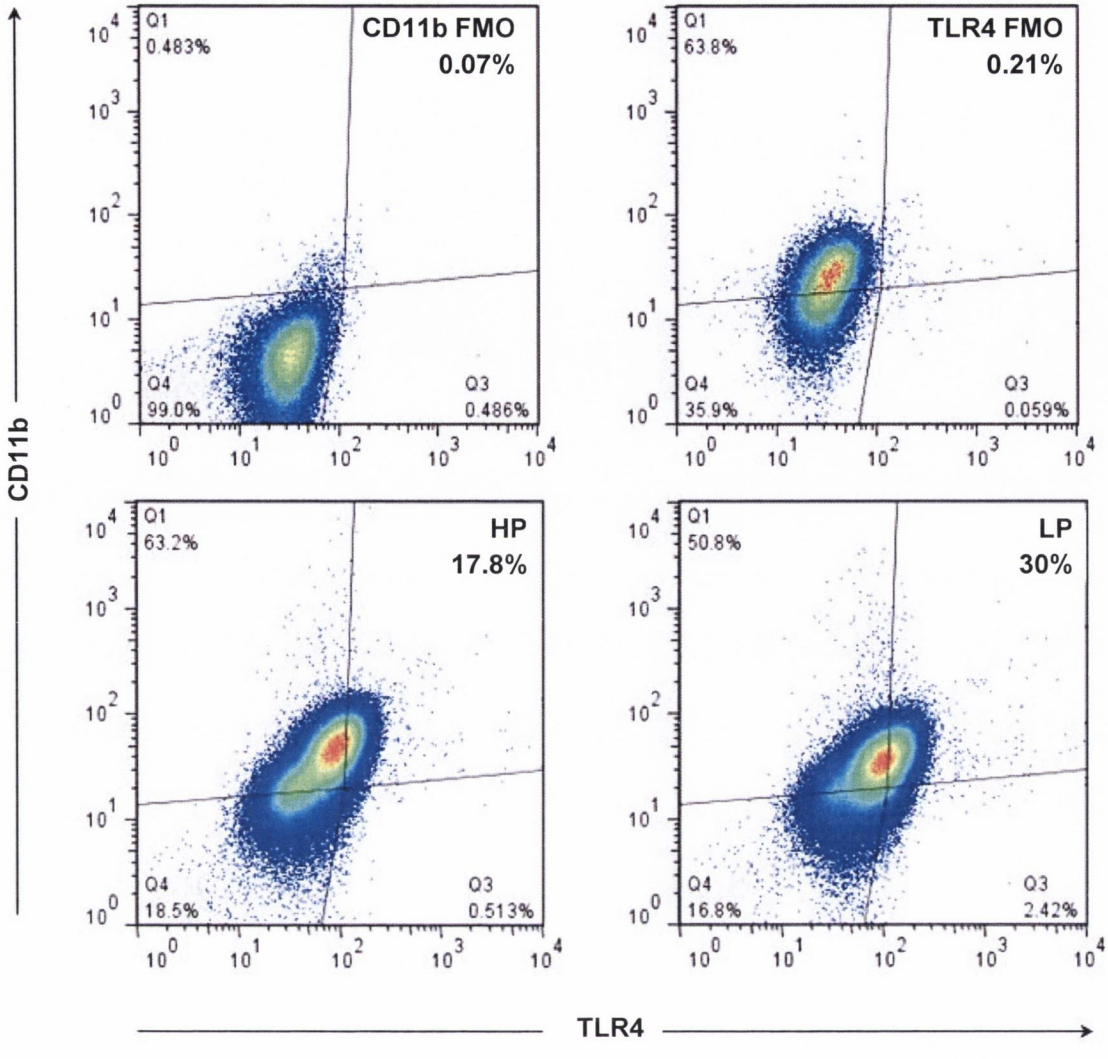

Figure 7.7b Gating strategy for the analysis of TLR4 expression in MDMs.

Debris and non-cellular events were initially excluded using forward/side scatter, with all further analysis gated on $CD11b^+$ MDMs identified by the appropriate FMO. Representative dot plots from HP and LP subjects are presented plotting CD11b versus TLR4, with the percentage of $CD11b^+TLR4^+$ cells in the top right-hand quadrant.

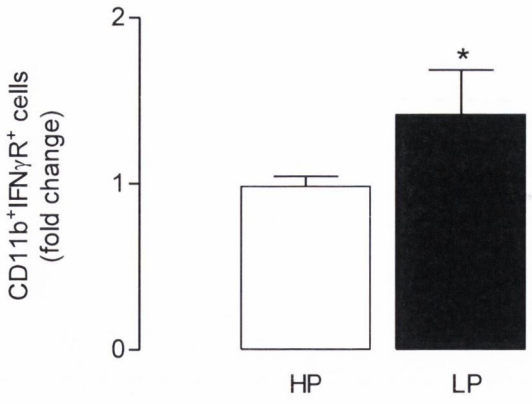

Figure 7.8 IFNγR expression was enhanced in MDMs derived from LP compared with HP subjects.

Monocytes, isolated from the PBMCs of HP and LP subjects, were cultured for 7 days with GM-CSF to generate MDMs. After 7 days, MDMs were assessed for expression of IFNγR using flow cytometry. Debris and non-cellular events were initially excluded using forward/side scatter, with all further analysis gated on $CD11b^+$ MDMs identified by the appropriate FMO. Protein expression of IFNγR ($p<0.05$) was increased in MDMs derived from LP compared with HP subjects. Data are expressed as means + SEM (n=12-35). *$p<0.05$ versus HP group (Student's t-test for independent means).

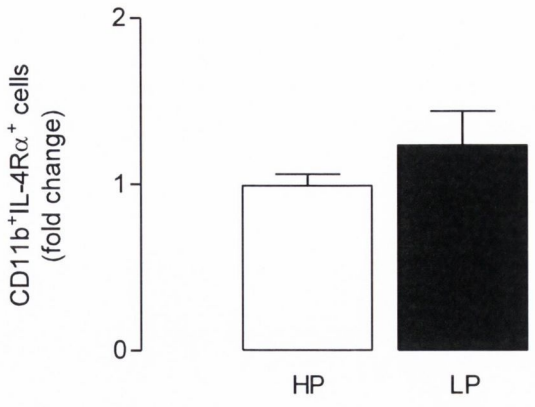

Figure 7.9 IL-4Rα expression was unchanged in MDMs derived from LP compared with HP subjects.

Monocytes, isolated from the PBMCs of HP and LP subjects, were cultured for 7 days with GM-CSF to generate MDMs. After 7 days, MDMs were assessed for expression of IL-4Rα using flow cytometry. Debris and non-cellular events were initially excluded using forward/side scatter, with all further analysis gated on $CD11b^+$ MDMs identified by the appropriate FMO. The data show that expression of IL-4Rα was unchanged between HP and LP subjects. Data are expressed as means + SEM (n=12-35).

7.3.5 Analysis of the effect of LPS on cytokine release from MDMs derived from LP and HP subjects

Monocytes, isolated from the PBMCs of HP and LP subjects, were cultured for 7 days with GM-CSF to generate MDMs. After 7 days, cells were stimulated with LPS (100ng/ml) for 24 hours and supernatants were assessed for the release of IL-1β, IFNγ, TNFα, IL-6, IL-12p70 and IL-10 by multiplex ELISA.

A 2-way AVOVA followed by *post-hoc* analysis demonstrated that LPS induced the release of IL-1β and IFNγ ($p<0.01$) by MDMs derived from both HP and LP subjects as shown in figures 7.10 and 7.11 respectively. No difference in the production of IL-1β and IFNγ from MDMs was observed between HP and LP subjects.

A 2-way AVOVA and *post-hoc* analysis further demonstrated that LPS also stimulated the release of TNFα, IL-6, IL-12p70 and IL-10 ($p<0.01$) by MDMs derived from HP and LP subjects as shown in figures 7.12 – 7.15, however release of these cytokines was exaggerated in MDMs derived from LP compared with HP subjects ($p<0.05$).

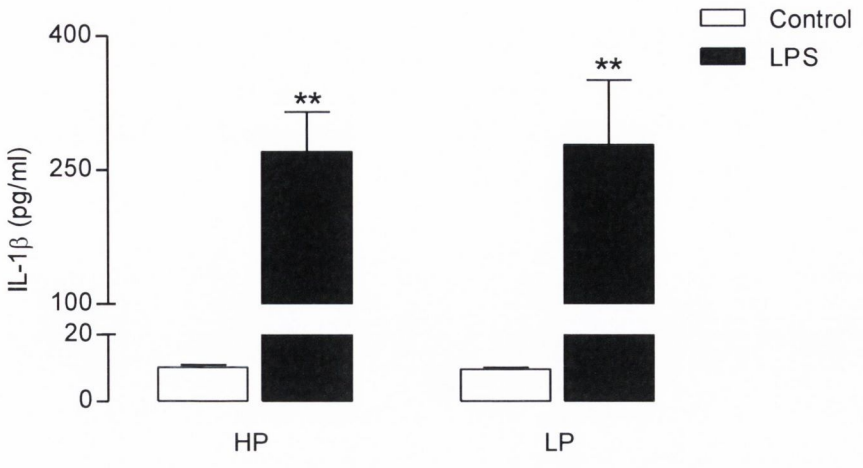

Figure 7.10 IL-1β release in MDMs stimulated with LPS was unchanged between LP and HP subjects.

Monocytes, isolated from the PBMCs of HP and LP subjects, were cultured for 7 days with GM-CSF to generate MDMs. After 7 days, cells were stimulated with LPS (100ng/ml) for 24 hours and supernatants assessed for the presence of IL-1β by multiplex ELISA. LPS induced the release of IL-1β ($p<0.01$) by MDMs derived from HP and LP subjects but no further differences were observed between groups. Data are expressed as means + SEM (n=12-35). **$p<0.01$ versus vehicle control (2-way ANOVA followed by Newman-Keuls *post-hoc* analysis).

LPS_{effect} [$F_{(1,76)}$=40.239, $p<0.0001$], $group_{effect}$ [$F_{(1,76)}$=0.008, p=0.9307], $interaction_{effect}$ [$F_{(1,12)}$=0.01, p=0.9179].

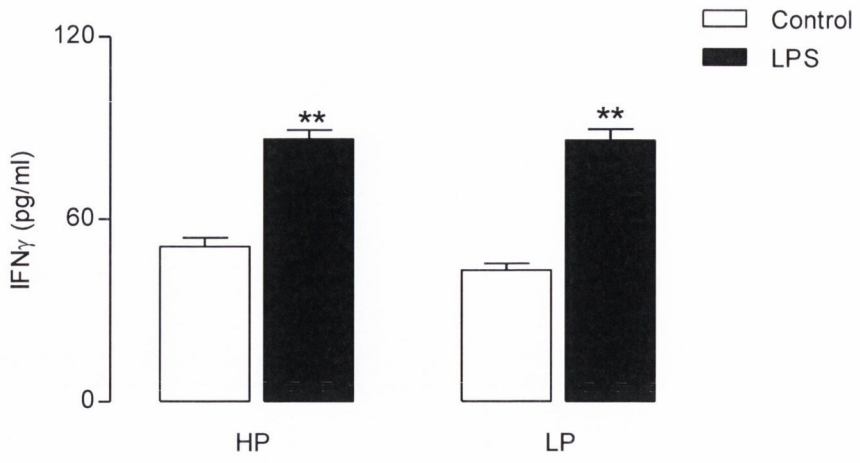

Figure 7.11 IFNγ release in MDMs stimulated with LPS was unchanged between LP and HP subjects.

Monocytes, isolated from the PBMCs of HP and LP subjects, were cultured for 7 days with GM-CSF to generate MDMs. After 7 days, cells were stimulated with LPS (100ng/ml) for 24 hours and supernatants were assessed for the presence of IFNγ by multiplex ELISA. LPS induced the release of IFNγ ($p<0.01$) by MDMs derived from both HP and LP subjects but no further differences were observed between groups. Data are expressed as means + SEM (n=12-35). **$p<0.01$ versus vehicle control (2-way ANOVA followed by Newman-Keuls *post-hoc* analysis).

LPS_{effect} [$F_{(1,76)}$=113.37, $p<0.0001$], $group_{effect}$ [$F_{(1,76)}$=1.26, p=0.2654], $interaction_{effect}$ [$F_{(1,12)}$=0.988, p=0.3235].

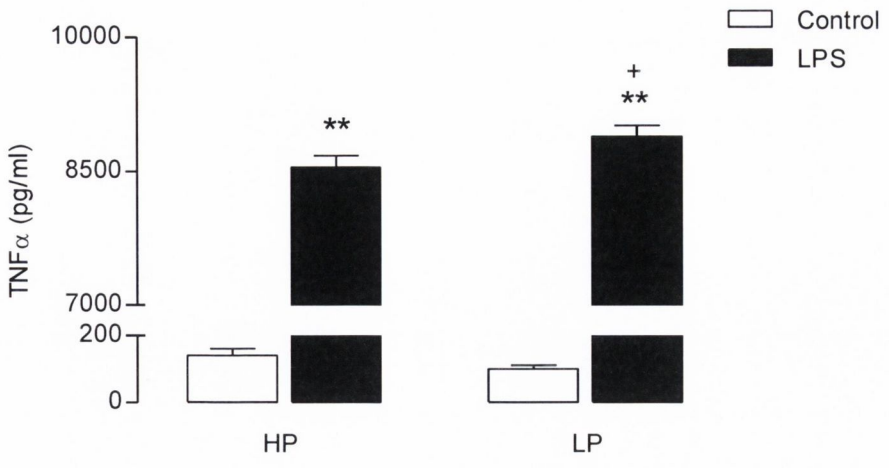

Figure 7.12 LPS induced a greater release of TNFα in MDMs derived from LP compared with HP subjects.

Monocytes, isolated from the PBMCs of HP and LP subjects, were cultured for 7 days with GM-CSF to generate MDMs. After 7 days, cells were stimulated with LPS (100ng/ml) for 24 hours and supernatants were assessed for the presence of TNFα by multiplex ELISA. LPS induced the release of TNFα ($p<0.01$) by MDMs derived from both LP and HP subjects, however this was exaggerated in MDMs prepared from LP subjects ($p<0.05$). Data are expressed as means + SEM (n=12-35). $^{**}p<0.01$ versus vehicle control; $^{+}p<0.05$ versus HP group (2-way ANOVA followed by Newman-Keuls *post-hoc* analysis).

LPS_{effect} $[F_{(1,76)}=5491.2, p<0.0001]$, $group_{effect}$ $[F_{(1,76)}=1.733, p=0.1932]$, $interaction_{effect}$ $[F_{(1,12)}=2.77, p=0.1004]$.

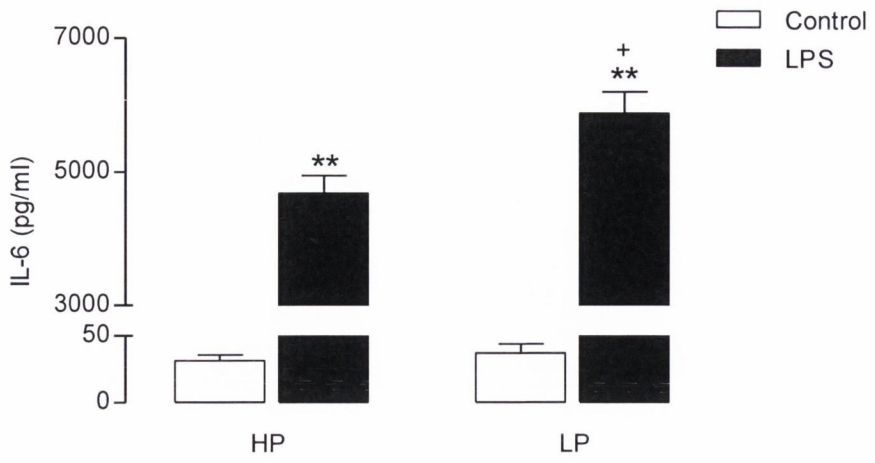

Figure 7.13 LPS induced IL-6 was exacerbated in MDMs derived from LP compared with HP subjects.

Monocytes, isolated from the PBMCs of HP and LP subjects, were cultured for 7 days with GM-CSF to generate MDMs. After 7 days, cells were stimulated with LPS (100ng/ml) for 24 hours and supernatants were assessed for the presence of IL-6 by multiplex ELISA. LPS induced the release of IL-6 ($p<0.01$) by MDMs derived from both LP and HP subjects, however this was exaggerated in MDMs prepared from LP subjects ($p<0.05$). Data are expressed as means + SEM (n=12-35). **$p<0.01$ versus vehicle control; $^{+}p<0.05$ versus HP group (2-way ANOVA followed by Newman-Keuls *post-hoc* analysis).

LPS_{effect} [$F_{(1,76)}$=449.6, $p<0.0001$], $group_{effect}$ [$F_{(1,76)}$=5.91, p=0.0176], $interaction_{effect}$ [$F_{(1,12)}$=5.8, p=0.0186].

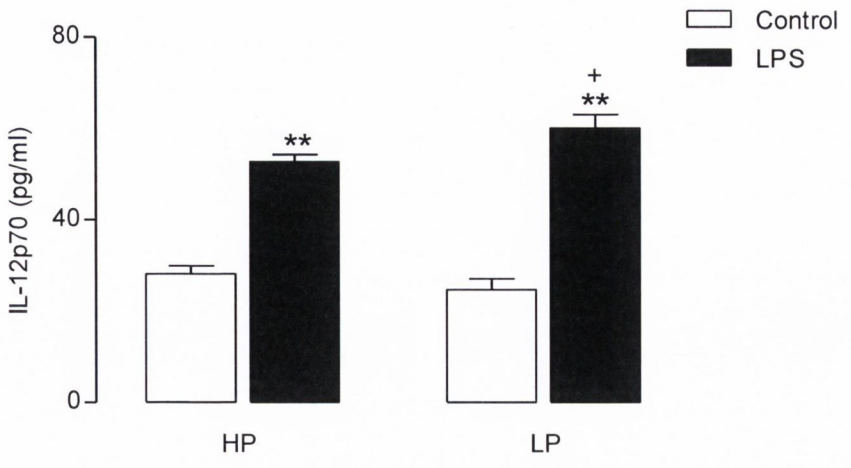

Figure 7.14 LPS induced IL-12p70 was exacerbated in MDMs derived from LP compared with HP subjects.

Monocytes, isolated from the PBMCs of HP and LP subjects, were cultured for 7 days with GM-CSF to generate MDMs. After 7 days, cells were stimulated with LPS (100ng/ml) for 24 hours and supernatants were assessed for the presence of IL-12p70 by multiplex ELISA. LPS induced the release of IL-12p70 ($p<0.01$) by MDMs derived from both LP and HP subjects, however this was exaggerated in MDMs prepared from LP subjects ($p<0.05$). Data are expressed as means + SEM (n=12-35). $^{**}p<0.01$ versus vehicle control; $^{+}p<0.05$ versus HP group (2-way ANOVA followed by Newman-Keuls *post-hoc* analysis).

LPS_{effect} [$F_{(1,76)}$=51.68, $p<0.0001$], $group_{effect}$ [$F_{(1,76)}$=0.006, p=0.9379], $interaction_{effect}$ [$F_{(1,12)}$=0.467, p=0.497].

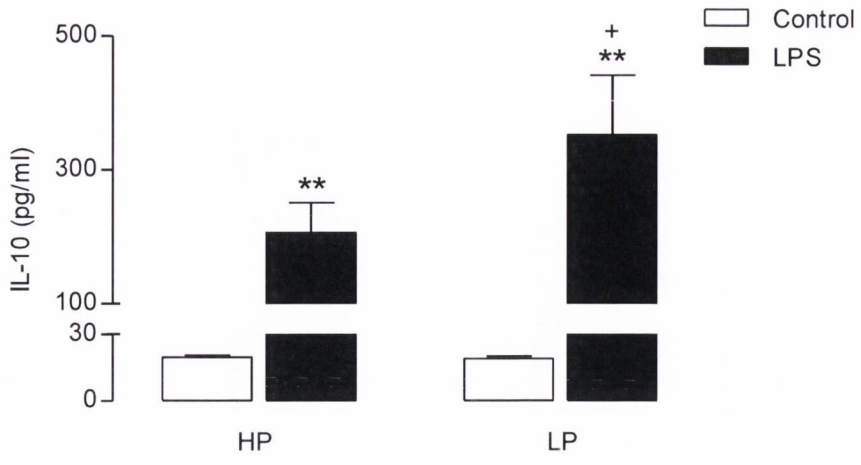

Figure 7.15 LPS induced a greater release of IL-10 in MDMs derived from LP compared with HP subjects.

Monocytes, isolated from the PBMCs of HP and LP subjects, were cultured for 7 days with GM-CSF to generate MDMs. After 7 days, cells were stimulated with LPS (100ng/ml) for 24 hours and supernatants were assessed for the presence of IL-10 by multiplex ELISA. LPS induced the release of IL-10 ($p<0.01$) by MDMs derived from both LP and HP subjects, however this was exaggerated in MDMs prepared from LP subjects ($p<0.05$). Data are expressed as means + SEM (n=12-35). **$p<0.01$ versus vehicle control; $^{+}p<0.05$ versus HP group (2-way ANOVA followed by Newman-Keuls *post-hoc* analysis).

LPS_{effect} [$F_{(1,76)}=32.91$, $p<0.0001$], $group_{effect}$ [$F_{(1,76)}=2.574$, $p=0.1128$], $interaction_{effect}$ [$F_{(1,12)}=2.62$, $p=0.1097$].

7.4 Discussion

The aim of this study was to assess whether inflammatory changes in MDMs accompany subtle episodic memory loss in older individuals and thus have the potential to provide a robust marker of early disease. This was assessed in a cohort of elderly individuals with episodic memory lower than expected for their IQ compared with healthy age-matched controls. It is important to note that this study was carried out in a non-clinical cohort with no apparent symptoms of MCI or AD. However, while only very early cognitive changes are reported here, these were found to be accompanied by alterations in MDMs and their susceptibly to inflammatory insult. The most significant findings indicate that MDMs isolated from LP subjects displayed enhanced expression of CD11b, TLR2 and TLR4, compared with those from HP subjects, and that stimulation of MDMs with LPS promoted exaggerated cytokine production by MDMs isolated from LP subjects.

Presence of the inflammatory C-reactive protein (CRP) was initially assessed in plasma from HP and LP subjects (data not shown here), where no difference was observed between groups, indicative of an equivalent infection index at the time of analysis. This was important to assess as neurological symptoms of patients suffering from neurodegenerative conditions are reported to be exacerbated by infection (Perry *et al.*, 2007). Evidence that systemic events affect the progression of AD were demonstrated in a study showing that peripheral infections and raised plasma levels of IL-1β were associated with accelerated cognitive decline (Holmes *et al.*, 2003). Studies have shown that the presence of inflammatory plasma proteins, such as CRP, were increased 5 years before the clinical onset of dementia compared with age-matched controls who did not go on to develop dementia (Engelhart *et al.*, 2004). In accordance with this, the suppression of inflammation has been linked with the efficacy of long-term use of NSAIDs in offering some level of protection against the development of AD (Etminan *et al.*, 2003).

A further aim of this study was to compare plasma concentrations of $A\beta_{1-38}$, $A\beta_{1-40}$ and $A\beta_{1-42}$ between HP and LP subjects in order to correlate this with inflammatory changes. Low concentrations of Aβ in plasma necessitate a sensitive and reliable quantitation assay, and in the case of the current study, the presence of $A\beta_{1-42}$ in plasma was found to be below the limit of detection. Results indicate that plasma concentrations of $A\beta_{1-38}$ and $A\beta_{1-40}$ were unchanged between HP and LP subjects. Decreased $A\beta_{1-42}$ and increased tau in CSF have previously been described as biomarkers for AD (Haldenwanger *et al.*, 2010). However, collection of CSF via lumbar puncture is an invasive and time-consuming procedure requiring medically trained personnel, and thus the identification of a blood-based biomarker would be more desirable. Although many studies have investigated plasma Aβ as a potential biomarker for AD, the findings indicate that this may not be a completely reliable measure of disease progression. Several cross-sectional studies and two longitudinal studies investigating plasma Aβ concentrations in AD identified no differences between AD patients and controls, suggesting that plasma Aβ is unlikely to be useful in predicting AD (Irizarry, 2004). These results are likely due to the fact that the majority of plasma Aβ is derived from peripheral tissues, and therefore does not reflect turnover or metabolism of Aβ within the brain (Mehta *et al.*, 2000). While the subjects used in this study have no apparent symptoms of AD, it was of interest to assess this measure in a group that may be more susceptible in progressing to develop MCI or AD.

Cells of the innate immune system, such as monocytes/macrophages, are the first line of defence against infection, acting as critical regulators of the inflammatory response. Monocytes circulate in the bloodstream for 1-3 days, and then typically migrate to tissues where they differentiate into multifunctional tissue-specific macrophages. The transformation from a monocyte to a macrophage involves the cell enlarging, increasing the number and complexity of its intracellular organelles and producing higher levels of hydrolytic enzymes in order to increase its phagocytic capability. Macrophages usually enter tissue within hours to a few days following the initiation of

inflammation, where their main biological function is to ingest and destroy foreign material and subsequently process and present it to lymphocytes via MHC.

CD11b is an cellular adhesion molecule, primarily expressed on the surface of monocytes/macrophages, but also on activated lymphocytes and a subset of NK cells, that mediates leukocyte adhesion and migration in order to promote an inflammatory response (Springer, 1990). Recent work has suggested that expression patterns of other monocytic cell adhesion molecules, such as intracellular adhesion molecule 1 (ICAM1), are altered in patients with MCI and AD (Hochstrasser *et al.*, 2010). Monocytes/macrophages also express a wide range of TLRs, each of which recognise a distinct class of conserved microbial molecules and elicits a tailored pattern of inflammatory gene expression. Activation of TLRs directly mediates innate immune responses by regulating phagocytosis and triggering anti-microbial activity, but also initiates the adaptive immune response by inducing the release of cytokines (Krutzik *et al.*, 2005). In the present study the focus was on examining expression of TLR2 and TLR4 since much evidence indicates the role of these receptors in AD, as has been described in previous chapters. Expression of TLR2 and TLR4 mRNA is also reported to be upregulated in PBMCs from patients with late-onset AD compared with age-matched controls (Zhang *et al.*, 2012). Presence of the IFNγR was assessed due to its pivotal role in stimulation of classical activation in macrophages.

PBMCs predominantly constitute lymphocytes and monocytes, with lower numbers of NK and dendritic cells. Results presented here indicate there was no difference in the expression of CD11b, TLR2, TLR4 or IFNγR on macrophage/monocytes on PBMCs derived from HP and LP subjects. However, it must be noted that this analysis was carried out on only half of the cohort, and perhaps if the full population had been assessed, significance may have been attained, particularly in the case of TLR4.

The uptake of fluorescently-labelled beads by monocytes/macrophages isolated from HP and LP subjects was also investigated. As predicted, cells expressing CD11b were

significantly more phagocytic than those without it, in accordance with its role in role cell migration and phagocytosis (Solovjov *et al.*, 2005). However, no overall change was observed in the phagocytic capacity of monocytes/macrophages isolated from HP and LP groups. A recent study has suggested that the phagocytic capacity of monocytes/macrophages isolated from the blood of AD patients was decreased compared with age-matched controls (Fiala *et al.*, 2005). Monocytes from healthy controls were reported to display excellent differentiation into macrophages and intracellular phagocytosis of Aβ, while AD monocytes showed poor differentiation and only surface uptake of Aβ. Monocytes incubated with AD brains sections *in vitro* were also unable to degrade Aβ efficiently (Fiala *et al.*, 2007). In contrast, macrophages from age-matched controls transported Aβ to endosomes and lysosomes, aiding the clearance of Aβ from AD brain sections. Work carried out by the same lab has suggested the use of a flow cytometric assay of phagocytosis as an early biomarker of AD (Avagyan *et al.*, 2009).

The next step in this study was to differentiate $CD14^+$ monocytes to become MDMs, type I or classically activated (M1) macrophages displaying a pro-inflammatory phenotype (Hendriks *et al.*, 2005). MDMs are considered to be the peripheral counterpart of microglia, sharing the same progenitor and antigen markers, and having similar biological behaviours that mirror microglial function in the brain (Templeton *et al.*, 2008, Dalmau *et al.*, 2003). Results demonstrate that MDMs derived from LP subjects displayed increased protein expression of CD11b compared with those derived from HP subjects. TLR2 mRNA expression was enhanced in MDMs derived from LP subjects, while both mRNA and protein expression of TLR4 were also increased in MDMs derived from LP compared with HP subjects. MDMs derived from LP subjects also displayed higher surface expression of IFNγR, while no change was observed in the expression of IL-4Rα.

These results perhaps indicate that MDMs from LP subjects may be more responsive to ligands of CD11b, TLR2, TLR4 and IFNγR, resulting in enhanced inflammatory

responses following stimulation. Given that TLR4 acts as the primary signalling receptor for Gram-negative bacterial LPS (Akira *et al.*, 2006), with TLR2 also required for LPS-induced TLR4 signalling (Good *et al.*, 2012), the effect of LPS on cytokine production in MDMs from HP and LP groups was determined. Stimulation of TLR4 by LPS initiates a complex signal-transduction pathway ultimately leading to activation of NFκB and an increase in the expression of pro-inflammatory cytokines. Here, LPS significantly increased cytokine production of IL-1β, IFNγ, TNFα, IL-6, IL-10 and IL-12p70 in MDMs from both groups, and importantly the production of TNFα, IL-6, IL-12p70 and IL-10 was exaggerated in MDMs prepared from LP compared with HP subjects.

The exaggerated release of these cytokines following stimulation with LPS indicates that MDMs prepared from LP subjects display an over-activated phenotype, at least in terms of cytokine production, and the increase in TLR4 and TLR2 expression provides a plausible mechanism for this effect. Increased expression of IFNγR may also have played a role in the enhanced response of MDMs from LP subjects to LPS, as IFNγ released following LPS stimulation presumably interacted with its cognate receptor resulting in the further release of cytokines involved in classical activation. No change in expression of IL-4Rα was observed, which may have been beneficial in promoting an anti-inflammatory response.

Plasma concentrations of IL-1β and IL-6 are reported to be increased in patients with AD compared with age-matched controls (Licastro *et al.*, 2000). Evidence has also demonstrated that PBMCs isolated from AD patients release enhanced levels of IL-1β, IL-6 and TNFα, and less IL-4 than those from healthy controls (Reale *et al.*, 2004). A recent study has also shown that LPS-stimulation of PBMCs isolated from AD patients released higher amounts of IL-6 compared with controls (Kaplin *et al.*, 2009). These findings suggest that PBMC function is dysregulated in AD. The present study expands on this to demonstrate that similar changes can be determined in MDMs

prepared from a group of otherwise healthy adults whose memory performance was discrepant with their estimated IQ.

The use of biomarkers to predict development of AD among pre-dementia or MCI stage individuals would yield substantial therapeutic and economic benefits. The most significant data reported here identifies changes in expression of CD11b, TLR2, TLR4 and IFNγR on MDMs isolated from a unique cohort of elderly individuals whose memory was in the normal range but whose memory performance was lower than expected for their educational and intellectual level. It was further shown that *in vitro* treatment with LPS promoted exaggerated cytokine production in MDMs from LP compared with HP subjects, with the observed increases in TLR4 and TLR2 expression suggested as probable candidates for this effect. This study thus identifies a novel association between MDM receptor and cytokine expression, and a population with episodic memory loss. These changes in peripheral cells are indicative of inflammation and may be associated with cellular events further leading to the development of neurodegenerative disease.

8: Conclusions

8.1 Conclusions

AD is reported to affect over 41,000 people in Ireland and more than 35.6 million people worldwide (www.alzheimer.ie). It is the fifth leading cause of death amongst people over 65, and the seventh leading cause of death across all age-groups. Due to the rapidly ageing population, the number of people suffering from AD is expected to triple by the year 2050. However, if it were possible to delay AD by only one year it is reported that there would be 9.5 million fewer people suffering from the disease in 2050. The World Alzheimer Report recently revealed that in 2010, the worldwide cost of dementia exceeded 1% of global GDP, priced at US$604 billion. Strikingly, if the cost of dementia care were a country, it would be the world's 18th largest economy (www.alz.org.uk).

The first objective of this study was to assess the impact of exogenous and endogenous Aβ on microglia and astrocytes both *in vitro* and *in vivo,* with specific regard to its effect on phagocytosis, cytokine release and the expression of putative Aβ binding receptors. A particular emphasis was placed on evaluating the potential receptors and signalling pathways involved in the response of astrocytes to Aβ, due to the relative scarcity of data compared with that of microglia. The modulatory effect of age on the accumulation of endogenous Aβ was examined in APP/PS1 mice, with attention focused on evaluating the expression profile of markers of classical, alternative and acquired deactivation in microglia, in addition to factors that serve to induce these phenotypes. In an effort to translate findings, which indicated that inflammation was a key component in age-related changes observed in a mouse model of AD, inflammatory changes in MDMs from an elderly human cohort with subtle cognitive deficits were investigated in an attempt to identify a potential biomarker in a prodromal condition that may preface AD.

Among the most significant findings described in this thesis is that astrocytes are efficient phagocytes. The phagocytic function of activated microglia has been known

for decades. In contrast, there are relatively few reports in the literature indicating that astrocytes have phagocytic potential. A recently-generated transcriptome database demonstrated that astrocytes highly express some of the evolutionarily conserved phagocytic pathways present in *Drosophila* and *Caenorhabditis elegans* (Cahoy *et al.*, 2008). These include specific cell death abnormality (ced) proteins, such as ced-1 and ced-7, which form parallel pathways leading to ced-10 (Rac1) cytoskeletal activation and target engulfment. The molecular components for other well-defined phagocytic pathways, including receptor tyrosine kinase and αvβ5 integrin, which modulates stabilin-2-mediated phagocytosis (Kim *et al.*, 2012), were also found to be expressed by astrocytes (Cahoy *et al.*, 2008). The authors proposed these phagocytic pathways might be excellent candidates in mediating the phagocytosis of Aβ by astrocytes. The present data are consistent with the proposal that astrocytes have the ability to phagocytose Aβ, as they were shown to efficiently engulf fluorescently-labelled Aβ in a manner dependent on actin polymerisation.

There are conflicting data regarding the modulatory effect of inflammatory cytokines on phagocytosis by microglia, with some groups suggesting a stimulatory effect (Shaftel *et al.*, 2007, Chakrabarty *et al.*, 2010) and others reporting the opposite (Koenigsknecht-Talboo and Landreth, 2005). Aβ results in the release of several inflammatory cytokines by microglia and astrocytes *in vitro* (Floden *et al.*, 2005, Lindberg *et al.*, 2005, Benveniste *et al.*, 2001, Veerhuis *et al.*, 2005, Butovsky *et al.*, 2005). A further significant finding reported here is that Aβ enhanced phagocytosis by astrocytes, as well as microglia, in addition to increasing mRNA and protein expression of markers of activation and inflammation. These findings suggest that phagocytosis can occur by both cell types, even when inflammatory changes persist.

In the case of astrocytes, phagocytic function and the production of pro-inflammatory cytokines appeared to involve CD36, CD47, TLR2 and RAGE, as blocking these receptors using neutralising antibodies modulated the release of pro-inflammatory cytokines and phagocytosis following exposure to Aβ. The finding that these proteins

are expressed on astrocytes is consistent with previous observations (Sick *et al.*, 2011, Bao *et al.*, 2012, Askarova *et al.*, 2011) although earlier findings had suggested that RAGE was only expressed on microglia (Alarcon *et al.*, 2005). Interestingly, in the case of all but TLR2, neutralising antibodies decreased uptake of beads even in the absence of Aβ. A role for these proteins in phagocytosis by macrophages or microglia has been reported (Matozaki *et al.*, 2009, Greenberg *et al.*, 2006, Friggeri *et al.*, 2011, Bao *et al.*, 2012, Gitik *et al.*, 2011) but, to our knowledge, there is no previous evidence that they play a role in phagocytosis by astrocytes. Furthermore, the data suggest a role for NFκB signalling following downstream activation of these receptors by Aβ, as inhibition of its activity significantly attenuated both phagocytosis and the Aβ-induced release of IL-1β, IL-6 and TNFα.

Having shown that short-term exposure of microglia and astrocytes to Aβ *in vitro* triggers inflammatory responses and phagocytosis, the effect of intracerebroventricular infusion of Aβ for 28 days was examined. This experiment was designed to assess the effect of exogenous Aβ accumulation in the brain, as has been shown to occur following this infusion protocol (unpublished data, Belinda Grehan). The number of $CD11b^+$ cells was found to be increased in tissue prepared from Aβ- compared with control-treated rats indicating an increase in microglial activation; this is consistent with previous findings which reported that chronic infusion of Aβ increased the number of F4/80-positive microglia (Craft *et al.*, 2004). Oxidative stress (Malm *et al.*, 2006, Frautschy *et al.*, 2001). Long-lasting increases in IL-1β and TNFα have also been reported following chronic Aβ infusion (Craft *et al.*, 2004). These changes were accompanied by a decreased neuronal count, downregulation of markers of synaptic function and, in some cases, reduced cognitive function, thus emphasising the negative impact of persistent inflammatory changes on neuronal function (Frautschy *et al.*, 2001).

Although Aβ increased the number of $CD11b^+$ cells following intracerebroventricular infusion, uptake of fluorescently-labelled latex beads by these cells was similar in

preparations obtained from control- and Aβ-treated rats. In contrast, while no change in the number of $GLAST^+$ cells was observed, Aβ infusion was found to increase mRNA expression of GFAP, consistent with previous reports (Craft *et al.*, 2004). Interestingly, Aβ increased the number of $GLAST^+$ cells that engulfed fluorescently-labelled latex beads indicating that chronic infusion of Aβ enhanced the phagocytic activity of astrocytes but not microglia. It appears, therefore, that astrocytes have a more important role to play in clearing Aβ *in vivo* under these experimental conditions, further indicating the phagocytic role of astrocytes may be more important than previously suspected.

These results are particularly interesting in context of the recent finding that ablation of microglia resulted in no change in Aβ accumulation in two transgenic mouse models of AD (Grathwohl *et al.*, 2009). These findings indicated that the almost-complete absence of microglia for a 4-week period exerted no effect on either congophilic Aβ deposits or dystrophic neuritic structures, suggesting that the role of microglia, at least during a specified time period, exerts limited effect on the *de novo* formation or clearance of Aβ-plaques. While results from the study by Grathwohl *et al.* also report a concomitant increase in GFAP expression, the question as to whether or not these functions are controlled by astrocytes remains to be further elucidated, as they were not assessed for phagocytic function. Either way, the current data certainly indicate that astrocytes are efficient phagocytes.

While the etiology of AD remains unclear, it is suggested that soluble oligomers rather than fibrillar plaques represent the most toxic species of Aβ. Soluble Aβ present in the brain and CSF is reported to better correlate with disease severity than the presence of plaques (Kuo *et al.*, 1996). Studies have shown that concentrations of soluble Aβ in the cortex are increased 3-fold in AD and correlate highly with other markers of disease severity, in contrast to insoluble Aβ which was found merely to discriminate AD patients from healthy controls (McLean *et al.*, 1999). Even so, the beneficial effects

of inhibiting Aβ production would undoubtedly be useful as a therapeutic strategy due to ample evidence attributing the toxic effects of excess soluble Aβ to AD pathology.

Utilising an APP/PS1 model of AD, the present data demonstrate that concentrations of both soluble and insoluble Aβ were increased with age in the hippocampus. It is of interest that no plateau effect appeared to exist in the age-related accumulation of Aβ, at least at the time-points investigated here. This finding was accompanied by evidence of enhanced activation of microglia and astrocytes with age, as revealed by the exaggerated expression of markers such as CD11b, CD68 and GFAP. Unfortunately, it still remains uncertain as to whether inflammatory changes contribute to pathogenesis of the disease and result in increased production of Aβ, or whether they are secondary to deposition of Aβ and other pathological changes. A deeper understanding of the precise sequence of events by assessing groups of mice at several ages would address this question, and a clear result would aid the development of strategies aimed at delaying disease progression.

Expression of the putative Aβ-binding receptors, TLR2 and TLR4, were increased in the cortex and hippocampus of APP/PS1 mice, and in the case of TLR2, this was further enhanced in older animals. The presence of increased Aβ, as well as enhanced expression of its putative receptor is likely to contribute to the release of pro-inflammatory cytokines following activation of NF-κB signalling pathways. Predictably, the data describe enhanced expression of markers of classical activation of microglia, such as TNFα and IL-1β, in the brains of aged, compared with middle-aged, APP/PS1 mice. There was no change in expression of MR, arginase-1 or FIZZ-1, all of which are markers of alternatively activated microglia; indeed decreased expression of IL-4Rα, NGF and BDNF were observed. These inflammatory changes were accompanied by breakdown of the BBB and enhanced chemokine expression in the hippocampus, with further evidence indicating that T cells, monocytes/macrophages and neutrophils infiltrated the brain parenchyma of APP/PS1 mice. The effect of leukocyte infiltration remains to be unequivocally determined, with some data indicating that it is detrimental

to neuronal function (Nikolic *et al.*, 2007) and others suggesting that infiltration of macrophages limits Aβ accumulation (Town *et al.*, 2008), and infiltrating leukocytes may be protective (Yong and Rivest, 2009). In the current study, however, it is proposed that accumulation of Aβ and infiltration of peripheral leukocytes combine to induce an age-related shift towards a classical pro-inflammatory phenotype in aged APP/PS1 mice.

In an effort to translate findings indicating that inflammation is a key component of the age-related changes reported in an APP/PS1 mouse model of AD, MDMs were isolated from the blood of a unique group of healthy elderly adults classified as IQ memory-discrepant (LP) or IQ memory-consistent (HP); this cohort consisted of elderly individuals whose memory performance was lower than predicted for their educational and intellectual level. Consistent with a role for inflammatory changes in the very early stages of cognitive deterioration, MDMs from the LP group displayed increased expression of CD11b, TLR2, TLR4 and IFNγR, suggesting an enhanced activation state, and it was further shown that when stimulated with LPS *in vitro*, MDMs from LP subjects were hypersensitive such that the release of the cytokines TNFα, IL-6, IL-12p70 and IL-10 was greater than in MDMs prepared from HP subjects. This is suggested to occur as a result of the observed increases in expression of TLR2 and TLR4.

A great deal of evidence, include some detailed in the current thesis, suggests that neuroinflammatory changes are a key component in the pathogenesis of AD. The finding that long-term treatment with NSAIDs results in a reduced risk of developing AD further suggests that such changes may occur early in the disease process and contribute to its development. Numerous studies have reported the presence of increased plasma cytokines (Magaki *et al.*, 2007), chemokines (Bjorkqvist *et al.*, 2012, Westin *et al.*, 2012, Kim *et al.*, 2008) and complement (Thambisetty *et al.*, 2011) in patients with MCI and AD, all of which are further indicative of inflammatory changes.

There is no doubt that early intervention with disease-modifying therapy would be vital in reducing the impact of AD, however this is hampered by a distinct lack of diagnostic tools to allow detection of early changes in cognitive dysfunction which may be indicative of prodromal conditions relating to AD. Existing technologies are reliant on assessment using invasive lumbar puncture or expensive MRI procedures. In addition to changes in $A\beta_{1-42}$ and tau in CSF, increased phospholipase A_2 (PLA_2) activity (Chalbot *et al.*, 2009) and the presence of isoprostane (Kester *et al.*, 2012, Pratico *et al.*, 2002), have been suggested as potential biomarkers for AD. While these results are of great interest, the ultimate goal in diagnostic research is to identify a simple blood-based biomarker to enable routine and repeated measurement before neuronal damage occurs. Therefore, a specific focus of this study was to assess whether changes in MDMs accompany subtle cognitive deficits in older individuals and thus have the potential to provide a robust marker of early disease.

This study thus identifies a novel association between cognitive dysfunction and expression of receptors and cytokines involved with an inflammatory response in MDMs. These inflammatory changes in peripheral cells may be associated with cellular events that contribute to the development of more profound cognitive dysfunction. These results are interesting, not only as is it a simple blood-based assay, but also because the test is subtle enough to identify changes in a non-clinical cohort of subjects. If will be of particular interest to pursue the present findings in a study which assesses whether these changes are associated with further cognitive dysfunction such as that which occurs in MCI or AD. If these were found to correlate, it may provide a method to continuously assess deteriorating cognitive dysfunction and disease progression. Such an assay could also be useful in clinical trials to examine the efficacy of potential disease-modifying treatments. Additionally, confirmation of these early changes in a larger cohort may trigger development of preventative strategies and novel disease-modifying treatments.

Overall, the data identify a role for the modulation of astrocytes as an important area to explore in finding ways to clear Aβ from the AD brain, provide evidence that inflammation is a key component of age-related changes in a mouse model of AD and establish a novel association between inflammatory changes in a population with episodic memory loss.

9: References

ADEREM, A. 2003. Phagocytosis and the inflammatory response. *J Infect Dis,* 187 Suppl 2, S340-5.

AKIRA, S., UEMATSU, S. & TAKEUCHI, O. 2006. Pathogen recognition and innate immunity. *Cell,* 124, 783-801.

AKIYAMA, H. & MCGEER, P. L. 1990. Brain microglia constitutively express beta-2 integrins. *J Neuroimmunol,* 30, 81-93.

AL-ALI, S. Y. & AL-HUSSAIN, S. M. 1996. An ultrastructural study of the phagocytic activity of astrocytes in adult rat brain. *J Anat,* 188 (Pt 2), 257-62.

ALARCON, R., FUENZALIDA, C., SANTIBANEZ, M. & VON BERNHARDI, R. 2005. Expression of scavenger receptors in glial cells. Comparing the adhesion of astrocytes and microglia from neonatal rats to surface-bound beta-amyloid. *J Biol Chem,* 280, 30406-15.

ALBANI, D., ROITER, I., ARTUSO, V., BATELLI, S., PRATO, F., PESARESI, M., GALIMBERTI, D., SCARPINI, E., BRUNI, A., FRANCESCHI, M., PIRAS, M. R., CONFALONI, A. & FORLONI, G. 2007. Presenilin-1 mutation E318G and familial Alzheimer's disease in the Italian population. *Neurobiol Aging,* 28, 1682-8.

ALLAN, S. M., TYRRELL, P. J. & ROTHWELL, N. J. 2005. Interleukin-1 and neuronal injury. *Nat Rev Immunol,* 5, 629-40.

AMITAI, Y. 2010. Physiologic role for "inducible" nitric oxide synthase: a new form of astrocytic-neuronal interface. *Glia,* 58, 1775-81.

APELT, J. & SCHLIEBS, R. 2001. Beta-amyloid-induced glial expression of both pro- and anti-inflammatory cytokines in cerebral cortex of aged transgenic Tg2576 mice with Alzheimer plaque pathology. *Brain Res,* 894, 21-30.

ASKAROVA, S., YANG, X., SHENG, W., SUN, G. Y. & LEE, J. C. 2011. Role of Abeta-receptor for advanced glycation endproducts interaction in oxidative stress and cytosolic phospholipase A(2) activation in astrocytes and cerebral endothelial cells. *Neuroscience,* 199, 375-85.

AVAGYAN, H., GOLDENSON, B., TSE, E., MASOUMI, A., PORTER, V., WIEDAU-PAZOS, M., SAYRE, J., ONG, R., MAHANIAN, M., KOO, P., BAE, S., MICIC, M., LIU, P. T., ROSENTHAL, M. J. & FIALA, M. 2009. Immune blood biomarkers of Alzheimer disease patients. *J Neuroimmunol,* 210, 67-72.

AVISON, M. J., NATH, A., GREENE-AVISON, R., SCHMITT, F. A., GREENBERG, R. N. & BERGER, J. R. 2004. Neuroimaging correlates of HIV-associated BBB compromise. *J Neuroimmunol,* 157, 140-6.

AWATSUJI, H., FURUKAWA, Y., HIROTA, M., MURAKAMI, Y., NII, S., FURUKAWA, S. & HAYASHI, K. 1993. Interleukin-4 and -5 as modulators of nerve growth factor synthesis/secretion in astrocytes. *J Neurosci Res,* 34, 539-45.

AZEVEDO, F. A., CARVALHO, L. R., GRINBERG, L.T., FARFEL, J.M., FERRETTI, R. E., LEITE, R. E., JACOB FILHO, W., LENT, R., HERCULANO-HOUZEL, S. 2009. Equal numbers of neuronal and nonneuronal cells make the human brain an isometrically scaled-up primate brain. *J Comp Neurol.*, 513(5):532-41.

BABIOR, B. M. 2000. Phagocytes and oxidative stress. *Am J Med,* 109, 33-44.

BAJETTO, A., BONAVIA, R., BARBERO, S. & SCHETTINI, G. 2002. Characterization of chemokines and their receptors in the central nervous system: physiopathological implications. *J Neurochem,* 82, 1311-29.

BAMBERGER, M. E., HARRIS, M. E., MCDONALD, D. R., HUSEMANN, J. & LANDRETH, G. E. 2003. A cell surface receptor complex for fibrillar beta-amyloid mediates microglial activation. *J Neurosci,* 23, 2665-74.

BAO, Y., QIN, L., KIM, E., BHOSLE, S., GUO, H., FEBBRAIO, M., HASKEW-LAYTON, R. E., RATAN, R. & CHO, S. 2012. CD36 is involved in astrocyte activation and astroglial scar formation. *J Cereb Blood Flow Metab,* 32, 1567-77.
BARTON, B. E. 1997. IL-6: insights into novel biological activities. *Clin Immunol Immunopathol,* 85, 16-20.

BARD, F., CANNON, C., BARBOUR, R., BURKE, R. L., GAMES, D., GRAJEDA, H., GUIDO, T., HU, K., HUANG, J., JOHNSON-WOOD, K., KHAN, K., KHOLODENKO, D., LEE, M., LIEBERBURG, I., MOTTER, R., NGUYEN, M., SORIANO, F., VASQUEZ, N., WEISS, K., WELCH, B., SEUBERT, P., SCHENK, D. & YEDNOCK, T. 2000. Peripherally administered antibodies against amyloid beta-peptide enter the central nervous system and reduce pathology in a mouse model of Alzheimer disease. *Nat Med,* 6, 916-9.

BASTA, G., LAZZERINI, G., MASSARO, M., SIMONCINI, T., TANGANELLI, P., FU, C., KISLINGER, T., STERN, D. M., SCHMIDT, A. M. & DE CATERINA, R. 2002. Advanced glycation end products activate endothelium through signal-transduction receptor RAGE: a mechanism for amplification of inflammatory responses. *Circulation,* 105, 816-22.

BASU, A., KRADY, J. K. & LEVISON, S. W. 2004. Interleukin-1: a master regulator of neuroinflammation. *J Neurosci Res,* 78, 151-6.

BECHMANN, I. & NITSCH, R. 1997. Astrocytes and microglial cells incorporate degenerating fibers following entorhinal lesion: a light, confocal, and electron microscopical study using a phagocytosis-dependent labeling technique. *Glia,* 20, 145-54.

BECKSTROM, H., JULSRUD, L., HAUGETO, O., DEWAR, D., GRAHAM, D. I., LEHRE, K. P., STORM-MATHISEN, J. & DANBOLT, N. C. 1999. Interindividual differences in the levels of the glutamate transporters GLAST and GLT, but no clear correlation with Alzheimer's disease. *J Neurosci Res,* 55, 218-29.

BEKRIS, L. M., YU, C. E., BIRD, T. D. & TSUANG, D. W. 2010. Genetics of Alzheimer disease. *J Geriatr Psychiatry Neurol,* 23, 213-27.

BENVENISTE, E. N. & BENOS, D. J. 1995. TNF-alpha- and IFN-gamma-mediated signal transduction pathways: effects on glial cell gene expression and function. *FASEB J,* 9, 1577-84.

BENVENISTE, E. N., NGUYEN, V. T. & O'KEEFE, G. M. 2001. Immunological aspects of microglia: relevance to Alzheimer's disease. *Neurochem Int,* 39, 381-91.

BERBAUM, K., SHANMUGAM, K., STUCHBURY, G., WIEDE, F., KORNER, H. & MUNCH, G. 2008. Induction of novel cytokines and chemokines by advanced glycation endproducts determined with a cytometric bead array. *Cytokine,* 41, 198-203.

BERBEL, P. & INNOCENTI, G. M. 1988. The development of the corpus callosum in cats: a light- and electron-microscopic study. *J Comp Neurol,* 276, 132-56.

BIRMINGHAM, K. & FRANTZ, S. 2002. Set back to Alzheimer vaccine studies. *Nat Med,* 8, 199-200.

BIRON, K. E., DICKSTEIN, D. L., GOPAUL, R. & JEFFERIES, W. A. 2011. Amyloid triggers extensive cerebral angiogenesis causing blood brain barrier permeability and hypervascularity in Alzheimer's disease. *PLoS One,* 6, e23789.

BJORKQVIST, M., OHLSSON, M., MINTHON, L. & HANSSON, O. 2012. Evaluation of a previously suggested plasma biomarker panel to identify Alzheimer's disease. *PLoS One,* 7, e29868.

BLENNOW, K., DE LEON, M. J. & ZETTERBERG, H. 2006. Alzheimer's disease. *Lancet,* 368, 387-403.

BORCHELT, D. R., RATOVITSKI, T., VAN LARE, J., LEE, M. K., GONZALES, V., JENKINS, N. A., COPELAND, N. G., PRICE, D. L. & SISODIA, S. S. 1997. Accelerated amyloid deposition in the brains of transgenic mice coexpressing mutant presenilin 1 and amyloid precursor proteins. *Neuron,* 19, 939-45.

BRAAK, H. & BRAAK, E. 1991. Neuropathological stageing of Alzheimer-related changes. *Acta Neuropathol,* 82, 239-59.

BRIKOS, C. & O'NEILL, L. A. 2008. Signalling of toll-like receptors. *Handb Exp Pharmacol*, 21-50.

BRODIE, C., GOLDREICH, N., HAIMAN, T. & KAZIMIRSKY, G. 1998. Functional IL-4 receptors on mouse astrocytes: IL-4 inhibits astrocyte activation and induces NGF secretion. *J Neuroimmunol,* 81, 20-30.

BROOKMEYER, R., GRAY, S. & KAWAS, C. 1998. Projections of Alzheimer's disease in the United States and the public health impact of delaying disease onset. *Am J Public Health,* 88, 1337-42.

BROWNE, T. C., MCQUILLAN, K., MCMANUS, R. M., O'REILLY, J. A., MILLS, K. H. & LYNCH, M. A. 2013. IFN-gamma Production by Amyloid beta-Specific Th1 Cells Promotes Microglial Activation and Increases Plaque Burden in a Mouse Model of Alzheimer's Disease. *J Immunol.*

BURGESS, B. L., MCISAAC, S. A., NAUS, K. E., CHAN, J. Y., TANSLEY, G. H., YANG, J., MIAO, F., ROSS, C. J., VAN ECK, M., HAYDEN, M. R., VAN NOSTRAND, W., ST GEORGE-HYSLOP, P., WESTAWAY, D. & WELLINGTON, C. L. 2006. Elevated plasma triglyceride levels precede amyloid deposition in Alzheimer's disease mouse models with abundant A beta in plasma. *Neurobiol Dis,* 24, 114-27.

BUTOVSKY, O., TALPALAR, A. E., BEN-YAAKOV, K. & SCHWARTZ, M. 2005. Activation of microglia by aggregated beta-amyloid or lipopolysaccharide impairs MHC-II expression and renders them cytotoxic whereas IFN-gamma and IL-4 render them protective. *Mol Cell Neurosci,* 29, 381-93.

CAHOY, J. D., EMERY, B., KAUSHAL, A., FOO, L. C., ZAMANIAN, J. L., CHRISTOPHERSON, K. S., XING, Y., LUBISCHER, J. L., KRIEG, P. A., KRUPENKO, S. A., THOMPSON, W. J. & BARRES, B. A. 2008. A transcriptome database for astrocytes, neurons, and oligodendrocytes: a new resource for understanding brain development and function. *J Neurosci,* 28, 264-78.

CALLAWAY, E. 2012. Gene mutation defends against Alzheimer's disease. *Nature,* 487, 153.

CAMANDOLA, S. & MATTSON, M. P. 2007. NF-kappa B as a therapeutic target in neurodegenerative diseases. *Expert Opin Ther Targets,* 11, 123-32.

CAMERON, B. & LANDRETH, G. E. 2010. Inflammation, microglia, and Alzheimer's disease. *Neurobiol Dis,* 37, 503-9.

CAO, C., ARENDASH, G. W., DICKSON, A., MAMCARZ, M. B., LIN, X. & ETHELL, D. W. 2009. Abeta-specific Th2 cells provide cognitive and pathological benefits to Alzheimer's mice without infiltrating the CNS. *Neurobiol Dis,* 34, 63-70.

CARPENTER, S. & O'NEILL, L. A. 2009. Recent insights into the structure of Toll-like receptors and post-translational modifications of their associated signalling proteins. *Biochem J,* 422, 1-10.

CARPENTIER, P. A., DUNCAN, D. S. & MILLER, S. D. 2008. Glial toll-like receptor signaling in central nervous system infection and autoimmunity. *Brain Behav Immun,* 22, 140-7.

CARTY, M. & BOWIE, A. G. 2011. Evaluating the role of Toll-like receptors in diseases of the central nervous system. *Biochem Pharmacol,* 81, 825-37.

CASULA, M., IYER, A. M., SPLIET, W. G., ANINK, J. J., STEENTJES, K., STA, M., TROOST, D. & ARONICA, E. 2011. Toll-like receptor signaling in amyotrophic lateral sclerosis spinal cord tissue. *Neuroscience.*

CHAKRABARTY, P., JANSEN-WEST, K., BECCARD, A., CEBALLOS-DIAZ, C., LEVITES, Y., VERBEECK, C., ZUBAIR, A. C., DICKSON, D., GOLDE, T. E. & DAS, P. 2010. Massive gliosis induced by interleukin-6 suppresses Abeta deposition in vivo: evidence against inflammation as a driving force for amyloid deposition. *FASEB J,* 24, 548-59.

CHALBOT, S., ZETTERBERG, H., BLENNOW, K., FLADBY, T., GRUNDKE-IQBAL, I. & IQBAL, K. 2009. Cerebrospinal fluid secretory Ca2+-dependent phospholipase A2 activity is increased in Alzheimer disease. *Clin Chem,* 55, 2171-9.

CHEN, G., CHEN, K. S., KNOX, J., INGLIS, J., BERNARD, A., MARTIN, S. J., JUSTICE, A., MCCONLOGUE, L., GAMES, D., FREEDMAN, S. B. & MORRIS, R. G. 2000. A learning deficit related to age and beta-amyloid plaques in a mouse model of Alzheimer's disease. *Nature,* 408, 975-9.

CHEN, G. & GOEDDEL, D. V. 2002. TNF-R1 signaling: a beautiful pathway. *Science,* 296, 1634-5.

CHEN, H. L., PISTOLLATO, F., HOEPPNER, D. J., NI, H. T., MCKAY, R. D. & PANCHISION, D. M. 2007. Oxygen tension regulates survival and fate of mouse central nervous system precursors at multiple levels. *Stem Cells,* 25, 2291-301.

CHIEPPA, M., BIANCHI, G., DONI, A., DEL PRETE, A., SIRONI, M., LASKARIN, G., MONTI, P., PIEMONTI, L., BIONDI, A., MANTOVANI, A., INTRONA, M. & ALLAVENA, P. 2003. Cross-linking of the mannose receptor on monocyte-derived dendritic cells activates an anti-inflammatory immunosuppressive program. *J Immunol,* 171, 4552-60.

CITRON, M., OLTERSDORF, T., HAASS, C., MCCONLOGUE, L., HUNG, A. Y., SEUBERT, P., VIGO-PELFREY, C., LIEBERBURG, I. & SELKOE, D. J. 1992. Mutation of the beta-amyloid precursor protein in familial Alzheimer's disease increases beta-protein production. *Nature,* 360, 672-4.

CLASSEN, A., LLOBERAS, J. & CELADA, A. 2009. Macrophage activation: classical versus alternative. *Methods Mol Biol,* 531, 29-43.

COLTON, C. A. 2009. Heterogeneity of microglial activation in the innate immune response in the brain. *J Neuroimmune Pharmacol,* 4, 399-418.

COLTON, C. A., MOTT, R. T., SHARPE, H., XU, Q., VAN NOSTRAND, W. E. & VITEK, M. P. 2006. Expression profiles for macrophage alternative activation genes in AD and in mouse models of AD. *J Neuroinflammation,* 3, 27.

COLTON, C. A. & WILCOCK, D. M. 2010. Assessing activation states in microglia. *CNS Neurol Disord Drug Targets,* 9, 174-91.

COMBS, C. K. 2009. Inflammation and microglia actions in Alzheimer's disease. *J Neuroimmune Pharmacol,* 4, 380-8.

CORBETT, A. & BALLARD, C. 2012. New and emerging treatments for Alzheimer's disease. *Expert Opin Emerg Drugs,* 17, 147-56.

CRAFT, J. M., WATTERSON, D. M., FRAUTSCHY, S. A. & VAN ELDIK, L. J. 2004. Aminopyridazines inhibit beta-amyloid-induced glial activation and neuronal damage in vivo. *Neurobiol Aging,* 25, 1283-92.

CZEH, M., GRESSENS, P. & KAINDL, A. M. 2011. The yin and yang of microglia. *Dev Neurosci,* 33, 199-209.

DA SILVA, R. P. & GORDON, S. 1999. Phagocytosis stimulates alternative glycosylation of macrosialin (mouse CD68), a macrophage-specific endosomal protein. *Biochem J,* 338 (Pt 3), 687-94.

DALMAU, I., VELA, J. M., GONZALEZ, B., FINSEN, B. & CASTELLANO, B. 2003. Dynamics of microglia in the developing rat brain. *J Comp Neurol,* 458, 144-57.

DAVIES, P. & MALONEY, A. J. 1976. Selective loss of central cholinergic neurons in Alzheimer's disease. *Lancet,* 2, 1403.

DAVOUST, N., VUAILLAT, C., ANDRODIAS, G. & NATAF, S. 2008. From bone marrow to microglia: barriers and avenues. *Trends Immunol,* 29, 227-34.

DEANE, R., SINGH, I., SAGARE, A. P., BELL, R. D., ROSS, N. T., LARUE, B., LOVE, R., PERRY, S., PAQUETTE, N., DEANE, R. J., THIYAGARAJAN, M., ZARCONE, T., FRITZ, G., FRIEDMAN, A. E., MILLER, B. L. & ZLOKOVIC, B. V. 2012. A multimodal RAGE-specific inhibitor reduces amyloid beta-mediated brain disorder in a mouse model of Alzheimer disease. *J Clin Invest,* 122, 1377-92.

DELRIEU, J., OUSSET, P. J., CAILLAUD, C. & VELLAS, B. 2012. 'Clinical trials in Alzheimer's disease': immunotherapy approaches. *J Neurochem,* 120 Suppl 1, 186-93.

DERECKI, N. C., CARDANI, A. N., YANG, C. H., QUINNIES, K. M., CRIHFIELD, A., LYNCH, K. R. & KIPNIS, J. 2010. Regulation of learning and memory by meningeal immunity: a key role for IL-4. *J Exp Med,* 207, 1067-80.

DINARELLO, C. A. 1996. Biologic basis for interleukin-1 in disease. *Blood,* 87, 2095-147.

DIXIT, R., ROSS, J. L., GOLDMAN, Y. E. & HOLZBAUR, E. L. 2008. Differential regulation of dynein and kinesin motor proteins by tau. *Science,* 319, 1086-9.

DODART, J. C., MEZIANE, H., MATHIS, C., BALES, K. R., PAUL, S. M. & UNGERER, A. 1999. Behavioral disturbances in transgenic mice overexpressing the V717F beta-amyloid precursor protein. *Behav Neurosci,* 113, 982-90.

DOETSCH, F. 2003. The glial identity of neural stem cells. *Nat Neurosci,* 6, 1127-34.

DONG, X. Q., YANG, S. B., ZHU, F. L., LV, Q. W., ZHANG, G. H. & HUANG, H. B. 2010. Resistin is associated with mortality in patients with traumatic brain injury. *Crit Care,* 14, R190.

DUAN, R. S., YANG, X., CHEN, Z. G., LU, M. O., MORRIS, C., WINBLAD, B. & ZHU, J. 2008. Decreased fractalkine and increased IP-10 expression in aged brain of APP(swe) transgenic mice. *Neurochem Res,* 33, 1085-9.

EL KHOURY, J. & LUSTER, A. D. 2008. Mechanisms of microglia accumulation in Alzheimer's disease: therapeutic implications. *Trends Pharmacol Sci,* 29, 626-32.

EMONTS, M., HAZELZET, J. A., DE GROOT, R. & HERMANS, P. W. 2003. Host genetic determinants of Neisseria meningitidis infections. *Lancet Infect Dis,* 3, 565-77.

ENG, L. F. & GHIRNIKAR, R. S. 1994. GFAP and astrogliosis. *Brain Pathol,* 4, 229-37.

ENG, L. F., GHIRNIKAR, R. S. & LEE, Y. L. 2000. Glial fibrillary acidic protein: GFAP-thirty-one years (1969-2000). *Neurochem Res,* 25, 1439-51.

ENGELHART, M. J., GEERLINGS, M. I., MEIJER, J., KILIAAN, A., RUITENBERG, A., VAN SWIETEN, J. C., STIJNEN, T., HOFMAN, A., WITTEMAN, J. C. & BRETELER, M. M. 2004. Inflammatory proteins in plasma and the risk of dementia: the rotterdam study. *Arch Neurol,* 61, 668-72.

ERNST, J. S., O 2006. *Phagocytosis of Bacteria and Bacterial Pathogenicity*, Cambridge University Press.

ETMINAN, M., GILL, S. & SAMII, A. 2003. Effect of non-steroidal anti-inflammatory drugs on risk of Alzheimer's disease: systematic review and meta-analysis of observational studies. *BMJ,* 327, 128.

EVIN, G., SERNEE, M. F. & MASTERS, C. L. 2006. Inhibition of gamma-secretase as a therapeutic intervention for Alzheimer's disease: prospects, limitations and strategies. *CNS Drugs,* 20, 351-72.

FAMILIAN, A., EIKELENBOOM, P. & VEERHUIS, R. 2007. Minocycline does not affect amyloid beta phagocytosis by human microglial cells. *Neurosci Lett,* 416, 87-91.

FANG, F. C. 1997. Perspectives series: host/pathogen interactions. Mechanisms of nitric oxide-related antimicrobial activity. *J Clin Invest,* 99, 2818-25.

FARINA, C., ALOISI, F. & MEINL, E. 2007. Astrocytes are active players in cerebral innate immunity. *Trends Immunol,* 28, 138-45.

FIALA, M., LIN, J., RINGMAN, J., KERMANI-ARAB, V., TSAO, G., PATEL, A., LOSSINSKY, A. S., GRAVES, M. C., GUSTAVSON, A., SAYRE, J., SOFRONI, E., SUAREZ, T., CHIAPPELLI, F. & BERNARD, G. 2005. Ineffective phagocytosis of amyloid-beta by macrophages of Alzheimer's disease patients. *J Alzheimers Dis,* 7, 221-32; discussion 255-62.

FIALA, M., LIU, P. T., ESPINOSA-JEFFREY, A., ROSENTHAL, M. J., BERNARD, G., RINGMAN, J. M., SAYRE, J., ZHANG, L., ZAGHI, J., DEJBAKHSH, S., CHIANG, B., HUI, J., MAHANIAN, M., BAGHAEE, A., HONG, P. & CASHMAN, J. 2007. Innate immunity and transcription of MGAT-III and Toll-like receptors in Alzheimer's disease patients are improved by bisdemethoxycurcumin. *Proc Natl Acad Sci U S A,* 104, 12849-54.

FIALA, M. & VEERHUIS, R. 2010. Biomarkers of inflammation and amyloid-beta phagocytosis in patients at risk of Alzheimer disease. *Exp Gerontol,* 45, 57-63.

FINCH, C. E. & COHEN, D. M. 1997. Aging, metabolism, and Alzheimer disease: review and hypotheses. *Exp Neurol,* 143, 82-102.

FLANNAGAN, R. S., COSIO, G. & GRINSTEIN, S. 2009. Antimicrobial mechanisms of phagocytes and bacterial evasion strategies. *Nat Rev Microbiol,* 7, 355-66.

FLODEN, A. M. & COMBS, C. K. 2006. Beta-amyloid stimulates murine postnatal and adult microglia cultures in a unique manner. *J Neurosci,* 26, 4644-8.

FLODEN, A. M., LI, S. & COMBS, C. K. 2005. Beta-amyloid-stimulated microglia induce neuron death via synergistic stimulation of tumor necrosis factor alpha and NMDA receptors. *J Neurosci,* 25, 2566-75.

FONTANA, A., FIERZ, W. & WEKERLE, H. 1984. Astrocytes present myelin basic protein to encephalitogenic T-cell lines. *Nature,* 307, 273-6.

FRAUTSCHY, S. A., HU, W., KIM, P., MILLER, S. A., CHU, T., HARRIS-WHITE, M. E. & COLE, G. M. 2001. Phenolic anti-inflammatory antioxidant reversal of Abeta-induced cognitive deficits and neuropathology. *Neurobiol Aging,* 22, 993-1005.

FRIGGERI, A., BANERJEE, S., BISWAS, S., DE FREITAS, A., LIU, G., BIERHAUS, A. & ABRAHAM, E. 2011. Participation of the receptor for advanced glycation end products in efferocytosis. *J Immunol,* 186, 6191-8.

GALLAGHER, J. J., MINOGUE, A. M. & LYNCH, M. A. 2012. Impaired Performance of Female APP/PS1 Mice in the Morris Water Maze Is Coupled with Increased Abeta Accumulation and Microglial Activation. *Neurodegener Dis.*

GAMES, D., ADAMS, D., ALESSANDRINI, R., BARBOUR, R., BERTHELETTE, P., BLACKWELL, C., CARR, T., CLEMENS, J., DONALDSON, T., GILLESPIE, F. & ET AL. 1995. Alzheimer-type neuropathology in transgenic mice overexpressing V717F beta-amyloid precursor protein. *Nature,* 373, 523-7.

GARDEN, G. A. & MOLLER, T. 2006. Microglia biology in health and disease. *J Neuroimmune Pharmacol,* 1, 127-37.

GATE, D., REZAI-ZADEH, K., JODRY, D., RENTSENDORJ, A. & TOWN, T. 2010. Macrophages in Alzheimer's disease: the blood-borne identity. *J Neural Transm,* 117, 961-70.

GAWRONSKI, J. D. & BENSON, D. R. 2004. Microtiter assay for glutamine synthetase biosynthetic activity using inorganic phosphate detection. *Anal Biochem,* 327, 114-8.

GEORGE, P. M., BADIGER, R., ALAZAWI, W., FOSTER, G. R. & MITCHELL, J. A. 2012. Pharmacology and therapeutic potential of interferons. *Pharmacol Ther,* 135, 44-53.

GIMBEL, D. A., NYGAARD, H. B., COFFEY, E. E., GUNTHER, E. C., LAUREN, J., GIMBEL, Z. A. & STRITTMATTER, S. M. 2010. Memory impairment in transgenic Alzheimer mice requires cellular prion protein. *J Neurosci,* 30, 6367-74.

GINHOUX, F., GRETER, M., LEBOEUF, M., NANDI, S., SEE, P., GOKHAN, S., MEHLER, MF., CONWAY, SJ., STANLEY, ER., SAMOKHVALOV, IM., MERAD, M. Fate mapping analysis reveals that adult microglia derive from primitive macrophages. *Science*, 2010 Nov 5;330(6005):841-5.

GITIK, M., LIRAZ-ZALTSMAN, S., OLDENBORG, P. A., REICHERT, F. & ROTSHENKER, S. 2011. Myelin down-regulates myelin phagocytosis by microglia and macrophages through interactions between CD47 on myelin and SIRPalpha (signal regulatory protein-alpha) on phagocytes. *J Neuroinflammation,* 8, 24.

GLOCKER, E. O., KOTLARZ, D., KLEIN, C., SHAH, N. & GRIMBACHER, B. 2011. IL-10 and IL-10 receptor defects in humans. *Ann N Y Acad Sci,* 1246, 102-7.

GOOD, D. W., GEORGE, T. & WATTS, B. A., 3RD 2012. Toll-like receptor 2 is required for LPS-induced Toll-like receptor 4 signaling and inhibition of ion transport in renal thick ascending limb. *J Biol Chem,* 287, 20208-20.

GORDON, S. & TAYLOR, P. R. 2005. Monocyte and macrophage heterogeneity. *Nat Rev Immunol,* 5, 953-64.

GRAMMAS, P. & OVASE, R. 2001. Inflammatory factors are elevated in brain microvessels in Alzheimer's disease. *Neurobiol Aging,* 22, 837-42.

GRAS, G., CHRETIEN, F., VALLAT-DECOUVELAERE, A. V., LE PAVEC, G., PORCHERAY, F., BOSSUET, C., LEONE, C., MIALOCQ, P., DEREUDDRE-BOSQUET, N., CLAYETTE, P., LE GRAND, R., CREMINON, C., DORMONT, D., RIMANIOL, A. C. & GRAY, F. 2003. Regulated expression of sodium-dependent glutamate transporters and synthetase: a neuroprotective role for activated microglia and macrophages in HIV infection? *Brain Pathol,* 13, 211-22.

GRATHWOHL, S. A., KALIN, R. E., BOLMONT, T., PROKOP, S., WINKELMANN, G., KAESER, S. A., ODENTHAL, J., RADDE, R., ELDH, T., GANDY, S., AGUZZI, A., STAUFENBIEL, M., MATHEWS, P. M., WOLBURG, H., HEPPNER, F. L. & JUCKER, M. 2009. Formation and maintenance of Alzheimer's disease beta-amyloid plaques in the absence of microglia. *Nat Neurosci,* 12, 1361-3.

GREENBERG, M. E., SUN, M., ZHANG, R., FEBBRAIO, M., SILVERSTEIN, R. & HAZEN, S. L. 2006. Oxidized phosphatidylserine-CD36 interactions play an essential role in macrophage-dependent phagocytosis of apoptotic cells. *J Exp Med,* 203, 2613-25.

GRIFFIN, W. S., STANLEY, L. C., LING, C., WHITE, L., MACLEOD, V., PERROT, L. J., WHITE, C. L., 3RD & ARAOZ, C. 1989. Brain interleukin 1 and S-100 immunoreactivity are elevated in Down syndrome and Alzheimer disease. *Proc Natl Acad Sci U S A,* 86, 7611-5.

GROVES, E., DART, A. E., COVARELLI, V. & CARON, E. 2008. Molecular mechanisms of phagocytic uptake in mammalian cells. *Cell Mol Life Sci,* 65, 1957-76.

HALDENWANGER, A., ELING, P., KASTRUP, A. & HILDEBRANDT, H. 2010. Correlation between cognitive impairment and CSF biomarkers in amnesic MCI, non-amnesic MCI, and Alzheimer's disease. *J Alzheimers Dis,* 22, 971-80.

HALLE, A., HORNUNG, V., PETZOLD, G. C., STEWART, C. R., MONKS, B. G., REINHECKEL, T., FITZGERALD, K. A., LATZ, E., MOORE, K. J. & GOLENBOCK, D. T. 2008. The NALP3 inflammasome is involved in the innate immune response to amyloid-beta. *Nat Immunol,* 9, 857-65.

HAN, M. H., LUNDGREN, D. H., JAISWAL, S., CHAO, M., GRAHAM, K. L., GARRIS, C. S., AXTELL, R. C., HO, P. P., LOCK, C. B., WOODARD, J. I., BROWNELL, S. E., ZOUDILOVA, M., HUNT, J. F., BARANZINI, S. E., BUTCHER, E. C., RAINE, C. S., SOBEL, R. A., HAN, D. K., WEISSMAN, I. & STEINMAN, L. 2012. Janus-like opposing roles of CD47 in autoimmune brain inflammation in humans and mice. *J Exp Med,* 209, 1325-34.

HAN, S. H., KIM, Y. H. & MOOK-JUNG, I. 2011. RAGE: the beneficial and deleterious effects by diverse mechanisms of actions. *Mol Cells,* 31, 91-7.

HANAMSAGAR, R., HANKE, M. L. & KIELIAN, T. 2012. Toll-like receptor (TLR) and inflammasome actions in the central nervous system. *Trends Immunol,* 33, 333-42.

HANISCH, U. K. 2002. Microglia as a source and target of cytokines. *Glia,* 40, 140-55.

HANISCH, U. K., JOHNSON, T. V. & KIPNIS, J. 2008. Toll-like receptors: roles in neuroprotection? *Trends Neurosci,* 31, 176-82.

HARDY, J. & SELKOE, D. J. 2002. The amyloid hypothesis of Alzheimer's disease: progress and problems on the road to therapeutics. *Science,* 297, 353-6.

HARRY, G. J. & KRAFT, A. D. 2012. Microglia in the developing brain: a potential target with lifetime effects. *Neurotoxicology,* 33, 191-206.

HART, S. P., SMITH, J. R. & DRANSFIELD, I. 2004. Phagocytosis of opsonized apoptotic cells: roles for 'old-fashioned' receptors for antibody and complement. *Clin Exp Immunol,* 135, 181-5.

HARVATH, L. & TERLE, D. A. 1999. Assay for phagocytosis. *Methods Mol Biol,* 115, 281-90.

HASHIOKA, S., KLEGERIS, A., SCHWAB, C., YU, S. & MCGEER, P. L. 2010. Differential expression of interferon-gamma receptor on human glial cells in vivo and in vitro. *J Neuroimmunol,* 225, 91-9.

HE, P., ZHONG, Z., LINDHOLM, K., BERNING, L., LEE, W., LEMERE, C., STAUFENBIEL, M., LI, R. & SHEN, Y. 2007. Deletion of tumor necrosis factor death receptor inhibits amyloid beta generation and prevents learning and memory deficits in Alzheimer's mice. *J Cell Biol,* 178, 829-41.

HENDRIKS, J. J., TEUNISSEN, C. E., DE VRIES, H. E. & DIJKSTRA, C. D. 2005. Macrophages and neurodegeneration. *Brain Res Brain Res Rev,* 48, 185-95.

HENEKA, M. T., O'BANION, M. K., TERWEL, D. & KUMMER, M. P. 2010. Neuroinflammatory processes in Alzheimer's disease. *J Neural Transm,* 117, 919-47.

HICKMAN, S. E., ALLISON, E. K. & EL KHOURY, J. 2008. Microglial dysfunction and defective beta-amyloid clearance pathways in aging Alzheimer's disease mice. *J Neurosci,* 28, 8354-60.

HOCHSTRASSER, T., WEISS, E., MARKSTEINER, J. & HUMPEL, C. 2010. Soluble cell adhesion molecules in monocytes of Alzheimer's disease and mild cognitive impairment. *Exp Gerontol,* 45, 70-4.

HOENICKA, J. 2006. [Genes in Alzheimer's disease]. *Rev Neurol,* 42, 302-5.

HOFER, U., LEHMANN, A. D., WAELTI, E., AMACKER, M., GEHR, P. & ROTHEN-RUTISHAUSER, B. 2009. Virosomes can enter cells by non-phagocytic mechanisms. *J Liposome Res,* 19, 301-9.

HOFFBRAND, A., PETTIT, J. & MOSS, P. 2005. *Essential Haematology,* London, Blackwell Science.

HOGAN, S. P., ROSENBERG, H. F., MOQBEL, R., PHIPPS, S., FOSTER, P. S., LACY, P., KAY, A. B. & ROTHENBERG, M. E. 2008. Eosinophils: biological properties and role in health and disease. *Clin Exp Allergy,* 38, 709-50.

HOLMES, C., EL-OKL, M., WILLIAMS, A. L., CUNNINGHAM, C., WILCOCKSON, D. & PERRY, V. H. 2003. Systemic infection, interleukin 1beta, and cognitive decline in Alzheimer's disease. *J Neurol Neurosurg Psychiatry,* 74, 788-9.

HSIAO, K., CHAPMAN, P., NILSEN, S., ECKMAN, C., HARIGAYA, Y., YOUNKIN, S., YANG, F. & COLE, G. 1996. Correlative memory deficits, Abeta elevation, and amyloid plaques in transgenic mice. *Science,* 274, 99-102.

HUANG, X., REYNOLDS, A. D., MOSLEY, R. L. & GENDELMAN, H. E. 2009. CD 4+ T cells in the pathobiology of neurodegenerative disorders. *J Neuroimmunol,* 211, 3-15.

HUANG, Y. 2010. Abeta-independent roles of apolipoprotein E4 in the pathogenesis of Alzheimer's disease. *Trends Mol Med,* 16, 287-94.

HUELL, M., STRAUSS, S., VOLK, B., BERGER, M. & BAUER, J. 1995. Interleukin-6 is present in early stages of plaque formation and is restricted to the brains of Alzheimer's disease patients. *Acta Neuropathol,* 89, 544-51.

HUSEMANN, J., LOIKE, J. D., ANANKOV, R., FEBBRAIO, M. & SILVERSTEIN, S. C. 2002. Scavenger receptors in neurobiology and neuropathology: their role on microglia and other cells of the nervous system. *Glia,* 40, 195-205.

INSALL, R. H. & MACHESKY, L. M. 2009. Actin dynamics at the leading edge: from simple machinery to complex networks. *Dev Cell,* 17, 310-22.

IRIZARRY, M. C. 2004. Biomarkers of Alzheimer disease in plasma. *NeuroRx,* 1, 226-34.

ISAACS, A. & LINDENMANN, J. 1957. Virus interference. I. The interferon. *Proc R Soc Lond B Biol Sci,* 147, 258-67.

ISHIZUKA, K., KIMURA, T., IGATA-YI, R., KATSURAGI, S., TAKAMATSU, J. & MIYAKAWA, T. 1997. Identification of monocyte chemoattractant protein-1 in senile plaques and reactive microglia of Alzheimer's disease. *Psychiatry Clin Neurosci,* 51, 135-8.

ITAGAKI, S., MCGEER, P. L. & AKIYAMA, H. 1988. Presence of T-cytotoxic suppressor and leucocyte common antigen positive cells in Alzheimer's disease brain tissue. *Neurosci Lett,* 91, 259-64.

ITTNER, L. M. & GOTZ, J. 2011. Amyloid-beta and tau--a toxic pas de deux in Alzheimer's disease. *Nat Rev Neurosci,* 12, 65-72.

JACK, C. R., JR. 2012. Alzheimer disease: new concepts on its neurobiology and the clinical role imaging will play. *Radiology,* 263, 344-61.

JACK, C. R., JR., KNOPMAN, D. S., JAGUST, W. J., SHAW, L. M., AISEN, P. S., WEINER, M. W., PETERSEN, R. C. & TROJANOWSKI, J. Q. 2010. Hypothetical model of dynamic biomarkers of the Alzheimer's pathological cascade. *Lancet Neurol,* 9, 119-28.

JADIDI-NIARAGH, F. & MIRSHAFIEY, A. 2011. Th17 cell, the new player of neuroinflammatory process in multiple sclerosis. *Scand J Immunol,* 74, 1-13.

JANA, M., PALENCIA, C. A. & PAHAN, K. 2008. Fibrillar amyloid-beta peptides activate microglia via TLR2: implications for Alzheimer's disease. *J Immunol,* 181, 7254-62.

JANEWAY, C. A., JR. & MEDZHITOV, R. 2002. Innate immune recognition. *Annu Rev Immunol,* 20, 197-216.

JANKOWSKY, J. L., FADALE, D. J., ANDERSON, J., XU, G. M., GONZALES, V., JENKINS, N. A., COPELAND, N. G., LEE, M. K., YOUNKIN, L. H., WAGNER, S. L., YOUNKIN, S. G. & BORCHELT, D. R. 2004. Mutant presenilins specifically elevate the levels of the 42 residue beta-amyloid peptide in vivo: evidence for augmentation of a 42-specific gamma secretase. *Hum Mol Genet,* 13, 159-70.

JOHNSTON, H., BOUTIN, H. & ALLAN, S. M. 2011. Assessing the contribution of inflammation in models of Alzheimer's disease. *Biochem Soc Trans,* 39, 886-90.

JOHNSTONE, M., GEARING, A. J. & MILLER, K. M. 1999. A central role for astrocytes in the inflammatory response to beta-amyloid; chemokines, cytokines and reactive oxygen species are produced. *J Neuroimmunol,* 93, 182-93.

JONSSON, T., ATWAL, J. K., STEINBERG, S., SNAEDAL, J., JONSSON, P. V., BJORNSSON, S., STEFANSSON, H., SULEM, P., GUDBJARTSSON, D., MALONEY, J., HOYTE, K., GUSTAFSON, A., LIU, Y., LU, Y., BHANGALE, T., GRAHAM, R. R., HUTTENLOCHER, J., BJORNSDOTTIR, G., ANDREASSEN, O. A., JONSSON, E. G., PALOTIE, A., BEHRENS, T. W., MAGNUSSON, O. T., KONG, A., THORSTEINSDOTTIR, U., WATTS, R. J. & STEFANSSON, K. 2012. A mutation in APP protects against Alzheimer's disease and age-related cognitive decline. *Nature,* 488, 96-9.

JOU, M. J. 2008. Pathophysiological and pharmacological implications of mitochondria-targeted reactive oxygen species generation in astrocytes. *Adv Drug Deliv Rev,* 60, 1512-26.

JUNGBLUT, M., TIVERON, M. C., BARRAL, S., ABRAHAMSEN, B., KNOBEL, S., PENNARTZ, S., SCHMITZ, J., PERRAUT, M., PFRIEGER, F. W., STOFFEL, W., CREMER, H. & BOSIO, A. 2012. Isolation and characterization of living primary astroglial cells using the new GLAST-specific monoclonal antibody ACSA-1. *Glia,* 60, 894-907.

KAGAN, B. L., GANZ, T. & LEHRER, R. I. 1994. Defensins: a family of antimicrobial and cytotoxic peptides. *Toxicology,* 87, 131-49.

KAPLIN, A., CARROLL, K. A., CHENG, J., ALLIE, R., LYKETSOS, C. G., CALABRESI, P. & ROSENBERG, P. B. 2009. IL-6 release by LPS-stimulated peripheral blood mononuclear cells as a potential biomarker in Alzheimer's disease. *Int Psychogeriatr,* 21, 413-4.

KAWAI, K., TSUNO, N. H., MATSUHASHI, M., KITAYAMA, J., OSADA, T., YAMADA, J., TSUCHIYA, T., YONEYAMA, S., WATANABE, T., TAKAHASHI, K. & NAGAWA, H. 2005. CD11b-mediated migratory property of peripheral blood B cells. *J Allergy Clin Immunol,* 116, 192-7.

KERCHNER, G. A. & BOXER, A. L. 2010. Bapineuzumab. *Expert Opin Biol Ther,* 10, 1121-30.

KESTER, M. I., SCHEFFER, P. G., KOEL-SIMMELINK, M. J., TWAALFHOVEN, H., VERWEY, N. A., VEERHUIS, R., TWISK, J. W., BOUWMAN, F. H., BLANKENSTEIN,

M. A., SCHELTENS, P., TEUNISSEN, C. & VAN DER FLIER, W. M. 2012. Serial CSF sampling in Alzheimer's disease: specific versus non-specific markers. *Neurobiol Aging,* 33, 1591-8.

KIM, S., PARK, S. Y., KIM, S. Y., BAE, D. J., PYO, J. H., HONG, M. & KIM, I. S. 2012. Cross Talk between Engulfment Receptors Stabilin-2 and Integrin alphavbeta5 Orchestrates Engulfment of Phosphatidylserine-Exposed Erythrocytes. *Mol Cell Biol,* 32, 2698-708.

KIM, S. U. & DE VELLIS, J. 2005. Microglia in health and disease. *J Neurosci Res,* 81, 302-13.

KIM, T. S., LIM, H. K., LEE, J. Y., KIM, D. J., PARK, S., LEE, C. & LEE, C. U. 2008. Changes in the levels of plasma soluble fractalkine in patients with mild cognitive impairment and Alzheimer's disease. *Neurosci Lett,* 436, 196-200.

KIMELBERG, H. K. & NEDERGAARD, M. 2010. Functions of astrocytes and their potential as therapeutic targets. *Neurotherapeutics,* 7, 338-53.

KIYOTA, T., OKUYAMA, S., SWAN, R. J., JACOBSEN, M. T., GENDELMAN, H. E. & IKEZU, T. 2010. CNS expression of anti-inflammatory cytokine interleukin-4 attenuates Alzheimer's disease-like pathogenesis in APP+PS1 bigenic mice. *FASEB J,* 24, 3093-102.

KLEGERIS, A. & MCGEER, P. L. 1997. beta-amyloid protein enhances macrophage production of oxygen free radicals and glutamate. *J Neurosci Res,* 49, 229-35.

KNIGHT, J. A. 2000. Review: Free radicals, antioxidants, and the immune system. *Ann Clin Lab Sci,* 30, 145-58.

KOENIGSKNECHT-TALBOO, J. & LANDRETH, G. E. 2005. Microglial phagocytosis induced by fibrillar beta-amyloid and IgGs are differentially regulated by proinflammatory cytokines. *J Neurosci,* 25, 8240-9.

KOENIGSKNECHT, J. & LANDRETH, G. 2004. Microglial phagocytosis of fibrillar beta-amyloid through a beta1 integrin-dependent mechanism. *J Neurosci,* 24, 9838-46.

KONG, L. & GE, B. X. 2008. MyD88-independent activation of a novel actin-Cdc42/Rac pathway is required for Toll-like receptor-stimulated phagocytosis. *Cell Res,* 18, 745-55.

KRONCKE, K. D., FEHSEL, K. & KOLB-BACHOFEN, V. 1997. Nitric oxide: cytotoxicity versus cytoprotection--how, why, when, and where? *Nitric Oxide,* 1, 107-20.

KRUTZIK, S. R., TAN, B., LI, H., OCHOA, M. T., LIU, P. T., SHARFSTEIN, S. E., GRAEBER, T. G., SIELING, P. A., LIU, Y. J., REA, T. H., BLOOM, B. R. & MODLIN, R. L. 2005. TLR activation triggers the rapid differentiation of monocytes into macrophages and dendritic cells. *Nat Med,* 11, 653-60.

KUO, Y. M., EMMERLING, M. R., VIGO-PELFREY, C., KASUNIC, T. C., KIRKPATRICK, J. B., MURDOCH, G. H., BALL, M. J. & ROHER, A. E. 1996. Water-soluble Abeta (N-40, N-42) oligomers in normal and Alzheimer disease brains. *J Biol Chem,* 271, 4077-81.

KURIHARA, T., WARR, G., LOY, J. & BRAVO, R. 1997. Defects in macrophage recruitment and host defense in mice lacking the CCR2 chemokine receptor. *J Exp Med,* 186, 1757-62.

KURUSHIMA, H., RAMPRASAD, M., KONDRATENKO, N., FOSTER, D. M., QUEHENBERGER, O. & STEINBERG, D. 2000. Surface expression and rapid internalization of macrosialin (mouse CD68) on elicited mouse peritoneal macrophages. *J Leukoc Biol,* 67, 104-8.

LADU, M. J., SHAH, J. A., REARDON, C. A., GETZ, G. S., BU, G., HU, J., GUO, L. & VAN ELDIK, L. J. 2000. Apolipoprotein E receptors mediate the effects of beta-amyloid on astrocyte cultures. *J Biol Chem,* 275, 33974-80.

LAI, J. C. & COOPER, A. J. 1986. Brain alpha-ketoglutarate dehydrogenase complex: kinetic properties, regional distribution, and effects of inhibitors. *J Neurochem,* 47, 1376-86.

LANTOS, P. L. 1974. An electron microscope study of reacting astrocytes in gliomas induced by n-ethyl-n-nitrosourea in rats. *Acta Neuropathol,* 30, 175-81.

LAWS, S. M., HONE, E., GANDY, S. & MARTINS, R. N. 2003. Expanding the association between the APOE gene and the risk of Alzheimer's disease: possible roles for APOE promoter polymorphisms and alterations in APOE transcription. *J Neurochem,* 84, 1215-36.

LAWSON, L. J., PERRY, V. H., DRI, P. & GORDON, S. 1990. Heterogeneity in the distribution and morphology of microglia in the normal adult mouse brain. *Neuroscience,* 39, 151-70.

LEE, C. Y. & LANDRETH, G. E. 2010. The role of microglia in amyloid clearance from the AD brain. *J Neural Transm,* 117, 949-60.

LEMERE, C. A., MARON, R., SPOONER, E. T., GRENFELL, T. J., MORI, C., DESAI, R., HANCOCK, W. W., WEINER, H. L. & SELKOE, D. J. 2000. Nasal A beta treatment induces anti-A beta antibody production and decreases cerebral amyloid burden in PD-APP mice. *Ann N Y Acad Sci,* 920, 328-31.

LEONG, J. W. & FEHNIGER, T. A. 2011. Human NK cells: SET to kill. *Blood,* 117, 2297-8.

LEWANDOWSKA, E., WIERZBA-BOBROWICZ, T., KOSNO-KRUSZEWSKA, E., LECHOWICZ, W., SCHMIDT-SIDOR, B., SZPAK, G. M., BERTRAND, E., PASENNIK, E. & GWIAZDA, E. 2004. Ultrastructural evaluation of activated forms of microglia in human brain in selected neurological diseases (SSPE, Wilson's disease and Alzheimer's disease). *Folia Neuropathol,* 42, 81-91.

LIANG, Z., VALLA, J., SEFIDVASH-HOCKLEY, S., ROGERS, J. & LI, R. 2002. Effects of estrogen treatment on glutamate uptake in cultured human astrocytes derived from cortex of Alzheimer's disease patients. *J Neurochem,* 80, 807-14.

LIAO, M. C., AHMED, M., SMITH, S. O. & VAN NOSTRAND, W. E. 2009. Degradation of amyloid beta protein by purified myelin basic protein. *J Biol Chem,* 284, 28917-25.

LICASTRO, F., PEDRINI, S., CAPUTO, L., ANNONI, G., DAVIS, L. J., FERRI, C., CASADEI, V. & GRIMALDI, L. M. 2000. Increased plasma levels of interleukin-1, interleukin-6 and alpha-1-antichymotrypsin in patients with Alzheimer's disease: peripheral inflammation or signals from the brain? *J Neuroimmunol,* 103, 97-102.

LIM, S., JANG, H. J., PARK, E. H., KIM, J. K., KIM, J. M., KIM, E. K., YEA, K., KIM, Y. H., LEE-KWON, W., RYU, S. H. & SUH, P. G. 2012. Wedelolactone inhibits adipogenesis through the ERK pathway in human adipose tissue-derived mesenchymal stem cells. *J Cell Biochem.*

LINDBERG, C., HJORTH, E., POST, C., WINBLAD, B. & SCHULTZBERG, M. 2005. Cytokine production by a human microglial cell line: effects of beta-amyloid and alpha-melanocyte-stimulating hormone. *Neurotox Res,* 8, 267-76.

LIU, M. H., TSUANG, F. Y., SHEU, S. Y., SUN, J. S. & SHIH, C. M. 2011. The protective effects of coumestrol against amyloid-beta peptide- and lipopolysaccharide-induced toxicity on mice astrocytes. *Neurol Res,* 33, 663-72.

LIU, S., LIU, Y., HAO, W., WOLF, L., KILIAAN, A. J., PENKE, B., RUBE, C. E., WALTER, J., HENEKA, M. T., HARTMANN, T., MENGER, M. D. & FASSBENDER, K. 2012. TLR2 is a primary receptor for Alzheimer's amyloid beta peptide to trigger neuroinflammatory activation. *J Immunol,* 188, 1098-107.

LOMBARDI, V. R., GARCIA, M., REY, L. & CACABELOS, R. 1999. Characterization of cytokine production, screening of lymphocyte subset patterns and in vitro apoptosis in healthy and Alzheimer's Disease (AD) individuals. *J Neuroimmunol,* 97, 163-71.

LOWENSTEIN, C. J. & PADALKO, E. 2004. iNOS (NOS2) at a glance. *J Cell Sci,* 117, 2865-7.

LUCIN, K. M. & WYSS-CORAY, T. 2009. Immune activation in brain aging and neurodegeneration: too much or too little? *Neuron,* 64, 110-22.

LUE, L. F., RYDEL, R., BRIGHAM, E. F., YANG, L. B., HAMPEL, H., MURPHY, G. M., JR., BRACHOVA, L., YAN, S. D., WALKER, D. G., SHEN, Y. & ROGERS, J. 2001a. Inflammatory repertoire of Alzheimer's disease and nondemented elderly microglia in vitro. *Glia,* 35, 72-9.

LUE, L. F., WALKER, D. G., BRACHOVA, L., BEACH, T. G., ROGERS, J., SCHMIDT, A. M., STERN, D. M. & YAN, S. D. 2001b. Involvement of microglial receptor for advanced glycation endproducts (RAGE) in Alzheimer's disease: identification of a cellular activation mechanism. *Exp Neurol,* 171, 29-45.

LUTH, H. J., HOLZER, M., GARTNER, U., STAUFENBIEL, M. & ARENDT, T. 2001. Expression of endothelial and inducible NOS-isoforms is increased in Alzheimer's disease, in APP23 transgenic mice and after experimental brain lesion in rat: evidence for an induction by amyloid pathology. *Brain Res,* 913, 57-67.

LYNCH, A. M., LOANE, D. J., MINOGUE, A. M., CLARKE, R. M., KILROY, D., NALLY, R. E., ROCHE, O. J., O'CONNELL, F. & LYNCH, M. A. 2007. Eicosapentaenoic acid confers neuroprotection in the amyloid-beta challenged aged hippocampus. *Neurobiol Aging,* 28, 845-55.

LYNCH, A. M., MURPHY, K. J., DEIGHAN, B. F., O'REILLY, J. A., GUN'KO, Y. K., COWLEY, T. R., GONZALEZ-REYES, R. E. & LYNCH, M. A. 2010. The impact of glial activation in the aging brain. *Aging Dis,* 1, 262-78.

LYONS, A., GRIFFIN, R. J., COSTELLOE, C. E., CLARKE, R. M. & LYNCH, M. A. 2007. IL-4 attenuates the neuroinflammation induced by amyloid-beta in vivo and in vitro. *J Neurochem,* 101, 771-81.

MA, X. & TRINCHIERI, G. 2001. Regulation of interleukin-12 production in antigen-presenting cells. *Adv Immunol,* 79, 55-92.

MAGAKI, S., MUELLER, C., DICKSON, C. & KIRSCH, W. 2007. Increased production of inflammatory cytokines in mild cognitive impairment. *Exp Gerontol,* 42, 233-40.

MAJUMDAR, A., CRUZ, D., ASAMOAH, N., BUXBAUM, A., SOHAR, I., LOBEL, P. & MAXFIELD, F. R. 2007. Activation of microglia acidifies lysosomes and leads to degradation of Alzheimer amyloid fibrils. *Mol Biol Cell,* 18, 1490-6.

MALININ, N. L., BOLDIN, M. P., KOVALENKO, A. V. & WALLACH, D. 1997. MAP3K-related kinase involved in NF-kappaB induction by TNF, CD95 and IL-1. *Nature,* 385, 540-4.

MALM, T., ORT, M., TAHTIVAARA, L., JUKARAINEN, N., GOLDSTEINS, G., PUOLIVALI, J., NURMI, A., PUSSINEN, R., AHTONIEMI, T., MIETTINEN, T. K., KANNINEN, K., LESKINEN, S., VARTIAINEN, N., YRJANHEIKKI, J., LAATIKAINEN, R., HARRIS-WHITE, M. E., KOISTINAHO, M., FRAUTSCHY, S. A., BURES, J. & KOISTINAHO, J. 2006. beta-Amyloid infusion results in delayed and age-dependent learning deficits without role of inflammation or beta-amyloid deposits. *Proc Natl Acad Sci U S A,* 103, 8852-7.

MAN, S. M., MA, Y. R., SHANG, D. S., ZHAO, W. D., LI, B., GUO, D. W., FANG, W. G., ZHU, L. & CHEN, Y. H. 2007. Peripheral T cells overexpress MIP-1alpha to enhance its transendothelial migration in Alzheimer's disease. *Neurobiol Aging,* 28, 485-96.

MANAYE, K. F., WANG, P. C., O'NEIL, J. N., HUANG, S. Y., XU, T., LEI, D. L., TIZABI, Y., OTTINGER, M. A., INGRAM, D. K. & MOUTON, P. R. 2007. Neuropathological quantification of dtg APP/PS1: neuroimaging, stereology, and biochemistry. *Age (Dordr),* 29, 87-96.

MANDREKAR-COLUCCI, S., KARLO, J. C. & LANDRETH, G. E. 2012. Mechanisms Underlying the Rapid Peroxisome Proliferator-Activated Receptor-gamma-Mediated Amyloid Clearance and Reversal of Cognitive Deficits in a Murine Model of Alzheimer's Disease. *J Neurosci,* 32, 10117-28.

MANDREKAR, S., JIANG, Q., LEE, C. Y., KOENIGSKNECHT-TALBOO, J., HOLTZMAN, D. M. & LANDRETH, G. E. 2009. Microglia mediate the clearance of soluble Abeta through fluid phase macropinocytosis. *J Neurosci,* 29, 4252-62.

MARKESBERY, W. R. & CARNEY, J. M. 1999. Oxidative alterations in Alzheimer's disease. *Brain Pathol,* 9, 133-46.

MATOZAKI, T., MURATA, Y., OKAZAWA, H. & OHNISHI, H. 2009. Functions and molecular mechanisms of the CD47-SIRPalpha signalling pathway. *Trends Cell Biol,* 19, 72-80.

MATTSON, M. P., CHENG, B., CULWELL, A. R., ESCH, F. S., LIEBERBURG, I. & RYDEL, R. E. 1993. Evidence for excitoprotective and intraneuronal calcium-regulating roles for secreted forms of the beta-amyloid precursor protein. *Neuron,* 10, 243-54.

MCLEAN, C. A., CHERNY, R. A., FRASER, F. W., FULLER, S. J., SMITH, M. J., BEYREUTHER, K., BUSH, A. I. & MASTERS, C. L. 1999. Soluble pool of Abeta amyloid as a determinant of severity of neurodegeneration in Alzheimer's disease. *Ann Neurol,* 46, 860-6.

MCQUILLAN, K., LYNCH, M. A. & MILLS, K. H. 2010. Activation of mixed glia by Abeta-specific Th1 and Th17 cells and its regulation by Th2 cells. *Brain Behav Immun,* 24, 598-607.

MEDZHITOV, R. & JANEWAY, C. A., JR. 1997. Innate immunity: impact on the adaptive immune response. *Curr Opin Immunol,* 9, 4-9.

MEHTA, P. D., PIRTTILA, T., MEHTA, S. P., SERSEN, E. A., AISEN, P. S. & WISNIEWSKI, H. M. 2000. Plasma and cerebrospinal fluid levels of amyloid beta proteins 1-40 and 1-42 in Alzheimer disease. *Arch Neurol,* 57, 100-5.

MILLER, A. M., PIAZZA, A., MARTIN, D. S., WALSH, M., MANDEL, A., BOLTON, A. E., LYNCH, M. A. 2009. The deficit in long-term potentiation induced by chronic administration of amyloid-beta is attenuated by treatment of rats with a novel phospholipid-based drug formulation, VP025. *Exp Gerontol.* 44(4):300-4.

MILLER, G. 2012. Alzheimer's research. Stopping Alzheimer's before it starts. *Science,* 337, 790-2.

MINAKAMI, R. & SUMIMOTOA, H. 2006. Phagocytosis-coupled activation of the superoxide-producing phagocyte oxidase, a member of the NADPH oxidase (nox) family. *Int J Hematol,* 84, 193-8.

MIZWICKI, M. T., MENEGAZ, D., ZHANG, J., BARRIENTOS-DURAN, A., TSE, S., CASHMAN, J. R., GRIFFIN, P. R. & FIALA, M. 2012. Genomic and nongenomic signaling induced by 1alpha,25(OH)2-vitamin D3 promotes the recovery of amyloid-beta phagocytosis by Alzheimer's disease macrophages. *J Alzheimers Dis,* 29, 51-62.

MONTGOMERY, S. L. & BOWERS, W. J. 2012. Tumor necrosis factor-alpha and the roles it plays in homeostatic and degenerative processes within the central nervous system. *J Neuroimmune Pharmacol,* 7, 42-59.

MONTGOMERY, S. L., MASTRANGELO, M. A., HABIB, D., NARROW, W. C., KNOWLDEN, S. A., WRIGHT, T. W. & BOWERS, W. J. 2011. Ablation of TNF-RI/RII expression in Alzheimer's disease mice leads to an unexpected enhancement of pathology: implications for chronic pan-TNF-alpha suppressive therapeutic strategies in the brain. *Am J Pathol,* 179, 2053-70.

MOORE, K. W., DE WAAL MALEFYT, R., COFFMAN, R. L. & O'GARRA, A. 2001. Interleukin-10 and the interleukin-10 receptor. *Annu Rev Immunol,* 19, 683-765.
MOSSER, D. M. 2003. The many faces of macrophage activation. *J Leukoc Biol,* 73, 209-12.

MOSSER, D. M. & EDWARDS, J. P. 2008. Exploring the full spectrum of macrophage activation. *Nat Rev Immunol,* 8, 958-69.

MUFSON, E. J., BOTHWELL, M. & KORDOWER, J. H. 1989. Loss of nerve growth factor receptor-containing neurons in Alzheimer's disease: a quantitative analysis across subregions of the basal forebrain. *Exp Neurol,* 105, 221-32.

MULLAN, M., TSUJI, S., MIKI, T., KATSUYA, T., NARUSE, S., KANEKO, K., SHIMIZU, T., KOJIMA, T., NAKANO, I., OGIHARA, T. & ET AL. 1993. Clinical comparison of Alzheimer's disease in pedigrees with the codon 717 Val-->Ile mutation in the amyloid precursor protein gene. *Neurobiol Aging,* 14, 407-19.

MUNOZ-FERNANDEZ, M. A. & FRESNO, M. 1998. The role of tumour necrosis factor, interleukin 6, interferon-gamma and inducible nitric oxide synthase in the development and pathology of the nervous system. *Prog Neurobiol,* 56, 307-40.

MURPHY, K. J., MILLER, A. M., THELMA, R., COWLEY, F., COX, F. F., LYNCH, M. A. 2011. The age- and amyloid-β-related increases in Nogo B contribute to microglial activation. *Neurochem Int*, 58(2):161-8.

NAERT, G. & RIVEST, S. 2011. CC chemokine receptor 2 deficiency aggravates cognitive impairments and amyloid pathology in a transgenic mouse model of Alzheimer's disease. *J Neurosci,* 31, 6208-20.

NAG, S., SARKAR, B., BANDYOPADHYAY, A., SAHOO, B., SREENIVASAN, V. K., KOMBRABAIL, M., MURALIDHARAN, C. & MAITI, S. 2011. The nature of the amyloid-{beta} monomer and the monomer-oligomer equilibrium. *J Biol Chem.*

NAGAI, A., MISHIMA, S., ISHIDA, Y., ISHIKURA, H., HARADA, T., KOBAYASHI, S. & KIM, S. U. 2005. Immortalized human microglial cell line: phenotypic expression. *J Neurosci Res,* 81, 342-8.

NAGELE, R. G., D'ANDREA, M. R., LEE, H., VENKATARAMAN, V. & WANG, H. Y. 2003. Astrocytes accumulate A beta 42 and give rise to astrocytic amyloid plaques in Alzheimer disease brains. *Brain Res,* 971, 197-209.

NAKANISHI, S., NAKAJIMA, Y., MASU, M., UEDA, Y., NAKAHARA, K., WATANABE, D., YAMAGUCHI, S., KAWABATA, S. & OKADA, M. 1998. Glutamate receptors: brain function and signal transduction. *Brain Res Brain Res Rev,* 26, 230-5.

NGUYEN, J. V., SOTO, I., KIM, K. Y., BUSHONG, E. A., OGLESBY, E., VALIENTE-SORIANO, F. J., YANG, Z., DAVIS, C. H., BEDONT, J. L., SON, J. L., WEI, J. O., BUCHMAN, V. L., ZACK, D. J., VIDAL-SANZ, M., ELLISMAN, M. H. & MARSH-ARMSTRONG, N. 2011. Myelination transition zone astrocytes are constitutively phagocytic and have synuclein dependent reactivity in glaucoma. *Proc Natl Acad Sci U S A,* 108, 1176-81.

NIELSEN, H. M., MULDER, S. D., BELIEN, J. A., MUSTERS, R. J., EIKELENBOOM, P. & VEERHUIS, R. 2010. Astrocytic A beta 1-42 uptake is determined by A beta-aggregation state and the presence of amyloid-associated proteins. *Glia,* 58, 1235-46.

NIELSEN, H. M., VEERHUIS, R., HOLMQVIST, B. & JANCIAUSKIENE, S. 2009. Binding and uptake of A beta1-42 by primary human astrocytes in vitro. *Glia,* 57, 978-88.

O'NEILL, L. A. & KALTSCHMIDT, C. 1997. NF-kappa B: a crucial transcription factor for glial and neuronal cell function. *Trends Neurosci,* 20, 252-8.

OAKLEY, H., COLE, S. L., LOGAN, S., MAUS, E., SHAO, P., CRAFT, J., GUILLOZET-BONGAARTS, A., OHNO, M., DISTERHOFT, J., VAN ELDIK, L., BERRY, R. & VASSAR, R. 2006. Intraneuronal beta-amyloid aggregates, neurodegeneration, and neuron loss in transgenic mice with five familial Alzheimer's disease mutations: potential factors in amyloid plaque formation. *J Neurosci,* 26, 10129-40.

OBERHEIM, N. A., WANG, X., GOLDMAN, S. & NEDERGAARD, M. 2006. Astrocytic complexity distinguishes the human brain. *Trends Neurosci,* 29, 547-53.

OLABARRIA, M., NORISTANI, H. N., VERKHRATSKY, A. & RODRIGUEZ, J. J. 2010. Concomitant astroglial atrophy and astrogliosis in a triple transgenic animal model of Alzheimer's disease. *Glia,* 58, 831-8.

OSBORN, G. G. & SAUNDERS, A. V. 2010. Current treatments for patients with Alzheimer disease. *J Am Osteopath Assoc,* 110, S16-26.

PALSSON-MCDERMOTT, E. M. & O'NEILL, L. A. 2007. The potential of targeting Toll-like receptor 2 in autoimmune and inflammatory diseases. *Ir J Med Sci,* 176, 253-60.

PARAMESWARAN, N. & PATIAL, S. 2010. Tumor necrosis factor-alpha signaling in macrophages. *Crit Rev Eukaryot Gene Expr,* 20, 87-103.

PARESCE, D. M., GHOSH, R. N. & MAXFIELD, F. R. 1996. Microglial cells internalize aggregates of the Alzheimer's disease amyloid beta-protein via a scavenger receptor. *Neuron,* 17, 553-65.

PARPURA, V., BASARSKY, T. A., LIU, F., JEFTINIJA, K., JEFTINIJA, S. & HAYDON, P. G. 1994. Glutamate-mediated astrocyte-neuron signalling. *Nature,* 369, 744-7.

PASINETTI, G. M. 2002. From epidemiology to therapeutic trials with anti-inflammatory drugs in Alzheimer's disease: the role of NSAIDs and cyclooxygenase in beta-amyloidosis and clinical dementia. *J Alzheimers Dis,* 4, 435-45.

PASSOS, G. F., FIGUEIREDO, C. P., PREDIGER, R. D., PANDOLFO, P., DUARTE, F. S., MEDEIROS, R. & CALIXTO, J. B. 2009. Role of the macrophage inflammatory protein-1alpha/CC chemokine receptor 5 signaling pathway in the neuroinflammatory response and cognitive deficits induced by beta-amyloid peptide. *Am J Pathol,* 175, 1586-97.

PERRY, V. H., CUNNINGHAM, C. & HOLMES, C. 2007. Systemic infections and inflammation affect chronic neurodegeneration. *Nat Rev Immunol,* 7, 161-7.

PERRY, V. H. & GORDON, S. 1988. Macrophages and microglia in the nervous system. *Trends Neurosci,* 11, 273-7.

PERSSON, M. & RONNBACK, L. 2012. Microglial self-defence mediated through GLT-1 and glutathione. *Amino Acids,* 42, 207-19.

PFEIFER, M., BONCRISTIANO, S., BONDOLFI, L., STALDER, A., DELLER, T., STAUFENBIEL, M., MATHEWS, P. M. & JUCKER, M. 2002. Cerebral hemorrhage after passive anti-Abeta immunotherapy. *Science,* 298, 1379.

PHAM, C. T. 2006. Neutrophil serine proteases: specific regulators of inflammation. *Nat Rev Immunol,* 6, 541-50.

PHILLIPS, H. S., HAINS, J. M., ARMANINI, M., LARAMEE, G. R., JOHNSON, S. A. & WINSLOW, J. W. 1991. BDNF mRNA is decreased in the hippocampus of individuals with Alzheimer's disease. *Neuron,* 7, 695-702.

PIHLAJA, R., KOISTINAHO, J., KAUPPINEN, R., SANDHOLM, J., TANILA, H. & KOISTINAHO, M. 2011. Multiple cellular and molecular mechanisms are involved in human Abeta clearance by transplanted adult astrocytes. *Glia,* 59, 1643-57.

PIHLAJA, R., KOISTINAHO, J., MALM, T., SIKKILA, H., VAINIO, S. & KOISTINAHO, M. 2008. Transplanted astrocytes internalize deposited beta-amyloid peptides in a transgenic mouse model of Alzheimer's disease. *Glia,* 56, 154-63.

PLOWDEN, J., RENSHAW-HOELSCHER, M., ENGLEMAN, C., KATZ, J. & SAMBHARA, S. 2004. Innate immunity in aging: impact on macrophage function. *Aging Cell,* 3, 161-7.

POIRIER, J., DAVIGNON, J., BOUTHILLIER, D., KOGAN, S., BERTRAND, P. & GAUTHIER, S. 1993. Apolipoprotein E polymorphism and Alzheimer's disease. *Lancet,* 342, 697-9.

POPKO, B., CORBIN, J. G., BAERWALD, K. D., DUPREE, J. & GARCIA, A. M. 1997. The effects of interferon-gamma on the central nervous system. *Mol Neurobiol,* 14, 19-35.

PRATICO, D., CLARK, C. M., LIUN, F., ROKACH, J., LEE, V. Y. & TROJANOWSKI, J. Q. 2002. Increase of brain oxidative stress in mild cognitive impairment: a possible predictor of Alzheimer disease. *Arch Neurol,* 59, 972-6.

PRESKY, D. H., YANG, H., MINETTI, L. J., CHUA, A. O., NABAVI, N., WU, C. Y., GATELY, M. K. & GUBLER, U. 1996. A functional interleukin 12 receptor complex is composed of two beta-type cytokine receptor subunits. *Proc Natl Acad Sci U S A,* 93, 14002-7.

PRILLER, C., BAUER, T., MITTEREGGER, G., KREBS, B., KRETZSCHMAR, H. A. & HERMS, J. 2006. Synapse formation and function is modulated by the amyloid precursor protein. *J Neurosci,* 26, 7212-21.

QIU, C., KIVIPELTO, M. & VON STRAUSS, E. 2009. Epidemiology of Alzheimer's disease: occurrence, determinants, and strategies toward intervention. *Dialogues Clin Neurosci,* 11, 111-28.

RACHAL PUGH, C., FLESHNER, M., WATKINS, L. R., MAIER, S. F. & RUDY, J. W. 2001. The immune system and memory consolidation: a role for the cytokine IL-1beta. *Neurosci Biobehav Rev,* 25, 29-41.

RANSOHOFF, R. M. & BROWN, M. A. 2012. Innate immunity in the central nervous system. *J Clin Invest,* 122, 1164-71.

REALE, M., IARLORI, C., GAMBI, F., FELICIANI, C., SALONE, A., TOMA, L., DELUCA, G., SALVATORE, M., CONTI, P. & GAMBI, D. 2004. Treatment with an acetylcholinesterase inhibitor in Alzheimer patients modulates the expression and production of the pro-inflammatory and anti-inflammatory cytokines. *J Neuroimmunol,* 148, 162-71.

REED-GEAGHAN, E. G., REED, Q. W., CRAMER, P. E. & LANDRETH, G. E. 2010. Deletion of CD14 attenuates Alzheimer's disease pathology by influencing the brain's inflammatory milieu. *J Neurosci,* 30, 15369-73.

REED-GEAGHAN, E. G., SAVAGE, J. C., HISE, A. G. & LANDRETH, G. E. 2009. CD14 and toll-like receptors 2 and 4 are required for fibrillar A{beta}-stimulated microglial activation. *J Neurosci,* 29, 11982-92.

RICHNER, M., BACH, G. & WEST, M. J. 2009. Over expression of amyloid beta-protein reduces the number of neurons in the striatum of APPswe/PS1DeltaE9. *Brain Res,* 1266, 87-92.

RODRIGUEZ, J. J., OLABARRIA, M., CHVATAL, A. & VERKHRATSKY, A. 2009. Astroglia in dementia and Alzheimer's disease. *Cell Death Differ,* 16, 378-85.

ROGERS, J., LUBER-NAROD, J., STYREN, S. D. & CIVIN, W. H. 1988. Expression of immune system-associated antigens by cells of the human central nervous system: relationship to the pathology of Alzheimer's disease. *Neurobiol Aging,* 9, 339-49.

ROTHWELL, N. J. & LUHESHI, G. N. 2000. Interleukin 1 in the brain: biology, pathology and therapeutic target. *Trends Neurosci,* 23, 618-25.

ROWAN, A.G., FLETCHER, J.M., RYAN, E.J., MORAN, B., HEGARTY, J.E., O'FARRELLY, C. & MILLS, K.H. 2008. Hepatitis C virus-specific Th17 cells are suppressed by virus-induced TGF-beta. *J Immunol* 181: 4485-4494.

RUAN, L., KANG, Z., PEI, G. & LE, Y. 2009. Amyloid deposition and inflammation in APPswe/PS1dE9 mouse model of Alzheimer's disease. *Curr Alzheimer Res,* 6, 531-40.

RUBIO-PEREZ, J. M. & MORILLAS-RUIZ, J. M. 2012. A review: inflammatory process in Alzheimer's disease, role of cytokines. *ScientificWorldJournal,* 2012, 756357.

SANTACRUZ, K., LEWIS, J., SPIRES, T., PAULSON, J., KOTILINEK, L., INGELSSON, M., GUIMARAES, A., DETURE, M., RAMSDEN, M., MCGOWAN, E., FORSTER, C., YUE, M., ORNE, J., JANUS, C., MARIASH, A., KUSKOWSKI, M., HYMAN, B., HUTTON, M. & ASHE, K. H. 2005. Tau suppression in a neurodegenerative mouse model improves memory function. *Science,* 309, 476-81.

SARAIVA, M. & O'GARRA, A. 2010. The regulation of IL-10 production by immune cells. *Nat Rev Immunol,* 10, 170-81.

SAVARIN-VUAILLAT, C. & RANSOHOFF, R. M. 2007. Chemokines and chemokine receptors in neurological disease: raise, retain, or reduce? *Neurotherapeutics,* 4, 590-601.

SCHENTEN, D. & MEDZHITOV, R. 2011. The control of adaptive immune responses by the innate immune system. *Adv Immunol,* 109, 87-124.

SCHRODER, K., HERTZOG, P. J., RAVASI, T. & HUME, D. A. 2004. Interferon-gamma: an overview of signals, mechanisms and functions. *J Leukoc Biol,* 75, 163-89.

SCHROEDER, J. T. 2009. Basophils beyond effector cells of allergic inflammation. *Adv Immunol,* 101, 123-61.

SERRANO-POZO, A., WILLIAM, C. M., FERRER, I., URO-COSTE, E., DELISLE, M. B., MAURAGE, C. A., HOCK, C., NITSCH, R. M., MASLIAH, E., GROWDON, J. H., FROSCH, M. P. & HYMAN, B. T. 2010. Beneficial effect of human anti-amyloid-beta active immunization on neurite morphology and tau pathology. *Brain,* 133, 1312-27.

SHAFTEL, S. S., CARLSON, T. J., OLSCHOWKA, J. A., KYRKANIDES, S., MATOUSEK, S. B. & O'BANION, M. K. 2007a. Chronic interleukin-1beta expression in mouse brain leads to leukocyte infiltration and neutrophil-independent blood brain barrier permeability without overt neurodegeneration. *J Neurosci,* 27, 9301-9.

SHAFTEL, S. S., GRIFFIN, W. S. & O'BANION, M. K. 2008. The role of interleukin-1 in neuroinflammation and Alzheimer disease: an evolving perspective. *J Neuroinflammation,* 5, 7.

SHAFTEL, S. S., KYRKANIDES, S., OLSCHOWKA, J. A., MILLER, J. N., JOHNSON, R. E. & O'BANION M, K. 2007b. Sustained hippocampal IL-1beta overexpression mediates chronic neuroinflammation and ameliorates Alzheimer plaque pathology. *J Clin Invest,* 117, 1595-604.

SHAPIRO, L. A., BIALOWAS-MCGOEY, L. A. & WHITAKER-AZMITIA, P. M. 2010. Effects of S100B on Serotonergic Plasticity and Neuroinflammation in the Hippocampus in Down Syndrome and Alzheimer's Disease: Studies in an S100B Overexpressing Mouse Model. *Cardiovasc Psychiatry Neurol,* 2010.

SHENG, J. G., GRIFFIN, W. S., ROYSTON, M. C. & MRAK, R. E. 1998. Distribution of interleukin-1-immunoreactive microglia in cerebral cortical layers: implications for neuritic plaque formation in Alzheimer's disease. *Neuropathol Appl Neurobiol,* 24, 278-83.

SHI, J. Q., SHEN, W., CHEN, J., WANG, B. R., ZHONG, L. L., ZHU, Y. W., ZHU, H. Q., ZHANG, Q. Q., ZHANG, Y. D. & XU, J. 2011. Anti-TNF-alpha reduces amyloid plaques and tau phosphorylation and induces CD11c-positive dendritic-like cell in the APP/PS1 transgenic mouse brains. *Brain Res,* 1368, 239-47.

SHIMIZU, E., KAWAHARA, K., KAJIZONO, M., SAWADA, M. & NAKAYAMA, H. 2008. IL-4-induced selective clearance of oligomeric beta-amyloid peptide(1-42) by rat primary type 2 microglia. *J Immunol,* 181, 6503-13.

SICK, E., BOUKHARI, A., DERAMAUDT, T., RONDE, P., BUCHER, B., ANDRE, P., GIES, J. P. & TAKEDA, K. 2011. Activation of CD47 receptors causes proliferation of human astrocytoma but not normal astrocytes via an Akt-dependent pathway. *Glia,* 59, 308-19.

SIMARD, M., ARCUINO, G., TAKANO, T., LIU, Q. S. & NEDERGAARD, M. 2003. Signaling at the gliovascular interface. *J Neurosci,* 23, 9254-62.

SKAPER, S. D. 2008. The biology of neurotrophins, signalling pathways, and functional peptide mimetics of neurotrophins and their receptors. *CNS Neurol Disord Drug Targets,* 7, 46-62.

SLY, L. M., KRZESICKI, R. F., BRASHLER, J. R., BUHL, A. E., MCKINLEY, D. D., CARTER, D. B. & CHIN, J. E. 2001. Endogenous brain cytokine mRNA and inflammatory responses to lipopolysaccharide are elevated in the Tg2576 transgenic mouse model of Alzheimer's disease. *Brain Res Bull,* 56, 581-8.

SOKOLOVA, A., HILL, M. D., RAHIMI, F., WARDEN, L. A., HALLIDAY, G. M. & SHEPHERD, C. E. 2009. Monocyte chemoattractant protein-1 plays a dominant role in the chronic inflammation observed in Alzheimer's disease. *Brain Pathol,* 19, 392-8.

SOLOVJOV, D. A., PLUSKOTA, E. & PLOW, E. F. 2005. Distinct roles for the alpha and beta subunits in the functions of integrin alphaMbeta2. *J Biol Chem,* 280, 1336-45.

SONG, L., LEE, C. & SCHINDLER, C. 2011. Deletion of the murine scavenger receptor CD68. *J Lipid Res,* 52, 1542-50.

SPRINGER, T. A. 1990. Adhesion receptors of the immune system. *Nature,* 346, 425-34.

STEINER, J., BERNSTEIN, H. G., BIELAU, H., BERNDT, A., BRISCH, R., MAWRIN, C., KEILHOFF, G. & BOGERTS, B. 2007. Evidence for a wide extra-astrocytic distribution of S100B in human brain. *BMC Neurosci,* 8, 2.

STERN, A. S., PODLASKI, F. J., HULMES, J. D., PAN, Y. C., QUINN, P. M., WOLITZKY, A. G., FAMILLETTI, P. C., STREMLO, D. L., TRUITT, T., CHIZZONITE, R. & ET AL. 1990. Purification to homogeneity and partial characterization of cytotoxic lymphocyte maturation factor from human B-lymphoblastoid cells. *Proc Natl Acad Sci U S A,* 87, 6808-12.

STEWART, C. R., STUART, L. M., WILKINSON, K., VAN GILS, J. M., DENG, J., HALLE, A., RAYNER, K. J., BOYER, L., ZHONG, R., FRAZIER, W. A., LACY-HULBERT, A., EL KHOURY, J., GOLENBOCK, D. T. & MOORE, K. J. 2010. CD36 ligands promote sterile inflammation through assembly of a Toll-like receptor 4 and 6 heterodimer. *Nat Immunol,* 11, 155-61.

STREIT, W. J., MILLER, K. R., LOPES, K. O. & NJIE, E. 2008. Microglial degeneration in the aging brain--bad news for neurons? *Front Biosci,* 13, 3423-38.

STRLE, K., ZHOU, J. H., SHEN, W. H., BROUSSARD, S. R., JOHNSON, R. W., FREUND, G. G., DANTZER, R. & KELLEY, K. W. 2001. Interleukin-10 in the brain. *Crit Rev Immunol,* 21, 427-49.

STURCHLER, E., GALICHET, A., WEIBEL, M., LECLERC, E. & HEIZMANN, C. W. 2008. Site-specific blockade of RAGE-Vd prevents amyloid-beta oligomer neurotoxicity. *J Neurosci,* 28, 5149-58.

SUN, J. C., LOPEZ-VERGES, S., KIM, C. C., DERISI, J. L. & LANIER, L. L. 2011. NK cells and immune "memory". *J Immunol,* 186, 1891-7.

SZCZEPANIK, A. M., FUNES, S., PETKO, W. & RINGHEIM, G. E. 2001. IL-4, IL-10 and IL-13 modulate A beta(1--42)-induced cytokine and chemokine production in primary murine microglia and a human monocyte cell line. *J Neuroimmunol,* 113, 49-62.

TAGA, T., HIBI, M., HIRATA, Y., YAMASAKI, K., YASUKAWA, K., MATSUDA, T., HIRANO, T. & KISHIMOTO, T. 1989. Interleukin-6 triggers the association of its receptor with a possible signal transducer, gp130. *Cell,* 58, 573-81.

TAGUCHI, A., BLOOD, D. C., DEL TORO, G., CANET, A., LEE, D. C., QU, W., TANJI, N., LU, Y., LALLA, E., FU, C., HOFMANN, M. A., KISLINGER, T., INGRAM, M., LU, A., TANAKA, H., HORI, O., OGAWA, S., STERN, D. M. & SCHMIDT, A. M. 2000. Blockade of RAGE-amphoterin signalling suppresses tumour growth and metastases. *Nature,* 405, 354-60.

TAKEDA, K., KAISHO, T. & AKIRA, S. 2003. Toll-like receptors. *Annu Rev Immunol,* 21, 335-76.

TAKEUCHI, H., JIN, S., SUZUKI, H., DOI, Y., LIANG, J., KAWANOKUCHI, J., MIZUNO, T., SAWADA, M. & SUZUMURA, A. 2008. Blockade of microglial glutamate release protects against ischemic brain injury. *Exp Neurol,* 214, 144-6.
TAMM, I. 1989. IL-6. Current research and new questions. *Ann N Y Acad Sci,* 557, 478-89.

TEMPLETON, S. P., KIM, T. S., O'MALLEY, K. & PERLMAN, S. 2008. Maturation and localization of macrophages and microglia during infection with a neurotropic murine coronavirus. *Brain Pathol,* 18, 40-51.

THAMBISETTY, M., SIMMONS, A., HYE, A., CAMPBELL, J., WESTMAN, E., ZHANG, Y., WAHLUND, L. O., KINSEY, A., CAUSEVIC, M., KILLICK, R., KLOSZEWSKA, I., MECOCCI, P., SOININEN, H., TSOLAKI, M., VELLAS, B., SPENGER, C. & LOVESTONE, S. 2011. Plasma biomarkers of brain atrophy in Alzheimer's disease. *PLoS One,* 6, e28527.

TOGO, T., AKIYAMA, H., ISEKI, E., KONDO, H., IKEDA, K., KATO, M., ODA, T., TSUCHIYA, K. & KOSAKA, K. 2002. Occurrence of T cells in the brain of Alzheimer's disease and other neurological diseases. *J Neuroimmunol,* 124, 83-92.

TOWN, T., LAOUAR, Y., PITTENGER, C., MORI, T., SZEKELY, C. A., TAN, J., DUMAN, R. S. & FLAVELL, R. A. 2008. Blocking TGF-beta-Smad2/3 innate immune signaling mitigates Alzheimer-like pathology. *Nat Med,* 14, 681-7.

TOWN, T., VENDRAME, M., PATEL, A., POETTER, D., DELLEDONNE, A., MORI, T., SMEED, R., CRAWFORD, F., KLEIN, T., TAN, J. & MULLAN, M. 2002. Reduced Th1 and enhanced Th2 immunity after immunization with Alzheimer's beta-amyloid(1-42). *J Neuroimmunol,* 132, 49-59.

TOWN, T., TAN, J., FLAVELL, R. A. & MULLAN, M. 2005. T-cells in Alzheimer's disease. *Neuromolecular Med,* 7, 255-64.

TREMBLAY, M. E., STEVENS, B., SIERRA, A., WAKE, H., BESSIS, A. & NIMMERJAHN, A. 2011. The role of microglia in the healthy brain. *J Neurosci,* 31, 16064-9.

TRINCHIERI, G. 1998. Interleukin-12: a cytokine at the interface of inflammation and immunity. *Adv Immunol,* 70, 83-243.

TRINCHIERI, G. 2003. Interleukin-12 and the regulation of innate resistance and adaptive immunity. *Nat Rev Immunol,* 3, 133-46.

TRIPATHY, D., THIRUMANGALAKUDI, L. & GRAMMAS, P. 2007. Expression of macrophage inflammatory protein 1-alpha is elevated in Alzheimer's vessels and is regulated by oxidative stress. *J Alzheimers Dis,* 11, 447-55.

TRIPATHY, D., THIRUMANGALAKUDI, L. & GRAMMAS, P. 2010. RANTES upregulation in the Alzheimer's disease brain: a possible neuroprotective role. *Neurobiol Aging,* 31, 8-16.

TRUDLER, D., FARFARA, D. & FRENKEL, D. 2010. Toll-like receptors expression and signaling in glia cells in neuro-amyloidogenic diseases: towards future therapeutic application. *Mediators Inflamm,* 2010.

TURNER, P. R., O'CONNOR, K., TATE, W. P. & ABRAHAM, W. C. 2003. Roles of amyloid precursor protein and its fragments in regulating neural activity, plasticity and memory. *Prog Neurobiol,* 70, 1-32.

TUSZYNSKI, M. H., THAL, L., PAY, M., SALMON, D. P., U, H. S., BAKAY, R., PATEL, P., BLESCH, A., VAHLSING, H. L., HO, G., TONG, G., POTKIN, S. G., FALLON, J., HANSEN, L., MUFSON, E. J., KORDOWER, J. H., GALL, C. & CONNER, J. 2005. A phase 1 clinical trial of nerve growth factor gene therapy for Alzheimer disease. *Nat Med,* 11, 551-5.

UDAN, M. L., AJIT, D., CROUSE, N. R. & NICHOLS, M. R. 2008. Toll-like receptors 2 and 4 mediate Abeta(1-42) activation of the innate immune response in a human monocytic cell line. *J Neurochem,* 104, 524-33.

UJIIE, M., DICKSTEIN, D. L., CARLOW, D. A. & JEFFERIES, W. A. 2003. Blood-brain barrier permeability precedes senile plaque formation in an Alzheimer disease model. *Microcirculation,* 10, 463-70.

UNDERHILL, D. M. & GOODRIDGE, H. S. 2012. Information processing during phagocytosis. *Nat Rev Immunol,* 12, 492-502.

UNDERHILL, D. M. & OZINSKY, A. 2002. Phagocytosis of microbes: complexity in action. *Annu Rev Immunol,* 20, 825-52.

VAN AMERSFOORT, E. S. & VAN STRIJP, J. A. 1994. Evaluation of a flow cytometric fluorescence quenching assay of phagocytosis of sensitized sheep erythrocytes by polymorphonuclear leukocytes. *Cytometry,* 17, 294-301.

VAN DER ZEE, E. A., PLATT, B. & RIEDEL, G. 2011. Acetylcholine: future research and perspectives. *Behav Brain Res,* 221, 583-6.

VAN LANDEGHEM, F. K., STOVER, J. F., BECHMANN, I., BRUCK, W., UNTERBERG, A., BUHRER, C. & VON DEIMLING, A. 2001. Early expression of glutamate transporter proteins in ramified microglia after controlled cortical impact injury in the rat. *Glia,* 35, 167-79.

VEERHUIS, R., BOSHUIZEN, R. S. & FAMILIAN, A. 2005a. Amyloid associated proteins in Alzheimer's and prion disease. *Curr Drug Targets CNS Neurol Disord,* 4, 235-48.

VEERHUIS, R., BOSHUIZEN, R. S., MORBIN, M., MAZZOLENI, G., HOOZEMANS, J. J., LANGEDIJK, J. P., TAGLIAVINI, F., LANGEVELD, J. P. & EIKELENBOOM, P. 2005b. Activation of human microglia by fibrillar prion protein-related peptides is enhanced by amyloid-associated factors SAP and C1q. *Neurobiol Dis,* 19, 273-82.

VERDIER, Y., ZARANDI, M. & PENKE, B. 2004. Amyloid beta-peptide interactions with neuronal and glial cell plasma membrane: binding sites and implications for Alzheimer's disease. *J Pept Sci,* 10, 229-48.

VINCENT, B. & SMITH, J. D. 2000. Effect of estradiol on neuronal Swedish-mutated beta-amyloid precursor protein metabolism: reversal by astrocytic cells. *Biochem Biophys Res Commun,* 271, 82-5.

VITA, N., LEFORT, S., LAURENT, P., CAPUT, D. & FERRARA, P. 1995. Characterization and comparison of the interleukin 13 receptor with the interleukin 4 receptor on several cell types. *J Biol Chem,* 270, 3512-7.

VITKOVIC, L., KONSMAN, J. P., BOCKAERT, J., DANTZER, R., HOMBURGER, V. & JACQUE, C. 2000. Cytokine signals propagate through the brain. *Mol Psychiatry,* 5, 604-15.

VOLIANSKIS, A., KOSTNER, R., MOLGAARD, M., HASS, S. & JENSEN, M. S. 2010. Episodic memory deficits are not related to altered glutamatergic synaptic transmission and plasticity in the CA1 hippocampus of the APPswe/PS1deltaE9-deleted transgenic mice model of ss-amyloidosis. *Neurobiol Aging,* 31, 1173-87.

VYAS, J. M., VAN DER VEEN, A. G. & PLOEGH, H. L. 2008. The known unknowns of antigen processing and presentation. *Nat Rev Immunol,* 8, 607-18.

WALSH, D. M., HARTLEY, D. M., KUSUMOTO, Y., FEZOUI, Y., CONDRON, M. M., LOMAKIN, A., BENEDEK, G. B., SELKOE, D. J. & TEPLOW, D. B. 1999. Amyloid beta-protein fibrillogenesis. Structure and biological activity of protofibrillar intermediates. *J Biol Chem,* 274, 25945-52.

WALSH, D. M. & SELKOE, D. J. 2007. A beta oligomers - a decade of discovery. *J Neurochem,* 101, 1172-84.

WALZ, W. & LANG, M. K. 1998. Immunocytochemical evidence for a distinct GFAP-negative subpopulation of astrocytes in the adult rat hippocampus. *Neurosci Lett,* 257, 127-30.
WANG, D. D. & BORDEY, A. 2008. The astrocyte odyssey. *Prog Neurobiol,* 86, 342-67.

WANG, J., TANILA, H., PUOLIVALI, J., KADISH, I. & VAN GROEN, T. 2003. Gender differences in the amount and deposition of amyloidbeta in APPswe and PS1 double transgenic mice. *Neurobiol Dis,* 14, 318-27.

WANG, L. Z., TIAN, Y., YU, J. T., CHEN, W., WU, Z. C., ZHANG, Q., ZHANG, W. & TAN, L. 2011. Association between late-onset Alzheimer's disease and microsatellite polymorphisms in intron II of the human toll-like receptor 2 gene. *Neurosci Lett,* 489, 164-7.

WEI, R. & JONAKAIT, G. M. 1999. Neurotrophins and the anti-inflammatory agents interleukin-4 (IL-4), IL-10, IL-11 and transforming growth factor-beta1 (TGF-beta1) down-regulate T cell costimulatory molecules B7 and CD40 on cultured rat microglia. *J Neuroimmunol,* 95, 8-18.

WEST, M. A., WALLIN, R. P., MATTHEWS, S. P., SVENSSON, H. G., ZARU, R., LJUNGGREN, H. G., PRESCOTT, A. R. & WATTS, C. 2004. Enhanced dendritic cell antigen capture via toll-like receptor-induced actin remodeling. *Science,* 305, 1153-7.

WESTIN, K., BUCHHAVE, P., NIELSEN, H., MINTHON, L., JANCIAUSKIENE, S. & HANSSON, O. 2012. CCL2 is associated with a faster rate of cognitive decline during early stages of Alzheimer's disease. *PLoS One,* 7, e30525.

WHITE, J. A., MANELLI, A. M., HOLMBERG, K. H., VAN ELDIK, L. J. & LADU, M. J. 2005. Differential effects of oligomeric and fibrillar amyloid-beta 1-42 on astrocyte-mediated inflammation. *Neurobiol Dis,* 18, 459-65.

WILCOCK, D. M., LEWIS, M. R., VAN NOSTRAND, W. E., DAVIS, J., PREVITI, M. L., GHARKHOLONAREHE, N., VITEK, M. P. & COLTON, C. A. 2008. Progression of amyloid pathology to Alzheimer's disease pathology in an amyloid precursor protein transgenic mouse model by removal of nitric oxide synthase 2. *J Neurosci,* 28, 1537-45.

WILKINSON, B., KOENIGSKNECHT-TALBOO, J., GROMMES, C., LEE, C. Y. & LANDRETH, G. 2006. Fibrillar beta-amyloid-stimulated intracellular signaling cascades require Vav for induction of respiratory burst and phagocytosis in monocytes and microglia. *J Biol Chem,* 281, 20842-50.

WILKINSON, K. & EL KHOURY, J. 2012. Microglial scavenger receptors and their roles in the pathogenesis of Alzheimer's disease. *Int J Alzheimers Dis,* 2012, 489456.

WILLINGHAM, S. B., VOLKMER, J. P., GENTLES, A. J., SAHOO, D., DALERBA, P., MITRA, S. S., WANG, J., CONTRERAS-TRUJILLO, H., MARTIN, R., COHEN, J. D., LOVELACE, P., SCHEEREN, F. A., CHAO, M. P., WEISKOPF, K., TANG, C., VOLKMER, A. K., NAIK, T. J., STORM, T. A., MOSLEY, A. R., EDRIS, B., SCHMID,

S. M., SUN, C. K., CHUA, M. S., MURILLO, O., RAJENDRAN, P., CHA, A. C., CHIN, R. K., KIM, D., ADORNO, M., RAVEH, T., TSENG, D., JAISWAL, S., ENGER, P. O., STEINBERG, G. K., LI, G., SO, S. K., MAJETI, R., HARSH, G. R., VAN DE RIJN, M., TENG, N. N., SUNWOO, J. B., ALIZADEH, A. A., CLARKE, M. F. & WEISSMAN, I. L. 2012. The CD47-signal regulatory protein alpha (SIRPa) interaction is a therapeutic target for human solid tumors. *Proc Natl Acad Sci U S A,* 109, 6662-7.

WISNIEWSKI, H. M., BARCIKOWSKA, M. & KIDA, E. 1991. Phagocytosis of beta/A4 amyloid fibrils of the neuritic neocortical plaques. *Acta Neuropathol,* 81, 588-90.

WU, J., WANG, A., MIN, Z., XIONG, Y., YAN, Q., ZHANG, J., XU, J. & ZHANG, S. 2011. Lipoxin A4 inhibits the production of proinflammatory cytokines induced by beta-amyloid in vitro and in vivo. *Biochem Biophys Res Commun,* 408, 382-7.

WU, L., ROSA-NETO, P., HSIUNG, G. Y., SADOVNICK, A. D., MASELLIS, M., BLACK, S. E., JIA, J. & GAUTHIER, S. 2012. Early-onset familial Alzheimer's disease (EOFAD). *Can J Neurol Sci,* 39, 436-45.

WYSS-CORAY, T., LOIKE, J. D., BRIONNE, T. C., LU, E., ANANKOV, R., YAN, F., SILVERSTEIN, S. C. & HUSEMANN, J. 2003. Adult mouse astrocytes degrade amyloid-beta in vitro and in situ. *Nat Med,* 9, 453-7.

XIA, M. Q., BACSKAI, B. J., KNOWLES, R. B., QIN, S. X. & HYMAN, B. T. 2000. Expression of the chemokine receptor CXCR3 on neurons and the elevated expression of its ligand IP-10 in reactive astrocytes: in vitro ERK1/2 activation and role in Alzheimer's disease. *J Neuroimmunol,* 108, 227-35.

YANG, Y., GOZEN, O., VIDENSKY, S., ROBINSON, M. B. & ROTHSTEIN, J. D. 2010. Epigenetic regulation of neuron-dependent induction of astroglial synaptic protein GLT1. *Glia,* 58, 277-86.

YIN, K. J., CIRRITO, J. R., YAN, P., HU, X., XIAO, Q., PAN, X., BATEMAN, R., SONG, H., HSU, F. F., TURK, J., XU, J., HSU, C. Y., MILLS, J. C., HOLTZMAN, D. M. & LEE, J. M. 2006. Matrix metalloproteinases expressed by astrocytes mediate extracellular amyloid-beta peptide catabolism. *J Neurosci,* 26, 10939-48.

YONG, V. W. & RIVEST, S. 2009. Taking advantage of the systemic immune system to cure brain diseases. *Neuron,* 64, 55-60.

YU, H., IYER, R. K., KERN, R. M., RODRIGUEZ, W. I., GRODY, W. W. & CEDERBAUM, S. D. 2001. Expression of arginase isozymes in mouse brain. *J Neurosci Res,* 66, 406-22.

ZAIDI, M. R. & MERLINO, G. 2011. The two faces of interferon-gamma in cancer. *Clin Cancer Res,* 17, 6118-24.

ZHANG, W., WANG, L. Z., YU, J. T., CHI, Z. F. & TAN, L. 2012. Increased expressions of TLR2 and TLR4 on peripheral blood mononuclear cells from patients with Alzheimer's disease. *J Neurol Sci,* 315, 67-71.

ZHANG, Y., KIM, H. J., YAMAMOTO, S., KANG, X. & MA, X. 2010. Regulation of interleukin-10 gene expression in macrophages engulfing apoptotic cells. *J Interferon Cytokine Res,* 30, 113-22.

ZHONG, N. & WEISGRABER, K. H. 2009. Understanding the basis for the association of apoE4 with Alzheimer's disease: opening the door for therapeutic approaches. *Curr Alzheimer Res,* 6, 415-8.

ZHU, J. & PAUL, W. E. 2008. CD4 T cells: fates, functions, and faults. *Blood,* 112, 1557-69.

ZHU, J. & PAUL, W. E. 2010. Heterogeneity and plasticity of T helper cells. *Cell Res,* 20, 4-12.

ZLOKOVIC, B. V. 2002. Vascular disorder in Alzheimer's disease: role in pathogenesis of dementia and therapeutic targets. *Adv Drug Deliv Rev,* 54, 1553-9.

ZLOKOVIC, B. V. 2008. The blood-brain barrier in health and chronic neurodegenerative disorders. *Neuron,* 57, 178-201.

ZOTOVA, E., HOLMES, C., JOHNSTON, D., NEAL, J. W., NICOLL, J. A. & BOCHE, D. 2011. Microglial alterations in human Alzheimer's disease following Abeta42 immunization. *Neuropathol Appl Neurobiol,* 37, 513-24.

ZYGMUNT, B. & VELDHOEN, M. 2011. T helper cell differentiation more than just cytokines. *Adv Immunol,* 109, 159-96.

10: Appendix

10.1 Solutions and buffers

aCSF solution A	NaCl	8.66g
	KCl	0.224g
	$CaCl_2$	0.206g
	$MgCl_2$	0.163g
	Dissolve in 500ml pyrogen-free, sterile dH_2O	
aCSF solution B	Na_2HPO_4	0.214g
	NaH_2PO_4	0.027g
	Dissolve in 500ml pyrogen-free, sterile dH_2O	
	Combine solutions A and B in a 1:1 ratio	
Bis/Acrylamide	Acrylamide	29.2g
	N'N' Bisacrylamide	0.8g
	Make up to 100ml with dH_2O and filter	
Electrode running buffer (10X)	Tris base	30g
	SDS	10g
	Glycine	144g
	Make up to 1L with dH_2O	
FACS buffer	PBS (1X)	500ml
	FBS	10ml
	Sodium azide	0.5g
Guanidine buffer	Guanidine	5M
	Tris HCl (pH 8)	50mM

Laemmli sample buffer (2X, pH 6.8)	SDS	4%
	β-mercaptoethanol	10%
	Glycerol	20%
	Tris HCl	0.125M
	Bromophenol blue	0.004%
Lysis buffer	Tris HCl	50mM
	NaCl	150mM
	Triton-X	1%
	Protease inhibitors	1%
	Phosphatase inhibitors	1%
MACS buffer	PBS (1X)	500ml
	EDTA	2mM
	FBS	10ml
Medium A	1X HBSS	50ml
	Glucose (45%)	650µl
	HEPES (1M)	750µl
PBS (1X, pH 7.3)	NaCl	8g
	KCl	0.2g
	Na_2HPO_4	1.15g
	K_2PO_4	0.2g
	Make up to 1L with dH_2O and filter	

Running gel (7.5%)	Bis/Acrylamide	1.25ml
	H_2O	2.425ml
	1.5M Tris HCl (pH 8.8)	1.25ml
	10% SDS	50µl
	10% APS	25µl
	TEMED	3µl
Running gel (10%)	Bis/Acrylamide	1.6655ml
	H_2O	2.01ml
	1.5M Tris HCl (pH 8.8)	1.25ml
	10% SDS	50µl
	10% APS	25µl
	TEMED	3µl
Stacking gel (4%)	Bis/Acrylamide	0.325ml
	H_2O	1.525ml
	0.5M Tris HCl (pH 6.8)	0.625ml
	10% SDS	25µl
	10% APS	12.5µl
	TEMED	4µl
	Make up to 1L with dH_2O and filter	
TBS (1X, pH 7.6)	Tris base	24g
	NaCl	88g
	Make up to 1L with dH_2O and filter	
Transfer buffer (10X)	Tris base	30g
	Glycine	144g
	Make up to 1L with dH_2O	
	Add 20% methanol when making 1X transfer buffer	

10.2 Suppliers

Absolute ethanol	Hazmat, TCD
ALZET Osmotic Pumps	ALZET, USA
APP/PS1 mice	Originally purchased from Jackson Laboratory Bred in Bioresources Unit, TCD
Aβ	Invitrogen, UK
$A\beta_{1-42}$ HiLyte Fluor™ 488-labeled	Anaspec, Fremont, USA
Biocidal ZF™	WAK-Chemie Medical, Germany
Black fluorescent plates	Thermo Scientific, UK
CompBeads	BD Biosciences, USA
Coverslips (glass, 13 mm)	VWR Scientific, Ireland
Cryovials	Sigma-Aldrich, UK
Cytochalasin-D	Calbiochem, Germany
Cytotox 96® Assay	Promega Ltd., UK
Dimethyl sulfoxide (DMSO)	Sigma Aldrich, UK
Disposable sterile scalpels	Swann-Morton Ltd., UK
DNeasy Blood & Tissue Kit	Qiagen, Germany
DMEM	Invitrogen, UK
Dulbecco's PBS	Sigma Aldrich, UK
FACS tubes	BD Biosciences, USA
Filter units (33mm sterile Millex)	Millipore B.V., Ireland
FBS	Invitrogen, UK

Fungizone	Invitrogen Life Technologies, UK
GelRed™	Biotium, USA
General laboratory chemicals	Sigma-Aldrich, UK (unless otherwise stated)
General laboratory plasticware	Sarstedt Ltd., UK
GM-CSF	R&D Systems, UK
GoTaq® Green Master Mix	Promega Ltd., UK
HBSS	Invitrogen, UK
High capacity cDNA archive kit	Applied Biosystems, UK
IsoFlo	Abbott Animal Health, UK
Latex beads, 1.0µM	Sigma-Aldrich, UK
Lidocaine hydrofluoride	Abbott Animal Health, UK
LPS from *E. coli* serotype 0111:B4	Sigma-Aldrich, UK
Lymphoprep	Axis-Shield plc, Scotland
M-CSF	R&D Systems, UK
MACS Kit	MACS Miltenyi Biotec, Germany
Mesoscale Assays	Mesoscale Discovery, USA
Mycoplasma-OFF	Minerva Biolabs, Germany
Nucleospin® RNA II lisolation Kit	Macherney-Nagel, Germany
OptiPrep™	Axis-Shield plc, Scotland
Penicillin-streptomycin	Invitrogen, UK
Poly-L-lysine	Sigma Aldrich, UK
Prestained SDS-PAGE Standards	BioRad Laboratories Inc., UK

Resazurin	Sigma-Aldrich, UK
Rimadyl	Abbott Animal Health, UK
RNase-free microtubes	Ambion Inc., USA
RNaseZap® wipes	Ambion Inc., USA
RPMI	Invitrogen, UK
Sterile plasticware	Sarstedt Ltd., UK
Syringe filters (0.2µm)	Pall Corporation, USA
Syringes (20ml, 50 ml)	Unitech, Ireland
TaqMan® Universal PCR Master Mix	Applied Biosystems, UK
TaqMan® Gene Expression Assays	Applied Biosystems, UK
Trypan blue (0.4%)	Sigma Aldrich, UK
Trypsin-EDTA	Sigma Aldrich, UK
Virkon	Antec International, USA
Wedelolactone	Merck Millipore, Germany
Wistar rats	Bioresources Unit, TCD

10.3 Published abstracts

J Neuroimmune Pharmacol. 2012 Dec 14. [Epub ahead of print]

Amyloid-β-induced astrocytic phagocytosis is mediated by CD36, CD47 and RAGE

Jones, R.S., Minogue, A.M., Connor, T.J., Lynch, M.A.

Astrocytes, the most numerous glial cell in the brain, have multiple functions and are key to maintenance of homeostasis in the central nervous system. Microglia are the resident immunocompetent cells in the brain and share several functions with macrophages, including their phagocytic ability. Indeed microglia are the resident phagocytes in the brain and express numerous cell surface proteins which act to enable receptor-mediated phagocytosis. However recent evidence suggests that astrocytes express some genes which permit phagocytosis of phosphatidylserine-decorated cells and this probably explains sporadic reports in the literature which suggest that astrocytes become phagocytic following brain trauma. Here we examined the potential of astrocytes to phagocytose fluorescently-labelled latex beads and amyloid-β (Aβ) and report that they competently engulf both in a manner that relies on actin polymerization since it was inhibited by cytochalasin D. The data indicate that incubation of cultured astrocytes or microglia with Aβ increased phagocytosis and markers of activation of both cell types. Aβ was found to markedly increase expression of the putative Aβ-binding receptors CD36 and CD47 in astrocytes, while it decreased expression of the receptor for advanced glycation endproducts (RAGE). It is demonstrated that blocking these receptors using a neutralizing antibody attenuated Aβ-induced phagocytosis of latex beads by astrocytes. Interestingly blocking these receptors also decreased uptake of beads even in the absence of Aβ. We conclude that astrocytes are competent phagocytes and their ability to engulf Aβ may be important in the context of identifying strategies which might reduce Aβ accumulation in Alzheimer's disease.

Under secondary review by PLOS ONE, February 2013

Identifying early inflammatory changes in monocyte-derived macrophages from a population with IQ-discrepant episodic memory

*Downer, E.J., *Jones, R.S., Greco, E., Brennan, S., Connor T.J., Roberston, I.H., Lynch, M.A.

Background: Cells of the innate immune system including monocytes and macrophages are the first line of defence against infections and are critical regulators of the inflammatory response. These cells express toll-like receptors (TLRs), innate immune receptors which govern tailored inflammatory gene expression patterns. Monocytes, which produce pro-inflammatory mediators, are readily recruited to the central nervous system (CNS) in neurodegenerative diseases.

Methods: This study explored the expression of receptors (CD11b, TLR2 and TLR4) on circulating monocyte-derived macrophages (MDMs) and peripheral blood mononuclear cells (PBMCs) isolated from healthy elderly adults who we classified as either IQ memory-consistent (high-performing, HP) or IQ memory-discrepant (low-performing, LP).

Results: The expression of CD11b, TLR4 and TLR2 was increased in MDMs from the LP group when compared to HP cohort. MDMs from both groups responded robustly to treatment with the TLR4 activator, lipopolysaccharide (LPS), in terms of cytokine production. Significantly, MDMs from the LP group displayed hypersensitivity to LPS exposure.

Interpretation: Overall these findings define differential receptor expression and cytokine profiles that occur in MDMs derived from a cohort of IQ memory-discrepant individuals. These changes are indicative of inflammation and may be involved in the prodromal processes leading to the development of neurodegenerative disease.

*These authors contributed equally to this work

10th European Meeting on Glial Cells in Health and Disease, September 2011

Phagocytosis by astrocytes is enhanced by amyloid- β

Jones, R.S., Cowley, T.R., Connor, T.J., Lynch, M.A.

In Alzheimer's disease (AD), it is widely accepted that the build-up of amyloid-beta (Aβ) is detrimental and factors contributing to its accumulation are increased production of Aβ and/or decreased processing, and ineffective clearance. Microglia, and also infiltrating macrophages, are professional phagocytes and primarily responsible for Aβ clearance. However there is some evidence that astrocytes may also function as phagocytes.

In this study, we first investigated phagocytic activity in mixed glial cells prepared from 1 day old rats and report that fluorescently-labelled latex beads were engulfed by both $CD11b^+$ and $CD11b^-$ cells. We established that this preparation comprised approximately 10% $CD11b^+$ cells and 90% $CD11b^-$ cells, and that the $CD11b^-$ cells were predominantly astrocytes. Uptake of latex beads by both cell types was inhibited by pre-treatment with cytochalasin D, a cell permeable and potent inhibitor of actin polymerisation, indicating that the mechanism of cellular uptake involved the phagocytic process. Pre-treatment with Aβ was found to enhance the uptake of fluorescently-labelled latex beads by both $CD11b^+$ and $GFAP^+$ cells.

We then assessed uptake of fluorescently-labelled Aβ and found that it was engulfed by both $CD11b^+$ and $GFAP^+$ cells and that this was again inhibited by cytochalasin D. Confocal images demonstrate intracellular localisation of Aβ within both $CD11b^+$ and $GFAP^+$ cells. Analysis of the uptake of fluorescently-labelled Aβ in purified astrocytes confirmed the phagocytic capability of these cells. These results indicate that astrocytes are competent phagocytes and we suggest that astrocytic dysfunction could contribute to the accumulation of Aβ that occurs in AD.